

**DEVELOPMENT OF PLANT-PRODUCED SUBUNIT  
VACCINE AND THERAPEUTIC PROTEIN FOR COVID-19**



**Mr. Konlavat Siriwattananon**

จุฬาลงกรณ์มหาวิทยาลัย  
**CHULALONGKORN UNIVERSITY**

**A Dissertation Submitted in Partial Fulfillment of the Requirements  
for the Degree of Doctor of Philosophy in Pharmaceutical Sciences and  
Technology**

**Common Course**

**FACULTY OF PHARMACEUTICAL SCIENCES**

**Chulalongkorn University**

**Academic Year 2021**

**Copyright of Chulalongkorn University**

การพัฒนาซัพยูนิตวัคซีนและโปรตีนที่ใช้บำบัดโรคโคโรนาไวรัส 2019 จากพืช



วิทยานิพนธ์นี้เป็นส่วนหนึ่งของการศึกษาตามหลักสูตรปริญญาวิทยาศาสตรดุษฎีบัณฑิต

สาขาวิชาเภสัชศาสตร์และเทคโนโลยี ไม่สังกัดภาควิชา/เทียบเท่า

คณะเภสัชศาสตร์ จุฬาลงกรณ์มหาวิทยาลัย

ปีการศึกษา 2564

ลิขสิทธิ์ของจุฬาลงกรณ์มหาวิทยาลัย

Thesis Title DEVELOPMENT OF PLANT-PRODUCED SUBUNIT  
VACCINE AND THERAPEUTIC PROTEIN FOR  
COVID-19

By Mr. Konlavat Siriwattananon

Field of Study Pharmaceutical Sciences and Technology

Thesis Advisor Associate Professor WARANYOO PHOOLCHAROEN,  
Ph.D.

---

Accepted by the FACULTY OF PHARMACEUTICAL SCIENCES,  
Chulalongkorn University in Partial Fulfillment of the Requirement for the Doctor of  
Philosophy

..... Dean of the FACULTY OF  
PHARMACEUTICAL SCIENCES  
(Assistant Professor RUNGPETCH  
SAKULBUMRUNGSIL, Ph.D.)

#### DISSERTATION COMMITTEE

..... Chairman  
(Associate Professor Anchanee Kubera, Ph.D.)

..... Thesis Advisor  
(Associate Professor WARANYOO PHOOLCHAROEN,  
Ph.D.)

..... Examiner  
(Assistant Professor CHATCHAI CHAOTHAM, Ph.D.)

..... Examiner  
(WANATCHAPORN ARUNMANEE, Ph.D.)

..... Examiner  
(KANNIKA KHANTASUP, Ph.D.)

จุฬาลงกรณ์มหาวิทยาลัย  
CHULALONGKORN UNIVERSITY

กถาวัชระ ศิริวัฒนนานนท์ : การพัฒนาซบยูนิตวักซันและโปรตีนที่ใช้บับัดโรคโคโรนาไวรัส 2019 จากพืช. ( DEVELOPMENT OF PLANT-PRODUCED SUBUNIT VACCINE AND THERAPEUTIC PROTEIN FOR COVID-19) อ.ที่ปริกษาหลัก : รศ. ดร.วรัญญู พูลเจริญ

เนื่องจากการแพร่ระบาดของโรคติดเชื้อโคโรนาไวรัส 2019 (COVID-19) อย่างรวดเร็ว ส่งผลกระทบต่อด้านสาธารณสุขและเศรษฐกิจอย่างร้ายแรง ดังนั้นการพัฒนาวิธีการรักษาโรคที่มีประสิทธิภาพจึงมีความจำเป็นในการควบคุมโรคระบาดดังกล่าว โดยในการศึกษานี้ได้ผลิตโปรตีนรีคอมบิแนนท์ SARS-CoV-2 RBD และ ACE2 ของมนุษย์โดยเชื่อมต่อกับส่วน Fc ของ IgG1 มนุษย์ใน *Nicotiana benthamiana* เพื่อใช้เป็นวัคซีนป้องกันและโปรตีนบับัดโรคโคโรนาไวรัส 2019 ในการศึกษาระดับภูมิคุ้มกันของรีคอมบิแนนท์วัคซีนซบยูนิต SARS-CoV-2 RBD-Fc ในสัตว์ทดลองมีการเติมสารเสริมฤทธิ์ (adjuvant) ซึ่งประกอบด้วย aluminium hydroxide gel (Alum), AddaVax™, (MF59) monophosphoryl lipid A จากแบคทีเรีย *Salmonella Minnesota* R595 (mPLA-SM) และ polyinosinic-polycytidylic acid (poly(I:C)) เพื่อเพิ่มประสิทธิภาพในการกระตุ้นภูมิคุ้มกันในหนู และนอกจากนั้นยังได้ทำการศึกษาระดับภูมิคุ้มกันไวรัส SARS-CoV-2 ของโปรตีนรีคอมบิแนนท์ ACE2-Fc ในหลอดทดลอง โดยใช้เซลล์ Vero E6 โดยจากการศึกษาพบว่าโปรตีนรีคอมบิแนนท์ SARS-CoV-2 RBD-Fc จากพืชสามารถเพิ่มระดับภูมิคุ้มกัน ในแง่ของการกระตุ้นการสร้างแอนติบอดี (antibody) และตอบสนองของเซลล์ภูมิคุ้มกันชนิดที (T-lymphocyte) ที่จำเพาะ และนอกจากนั้นยังพบว่าโปรตีน ACE2-Fc จากพืชสามารถยับยั้งการติดเชื้อไวรัส SARS-CoV-2 ในหลอดทดลองได้อย่างมีประสิทธิภาพ จะเห็นได้ว่าโปรตีนรีคอมบิแนนท์ SARS-CoV-2 RBD-Fc และ ACE2-Fc จากพืชมีศักยภาพที่จะนำมาพัฒนาเป็นวัคซีนซบยูนิตและโปรตีนบับัดโรคโคโรนาไวรัส 2019 ในการทดลองทางคลินิกสำหรับมนุษย์ในอนาคตต่อไป



สาขาวิชา เกษศาสตร์และเทคโนโลยี  
ปีการศึกษา 2564

ลายมือชื่อนิติ .....  
ลายมือชื่อ อ.ที่ปริกษาหลัก .....

# # 6176452333 : MAJOR PHARMACEUTICAL SCIENCES AND TECHNOLOGY

KEYWORD COVID-19, SARS-CoV-2, Receptor-binding domain, Angiotensin-converting enzyme 2, Plant-produced biopharmaceuticals, Protein-based subunit vaccine, Therapeutic protein for COVID-19

Konlavat Siriwattananon : DEVELOPMENT OF PLANT-PRODUCED SUBUNIT VACCINE AND THERAPEUTIC PROTEIN FOR COVID-19. Advisor: Assoc. Prof. WARANYOO PHOOLCHAROEN, Ph.D.

Due to the rapid transmission of the Coronavirus Disease 2019 (COVID-19) causing serious public health problems and economic burden, the development of effective therapeutic interventions is urgently needed for controlling the ongoing pandemic disease. In this study, we have transiently produced recombinant SARS-CoV-2 RBD and human ACE2 fused with the Fc region of human IgG1 in *Nicotiana benthamiana* in order to use as a preventive subunit vaccine and therapeutic against SARS-CoV-2. The recombinant SARS-CoV-2 RBD-Fc subunit vaccine was formulated with different commercially available adjuvants including aluminium hydroxide gel (Alum), AddaVax™ (MF59), monophosphoryl lipid A from *Salmonella Minnesota* R595 (mPLA-SM), and polyinosinic-polycytidylic acid (poly(I:C)) and intramuscularly immunized in mice to appraise the immunogenicity as well as potent anti-SARS-CoV-2 activity of recombinant ACE2-Fc protein was assessed *in vitro* using Vero E6 cells. Importantly, the plant-produced recombinant SARS-CoV-2 RBD-Fc could exhibit effective immunogenicity profiles in terms of and specific potent antibodies vaccine-specific T-lymphocyte responses in mice. Additionally, plant-produced ACE2-Fc proteins could efficiently inhibit SARS-CoV-2 infection *in vitro*. Altogether, our results demonstrated that the plant-produced recombinant SARS-CoV-2 RBD-Fc and ACE2-Fc proteins have the potential to be used as an alternative subunit vaccine and therapeutic for COVID-19, which are possibly presented in the clinical trials for human uses in the near future.

จุฬาลงกรณ์มหาวิทยาลัย  
CHULALONGKORN UNIVERSITY

Field of Study:	Pharmaceutical Sciences and Technology	Student's Signature .....
Academic Year:	2021	Advisor's Signature .....

## ACKNOWLEDGEMENTS

I would like to express my sincere gratitude and appreciation to my advisor, Associate Professor WARANYOO PHOOLCHAROEN, Ph.D., from the Department of Pharmacognosy and Pharmaceutical Botany, Faculty of Pharmaceutical Sciences, Chulalongkorn University, for providing the opportunities to study in Ph.D. program and continuing in the interesting research field. Her guidance and encouragement supported of my Ph.D. study and research and carried me through all stages of my project and writing of this thesis. Besides my advisor, I would also like to thank to KAEWTA RATTANAPISIT, Ph.D. and BALAMURUGAN SHANMUGARAJ, Ph.D., postdoctoral researchers, and members of the Research Unit for Plant-Produced Pharmaceuticals (RU-PPP), Chulalongkorn University for valuable suggestions and supports in every steps of this thesis.

I would like to thank my committee members including Associate Professor ANCHANEE KUBERA, Ph.D., Assist. Prof. CHATCHAI CHAOTHAM, Ph.D., WANATCHAPORN ARUNMANEE, Ph.D., and KANNIKA KHANTASUP, Ph.D. for letting my thesis defense be a delightful moment and for your insightful comments and suggestions.

I greatly appreciate to PHARMACEUTICAL SCIENCES AND TECHNOLOGY (PST) PROGRAM, Faculty of Pharmaceutical Sciences, Chulalongkorn University for contribution of attractive courses as well as the good times during my three years as a Ph.D. student.

I am thankful to the Department of Disease Control, Ministry of Public Health, Thailand for providing clinical specimens for the viral isolate and sera from a COVID-19 survivor, 100th anniversary Chulalongkorn University for doctoral scholarship and Baiya Phytopharm Co., Ltd. for a financial support in this research.

Finally, my sincere thanks also go to my friends, my family, and my parents for their continuous and unparalleled love, help and support.

Konlavat Siriwattananon

# TABLE OF CONTENTS

	<b>Page</b>
.....	iii
ABSTRACT (THAI) .....	iii
.....	iv
ABSTRACT (ENGLISH).....	iv
ACKNOWLEDGEMENTS.....	v
TABLE OF CONTENTS.....	vi
LIST OF TABLES.....	xiii
LIST OF FIGURES .....	xiv
CHAPTER 1 .....	1
Rationale and Significance .....	1
Research Hypotheses .....	3
Literature Reviews.....	4
COVID-19 pandemic disease.....	4
Epidemiological characteristics of COVID-19 disease.....	4
Pathophysiology of SARS-CoV-2.....	5
• Classification and origin of SARS-CoV-2.....	5
• Structural biology of SARS-CoV-2 .....	8
• Entry of SARS-CoV-2 and pathogenesis.....	11
• Role of ACE2 in COVID-19.....	13
Potential anti-SARS-CoV-2 interventions for COVID-19 treatment.....	15
Anti-inflammatory agents.....	16
Systemic anticoagulants .....	16
Chloroquine and hydroxychloroquine.....	17
Renin-angiotensin system inhibitors .....	17
Serine protease inhibitors .....	18

Non-steroidal anti-inflammatory drugs .....	18
Repurposed anti-viral drugs .....	18
• Lopinavir and ritonavir .....	18
• Nelfinavir .....	19
• Remdesivir .....	19
• Favipiravir .....	19
Antibody-based therapy .....	20
ACE2 protein as the potential therapeutic agent for COVID-19 .....	23
Development of vaccine candidates for COVID-19 prevention .....	26
Vaccine platforms.....	26
• Live-attenuated platform .....	28
• Inactivated platform .....	29
• Viral RNA platform .....	31
• Viral DNA-based platform.....	34
• Viral vector platform.....	35
• Protein-based subunit platform .....	38
Selection of SARS-CoV-2 antigen.....	42
Selection of efficient immunoadjuvants.....	44
• Aluminum-based adjuvant (Alum) .....	45
• Oil in water emulsion .....	46
• Monophosphoryl lipid A (MPL) .....	47
• Toll-like receptor (TLR) agonists .....	48
- TLR9 agonists.....	49
- TLR7/8 agonists.....	49
- TLR3 agonists.....	50
Plants as alternative protein production factories.....	50
Plant-based expression system .....	50
Transient expression technologies.....	52
Protein processing and localization in plant cells .....	55



Plant-produced biopharmaceuticals in several clinical applications .....	57
Fc-based therapeutic candidates .....	59
CHAPTER 2 .....	61
Materials and Equipment .....	61
Genetic materials .....	61
Biological materials .....	62
Equipment .....	62
Materials .....	63
Proteins and antibodies .....	64
Immunoadjuvants .....	65
Chemical reagents .....	66
Software and database .....	69
Facilities .....	70
Experimental Procedures .....	70
Gene Design and Synthesis .....	70
Cloning and Construction of Expression Vectors .....	71
Preparation of Escherichia coli Competent Cells .....	73
Plasmid Propagation in E. coli .....	74
Preparation of Agrobacterium tumefaciens Electrocompetent Cells .....	75
Gene Transformation into A. tumefaciens by Electroporation .....	76
Transient Expression and Optimization of SARS-CoV-2 RBD-Fc and ACE2-Fc .....	76
Large-Scale Productions of SARS-CoV-2 RBD-Fc and ACE2-Fc .....	77
Protein Extraction and Purification .....	77
Protein Characterization by Sodium Dodecyl Sulfate Polyacrylamide Gel Electrophoresis (SDS-PAGE) and Western Blotting .....	78
Protein Quantification by Enzyme-linked Immunoassay (ELISA) Assay .....	79
In vitro Binding Activity of Plant-Produced SARS-CoV-2 RBD-Fc .....	80
In vitro Binding Activity of Plant-Produced ACE2-Fc .....	81

Vaccine Preparation and Formulation for Mice Immunization.....	81
Ethics Statement.....	82
Mice Immunogenicity Studies.....	82
Evaluation of SARS-CoV-2 RBD-Specific Antibody Responses by ELISA	
Assay.....	83
Cell culture.....	84
Virus preparation.....	85
In Vitro Microneutralization Assay.....	85
Quantification of Mouse IFN- $\gamma$ by ELISpot Assay.....	87
In Vitro Antiviral Activity of Plant-Produced ACE2-Fc.....	88
Statistical analysis.....	90
CHAPTER 3.....	91
Construction of SARS-CoV-2 RBD-Fc and ACE2-Fc for Plant Expression.....	93
Transient Expression of SARS-CoV-2 RBD-Fc and ACE2-Fc in <i>N. benthamiana</i> <i>via.</i> , Agroinfiltration.....	97
Purification and Characterization of SARS-CoV-2 RBD-Fc and ACE2-Fc Fusion Protein from <i>N. benthamiana</i> Leaves.....	100
<i>In vitro</i> Binding Activity of Plant-Produced RBD-Fc and ACE2-Fc Fusion Proteins .....	104
Identification of Immunoadjuvants and Mice Immunogenicity.....	109
SARS-CoV-2 RBD-specific IgG responses elicited in mice immunized by several plant-produced SARS-CoV-2 subunit vaccine formulations.....	112
SARS-CoV-2 RBD-specific IgG1 and IgG2a subtype responses elicited in mice immunized by several plant-produced SARS-CoV-2 subunit vaccine formulations.....	114
Protective efficacy against live SARS-CoV-2 <i>in vitro</i> .....	116
IFN- $\gamma$ -expressing T cells induced by several plant-produced SARS-CoV-2 subunit vaccine formulations.....	118
Anti-SARS-CoV-2 Activity of the Plant-Produced ACE2-Fc Fusion Protein.....	121
CHAPTER 4.....	124
REFERENCES.....	126

APPENDICES .....	152
APPENDIX 1.....	153
Synthesized Sequence of Signal Peptide-SARS-CoV-2 RBD-Peptide Linker .....	153
Synthesized Sequence of Human Fc of Immunoglobulin G1-SEKDEL Retention Signal .....	154
Sequence of SARS-CoV-2 RBD-Fc construct.....	155
APPENDIX 2.....	157
Synthesized Sequence of Signal Peptide-ACE2-Peptide Linker .....	157
Sequence of ACE2-Fc construct .....	159
APPENDIX 3.....	162
<i>Xba</i> I Restriction Enzyme.....	162
<i>Bam</i> HI Restriction Enzyme.....	162
<i>Sac</i> I Restriction Enzyme .....	162
APPENDIX 4.....	163
APPENDIX 5.....	164
LB Broth (Miller).....	164
LB Agar (Miller) .....	164
1xPBS Buffer (pH7.4).....	164
1xInfiltration Buffer (pH 5.5).....	165
1xRunning Buffer for SDS-PAGE.....	165
1xTransfer Buffer for Western Blotting.....	165
Coomassie Staining Solution.....	165
De-staining Solution.....	166
Z-buffer for Reducing Protein Loading Dye.....	166
Z-buffer for Non-Reducing Protein Loading Dye.....	166
Complete DMEM Medium .....	166
Blocking Solution for Microneutralization Assay.....	167
Diluent Solution for Antibody.....	167
R5 Medium.....	167

R10 Medium.....	167
1xACK Lysis Buffer .....	168
APPENDIX 6.....	169
Commercial HEK-Produced ACE2-Fc Protein Standard .....	169
Expression Levels of Plant-Produced ACE2-Fc Proteins .....	170
APPENDIX 7.....	171
Absorbance at 450 nm of Sample in the Various Concentrations Tested by Using HEK293-Produced ACE2 Protein. ....	171
Absorbance at 450 nm of Sample in the Various Concentrations Tested by Using CHO-Produced ACE2 Protein. ....	172
Absorbance at 450 nm of Sample in the Various Concentrations Tested by Using 1xPBS Buffer (Negative Control).....	173
APPENDIX 8.....	174
Absorbance at 450 nm of Sample in the Various Concentrations Tested by Using Sf9-Produced SARS-CoV-2 RBD-His Protein.....	174
Absorbance at 450 nm of Sample in the Various Concentrations Tested by Using Plant-Produced S1 of PEDV-His Protein (Negative Control). ....	175
Absorbance at 450 nm of Sample in the Various Concentrations Tested by Using 1xPBS Buffer (Negative Control).....	176
APPENDIX 9.....	177
Total IgG Titers .....	177
IgG1 subtype Titers .....	179
IgG2a subtype Titers .....	181
APPENDIX 10.....	183
APPENDIX 11.....	185
APPENDIX 12.....	190
APPENDIX 13.....	192
APPENDIX 14.....	194
Alum Adjuvant.....	194
AddaVax™ (MF59) Adjuvant .....	195
mPLA-SM Adjuvant .....	196

Poly (I:C)-High Molecular Weight Adjuvant ..... 197  
VITA..... 199



## LIST OF TABLES

	<b>Page</b>
Table 1 List of monoclonal antibodies developed for COVID-19 treatment .....	21
Table 2 Overview of available vaccine platforms developed for infectious diseases prevention .....	27
Table 3 List of clinical inactivated vaccine candidates for SARS-CoV-2.....	31
Table 4 List of clinical viral RNA-based vaccine candidates for SARS-CoV-2.....	33
Table 5 List of clinical viral DNA-based vaccine candidates for SARS-CoV-2.....	35
Table 6 List of clinical viral-vectored vaccine candidates for SARS-CoV-2.....	37
Table 7 List of clinical protein-based vaccine candidates for SARS-CoV-2 .....	39
Table 8 Comparison of clinical efficacy of commercial vaccine candidates, which are approved for emergency use .....	41
Table 9 Strengths and limitations of heterologous protein-based expression systems .....	51
Table 10 Overview of expression strategies for production of plant-derived biopharmaceuticals .....	54
Table 11 Examples of plant-produced biopharmaceuticals, which are available in clinical studies or approved for therapeutic use.....	58
Table 12 Examples of plant-produced vaccines, which are available in clinical studies or approved for therapeutic use.....	58
Table 13 Fc-fusion proteins approved for clinical use.....	60
Table 14 Components for restriction enzyme digestion .....	72
Table 15 Components for in vitro ligation.....	72
Table 16 Components for polymerase chain reaction.....	74
Table 17 Conditions for polymerase chain reaction .....	75
Table 18 Primers for polymerase chain reaction .....	75
Table 19 Experiment groups for immunogenicity study in mice .....	82

## LIST OF FIGURES

### Page

Figure 1 Timeline of the emergences of seven human coronaviruses consisting of human coronavirus 229E (HCoV-229E), HCoV-OC43, HCoV-NL63, HCoV-HKU1, Severe acute respiratory syndrome coronavirus (SARS-CoV), Middle-East respiratory syndrome coronavirus (MERS-CoV), and severe acute respiratory syndrome coronavirus 2 (SARS-CoV-2).....	7
Figure 2 Genome and viral structure of SARS-CoV-2. including 5'-untranslated region (5'-UTR), Open reading frame (ORF) 1a/b, non-structural proteins (papain-like protease; 3CL-protease; RNA-dependent RND polymerase (RdRp); Helicase; and endoribonuclease), structural proteins (spike (S); membrane (M); envelope (E); and nucleocapsid (N) proteins), accessory proteins (ORF3a, 6, 7a, 7b, 8, 9b, and 10), and 3'-UTR.....	9
Figure 3 Schematic illustration of SARS-CoV-2 spike protein, which is cleaved by specific protease into subunit S1 and S2. The S1 subunit consists of N-terminal domain (NTD), receptor-binding motif (RBM), and receptor-binding domain (RBD), receptor-binding motif (RBM). The S2 subunit consists of fusion peptide (FP), heptad repeat 1 and 2 (HR 1/2), and transmembrane anchor (TM).....	11
Figure 4 Renin-angiotensin-aldosterone system (RAAS) and ACE/ACE2 balance ..	15
Figure 5 Diagrammatic representation showing the mechanism of soluble ACE2 protein in anti-SARS-CoV-2 activity.....	26
Figure 6 Schematic representation of TLR agonists activated various TLRs on conventional and plasmacytoid dendritic cells (DCs) .....	49
Figure 7 Schematic representation of gene design for cloning with Fc region to construct A. SARS-CoV-2 RBD-Fc and B. ACE2-Fc sequences .....	71
Figure 8 Schematic representation of constructed protein expression vectors for expression in <i>N. benthamiana</i> including A. pBYR2e-SARS-CoV-2 RBD-Fc and B. pBYR2e-ACE2-Fc .....	73
Figure 9 Experimental design of plant-produced SARS-CoV-2 RBD-Fc immunization and sample collection in mice immunogenicity studies .....	83
Figure 10 Experimental design of in vitro anti-SARS-CoV-2 assay including A. post-infection phase; plant-produced ACE2-Fc added to SARS-CoV-2-infected Vero E6 cells (at 25TCID <sub>50</sub> ) and B. pre-infection phase; plant-produced ACE2-Fc and SARS-CoV-2 (at 25TCID <sub>50</sub> ) mixture added to Vero E6 cells.....	90

Figure 11 Digestion of commercially synthesized genes including A. pUC57-SARS-CoV-2 and B. pUC57-ACE2 by XbaI and BamHI restriction enzymes.....	94
Figure 12 Digestion of A. Fc fragment and B. pBYR2e vector by using its specific restriction enzymes including BamHI and SacI and XbaI and SacI restriction enzymes, respectively for preparation of expression constructs in plants .....	95
Figure 13 0.8% agarose gel of transformant <i>E. coli</i> colony PCR containing A. pBYR2e-SARS-CoV-2 RBD-Fc and B. pBYR2e-ACE2-Fc .....	96
Figure 14 0.8% agarose gel of transformant <i>A. tumefaciens</i> colony PCR containing A. pBYR2e-SARS-CoV-2 RBD-Fc and B. pBYR2e-ACE2-Fc .....	97
Figure 15 Phenotypic expression of infiltrated <i>N. benthamiana</i> leaves. A. leaf infiltrated with 1; <i>Agrobacterium</i> control and 2; <i>Agrobacterium</i> containing pBYR2e-SARS-CoV-2 RBD-Fc after 4 dpi. B. leaf infiltrated with <i>Agrobacterium</i> containing pBYR2e-ACE2-Fc after 6 dpi .....	98
Figure 16 Expression levels of plant-produced ACE2-Fc in each time course. The infiltrated leaves were collected from 3 individual plants in each day post infiltration. Data were analyzed by indirect ELISA assay using ACE2-specific antibody and presented as mean $\pm$ SD of triplicates.....	99
Figure 17 SDS-PAGE analysis of plant-produced A. SARS-CoV-2 RBD-Fc and B. ACE2-Fc fusion proteins stained with Coomassie staining. 1; SDS gel under reducing condition, 2; SDS gel under non-reducing condition.....	101
Figure 18 Western blotting analysis of A. plant-produced SARS-CoV-2 RBD-Fc and B. plant-produced ACE2-Fc fusion proteins probed with its specific antibody including a rabbit anti-SARS-CoV-2 RBD antibody and rabbit anti-human ACE2 antibody. 1; SDS gel under reducing condition, 2; SDS gel under non-reducing condition .....	103
Figure 19 Western blotting analysis of A. plant-produced SARS-CoV-2 RBD-Fc and B. plant-produced ACE2-Fc fusion proteins probed with Fc-specific antibody 1; SDS gel under reducing condition, 2; SDS gel under non-reducing condition.....	104
Figure 20 Binding activity of the plant-produced SARS-CoV-2 RBD-Fc using the commercial angiotensin-converting enzyme 2 (ACE2 proteins) derived from HEK293 and CHO cells and analyzed by ELISA. 1xPBS was used as negative control. Data are presented as mean $\pm$ standard deviation (SD) of triplicates in each sample dilution	105
Figure 21 Expression of S1 protein of porcine epidemic diarrhea virus (PEDV) in <i>N. benthamiana</i> . A. Schematic representation showing the plant expression construct pBYR2e PEDV S1-His used. B. Diagrammatic representation showing the overview of transient expression of PEDV S1 protein in <i>N. benthamiana</i> . C. Western blotting of	



plant-produced PEDV S1 under reducing conditions. SARS-CoV-2 RBD-His from Sf9 cells (Genscript Biotech, USA) (lane 1; positive control) and lane 2; purified plant-produced PEDV S1-His probed with anti-His-HRP conjugate antibody. The red and black arrows indicate the presence of S1-His of PEDV and SARS-CoV-2 RBD-His, respectively..... 107

Figure 22 Binding activity of the plant-produced ACE2-Fc using the commercial Sf9-produced SARS-CoV-2 RBD protein and analyzed by ELISA. PBS buffer and S1 protein of PEDV were used as negative controls. Data are presented as mean  $\pm$  standard deviation (SD) of triplicates in each sample dilution ..... 108

Figure 23 The SARS-CoV-2 RBD-specific total IgG antibody response elicited by mice immunized with different plant-produced SARS-CoV-2 RBD-Fc vaccine formulations. The titers were expressed as endpoint titers, which were analyzed by indirect ELISA using commercial SARS-CoV-2 RBD produced from Sf9 cells as a capture antigen and detected with goat-anti mouse IgG-HRP conjugated antibody. The immunological data were presented as mean  $\pm$  SD of the endpoint titers from five mice in each vaccination group (n = 5). \*p < 0.05; \*\*p < 0.01; \*\*\*p < 0.001; \*\*\*\*p < 0.0001..... 113

Figure 24 The endpoint titers of SARS-CoV-2 RBD-specific IgG1 detected in the immunized sera, which were collected on day 0, 14, and 35 and analyzed by indirect ELISA using commercial SARS-CoV-2 RBD produced from Sf9 cells as a capture antigen and the mouse-specific detection antibodies including goat-anti mouse IgG1-HRP and goat anti-mouse IgG2a-HRP antibody, respectively. The immunological data were presented as mean  $\pm$  SD of the endpoint titers from five mice in each vaccination group (n = 5). \*p < 0.05; \*\*p < 0.01; \*\*\*p < 0.001; \*\*\*\*p < 0.0001 ... 115

Figure 25 The endpoint titers of SARS-CoV-2 RBD-specific IgG2a detected in the immunized sera, which were collected on day 0, 14, and 35 and analyzed by indirect ELISA using commercial SARS-CoV-2 RBD produced from Sf9 cells as a capture antigen and the mouse-specific detection antibodies including goat-anti mouse IgG1-HRP and goat anti-mouse IgG2a-HRP antibody, respectively. The immunological data were presented as mean  $\pm$  SD of the endpoint titers from five mice in each vaccination group (n = 5). \*p < 0.05; \*\*p < 0.01; \*\*\*p < 0.001; \*\*\*\*p < 0.0001 ... 116

Figure 26 The neutralizing titers detected in mouse sera, which were elicited by mice immunized with several plant-produced SARS-CoV-2 RBD-Fc vaccine formulations against SARS-CoV-2. The in vitro neutralizing responses were assessed by microneutralization assay using Vero E6 cells. The infected cells were detected by anti-SARS-CoV-2 nucleocapsid mAb and goat anti-rabbit IgG-HRP antibody. The immunological data were presented as mean  $\pm$  SD of the endpoint titers from five

mice in each vaccination group (n = 5). \*p < 0.05; \*\*p < 0.01; \*\*\*p < 0.001; \*\*\*\*p < 0.0001..... 117

Figure 27 The levels of SARS-CoV-2 RBD-specific IFN- $\gamma$ -producing T cells expressing from mouse splenocytes immunized with different plant-produced SARS-CoV-2 RBD-Fc vaccine formulations. The IFN- $\gamma$  expression levels were quantified by mouse ELISpot assay. Data are expressed as mean  $\pm$  SD of the spot-forming cells (SFCs)/10<sup>6</sup> splenocytes from five mice in each vaccination group (n = 5). \* p < 0.05; \*\* p < 0.01; \*\*\* p < 0.001; \*\*\*\* p < 0.0001..... 120

Figure 28 Dose-dependent effect of plant-produced ACE2-Fc on live SARS-CoV-2 inhibition in vitro at the pre-infection phase. A. SARS-CoV-2 infection profiles in Vero E6 cells which were treated with eight concentrations of plant-produced ACE2-Fc. B. Percentage of SARS-CoV-2 inhibition in Vero E6 cells, which were treated with eight concentrations of plant-produced ACE2-Fc starting with 200  $\mu$ g/ml. C. Efficacy of SARS-CoV-2 inhibition in Vero E6 cells, which were treated by eight concentrations of plant-produced ACE2-Fc. The data were showed as mean  $\pm$  SD of triplicates in individual concentrations ..... 122

Figure 29 Dose-dependent effect of plant-produced ACE2-Fc on live SARS-CoV-2 inhibition in vitro at the post-infection phase. A. SARS-CoV-2 infection profiles in Vero E6 cells which were treated with eight concentrations of plant-produced ACE2-Fc. B. Percentage of SARS-CoV-2 inhibition in Vero E6 cells, which were treated with eight concentrations of plant-produced ACE2-Fc starting with 200  $\mu$ g/ml. C. Efficacy of SARS-CoV-2 inhibition in Vero E6 cells, which were treated by eight concentrations of plant-produced ACE2-Fc. The data were showed as mean  $\pm$  SD of triplicates in individual concentrations ..... 123

# CHAPTER 1

## INTRODUCTION

### Rationale and Significance

In December 2019, the outbreak of pneumonia has been first reported in Wuhan, Hubei Province, China, which was initially reported to be caused by novel coronavirus (nCoV-2019) and later named as severe acute respiratory syndrome virus 2 (SARS-CoV-2) (1). On January 30, 2020, World Health Organization (WHO) officially named the disease condition associated with current coronavirus as Coronavirus Disease 2019 (COVID-19) (2, 3). The virus outbreak has become the pandemic disease and rapidly spread to more than 200 countries and territories. As of 16 November, 2021, more than 252 million of cumulative confirmed cases with a toll of more than 5.1 million of cumulative deaths were globally reported (4). The number of infected patients and deaths have still been exponentially increasing daily with the ongoing pandemic, which directly affects national health care and global economy. Thus, the development of specific vaccines or therapeutics would be significant approaches to control and prevent the pandemic disease.

SARS-CoV-2 belongs to the family of *Coronaviridae* with the genus *Betacoronavirus*, which is known to infect mammals. Coronaviruses (CoVs) are enveloped and single-stranded positive sense RNA viruses (+ssRNA). The genome of CoVs contains several open reading frames encoding for non-structural and structural proteins with size of 27-32 kb (5). The structural proteins consist of nucleocapsid protein (N), which located outside the genome and viral genome is packed by three

structural proteins including spike (S), membrane (M), and envelope (E) proteins. The S, M, and E proteins are essential for viral assembly and infection (6). The spike (S) glycoprotein of SARS-CoV-2 contains a receptor-binding domain (RBD), which plays an important role in viral entry into the target cells by interacting to angiotensin-converting enzyme 2 (ACE2) receptor on the host cell membrane (7, 8). Hence, S glycoprotein and ACE2 receptor are attractive antiviral targets and can be considered for developing as either vaccines or therapeutics against SARS-CoV-2 infection (9-11).

Plants have received considerable attention due to several advantages in comparison to the competing available expression systems in terms of low-cost production, scalability, speed and lack of animal and human pathogens (12-14). Several potential biologics can be transiently expressed in plants, which is likely to continue with the increasing demand for cheaper medicines produced in the manufacturing scale (15, 16). Interestingly, plants provide the protein post-translational modification mechanisms, which are suitable for production of complex proteins, especially Fc-based therapeutic proteins as describes here (17-20). Hence, plants can be considered as an alternative platform for economical production of commercially viable biopharmaceuticals and vaccines especially for developing countries during pandemic situation.

Fc-based therapeutic proteins show the ability to provide several benefits in terms of increasing protein expression and secretion without unfolding and aggregation and enable to easy and cost-effective purification of recombinant protein by protein A chromatography (13, 21-23). Additionally, the Fc domain can also prolong the half-life of the proteins due to pH-dependent binding to the neonatal Fc

receptor that can prevent the protein degradation in endosomes (13, 24-26). Therefore, the construction of Fc fragment can help to overcome the negative aspects in the development of antibody and Fc-containing fusion therapeutics.

In this study, we aim to develop plant-produced recombinant SARS-CoV-2 RBD-based subunit vaccine candidate, which can act as a promising immunopotentiator to elicit the potent neutralizing antibody in mice. As well, we aim to demonstrate the biological activity and inhibitory efficacy of plant-produced recombinant ACE2 protein in inhibition of SARS-CoV-2 infection *in vitro* using Vero E6 cells. Both SARS-CoV-2 RBD and ACE2 proteins were developed by fusing Fc domain of human immunoglobulin G1 (IgG1) at the C-terminus providing SARS-CoV-2 RBD-Fc and ACE2-Fc and constructed by cloning into geminiviral vector for expression in *Nicotiana benthamiana* plants. The plant-produced recombinant SARS-CoV-2 RBD-Fc and ACE2-Fc could show high potential to be alternative therapeutic interventions for combating the SARS-CoV-2 pandemic.

### **Research Hypotheses**

1. Plant-produced SARS-CoV-2 RBD-Fc apparently shows the effective binding activity to the commercial HEK-produced and CHO-produced ACE2 proteins and it can induce SARS-CoV-2 RBD-specific antibodies in mice with highly potent activity with two doses of immunizations.
2. Plant-produced ACE2-Fc allows binding activity to commercial HEK-produced SARS-CoV-2 RBD protein with high affinity and show the inhibitory activity to effectively protect Vero E6 cells against SARS-CoV-2 infection.

## Literature Reviews

### COVID-19 pandemic disease

#### Epidemiological characteristics of COVID-19 disease

The coronavirus disease 2019 (COVID-19) outbreak was first reported in Huanan Seafood Wholesale market located in Wuhan City, Hubei Province, China in December 2019, which was initially confirmed to be caused by a novel coronavirus (termed 2019-nCoV) from genomic analysis from the clinical specimens of viral pneumonia patients (1). Later, the International committee on Taxonomy of Viruses (ICTV) officially renamed the causative virus as severe acute respiratory syndrome coronavirus 2 (SARS-CoV-2) (2, 3). The World Health Organization declared the current outbreak termed COVID-19 has become a pandemic disease, which rapidly spreads around the globe with 216 countries and territories within a short time period and causes the large-scale outbreak, especially in the United State, India, and Brazil (27). The main COVID-19 transmission route is human-human transmission *via*., virus-containing respiratory droplets or direct contact with the infected patients. In addition, COVID-19 has also been found to be exposure by airborne transmission through aerosols (28). The incubation period of COVID-19 is 2-14 days (mean incubation time of approximately 6 days) after the viral exposure (29, 30). The COVID-19 disease has pleomorphic clinical manifestations including asymptomatic individuals and symptomatic patients ranged from mild to severe involvements (4, 10, 31-34). The clinical presentations can be divided into 2 main stages including upper respiratory tract infections (URTIs) with fever, dry cough, shortness of breath,

fatigue, nausea, vomiting and diarrhea and lower respiratory tract infections (LRTIs) with common complications consisting of pneumonia, acute respiratory syndrome, liver injury, myocarditis, acute kidney injury, neurological complication, cardiopulmonary failure, acute cerebrovascular disease, and shock, which can increase mortality and disability rates among hospitalized patients (34-40). Some COVID-19 carriers may not express any symptoms, which can increase the transmissibility rate of COVID-19 epidemic (41). Currently, the viral respiratory pathogen, referred to SARS-CoV-2 has globally infected at least 252 million individuals and killed more than 5.1 million people (4). In Thailand, more than 2.07 million cumulative confirmed cases with more than 20 thousands deaths, which was reported by Department of Disease Control, Ministry of Public Health on November 22, 2021 (42). Moreover, the numbers of COVID-19-infected patients and deaths have still exponentially risen daily in many countries. The COVID-19 have been included in the list of Public Health Emergency of International Concern (PHEIC) and provides international crises and negative effects on national health care, global economy, and education (43).

#### Pathophysiology of SARS-CoV-2

- *Classification and origin of SARS-CoV-2*

Coronaviruses (CoVs) belong to the family of *Coronaviridae* with the subfamily of *Orthocoronavirinae*, consisting of four genera including *alphacoronavirus* ( $\alpha$ -CoVs), *betacoronavirus* ( $\beta$ -CoVs), *gammacoronavirus* ( $\gamma$ -CoVs), and *deltacoronavirus* ( $\delta$ -CoVs). The genera of  $\alpha$ -CoVs and  $\beta$ -CoVs generally infect human and mammalian species, whereas  $\gamma$ -CoVs and  $\delta$ -CoVs genera are specific to a

wide range of avian species (5). CoVs are known to be enveloped and positive-sense single-stranded RNA viruses and they are found to be pathogenic agents in humans, other mammals, and avian species that typically cause a wide range of respiratory, gastrointestinal, renal, and neurological diseases (44-47). There are seven types of coronaviruses, which are found to be causative agents in humans including human coronavirus 229E (HCoV-229E), HCoV-OC43, HCoV-NL63, HCoV-HKU1, Severe acute respiratory syndrome coronavirus (SARS-CoV), Middle-East respiratory syndrome coronavirus (MERS-CoV), and most recent SARS-CoV-2 virus (Figure 1). The human coronaviruses such as HCoV-229E, HCoV-OC43, HCoV-NL63, and HCoV-HKU1 have circulated in the population for a long time and usually cause mild respiratory tract infections with common cold symptoms (5, 32, 45, 48). The lethal coronaviruses containing of SARS-CoV, MERS-CoV, and SARS-CoV-2, are highly pathogenic viruses, which emerged in the human population over 20 years, and caused severe and life-threatening respiratory diseases and lung pathologies by infecting the upper respiratory tract cells, bronchial epithelial cells, and pneumocytes in humans (5, 49-51).



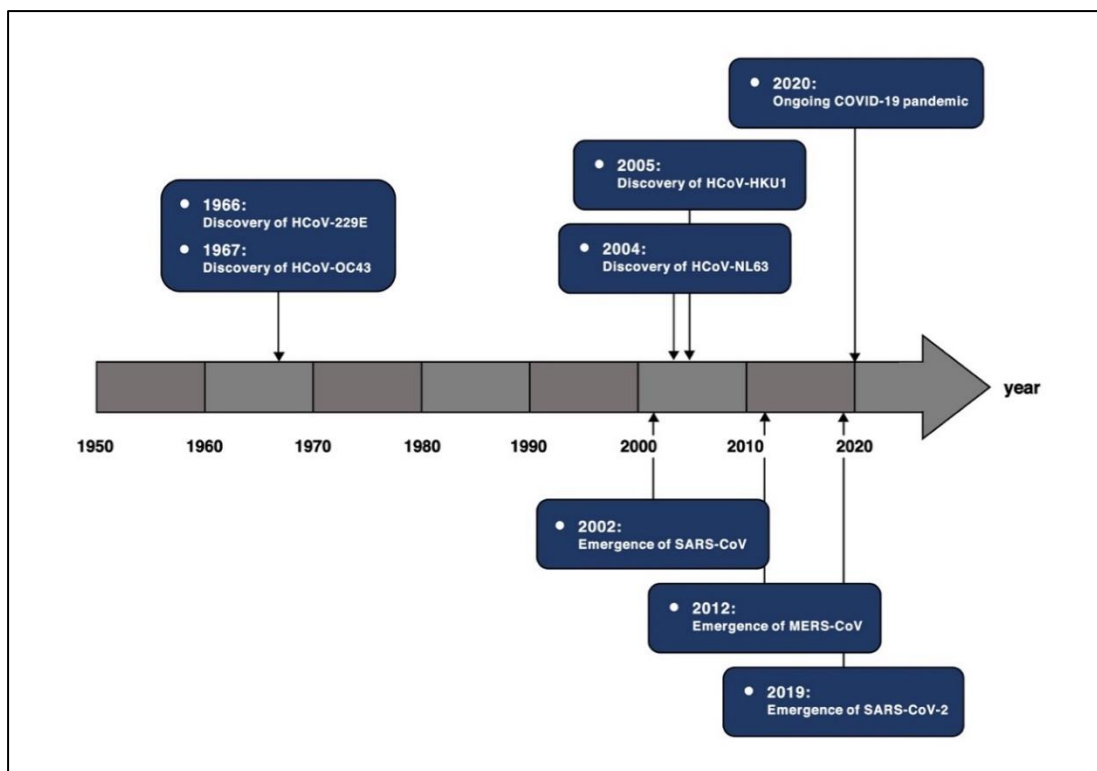


*Figure 1 Timeline of the emergences of seven human coronaviruses consisting of human coronavirus 229E (HCoV-229E), HCoV-OC43, HCoV-NL63, HCoV-HKU1, Severe acute respiratory syndrome coronavirus (SARS-CoV), Middle-East respiratory syndrome coronavirus (MERS-CoV), and severe acute respiratory syndrome coronavirus 2 (SARS-CoV-2)*

SARS-CoV-2 is the third highly zoonotic coronavirus, which emerged and globally spread in human in the past two decades containing SARS-CoV, which originated in Guangdong Province, China in November 2002 causing 8,098 documented cases and 774 deaths (lethal consequences of 10%) (52), MERS-CoV, which originated from the Arabian Peninsula resulting to 2,468 cumulative infected patients and 851 deaths with 35% case fatality rate (53), and most recent emerged SARS-CoV-2. Firstly, bats are believed to be natural reservoirs for progenitors of

zoonotic SARS-CoV-2, while the civets and camels are known to be the intermediate hosts for SARS-CoV and MERS-CoV infections. According to metagenomic sequencing results, it has been suggested that pangolins (*Manis javanica*) in Guangxi and Guangdong, China are considered as possible intermediary hosts between bats and humans due to closely related genetic profile with 91.02% genome identity (54-56).

- *Structural biology of SARS-CoV-2*

A novel *betacoronavirus* SARS-CoV-2 has spherical shape with a diameter of 60-140 nm and distinctive spikes 9-12 nm with the club-shaped projections (34, 44). The complete genomic material has been reported to be 29.9 kb (Figure 2). At the 5' end, the viral genomic RNA contains two main open reading frames (ORFs; ORF1a and ORF1b), which occupy two-thirds of the coding capped and polyadenylated genome. The ORF1a/b frame encodes 15-16 non-structural proteins (nsp), especially RNA-dependent RNA polymerase enzyme (RdRp), helicase enzyme, and endoribonuclease proofreading enzyme involving in viral replication and transcription (57, 58). The ORFs on one-third of viral RNA at 3'-terminus encode four major structural proteins including spike (S), envelope (E), membrane (M) proteins, which cooperatively create the viral envelop, and nucleocapsid (N) protein, holding the viral RNA genome (Figure 2) (2, 6, 10). Between the structural protein ORFs include accessory proteins including ORF3a, ORF6, ORF7a, ORF7b and ORF8 as well as ORF9b and 10, which are assumed to be located in the N gene (59, 60). The accessory genes are high variability among coronavirus groups and usually contain no similarity

with other viral sequences. The accessory proteins have an important role in viral pathogenicity during natural host infection (Figure 2) (46, 61).

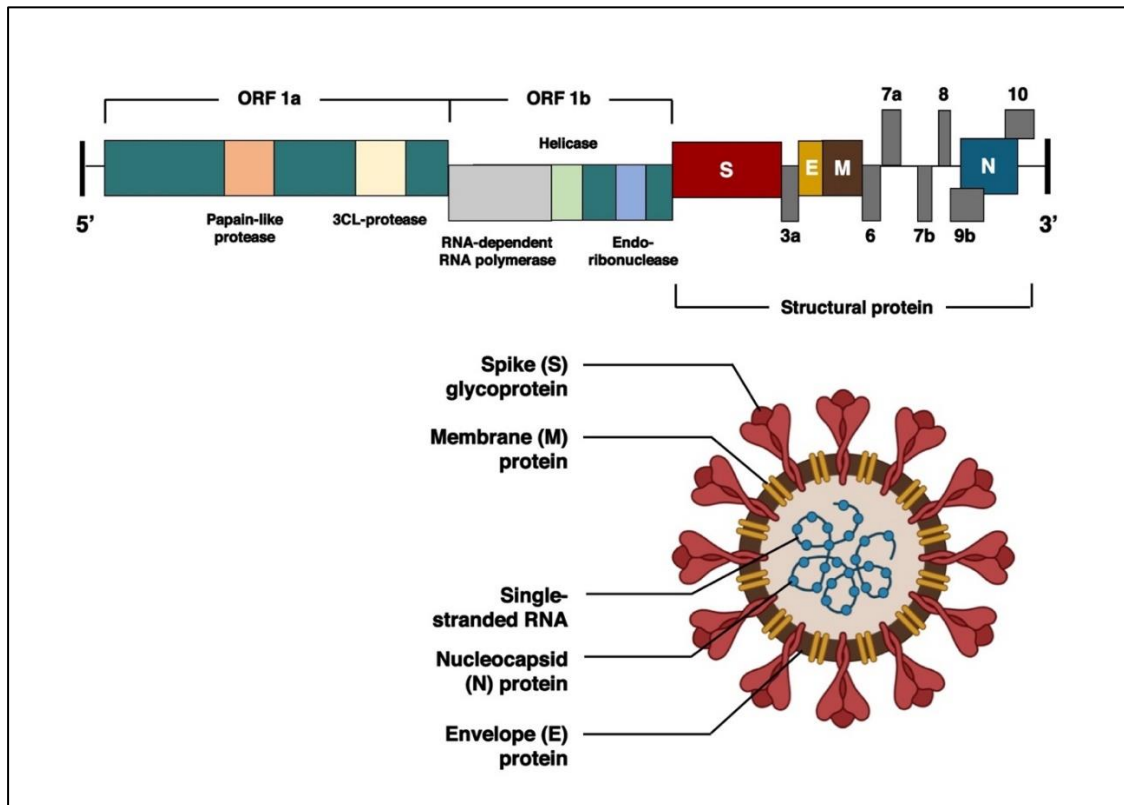


Figure 2 Genome and viral structure of SARS-CoV-2. including 5'-untranslated region (5'-UTR), Open reading frame (ORF) 1a/b, non-structural proteins (papain-like protease; 3CL-protease; RNA-dependent RND polymerase (RdRp); Helicase; and endoribonuclease), structural proteins (spike (S); membrane (M); envelope (E); and nucleocapsid (N) proteins), accessory proteins (ORF3a, 6, 7a, 7b, 8, 9b, and 10), and 3'-UTR

The S glycoprotein, which has the molecular weight of 150 kDa, forms into trimeric protein and expresses on the viral surface, providing crown-like shape of CoVs. S protein is classified into class-I viral fusion protein providing a metastable prefusion protein conformation for fusing the viral membrane with the target cells

(62). During the virus infection, S protein is cleaved by host proteases, especially furin, which cleaves at monobasic cleavage at the S1/S2 protease cleavage site into two functionally distinct parts consisting of N-terminus S1 subunit and C-terminus S2 subunit proteins, and another protease is transmembrane serine protease 2 (TMPRSS2), which cleaves at polybasic motifs (5, 7, 63-65). S1 subunit comprises of N-terminal domain (NTD) and receptor-binding domain (RBD), which is utilized to specifically interact with the host receptor named angiotensin-converting enzyme 2 resulting to virus cell tropism and viral pathogenicity (Figure 3). The transmembrane S2 subunit contains important parts, especially heptad repeat regions, transmembrane domain (TM), and fusion peptide (FP), which are used for fusion between virus and target cell enabling irreversible conformational rearrangements and allowing viral materials entering to the host cells (Figure 3) (2, 5, 8, 66). The M and E proteins allow the shape of viral envelop and facilitate virus-like protein (VLP) assembly release of new virions. N protein binds to viral genetic materials providing nucleocapsid protein involving in viral RNA replication and supporting the replication-transcription complex (6). The coronavirus structural proteins are assembled and proceeded into the new virions in the endoplasmic reticulum (ER) and followed by the secretory pathway, named as the endoplasmic reticulum-Golgi intermediate compartment complex (ERGIC), Subsequently the virions are secreted from infected cells by exocytosis (67-69).

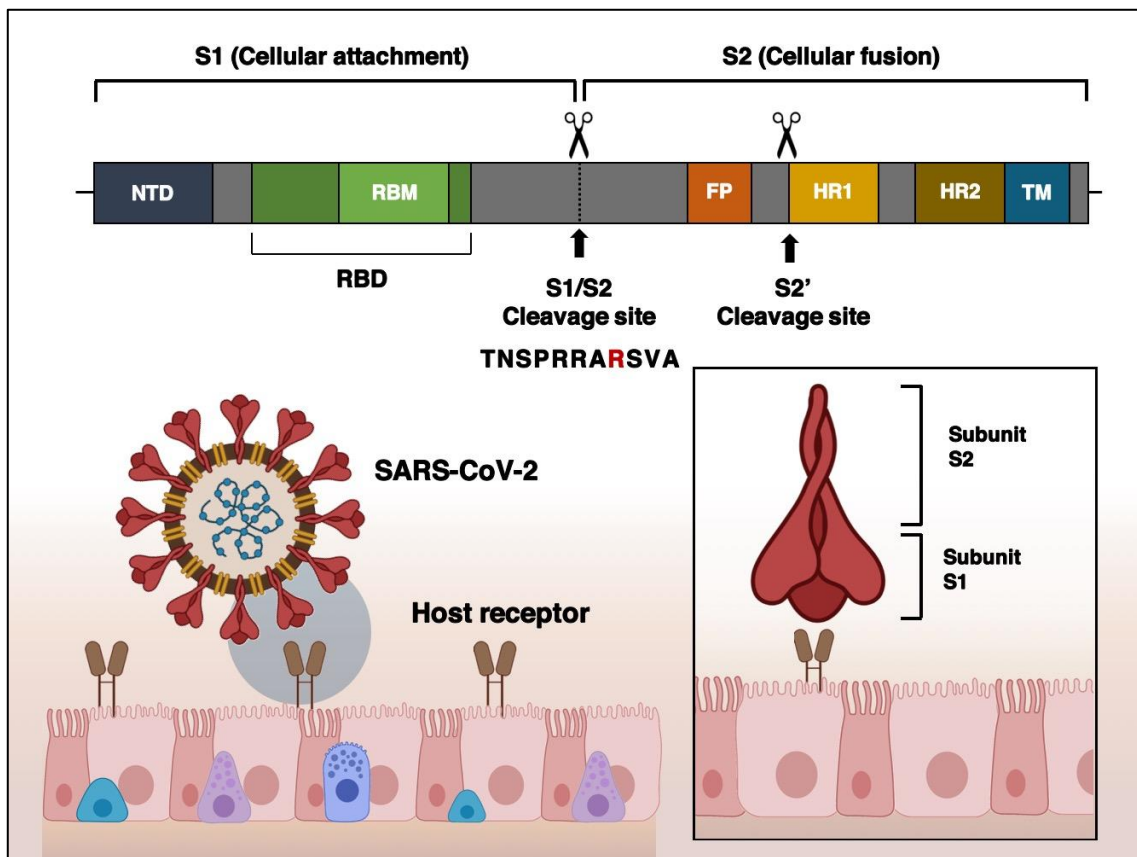


Figure 3 Schematic illustration of SARS-CoV-2 spike protein, which is cleaved by specific protease into subunit S1 and S2. The S1 subunit consists of N-terminal domain (NTD), receptor-binding motif (RBM), and receptor-binding domain (RBD), receptor-binding motif (RBM). The S2 subunit consists of fusion peptide (FP), heptad repeat 1 and 2 (HR 1/2), and transmembrane anchor (TM)

- *Entry of SARS-CoV-2 and pathogenesis*

The angiotensin-converting enzyme 2 (ACE2) has been reported to be a functional receptor for viruses in member of the species *severe acute respiratory syndrome-related coronavirus*, especially SARS-CoV and SARS-CoV-2 (7, 48, 70). The RBD of surface-exposed S1 subunit specifically interacts with cellular ACE2 receptor resulting to the priming of S1 at S1/S2 cleavage site by cellular furin protease

and other endosomal proteases. Fusion protein (FP) of transmembrane S2 subunit is exposed by cleavage of host cellular serine protease TMPRSS2 at S2' site allowing irreversible S protein formation and insertion of S2 subunit into host membrane (7, 8, 71). TMPRSS2 also plays an essential role on cellular entry of SARS-CoV-2 as well as SARS-CoV and MERS-CoV (72). According to previous study, the inhibition of serine TMPRSS2 protease by camostat mesylate can efficiently block the SARS-CoV-2 entry *in vitro* (7). CD147 is a transmembrane glycoprotein and extracellular matrix metalloproteinase inducer (EMMPRIN) involving in production of several matrix metalloproteinase for tissue modeling. CD147 is expressed on surface of erythrocytes, lymphocytes, macrophages, dendritic cells, and several organs such as lungs, heart, epithelial cells, intestines, and kidneys (73, 74). Meplazumab, a humanized anti-CD147, can block the interaction of SARS-CoV-2 S protein and cellular CD147 and decrease the replication SARS-CoV-2 *in vitro* (75). SARS-CoV and SARS-CoV-2 share the similarity in the use of receptor-mediated endocytosis through cellular ACE2 during its infection. Interestingly, SARS-CoV-2 RBD is able to bind ACE2 receptor with greater efficiency with 10-20-fold than the affinity of SARS-CoV RBD and ACE2 interaction (76). Following the entry, the viral RNA is released and uncoated for translation of ORF1a/b providing non-structural proteins (nsps), particularly viral proteases and RNA-dependent RNA polymerase (RdRp). The expression of nsps creates the protective environment for viral RNA replication and subgenomic mRNAs (sg mRNAs) transcription. The expression of structural proteins occurs in rough endoplasmic reticulum and all viral proteins are transited to the endoplasmic reticulum-Golgi intermediate compartment complex (ERGIC) of host

cell resulting in budding and viral assembly. Finally, the complete virions are released by exocytosis from the host cell (5, 77).

- *Role of ACE2 in COVID-19*

The renin-angiotensin-aldosterone system (RAAS) is complex signaling pathway involving in controlling the blood pressure, electrolyte and fluid homeostasis, natriuresis, and trophic responses to the stimuli (78-82). The RAAS also affects the function of several organs, especially heart, blood vessels, and kidneys. Commonly, renin converts the angiotensinogen into angiotensin I (Ang I) in the liver. Subsequently, angiotensin-converting enzyme (ACE) converts the Ang I into Ang II in the lungs by removing two amino acids at the carboxyl terminus. Ang II can promote different effects in accordance with different angiotensin receptor. Interaction of Ang II and angiotensin type 1 receptor (AT1R) results deleterious effects including vasoconstriction, oxidative stress, cell proliferation, fibrosis, apoptosis, and inflammation, whereas AT1R binding causes the opposite effects (Figure 4) (83-85).

In 2000, the ACE2, which is the homolog of ACE, was discovered. ACE2 is catalytic enzyme that also cleaves two amino acids at the carboxyl terminal phenylalanine in Ang II providing heptapeptide Ang (1-7) and hydrolyses the Ang I to Ang (1-9) (Figure 4). ACE2 plays a fundamental role in local and systemic haemodynamics by cleaving the Ang II into Ang (1-7), which can bind to the G-protein-coupled receptor MAS. The interaction of Ang (1-7) and MAS promotes vasodilation and anti-proliferation activities, which counterbalances the ACE or Ang

II and AT1R axis. Additionally, ACE2 regulates the RAAS pathway and ACE action by reducing Ang II and increasing the Ang (1-7) (83, 85, 86).

ACE2 is dominantly expressed on surface of alveolar endothelial cells and type I pneumocytes in lung tissues (87, 88). The alveolar epithelial type II cells in lungs have a potential to be viral reservoir, which can be damaged by SARS-CoV-2 infection. SARS-CoV-2 spike protein, particularly RBD domain binds to ACE2 competing with Ang II in viral internalization. The interaction of ACE2 and SARS-CoV-2 RBD can inhibit the ACE2 activities resulting to RAAS imbalance. The downregulation of ACE2 increases activities in ACE or Ang II and AT1R axis, especially tissue inflammation, which can result to epithelial cell death with apoptosis and pro-inflammatory program cell death or pyroptosis. The cell death induces release of pro-inflammatory cytokines such as interleukin-1 $\beta$  (IL-1 $\beta$ ), IL-18, IL-6, IL-8, Tumor necrosis factor- $\alpha$  (TNF- $\alpha$ ), Interferon gamma- induced protein 10 (IP-10), and monocyte chemoattractant protein 1 (MCP1), allowing pulmonary inflammation and lung damage (89-91). Dendritic cells (DCs) present the viral antigens to T-lymphocytes following activation of T-mediated immune responses. Helper CD4<sup>+</sup> T cells and B cells elicit the virus-specific antibodies, whereas Cytotoxic CD8<sup>+</sup> T cells kill the infected cells, resulting in increasing of pro-inflammatory cytokines (cytokine storm), particularly IL-6 and TNF- $\alpha$  (91-94). The high level of TNF- $\alpha$  promotes the overexpression of tissue factor (TF) in platelets and macrophage and may result in coagulation responses in severe COVID-19 patients (95).



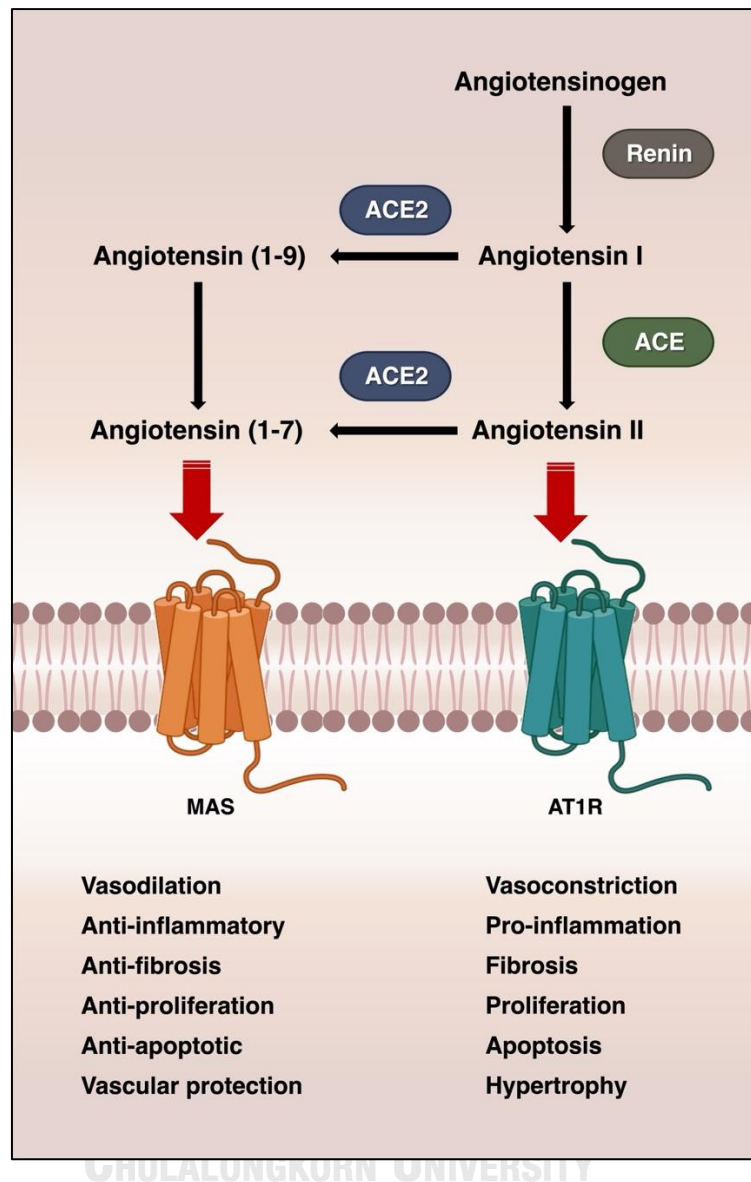


Figure 4 Renin-angiotensin-aldosterone system (RAAS) and ACE/ACE2 balance

### Potential anti-SARS-CoV-2 interventions for COVID-19 treatment

Due to the lack of specific antiviral treatments for SARS-CoV-2, the development of public health interventions such as anti-virals, antibodies, or vaccines is high essential strategy to control the transmission of the ongoing pandemic. Currently, there are several pharmacotherapeutic agents, which are repurposed from

experienced infectious disease treatments and possibly used as promising interventions for COVID-19 therapy.

#### Anti-inflammatory agents

During SARS-CoV-2 infection, the virus binds to ACE2 receptor on the target cells leading to activation of inflammatory cascade and cytokine release syndrome, especially IL-1, IL-6, IL-12, IL-18, or inflammatory mediators (91, 96). Tissue necrosis, lymphocyte infiltrations, cytokine storm, and hyperactivated pro-inflammatory T cells in gastrointestinal, heart, and lung mucosa are commonly seen in SARS-CoV-2-infected patients suggesting the use of anti-inflammatory agents for controlling the tissue damage from viral pathogenesis (97). Tocilizumab can bind to cell-related IL-6 eliciting or soluble IL-6 receptors providing the inhibition of immunosignal in significant pneumonia patients. The single dose of 400 mg tocilizumab can improve the lung function with 91% of hospitalized pneumonia patients (98) and show the benefits in the use of tocilizumab with the repeated doses in severe pneumonia cases (99). The systemic steroids are also used in COVID-19 patients due to the evidenced efficacy in treatment of systemic inflammatory response syndrome. The steroids can reduce the mortality rate in ventilated patients as observed as a trial study at the University of Oxford (100).

#### Systemic anticoagulants

Severe COVID-19 patients show the activation of coagulation cascade resulting to intravascular coagulation. In addition, lung inflammation may lead a microthrombotic phenomenon providing pulmonary embolism, venous thrombosis, and thrombotic arterial complications, especially ischemic stroke and myocardial

infarction among severe cases (101). Anticoagulants, especially heparin, can treat intravascular coagulation and venous thromboembolism, which are found in COVID-19 patients and it also reduces mortality rate compared to non-heparin users. Nevertheless, heparin is not the drug of choice for COVID-19 patients with atrial fibrillation due to various unpredicted side effects such as tachyarrhythmias, bradycardia, and severe bleeding (102, 103).

#### Chloroquine and hydroxychloroquine

Chloroquine (CQ) and hydroxychloroquine (HCQ) are anti-malaria drugs that are approved by US Food and Drug Administration (US-FDA) for emergency use for COVID-19 treatment. CQ and HCQ block fusion of viral and cellular membrane by interfering glycosylation of viral entry receptors and preventing endosomal acidification, which results to conformational changes of viral spike protein. The use of CQ in clinical trials can decrease the pneumonia symptoms and promote a virus-negative conversion. Additionally, CQ can inhibit Th1 immunity preventing a cytokine storm in COVID-19 patients. However, CQ and HCQ show toxic effects in human especially, promoting the development of irregular heart rhythm. Hence, these drugs have been warned against using outside of hospitalized applications or clinical trials (104-106).

#### Renin-angiotensin system inhibitors

Generally, SARS-CoV-2 utilizes RBD domain for viral infection through cellular ACE2 receptor. The use of ACE2 blocking agents, particularly renin-angiotensin system inhibitors or angiotensin II type 1 receptor blockers (ACEIs), is expected to allow prophylactic activity for preventing SARS-CoV-2 infection. ACEIs

allow effective activities in COVID-19 treatment terms of increasing immune cells, especially CD3 and CD8T, which are involved in viral clearance. ACEIs can decrease viral load in comparison to other antihypertensive drugs that can be used for treating the patients with hypertension, diabetes, and cardiovascular disorders (102, 107, 108).

#### Serine protease inhibitors

The serine protease inhibitors, consisting of camostat mesylate (NI-03), gabexate mesylate (Factor X inhibitor), and nafamostat mesylate (futhan), can inhibit viral entry by blocking the cellular enzyme transmembrane protease serine 2 (TMPRSS2), which leads to inactivation of SARS-CoV-2 S protein. These protease inhibitors were approved for using in treatment of unrelated coronavirus diseases. Thus, they have to be evaluated in the clinical studies (102, 109).

#### Non-steroidal anti-inflammatory drugs

Indomethacin, which is the one of NSAID drugs are widely used as anti-inflammatory and analgesic drugs. Additionally, it also shows anti-viral activities against canine coronavirus and SARS-CoV epidemic in 2003. Surprisingly, indomethacin has been found to inhibit SARS-CoV-2 pseudovirus *in vitro* that can be applied in further clinical study as an alternative strategy for COVID-19 treatment (102, 110).

#### Repurposed anti-viral drugs

- *Lopinavir and ritonavir*

The combination of lopinavir and ritonavir (LPV/RTV), which are intensively used for the treatment of HIV, has been suggested for treating COVID-19-infected

patients. LPV and RTV are FDA-approved protease inhibitors that disrupts viral replication by inhibition of 3CLPro activity *in vitro*. However, LPV/RTV did not show effective anti-viral efficacy in COVID-19 patients in comparison to the other standard cares terms of clinical improvement, mortality rate, and viral detection in each timepoint (34, 111-113).

- *Nelfinavir*

Protease inhibitor-based anti-viral drug, nelfinavir is approved antiviral drug for HIV treatment. Nelfinavir was also showed the benefits in anti-SARS-CoV-2 actions *in vitro*. Due to the anti-CoV activities, the nelfinavir was also chosen to be a potential inhibitor of SARS-CoV-2 in clinical studies (114, 115).

- *Remdesivir*

Remdesivir is used as an anti-viral drug against various viral infectious diseases including filoviruses, paramyxoviruses, pneumoviruses, SARS-CoV, MERS-CoV, mouse hepatitis virus (MHV), and porcine and bat-strained CoVs. Remdesivir blocks the viral replication by interfering viral RNA polymerase that leads to decreasing viral RNA replication. The anti-viral drug was reported to be active against SARS-CoV-2 infection with the success rate of 68% and provided higher potential than the use of LPV/RTV (34, 116-118).

- *Favipiravir*

Favipiravir was initially designed for treating throat and nose inflammatory symptoms. It can inhibit viral replication by blocking the RNA-dependent RNA polymerase (RdRp). Favipiravir was firstly approved for using as treatment strategy

of COVID-19 in China and also applied in phase III-clinical trial in India with high anti-viral efficacy and minimal unwanted side effects (34, 119).

#### Antibody-based therapy

However, many vaccines need a long period of time to activate immune response. Number of antibodies, which are usually present in antiserum, may not be effective for viral neutralization and infectious pathogen clearance depending on the host's ability (120, 121). Moreover, some diseases do not require the time for the body to develop its own immune responses due to a high risk of infection. Passive immunotherapy is regarded as an alternative method for clinical treatment of SARS-CoV-2 infectious disease.

Intravenous immunoglobulin (IVIg) is one of the passive antibody strategies that is prepared from blood samples of patients who recovered from viral infection. It transfers the active antibodies, which recognize the neutralizing epitopes on pathogenic virus surface leading to effective reduction of viral replication and severity (10, 44, 121). Based on the prior experiences, passive antibody was successfully used for treating various viral-infected diseases including influenza, Ebola, SARS-CoV, and MERS-CoV that could show high anti-viral efficacy and significantly reduce viral load and mortality rate among infected patients (122-124). However, passive immunization still has several limitations in terms of low potency of antiviral effect, safety due to high risk of human pathogen contamination, antibody demanding and several side effects consisting hypersensitivity and anaphylactic reactions and renal complications in glomerulonephritis patients (123, 125).

The use of monoclonal antibodies (mAbs) overcomes the drawbacks of passive immunizations with serum immunotherapy or intravenous immunoglobulin (IVIg) including specificity, safety due to low risk of human pathogen contamination, functionality, and purity. Monoclonal antibodies have become dominant class of pharmaceutical products, which are developed in recent years. Currently, therapeutic mAbs have been approved by FDA and successfully used in clinical application for treating several human diseases including cancers, autoimmune diseases, metabolic and infectious diseases (126-129). Generally, SARS-CoV-2 S protein of its RBD domain are used for interaction of cellular ACE2 receptor during viral entry. The development of either SARS-CoV-2 S or RBD-specific antibodies is an effective way against SARS-CoV-2 by blocking the binding of S protein and ACE2 receptor that results to prevention of viral penetration and infection (129-133). A list of antibody-based interventions developed for treatment against SARS-CoV-2 infection is shown in the Table 1.

*Table 1 List of monoclonal antibodies developed for COVID-19 treatment*

<b>mAb</b>	<b>Source</b>	<b>Specific site</b>	<b>Potency (IC<sub>50</sub>)</b>	<b>Status</b>	<b>Reference</b>
REGN-10987	SARS-CoV-2 immunized hu-mice and COVID-19 patients	SARS-CoV-2 RBD	< 10 ng/ml	Clinical trial phase III	(134-136)
P2C-1F11	COVID-19 patients	SARS-CoV-2 RBD	30 ng/ml	Clinical trial phase I	(137)
CB6-LALA (CA1)		SARS-CoV-2 RBD	36 ng/ml	Clinical trial phase I	(138)
C105		SARS-CoV-2 RBD	26 ng/ml	N/A	(139)

C002 (C121)		SARS-CoV-2 RBD	10 ng/ml	N/A	(140)
nAB cc12.1		SARS-CoV-2 RBD	19 ng/ml	Pre-clinical (Syrian hamsters)	(141)
B38/H4		SARS-CoV-2 RBD	200 ng/ml	Pre-clinical (hACE2 in transgenic mice)	(142)
311 mAb- 31B5 (32D4)		SARS-CoV-2 RBD	50 ng/ml	N/A	(143)
COVA1-18 (COVA2- 15, COVA2- 17)	COVID-19 patients	SARS-CoV-2 RBD	7 ng/ml	N/A	(144)
CV30/CV1		SARS-CoV-2 RBD	30 ng/ml 15,000 ng/ml	N/A	(145)
COV2-2196 (COV2- 2130)	COVID-19 patients	SARS-CoV-2 RBD	1-10 ng/ml	Pre-clinical (hACE2- expressing mice)	(146)
BD-368-2		SARS-CoV-2 RBD	15 ng/ml	Pre-clinical (hACE2 in transgenic mice)	(147)
4A8	COVID-19 patients	SARS-CoV-2 S1	500 ng/ml	N/A	(148)
CR3022	SAR-CoV patients	Cross- reactivity of SARS1/SARS2 RBD	114 ng/ml	N/A	(149-151)
47D11- H2L2	SAR-CoV hybridoma	Cross- reactivity of SARS1/SARS2	570 ng/ml	N/A	(152)



		RBD			
S309	SAR-CoV patients	Cross-reactivity of SARS1/SARS2 RBD	79 ng/ml	N/A	(133)
H014	Mice immunized SARS-CoV RBD	Cross-reactivity of SARS1/SARS2 RBD	38 ng/ml	Clinical trial phase I	(153)
ADI55689 (ADI56046)	SAR-CoV patients	Cross-reactivity of SARS1/SARS2 RBD	50-1400 ng/ml	N/A	(154)
VHH72-Fc	Llama immunized CoV S	Cross-reactivity of SARS1/SARS2 RBD	N/A	N/A	(155)

**\*\*N/A: not available**

#### ACE2 protein as the potential therapeutic agent for COVID-19

The development of neutralizing mAbs is facing several drawbacks that limit their uses as therapeutics for COVID-19. The SARS-CoV-2-specific mAbs are difficult to quickly validate a broadly neutralizing activity and confirm the neutralizing efficacy for protecting the escape of mutating viruses. Furthermore, the cocktail antibodies, which are used for treating the Ebola pandemic, provides more complicate validation and higher costs to the manufacturing process (26). Hence, the antibody-like molecule, which can bind to CoVs itself, would be a promising strategy and it overcomes the challenges in therapeutic development during the ongoing COVID-19 pandemic.

The recombinant ACE2 protein is purposed to interact with RBD, resulting to blocking and neutralizing the SARS-CoV-2 (Figure 5) (156-158). Interestingly, ACE2-based therapeutic was used to treat respiratory virus infections such as SARS-CoV and human coronavirus (HCoV)-NL63 coronaviruses (159, 160). Administration of soluble ACE2 proteins is able to effectively block the interactions of SARS-CoV and ACE2 receptor on cellular membrane, preventing the viral infection *in vitro*. Moreover, the affinity of soluble ACE2 in SARS-CoV inhibition was 1.70 nM, which is comparable to the uses of SARS-CoV-specific monoclonal antibodies (161, 162). According to Moore MJ. et al., (2020) study, the extracellular ACE2 domain engineered by fusing Fc of immunoglobulin G could also effectively neutralize SARS-CoV *in vitro* with IC<sub>50</sub> of 2 nM, while soluble ACE2 protein was not tested in animal model (163). Similar to SARS-CoV and SARS-CoV-2, utilize the same binding site on cellular ACE2 receptor for its attachment and binding. It could similarly apply the ACE2 blocking strategy in SARS-CoV-2 protection *in vitro* and COVID-19 therapy. Furthermore, no mutating SARS-CoV-2 strains are able to change the receptor for viral infection in the time frame of their pandemic. It has no concern about viral evasion form binding to ACE2 therapeutic agent (26, 164). The Apeiron biologics company developed APN01, which is a recombinant human ACE2 protein, for using as a therapeutic drug candidate for COVID-19 treatment. The APN01 was found to be safe in healthy volunteers during a pilot human trial in China. Currently, APN01 is currently running in phase II clinical trials to investigate the drug potency in Europe (88, 156). APN01, ACE2-based therapeutic, has potential to prevent the interaction of SARS-CoV-2 RBD to cellular receptor and reduce the organ injury and pathology by increase of Ang (1-7) resulting to reduction of injuries in

blood vessels, lungs, kidneys, and heart. It can also reduce the pro-inflammatory cytokines that involves in lung injury. APN01 was initially applied clinical phase II studies in April 2020 and completed in December 2020. The clinical results showed that APN01 could successfully protect severe respiratory diseases like acute lung injury (ALI), acute respiratory distress syndrome (ARDS) and pulmonary arterial hypertension (PAH) in the patient treated (165). Moreover, the recombinant ACE2 protein was also used in other clinical applications, especially, treatment of acute respiratory distress syndrome (ARDS). It could reduce ARDS effects caused by respiratory syncytial virus (RSV) and H5N1 influenza virus. Recombinant ACE2 was applied in phase I and II in clinical trials to treat the ARDS in critical patients. The results demonstrated that ACE2 provided higher tolerance of ARDS with no cardiovascular effects (166-168). Hence, the extracellular ACE2 protein has therefore the high potential to be regarded as the alternative therapeutic intervention for treatment of COVID-19 (156).

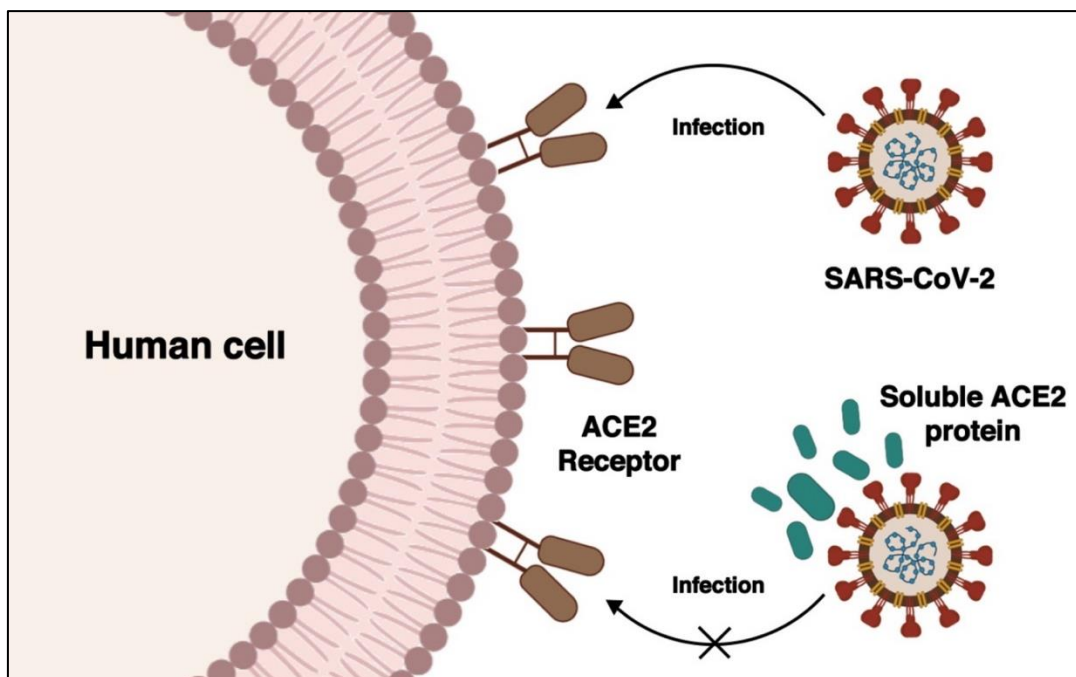


*Figure 5 Diagrammatic representation showing the mechanism of soluble ACE2 protein in anti-SARS-CoV-2 activity*

### **Development of vaccine candidates for COVID-19 prevention**

#### **Vaccine platforms**

Vaccination is one of effective strategies in prevention of infectious diseases, which provides active specific immune responses against pathogen-associated diseases and reduces morbidity and mortality from infection. Currently, there are several vaccine platforms, which are developed for prevention of infectious diseases. The commercially available vaccines can be classified into six platforms including live-attenuated, inactivated, RNA, DNA, viral vector, and recombinant protein vaccines (Table 2)

*Table 2 Overview of available vaccine platforms developed for infectious diseases prevention*

<b>Platform</b>	<b>Advantage</b>	<b>Disadvantage</b>	<b>Licensed vaccine</b>
Live-attenuated vaccine	<ul style="list-style-type: none"> <li>- Mimicking of natural infection</li> <li>- Efficient activation of cellular and humoral immune responses within one dose.</li> <li>- Providing long-lasting immune responses</li> </ul>	<ul style="list-style-type: none"> <li>- Not suitable for immunosuppressed people.</li> <li>- Virulent inversion</li> </ul>	Oral Polio, Yellow fever, Chickenpox, Mumps, Measles, Rotavirus, Rubella, Vaccinia, Bacillus Calmette-Guerin
Inactivated vaccine	<ul style="list-style-type: none"> <li>- Safer than live-attenuated vaccine due to the dead pathogen</li> <li>- Easy to handle termed of transportation and storage.</li> <li>- Scalability</li> </ul>	<ul style="list-style-type: none"> <li>- Low immunogenicity profiles due to the inactivation process.</li> <li>- Requirement of several booster doses.</li> </ul>	Rabies, Polio, Hepatitis A virus
Nucleic acid vaccine (DNA and RNA vaccines)	<ul style="list-style-type: none"> <li>- Fast and scalability</li> <li>- Safe due to no infectious agent</li> <li>- Efficient induction of humoral and cellular responses.</li> </ul>	<ul style="list-style-type: none"> <li>- No nucleic acid vaccine approved.</li> <li>- Requirement of a special delivery platform.</li> <li>- Instability</li> <li>- Requirement of efficient cold chain for transportation</li> </ul>	-
Viral-vectored vaccine	<ul style="list-style-type: none"> <li>- Efficient activation of cellular and humoral immune responses within one dose.</li> <li>- Safe immunogenicity profile.</li> </ul>	<ul style="list-style-type: none"> <li>- Pre-existing immunity against a human viral vector</li> <li>- Requirement of storage at &lt;math&gt;-20\text{ }^{\circ}\text{C}&lt;/math&gt;.</li> <li>- Requirement of Complicated manufacturing process</li> <li>- High risk of genomic</li> </ul>	Ebola

			integration genome
		-	Adverse effects e.g., inflammatory responses
Protein subunit vaccine	- Safe for immunosuppressed people.	-	Low immunogenicity.
	- No infectious agent	-	Requirement of several booster dose
		-	Requirement of immunoadjuvants.
		-	Inefficient activation of cellular responses.
		-	Limited antigen production scalability
			Hepatitis B virus, Hepatitis C virus, Influenza, Acellular pertussis vaccine, human papilloma virus

- *Live-attenuated platform*

The live-attenuated vaccines are made from laboratory-weakened version of the native pathogens. These vaccines preserve the viral native antigens that mimics the natural infection allowing strong immune responses and long-term immunity. The pathogens in live-attenuated vaccine can replicate in the host cells providing antigenic stimulation and induction of humoral and cell-mediated immune responses with high efficacy (169). However, vaccines still contain living microorganisms, which carry higher risk than other types of vaccine, especially inversion to the original virulent form. Consequently, live vaccines cannot be given to immunodeficient patients (170-173). The live-attenuated vaccines have been developed for using in treatment of several infectious diseases, especially measles, mumps, tuberculosis, rubella, varicella, influenza, and yellow fever (174).

The SARS-CoV-2 live-attenuated vaccines were developed by several either biotech companies or universities such as Indian Immunologicals company, Griffith University, and Mehmet Ali Aydinlar University. All live-attenuated vaccines are

recruiting in the pre-clinical studies. In addition, COVI-VAC, which was developed by Codagenix company, is the one of SARS-CoV-2 live-attenuated vaccines that can be applied in clinical phase I trial in UK (77, 175).

- *Inactivated platform*

The inactivated viral vaccines are produced from killed or inactivated whole virus by heat, radiation, chemical reagents, particularly formaldehyde and  $\beta$ -propiolactone. The inactivated vaccines are scalable to produce at a large scale without the several requirements compared to other types of viral vaccines. These vaccines are safer than live-attenuated platform but they still provide less immunogenic profile and weaker immunity. Therefore, additional booster adjuvants are required for effective immune activation (170-173).

CoronaVac is a SARS-CoV-2 inactivated vaccine formulated with alum adjuvant developed by Sinovac Research and Development Company. The Coronavac vaccine was produced from  $\beta$ -propiolactone-inactivated SARS-CoV-2 strain CN2, which is isolated from COVID-19 hospitalized patients. The vaccine showed highly immunogenic in animal studies, especially BALB/c mice, Wistar rats, and rhesus macaques (*Macaca mulatta*) with high titers of S- and RBD-specific antibodies and neutralizing antibodies as well as the protective efficacy in animal challenge (176). The CoronaVac was applied for testing the vaccine efficacy in clinical studies phase II in 600 healthy volunteers between 18 and 59 years old. It was found to be immunogenic by promoting the immunogenicity and neutralizing antibodies eliciting against SARS-CoV-2 in human. The neutralizing titers ranged from 23.8-65.4 after 28 days post second immunization and the titers were dropped in elderly participants

(177). However, the CoronaVac vaccine allows some unwanted side effects in clinical studies such as fever and pain at the injection site among vaccinated subjects (178). Currently, the CoronaVac vaccine is evaluating in clinical trials phase III with a two-dose injection regimen (14 days interval) using 8870 participants from Brazil, Indonesia, and Turkey.

The BBIBP-CorV vaccine is a  $\beta$ -propiolactone-mediated inactivation of SARS-CoV-2 strain HB02, which propagate in Vero E6 cells. The inactivated SARS-CoV-2 adjuvanted with alum hydroxide, which can activate pro-inflammatory molecules and promote the secretion of IL-1 $\beta$  and IL-18. BBIBP-CorV vaccine could induce high levels of neutralizing antibodies and protect rhesus macaques from SARS-CoV-2 infection within 7 days post vaccination as evidenced as viral loads in lung tissue and pathological analysis results (179). In phase I clinical study, BBIBP-CorV was tested in 192 participants and showed the safety profiles with mild or moderate and no serious adverse effects. The vaccine was found to be immunogenic by induction of immunity on day 42 after vaccination in adults with the neutralizing antibody titer of approximately 256 (180). 448 volunteers were participated for testing the vaccine efficacy in phase II trials. The vaccine was also showed the safety profiles with mild to moderate adverse reactions of less than 4%. BBIBP-CorV is being applied in phase III clinical trials in Argentina, Bahrain, Jordan, Egypt, and U.A.E.

The other current inactivated vaccine candidates, recruiting in pre-clinical studies and human clinical trials are shown in the Table 3.



*Table 3 List of clinical inactivated vaccine candidates for SARS-CoV-2*

<b>Vaccine</b>	<b>Developer</b>	<b>Status</b>	<b>Clinical trial registration</b>	<b>Reference</b>
CoronaVac	Sinovac	Phase III	NCT04456595 NCT04582344 669/UN6.KEP/EC/2020	(177)
Inactivated SARS-CoV-2 vaccine (Vero cell)	Wuhan Institute of Biological Products/ Sinopharm	Phase III	ChiCTR2000034780 ChiCTR2000039000	(181)
BBIBP-CorV	Beijing Institute of Biological Products/ Sinopharm	Phase III	ChiCTR2000034780 NCT04466085	(180)
BBV152A BBV152B BBV152C	Bharat Biotech	Phase I/II	NCT04471519 CTRI/2020/09/027674	-
Inactivated SARS-CoV-2 vaccine	Institute Medical Biology, Chinese	Phase I/II	NCT04470609	-
QazCovid-in	Research institute for Biological Safety Problems, Rep of Kazakhstan	Phase I/II	NCT04530357	-
Inactivated SARS-CoV-2 Vaccine	Beijing Minhai Biotechnology	Phase I	ChiCTR2000038804	-

- *Viral RNA platform*

The viral RNA platform is a new generation platform that can effectively activate immune responses similar to native viral infection. Viral RNA vaccines are made from synthetic viral mRNAs encoding the target antigenic agents in the cytosol of host cell. This platform allows low-cost, rapid, and ease manufacturing that is able to adapt to new pathogens. Nevertheless, mRNA vaccines are instability affecting their immunogenic profiles. Moreover, they require low temperature for storage and

transportation and provide high risk of RNA-induced interferon responses resulting to off-targets and unwanted side effects (170-173, 182).

There are several viral mRNA-based vaccine candidates, which are currently applying in clinical studies (Table 4). The mRNA-1273 vaccine, which is developed by Massachusetts-based biotechnology company (Moderna), is non-replicating viral mRNA encoding prefusion domain located in spike (S) protein of SARS-CoV-2 encapsulated in a lipid nanoparticle (LNP) vector for enhancing its immunogenicity. mRNA-1273 vaccine was designed for stabilizing pre-fusion form of the SARS-CoV-2 S protein. mRNA-1273 could induce immune responses in several animal such as BALB/cJ, C57BL/6J, and B6C3F1/J mice after receiving the two intramuscularly immunized doses. mRNA-1273 could elicit neutralizing antibodies and show neutralization activity against SARS-CoV-2 pseudovirus *in vitro*. mRNA-1273 was applied the phase I clinical trials in 45 healthy volunteers ranging from 18 to 55 years old with 2 doses of 28-day interval vaccine. The vaccine elicited strong immune responses, particularly CD4+ T cell responses with a minimum expression of T helper 2 (Th2) responses (183). mRNA-1273 vaccine entered a phase III trials July 27<sup>th</sup> 2020 with the enrollment of 30,000 participants in the U.S. The vaccine could prevent symptomatic and hospitalization for SARS-CoV-2 infection with no serious adverse effects among participants (178, 184).

BioNTech/ Pfizer launched two viral vaccines including BNT162b1, encoding SARS-CoV-2 RBD, and BNT162b2, which is translated into full-length spike protein of SARS-CoV-2, administered for two vaccinations with 3-week interval. BNT162b2 could induce strong immune responses in BALB/c mice and *Rhesus macaques* with high titers of neutralizing antibodies as well as T-mediated responses. BNT162b2 also

induced Th1-biased immunity, which is desired immune responses against coronaviruses, especially SARS-CoV and MERS-CoV. The vaccine could show the protective activities against USA-WA1/2020 strain of SARS-CoV-2 infection during viral challenge as judged by no viral RNA detection in their lungs and nasal swabs. In addition, the vaccinated animal did not show the clinical symptomatic induced from SARS-CoV-2 infection (185). The clinical data from phase I trials of BNT162b2 vaccine were collected from 2 groups of participants including younger (18–55 years old) and older adults (65–85 years old). The vaccine could induce minimum side effects in participants and elicit high neutralizing antibody titers as compared to SARS-CoV-2 convalescent sera (186). BNT162b2 vaccine also showed less systemic reactogenicity in older adults (187, 188). After completing a Phase I trials, BNT162b2 vaccine entered to phase II/III for evaluating safety and efficacy in 43,488 volunteers with chronic conditions and different genetic backgrounds. The vaccine also showed significant activation of SARS-CoV-2 specific CD8<sup>+</sup> T cell and CD4<sup>+</sup> as well as neutralizing antibodies against SARS-CoV-2 (189).

*Table 4 List of clinical viral RNA-based vaccine candidates for SARS-CoV-2*

<b>Vaccine</b>	<b>Developer</b>	<b>Status</b>	<b>Clinical registration</b>	<b>Reference</b>
mRNA-1273	Moderna/NIAID	Phase III	NCT04470427	(183, 184)
BNT162b1	BioNTech/Fosun Pharma/Pfizer	Phase III	NCT04368728	(186, 188,
BNT162b2				189)
CVnCoV	Curevac	Phase II	NCT04515147	-
ARCT-021	Arcturus/Duke-NUS	Phase I/II	NCT04480957	-
LNP-nCoVsaRNA	Imperial College London	Phase I	ISRCTN1707269	-
SARS-CoV-2 mRNA vaccine	People's Liberation Army (PLA) Academy of Military Sciences/	Phase I	ChiCTR2000034112	-

- *Viral DNA-based platform*

DNA-based vaccines work by injection of engineered plasmid containing specific viral antigen-coding DNA sequence that results to viral antigen expression and immunological responses onto the cells. Although DNA vaccination has theoretical advantages over viral-vectored and live-attenuated vaccines including specificity due to encoding antigenic epitopes known to activate immune cells, stability, and ease of manufacturing. This platform is still suffering from several limitations such as low immunogenicity, and high risk of genomic integration into human genome causing unpredictable abnormalities (170-173).

During COVID-19 pandemic, various viral DNA-based vaccine candidates were developed and tested in clinical trials (Table 5). INO-4800 is one of SARS-CoV-2 DNA-based vaccine candidates recruiting in the clinical trials. INO-4800, which was developed by Pennsylvania-based company, Inovio, are DNA sequence of SARS-CoV-2 S protein with a portable device named 'Celectra 2000'. Celectra 2000 is small electric pulse, which can facilitate the DNA uptake by nucleus through an electroporation method. The DNA vaccine could elicit neutralizing antibodies detected in lungs of immunized porcine and mice. The detected antibodies in lung could be important for SARS-CoV-2 protection (178, 190). Phase I clinical trials of INO-4800 were conducted in 36 volunteers with age ranged from 18–50 years old. The results showed that there were no serious adverse effects in participants. The vaccine could generate the protective antibodies against SARS-CoV-2/Australia/VIC01/2020

strain *in vitro* neutralization assay and showed strong Th1 and CD8+ T cell responses (191).

GX-19 is another DNA-based vaccine in clinical trials which are developed by Genexine consortium. GX-19 was initially tested the vaccine efficacy in mice and non-human primate models and it was found to induce a robust production of neutralizing antibodies against novel SARS-CoV-2 in animal models (178, 192).

*Table 5 List of clinical viral DNA-based vaccine candidates for SARS-CoV-2*

Vaccine	Developer	Status	Clinical trial registration	Reference
INO-4800	Inovio Pharmaceuticals/International Vaccine Institute	Phase II/III	NCT04447781 NCT04336410	(191)
AG0301-COVID19	Osaka University/ AnGes/Takara Bio	Phase I/II	NCT04463472 NCT04527081	-
nCov Vaccine	Cadila Healthcare Limited	Phase I/II	CTRI/2020/07/026352	-
GX-19	Genexine Consortium	Phase I/II	NCT04445389	-

- *Viral vector platform*

The viral-vectored platform is prepared from microbial DNA, which can be expressed in the recipients. These vaccines are able to induce stronger immune responses due to preservation of native antigenic agents and mimicking natural infection. Viral-vectored vaccines allow several limitations including more complicated manufacturing process, high risk of genomic integration into host genome, and induction of inflammatory responses. Additionally, the vectors might

negatively affect the vaccine efficacy and they are possibly damaged by pre-existing immunity (170-173).

CanSino Biologics and the Institute of Biology of China's Academy of Military Medical Sciences developed Adenovirus type-5-vectored coronavirus (Ad5-nCoV), which uses adenovirus serotype 5 vector (Ad5) for delivery of SARS-CoV-2 full-length S protein genome into host cells. Ad5-nCoV vaccine was found to be immunogenic in BALB/c mice within first immunization by induction strong humoral responses, especially SARS-CoV-2 S-specific IgA. Ad5-nCoV vaccine also protected mice-adapted SARS-CoV-2 (HRB26M) and ferrets from wild-type SARS-CoV-2 infection in animal challenge studies. The immunized animals shown no viral replication in their lungs and any clinical symptoms (193). Ad5-nCoV was evaluated in phase I clinical trials for dose escalation obtained from 108 participants between 18 and 60 years old with low, medium, and high doses of Ad5-nCoV vaccine (194). For phase II clinical trials, the Ad5-nCoV vaccine was applied to 508 volunteers with the ages of 18-83 years. Ad5-nCoV vaccine showed the benefits in participants termed of RBD-specific antibodies eliciting and neutralizing antibody against live SARS-CoV-2 *in vitro* as well as activation of specific T cell responses within 28 days post-immunization. Severe adverse effects were reported with less than 10% of participants per each vaccination group (195). The data in phase III efficacy trials of Ad5-nCoV vaccine is collecting from 40,000 volunteers in Saudi Arabia, Russia, and Pakistan.

ChAdOx1 nCoV-19 (AZD1222) is non-replicating viral vaccine developed by Oxford University and AstraZeneca using a chimpanzee adenovirus (ChAdOx1) platform. ChAdOx1 nCoV-19 contains full-length of wild-type SARS-CoV-2 S protein and plasminogen activator leader sequence. AZD1222 induced strong humoral

and cellular SARS-CoV-2-specific responses with Th1-biased responses in pre-clinical studies containing BALB/c and CD1 mice, pigs, rhesus macaques. The vaccine could reduce the viral load in lower respiratory tract from infection of SARS-CoV-2 strain nCoV-WA1-2020 (196). The phase I/II single-blinded, randomized, multicenter control study was evaluated in 1,090 healthy adult participants aged 18–55 years (197) and Phase III efficacy and safety trials was tested with more than 30,000 individuals from the U.S., India, Brazil, Russia, and South Africa (198). This vaccine is found to be immunogenic, which can induce high titer of neutralizing antibodies in the participants. However, the trials showed some serious adverse effects, particularly severe neurological symptoms. Later, it was concluded that serious adverse events were not related to the vaccine (199). Additionally, there are several viral-vectored vaccines that are developed and investigated in the clinical trials are reviewed in the Table 6.

*Table 6 List of clinical viral-vectored vaccine candidates for SARS-CoV-2*

<b>Vaccine</b>	<b>Developer</b>	<b>Status</b>	<b>Clinical trial registration</b>	<b>Reference</b>
AZD1222	University of Oxford/ AstraZeneca	Phase III	NCT04516746 NCT04540393 ISRCTN89951424 CTRI/2020/08/027170	(197, 198)
Ad5-nCoV	CanSino Biological Inc./ Beijing Institute of Biotechnology	Phase III	NCT04526990 NCT04540419	(194, 195)
Gam-COVID- Vac	Gamaleya Research Institute	Phase III	NCT04530396 NCT04564716	(200)
Ad26.COV2.S	Janssen Pharmaceutical Companies	Phase III	NCT04505722	(201)
hAd5-S- Fusion + N-	ImmunityBio, Inc. & NantKwest Inc	Phase I	NCT04591717	-

ETSD vaccine				
GRAd-COV2	ReiThera/LEUKOCARE/ Univercells	Phase I	NCT04528641	-
Ad5-nCoV	CanSino Biological Inc/ Institute of Biotechnology, Academy of Military Medical Sciences, PLA of China	Phase I	NCT04552366	-
VXA-CoV2-1	Vaxart	Phase I	NCT04563702	-
MVA-SARS-2- S	Ludwig-Maximilians University of Munich	Phase I	NCT04569383	-
V590	Merck Sharp & Dohme/ IAVI	Phase I	NCT04569786	-
TMV-083	Institute Pasteur/ Themis/University of Pittsburg CVR/Merck Sharp & Dohme	Phase I	NCT04497298	-
DelNS1-2019- nCoV- RBD- OPT1	Beijing Wantai Biological Pharmacy/Xiamen University	Phase I	ChiCTR2000037782	-

- *Protein-based subunit platform*

The protein-based vaccines carry viral antigenic agents produced by recombinant protein techniques. Protein subunit vaccines do not contain live component of the virion that are safe relative to whole virus and viral-vectored vaccines. Moreover, subunit vaccines readily stimulate the immune responses with the reduction of adverse reactions due to specific epitopes. Hence, these vaccines can be used in immunocompromised patients. The significant drawbacks of these vaccines are low immunogenic profile and requires either adjuvants or immunostimulatory molecules to improve the vaccine efficacy. In addition, antigenic epitopes need to be determined to increase vaccine specificity (170-173).

NVX-CoV2373 vaccine is recombinant protein-based subunit vaccine (Table 7) developed by Maryland-based Novavax company. NVX-CoV2373 is prepared



form baculovirus-Sf9-based full-length S protein of SARS-CoV-2 formulated with a saponin-based (Matrix-M1) adjuvant to improve its immunogenicity profiles by activation of cell-mediated immune responses. In addition, Matrix M-adjuvanted NVX-CoV2373 vaccine significantly increased the levels of SARS-CoV-2-specific neutralizing antibodies compared with antigen alone and induced strong T-cell mediated responses with Th1-biased immunity in immunized animals. The sera of immunized mice showed efficient neutralization by reducing the cytopathic effects of SARS-CoV-2 on Vero E6 cells *in vitro* and also protected the human ACE2-expressed mice and cynomolgus macaques from infection SARS-CoV-2 strain 2019-nCoV/USA-WA1/2020 as observed by protection of SARS-CoV-2 infection in upper and lower respiratory tract and pulmonary disease in immunized animals (202, 203). Saponin-based NVX-CoV2373 vaccine was launched in clinical trials phase I with 131 healthy adults. The results showed that the vaccine induced mild and short duration of adverse effects and enhanced Anti-S IgG and neutralizing antibodies eliciting with Th1-biased phenotype in the participants (204). NVX-CoV2373 was subsequently launched in phase III clinical trials with 9,000 subjects in the U.K., U.S., India, South Africa, and other countries.

*Table 7 List of clinical protein-based vaccine candidates for SARS-CoV-2*

<b>Vaccine</b>	<b>Developer</b>	<b>Status</b>	<b>Clinical trial registration</b>	<b>Reference</b>
NVX-CoV2373	Novavax	Phase III	2020-004123-16 NCT04533399	(204)
KBP-COVID-19	Kentucky Bioprocessing, Inc	Phase I/II	NCT04473690	-
SARS-CoV-2 vaccine	Sanofi Pasteur/GSK	Phase I/II	NCT04537208	-

RBD SARS-CoV-2 HBsAg VLP	SpyBiotech/Serum Institute of India	Phase I/II	ACTRN126200008179 43	-
SCB-2019	Clover Biopharmaceuticals Inc./GSK/ Dynavax	Phase I	NCT04405908	-
COVAX-19	Vaxine Pty Ltd/Medytox	Phase I	NCT04453852	-
SARS-CoV-2 Sclamp vaccine	University of Queensland/CSL/Seqirus	Phase I	ACTRN126200006749 32p ISRCTN51232965	-
MVC-COV1901	Medigen Vaccine Biologics Corporation/ NIAID/Dynavax	Phase I	NCT04487210	-
Soberana 01	Instituto Finlay de Vacunas, Cuba	Phase I	IFV/COR/04	-
EpiVacCorona	FBRI SRC VB VECTOR, Rospotrebnadzor, Koltsovo	Phase I	NCT04527575	-
Recombinant SARS- CoV-2 vaccine	West China Hospital, Sichuan University	Phase I	ChiCTR2000037518	-
IMP (CoVac-1)	University Hospital Tuebingen	Phase I	NCT04546841	-
UB-612	COVAXX	Phase I	NCT04545749	-
Recombinant Coronavirus-Like Particle COVID 19 Vaccine (VLP)	Medicago Inc	Phase I	NCT04450004	(205)

CHULALONGKORN UNIVERSITY

Several COVID-19 vaccine candidates have been tested in the clinical trials to assess their immunogenic profiles and vaccine efficacies that are reviewed in the Table 8.



CoronaVac	3 µg IM with 2 doses (0, 14)	N/A	N/A	N/A	N/A	N/A	N/A	N/A
BBiBP-CorV	4 µg IM with 2 doses (0, 21)	N/A	N/A	N/A	N/A	N/A	N/A	N/A
BBV152/Covaxin	3 µg IM with 2 doses (0, 28)	N/A	N/A	N/A	N/A	N/A	N/A	N/A

**\*\*N/A: not available**

### Selection of SARS-CoV-2 antigen

SARS-CoV-2 S protein is required for cellular entry by interaction with the host cells and viruses through ACE2 receptor. Additionally, S protein also induces pathogenicity and elicits the robust immune responses during the disease progression (206). The trimeric S protein contains S1 and S2 subunits. S1 subunit can be divided into two domains consisting of N-terminal domain (NTD) and C-terminal domain (CTD), which includes RBD domain. SARS-CoV-2 RBD is specifically binds to cellular ACE2 as an initial step during viral entry, triggering the conformational change of S protein for membrane fusion by elements in S2 subunit, particularly internal membrane fusion peptide (FP), two 7-peptide repeats (HR1/2), and transmembrane domain (TM) (207). According to previous studies, S protein-based vaccine could elicit potent immune responses, which showed SARS-CoV and MERS-CoV neutralization and protective activities in non-clinical and clinical studies (208-210). Similarly, S protein is regarded as a key target for development of possible vaccines with effective induction of neutralizing antibodies and protective immunity against SARS-CoV-2. The S protein, especially RBD domain could induce the neutralizing antibodies and T cell-mediated responses in animals (9, 11). Intriguingly, SARS-CoV-2 RBD was found to be strong neutralizing epitopes which are accounted for half of SARS-CoV-2 S-induced IgG antibody responses and can neutralize the

virus by inhibiting the interaction of RBD with ACE2 receptor as proved by a surrogate of neutralization assay. RBD also successfully elicited the potent neutralizing antibodies without adverse effects in vaccine-induced immunity, particularly antibody-independent enhancement (ADE), which caused by antigen-induced suboptimal antibody responses, facilitating the viral infectivity in rodents (211). Moreover, SARS-CoV-2 RBD-specific immune responses were detected in the sera of COVID-19 patients (212, 213). Hence, SARS-CoV-2 RBD-based vaccines are promising candidates for protection of COVID-19.

Aside from SARS-CoV-2 S protein, other structures, particularly M protein, E protein, N protein, and accessory proteins may also be served as vaccine antigens. Full-length SARS-CoV M protein has the potential in induction of neutralizing antibodies in infected patients and triggers a robust cytotoxic T-lymphocyte responses (214). E protein has found to be an inducer of inflammatory molecules and ultimately activates IL-1 $\beta$  production and inflammatory responses leading to cytokine storm (215). Therefore, the E protein-induced immunity is difficult to control in recipients. N protein showed strong antigenicity, which could induce high titers of SARS-CoV N-specific IgG responses in C57BL/6 mice immunized with DNA vaccine encoding SARS-CoV N protein (216). N protein-mediated cellular responses showed benefits in protection of avian contagious bronchitis virus infection, which decreased the clinical signs and viral load in lungs (217). However, immunization of N protein inefficiently elicited neutralizing antibodies and did not protect SARS-CoV infection in hamsters during animal challenge (218). Consequently, the efficacy of N protein immunization could not be guaranteed for SARS-CoV protection. Accessory proteins of CoV also elicit the host immune responses such as ORF8 activated the cytotoxic T

lymphocytes (CTLs)-mediated killing of virus-infected cells (219), and ORF9b targeted the mitochondrial antiviral signaling (MAVS) protein (220).

#### Selection of efficient immunoadjuvants

The recombinant protein-based subunit vaccines allow more secure and well-defined antigenic epitopes in comparison to other types of vaccines, especially live-attenuated vaccines, resulting to reduction of pathogenicity. Moreover, the protein-based vaccines are scalable and cost-effective (221-224). Unfortunately, the protein subunit vaccines inefficiently induce immunity with poor immunogenic profiles and activate only partial protective immune responses (225-229). To improve the immunogenicity of SARS-CoV-2 protein-based vaccines, the addition and selection of immunoadjuvants or delivery vehicles should be included in development of protein-based subunit vaccine. Immunoadjuvants are compounds, which are used for various purposes including enhancement of immunogenicity, reducing the amount of antigenic agent, improvement of vaccine efficacy in newborns, elderly and immunocompromised patients, and acting as the antigen delivery systems to specific target (230-233). Hence, the formulation of protein-based vaccines with the appropriate adjuvants has become high potential strategy to elicit the robust protective and long-lasting immune responses in recipients (230, 234). Several protein-based subunit vaccines for COVID-19 are adjuvanted with immunostimulatory molecules to enhance their immunogenicity profiles. NVX-CoV2373 developed by Novavax (USA) includes full-length of SARS-CoV-2 S protein along with saponin-based Matrix-M (202, 203, 235). Squalene-based AS03 immunoadjuvant is applied in numerous vaccines developed by Sanofi and Xiamen Innovax Biotech (235, 236).

Plant-produced SARS-CoV-2 virus-like particles (VLPs) vaccine developed from iBio (USA) is adjuvanted with glucopyranosyl lipid adjuvant and MPL (235, 237, 238). CoVaccine HT, an oil-in-water emulsion adjuvant (235, 239), was developed by Soligenix, Inc. (USA) for their vaccine formulation (240, 241). To date, very few immunoadjuvants have been licensed for clinical uses in human such as aluminum salts (alum), oil in water emulsions, particularly MF59 and AS03, and monophosphoryl lipid A (MPL).

- *Aluminum-based adjuvant (Alum)*

Alum were firstly used as a vaccine adjuvant over 70 years in several human vaccines such as HAV, HPV, HBV, Diphtheria and Tetanus (DT), Haemophilus influenza type B (HIB), and pneumococcal-associated vaccines (242). Alum enhances the vaccine efficacy by trapping of the soluble antigen resulting to expansion the circulation and duration of immune cell-antigen interaction. Alum salt allows complement and macrophage activations, which increases antigen uptake by the antigen presenting cells (APCs) to the immune cells. It also promotes interleukin-4 (IL-4) cytokine secretion involved in stimulation of Th2 immune responses and induce the high titer of immunoglobulin G1, E, and eosinophils resulting to anti-bacterial and anti-parasitic activities (243-246). Additionally, alum is inexpensive adjuvant with safety profile approved by the United States Food and Drug Administration for using in several available licensed human vaccines for Newcastle disease and foot-and-mouth disease (247-249). However, aluminum compound provides inefficient activation of Th1-type of cellular and humoral immunities, which are important to combat the viral infection and intracellular pathogens. Therefore, the

co-administration of other adjuvants stimulating Th-1 cell responses is required (234, 242).

- *Oil in water emulsion*

MF59 is an oil-in-water emulsion consisting of squalene in acid buffer and other stabilizer reagents, particularly Tween 80 and Span 85. Squalene is a naturally synthesized product found in plants and animals. Squalene is presented to be an intermediate in the pathway of human steroid hormones, cholesterol in skin, adipose tissue, muscles, and lymph nodes. Tween 80 and Span 85 surfactants are produced from plants. Hence, all components in MF59 are biodegradable, and safe, which can be used in the wide range of biopharmaceutical products (250, 251). MF59 and AS03 have been licensed in Europe for adjuvating with pandemic flu vaccines and widely used in H1N1 flu vaccine in 2009 to increase flu immunogenicity in the elderly (242, 252, 253). Oil-in-water adjuvants work through recruitment and activation of APCs enhancing the immune cells at the administration site that leads to induction of cytokine and chemokine secretions by macrophages and granulocytes and up-regulation of innate immunity genes, which promote CD11b<sup>+</sup> and MHCII<sup>+</sup> cell recruitment in the muscle (254-256). Additionally, MF59 and AS03 enhance dendritic cell differentiation resulting to more efficient antigen trafficking to lymph nodes (257, 258). This class of adjuvant elicits both Th1 and Th2 immunities, but prefers induction of Th2-biased immune response. The addition of TLR4 or TLR9 agonists is required to improve the adjuvant efficacy by inducing of Th1-type immunity to increase IgG2a antibody titer, which is effective isotype for viral clearance (251). Currently, MF59 has been approved to be used in a board spectrum of alternative



vaccines, especially influenza virus, herpes simplex virus (HSV-2), human immunodeficiency virus (HIV), hepatitis B virus (HBV), and hepatitis C virus (HCV) in US. and other 30 countries (251, 257, 259).

- *Monophosphoryl lipid A (MPL)*

MPL is made from lipopolysaccharide of Gram-negative *Salmonella Minnesota* strain R595. MPL enhances immunity by activating Toll-like receptor-4 (TLR4), which plays a role in the induction of innate and adaptive immunities through interactions with B-lymphocyte cells. MPL allows the preferential recruitment of TIR-domain-containing adapter-inducing interferon- $\beta$  (TRIF) responding to activation of TLR4, which leads to decreasing the induction of inflammatory cytokines (260-263). According to the studies, MPL adjuvant could induce a strong Th1 cytokines and trigger B cell proliferation in mice that are involved in production of IgG1 isotype antibody that is able to kill pathogens and pathogen-infected cells (264-266). In particular, AS04 is combination of MPL and alum, which induces the nuclear factor NF- $\kappa$ B pathway for inflammatory responses and cytokine production resulting to optimal activation of APCs. Additionally, alum in AS04 formulation could prolong cytokine eliciting at the injection site (266). Alum-MPL adjuvant is licensed in Europe (FENDrix) for use in the Hepatitis B virus vaccine and Australia (Cervarix) for use in the human papillomavirus vaccine and currently approved by USA's Food and Drug Administration. MPL has become the first generation of TLR-stimulatory adjuvant, which is widely used in human vaccines, especially cancer, HBV, malaria, and HPV vaccines (225, 260, 261).

- *Toll-like receptor (TLR) agonists*

Toll-like receptors (TLRs) is pattern recognition receptors (PRRs) in innate immune system, which play role in recognition of conserved microbial patterns called pathogen associated molecular patterns (PAMPs). TLRs are transmembrane signaling proteins located either on cellular surface (TLR1, 2, 3, 4, 5, 6, and 10) or endosomal and lysosomal membranes (TLR7, 8, and 9). TLRs are also predominantly expressed on phagocytes, particularly dendritic cells (DCs), which contains conventional DC (cDC) and plasmacytoid DC (pDC). cDC expresses TLR3, 4, 8 which involves in production cytokines such as IL-12, whilst pDC expresses TLR7 and 9 resulting to IFN- $\gamma$  production (Figure 6). Consequently, TLR influences the different cytokines production, which can be induced by various TLR agonists (Figure 6). Currently, several TLR agonists are adapted as high potential immunoadjuvants for improving the vaccine efficacy in clinical evaluations.

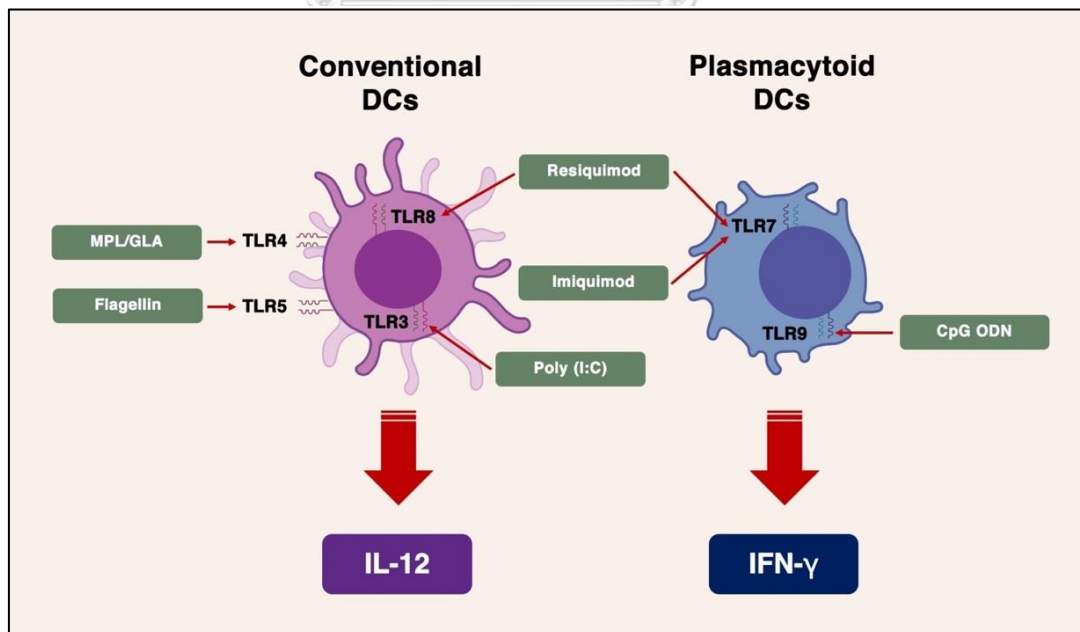


*Figure 6 Schematic representation of TLR agonists activated various TLRs on conventional and plasmacytoid dendritic cells (DCs)*

- TLR9 agonists

TLR9 is intracellularly expressed in endosomal membrane and pDC, which detects the bacterial and viral infection by interacting with repeat sequences of cytosine phosphoguanosine (CpG) motifs in pathogenic genome. TLR9 leads to pro-inflammatory cytokine responses including IFN- $\gamma$  and activation of Th1 immunity through myeloid differentiation primary response 88 (MyD88), which are required for bacterial and viral vaccine development (267-269). There are several TLR9 agonists are commercially available, especially 1018 ISS adjuvant, which is clinically used in hepatitis B vaccine and able to induce rapid production of protective antibodies in healthy adults (242, 270). Additional TLR9 agonist, IC31 is currently used in clinical vaccine against tuberculosis (TB) due to effective protection against the pathogenic bacteria in animal models (271-274).

- TLR7/8 agonists

TLR7 and 8 play a significant role in regulation of antiviral immunity, which detects PAMPs terms of short hairpin RNA (shRNA) sequences in viral genomes and synthetic small molecules such as imidazoquinolines imiquimod (TLR7 agonist) and resiquimod (TLR7/8 agonist). TLR 7 and 8 activation is responsible for the production of IFN- $\gamma$  and IL-12, respectively that are considered as an effective antiviral mechanisms terms of neutralizing antibody eliciting with effector mechanisms for viral clearance. Hence TLR7/8 agonists are considerable to be used as high potential vaccine adjuvants (275, 276). Moreover, TLR7 was licensed for

topical uses in treating malignant and non-malignant skin cell (242), and papillomavirus vaccine (277).

- TLR3 agonists

TLR3 agonists are regarded as attractive adjuvant candidates for vaccine development against tumors and pathogens. TLR3 agonists including dsRNA, ssRNA and DNA in viral genomes activate the signaling through TLR3 and cytosolic sensors including melanocyte differentiation-associated 5 (MDA-5) and retinoic acid-inducible protein I (RIG-I). TLR3 induces the production of IL-12 and type I IFNs eliciting anti-viral responses and increases the expression of MHC class II and cross-presentation of antigen. MDA-5 also induces type I IFNs production leading to activation of T and B lymphocyte responses (278-281). Polyinosinic-polycytidylic acid (poly(I:C)) and its derivatives, which are TLR3 agonists, are currently undergoing in the various clinical trials for influenza, HBV, HIV, and coronavirus vaccines (282-286).

### **Plants as alternative protein production factories**

#### **Plant-based expression system**

Plants have been practiced and optimized for using as exceptional bioreactors in biopharmaceutical production with high yield and low production costs. Plants are used for producing several valuable biopharmaceutical products such as therapeutic immunoglobulins, human lysosomal enzymes, cytokines, hormones, growth factor molecules, and vaccines (19, 20, 287, 288). Plant-based expression system offers many strengths over other competing platforms (Table 9). Plants have been domesticated to be effective platform to produce useful compounds by using normal

greenhouse, inexpensive sources, cheap growth conditions and well-understood manufacturing practices that can reduce capital investment costs (17, 18, 287-289). The production costs in plant biopharming process are commonly 0.1% of mammalian cell expression systems and 2-10% of prokaryotic expression systems (287). Plants are able to perform post-translational modifications maintaining protein structure and immunogenicity as produced in mammalian-derived counterparts (14, 288-291). Interestingly, recombinant protein expression can be localized to multiple subcellular compartments in plant cells, particularly chloroplast and endoplasmic reticulum (ER), for facilitating and accumulating the recombinant proteins (14, 292). In addition, plants have several attractive characteristics as therapeutic protein expression platform including scalability, rapid production timescales, and low risk of animal pathogen and toxin contaminations (289, 293). Plant bioreactor is a promising expression system that can be considered as an alternative platform for economic production of therapeutic proteins.

*Table 9 Strengths and limitations of heterologous protein-based expression systems*

<b>Expression system</b>	<b>Strength</b>	<b>Limitation</b>
Bacteria	<ul style="list-style-type: none"> <li>- Rapid expression rate</li> <li>- High expression level</li> <li>- Ease of scaling up and manipulate</li> <li>- Capacity for continuous fermentation</li> <li>- Cost-effective process</li> </ul>	<ul style="list-style-type: none"> <li>- Lack of post-translational modification</li> <li>- Endotoxin contamination</li> <li>- Improper folding</li> <li>- Insoluble protein produced in inclusion bodies</li> <li>- Degradation of proteins</li> </ul>
Yeast	<ul style="list-style-type: none"> <li>- High expression level</li> <li>- Cost-effective process</li> <li>- Rapid growth in chemical media</li> <li>- High productivity</li> <li>- No endotoxin contamination</li> <li>- Durability</li> <li>- Able to post-translational modifications</li> </ul>	<ul style="list-style-type: none"> <li>- Hypermannose glycosylation</li> <li>- Inefficient in secreting the recombinant proteins in culture media</li> <li>- Limited glycosylation capacity</li> </ul>

Insect cells	<ul style="list-style-type: none"> <li>- High expression level</li> <li>- Appropriate post-translational modifications</li> <li>- Suitable for glycoprotein production</li> <li>- No endotoxin contamination</li> <li>- Efficient cleavage of signaling peptides</li> <li>- Proper protein folding</li> </ul>	<ul style="list-style-type: none"> <li>- More demanding expensive media and culture conditions</li> <li>- High production costs</li> <li>- Time consuming</li> <li>- Not suitable for continuous expression</li> </ul>
Mammalian cells	<ul style="list-style-type: none"> <li>- Appropriate post-translational modifications</li> <li>- Proper protein folding</li> <li>- Full protein assembly</li> <li>- Existing regulatory approval</li> <li>- Authentic functions of recombinant proteins</li> </ul>	<ul style="list-style-type: none"> <li>- High production costs</li> <li>- Expensive media and complicated technology requirements</li> <li>- Time consuming</li> <li>- High risk of pathogen and toxin contamination</li> </ul>
Plants	<ul style="list-style-type: none"> <li>- High level of accumulation of recombinant proteins</li> <li>- Easy scaling up with low investment costs</li> <li>- Proper folding and assembly of complex proteins</li> <li>- Low risk of human pathogen contamination</li> <li>- Cost-effective process</li> <li>- Able to perform post-translational modifications</li> <li>- Protein localization in different organelles</li> </ul>	<ul style="list-style-type: none"> <li>- Limited glycosylation capacity</li> <li>- Regulatory approval</li> <li>- GMP conduct in manufacturing process</li> </ul>

### Transient expression technologies

Plants have several attractive characteristics as therapeutic protein expression platform including, cost-effective production, safety due to low risk of animal pathogen and toxin contaminations, and plants are able to perform efficient post-translational modifications maintaining protein structure and immunogenicity as produced in mammalian-derived counterparts (288, 294). The recombinant proteins can be expressed in plants by several strategies including stable expression, transient expression, and plant cell-based expression (Table 10). Interestingly, plant expression system can progress from the competing available expression systems in terms of

allowing more rapid production and high yield of recombinant protein *via.*, transient expression, which is suitable for the huge production of biopharmaceutical proteins to respond the demands of therapeutic uses during the emerging disease crisis (295). Transient expression technologies for therapeutic protein production have been developed for two decades ago. Transient expression technologies typically require *Agrobacterium* as gene carrier and viral-based expression machinery. Viral-based vectors for *Agrobacterium*-mediated gene transformation contain two major components including T-DNA and vector backbone. T-DNA, delimited by border sequence consisting of left (LB) and right (RB) border, incorporates multiple cloning sites, genes of interest, reporter genes, and selectable marker genes for plant transformation (15, 296-299). Viral-vectored backbone involves the replication and mobilization functions and antibiotic resistance for selection of bacteria-containing expression vector. The transient expression is widely used for production of therapeutic proteins in several plant species such as *Lactuca sativa*, *Arabidopsis thaliana*, *Nicotiana tabacum*, and *Nicotiana benthamiana* (15, 300). *Agrobacterium*-mediated transient expression provides various advantages termed of ease, speed, low cost, and high yield of recombinant proteins due to nonhomologous chromosomal integration into host genome and extra-chromosomal transgene, which is dependently replicated and expressed in plant cells resulting in unrestricted numbers of recombinant proteins (301). Transient expression strategies have been successfully used for production of effective vaccines and therapeutic proteins in pre-clinical and clinical studies. The VP1 protein of foot-and-mouth disease virus (FMDV) was the first viral antigen produced in plants using Tobacco Mosaic virus (TMV)-based transient expression vector providing the expression level of approximately 0.5-1  $\mu\text{g}$

per g leaf weight (302). The transient expression platform also used to produce the hepatitis B core antigen (HBcAg) (303) and Norwalk virus (NV)-derived virus-like particles (VLPs) (304) using the MagnICON-based expression system in *N. benthamiana* plants with the yields of 2.38 and 0.86 mg/g fresh weight, respectively. *N. benthamiana* with geminiviral-based transient expression vector expressed Ebola GP-based immune complex with maximum yield of 50 µg antigen per g leaf mass within 4 days after agroinfiltration (12). Plant-produced antigens are immunogenic as confirmed by their immunogenicity profiles in efficient induction of both humoral and cell-mediated immune responses and viral protection of *in vivo* studies. Plant-based transient expression is also used for production monoclonal antibodies such as chimeric D5 antibody against Enterovirus 71 (EV71) (305), anti-human PD1 antibody (306), and ZMapp antibody cocktail against Ebola virus, which was approved for emergency use by FDA (307).

Table 10 Overview of expression strategies for production of plant-derived biopharmaceuticals

Expression technique	Advantages	Disadvantages	Example
Stable expression	<ul style="list-style-type: none"> <li>- Scalability</li> <li>- High protein stability</li> <li>- Able to apply in many species</li> <li>- Unique post-translational modification</li> <li>- Able to provide seed bank generation</li> </ul>	<ul style="list-style-type: none"> <li>- Risk of gene silencing</li> <li>- Transgene contamination</li> <li>- Random of gene integration</li> <li>- Time-consuming</li> </ul>	<ul style="list-style-type: none"> <li>- Anti-HIV 2G12 IgG in transgenic tobacco and maize (308)</li> <li>- Chimeric IgA (CaroRx™) in transgenic tobacco (309)</li> <li>- Avicidin in transgenic maize and corn (20)</li> </ul>



Transient expression	<ul style="list-style-type: none"> <li>- Easy manipulation</li> <li>- Rapid expression</li> <li>- High yield</li> <li>- Time-saving upstream process</li> <li>- Simple technology in gene transformation</li> </ul>	<ul style="list-style-type: none"> <li>- Unstable yield of recombinant proteins</li> <li>- Limited scalability</li> <li>- High risk of gene transfer to the environment</li> <li>- Various effects on plant-produced biomass</li> <li>- Unable to generate the seed bank</li> </ul>	<ul style="list-style-type: none"> <li>- Anti-Ebola ZMapp antibody cocktail in tobacco (127)</li> <li>- Influenza virus (H5N1)-based VLP vaccine in tobacco (310)</li> <li>- Idiotype IgG-based cancer vaccine in tobacco (311)</li> </ul>
Suspension cells	<ul style="list-style-type: none"> <li>- Sterility and lack of human pathogen contamination</li> <li>- Well-defined downstream process</li> <li>- Scalability</li> <li>- Improving quality of recombinant protein</li> </ul>	<ul style="list-style-type: none"> <li>- low-yield</li> <li>- Instability of recombinant proteins</li> <li>- Complexity in large-scale production</li> <li>- High cost of cultivation</li> </ul>	<ul style="list-style-type: none"> <li>- Glucocerebrosidase enzyme (ELELYSO™) in carrot cells (312)</li> <li>- Human <math>\beta</math>-1,4-galactosyltransferase in BY-2 tobacco cell lines (313)</li> <li>- Alpha-galactosidase-A (Fabrazyme) in tobacco cell lines (314)</li> </ul>

### Protein processing and localization in plant cells

Plants offer several targets for protein expression in several subcellular compartments, where the recombinant protein can be accumulated, particularly apoplast, cytosol, chloroplast, endoplasmic reticulum (ER), or vacuole. Selection of subcellular localization affects the expression level and stability of heterologous proteins. Hence, it is an important point to be considered for recombinant protein production (315, 316). Most therapeutic proteins require post-translational modifications for their maturation and functionality. Glycosylation is a common process in posttranslational modification of therapeutic proteins such as monoclonal

antibodies and related compounds including bispecific antibodies, antibody-drug conjugates and Fc-fusion proteins (317). Protein glycosylation through endoplasmic reticulum (ER) pathway is a major traffic of membrane and secretory proteins processing in eukaryotic cells. After protein translation in ribosomes, the signaling peptide sequences localize the targeting proteins to the ER for protein glycosylation. The signaling peptides include the short chains of hydrophobic amino acids and they are cleaved from the polypeptide chain during transferring into the ER lumen. Protein glycosylation, particularly, asparagine (N)-linked glycosylation (ALG) involves many biological processes of proteins in secretory pathway consisting of protein solubility due to hydrophilic nature of carbohydrate chains, protein folding, protein stability, and protein-protein interaction (318, 319). Additionally, the N-glycans on polypeptide chains monitor the folding status of the glycoproteins in ER chaperone cycle (320). ER contains high concentration of quality control components, especially chaperones, co-chaperones, protein disulfide isomerases, glycosylating enzymes, and the ER-associated degradation (ERAD) machinery allowing the correct folding and assembly of glycoproteins (321). The complete glycosylated proteins are exported from ER to Golgi apparatus for protein maturation followed by the secretory vesicles for delivery to their final destinations. ER resident proteins require specific mechanism for protein retention in the compartment. The consensus tetrapeptides His/Lys-Asp-Glu-Leu (H/KDEL) presented at the C-terminus of soluble proteins have been identified as ER retention signals in mammals and plants leading to retardation of transport downstream in secretory pathway (322, 323). The tetrapeptides involve in quality control of the secretory proteins by interacting with chaperone-misfolded protein complexes and facilitating the escape of misfolded proteins from ER to lytic vacuole

for protein degradation (324). In addition, ER is a favorable subcellular compartment for protein storage enhancing protein accumulation levels and increasing the yield of recombinant proteins, especially scFVs produced in tobacco plants and rice callus (325-327). The production levels of scFV localized in ER found to be 14-fold higher than apoplast targeting (328).

#### Plant-produced biopharmaceuticals in several clinical applications

For three decades ago, many plant-based recombinant proteins have been developed and manufactured as practicable commercial proteins for several applications such as diagnostic, prevention, and therapeutic. Plants are high potential natural bioreactors and effective production system for valuable biopharmaceutical and medicinal molecules in term of economy, biosafety, purity, flexibility, rapid scalability, and consistency over available expression platforms (12, 13, 23, 287, 288, 295, 305, 315, 329, 330). Plants successfully express various therapeutic proteins, particularly antibodies such as IgG, IgA, IgM, IgA, Fab fragments, scFVs and even bispecific antibodies with complete biological activities (295, 305, 306, 330-339). Plants are also used for producing vaccine candidates for both veterinary and human applications. Plant expressing recombinant vaccines have been reported to be highly immunogenic, which elicit potent immune responses and protective activities against infectious diseases and cancers (12, 288, 331, 339-343). Hence, the concept of plant-produced biopharmaceuticals and vaccines has been developed and well explored by number of research centers, biotech companies and universities worldwide for commercialization and usage in the clinical applications. Currently, there are many

plant-produced pharmaceuticals (Table 11) and vaccines (Table 12), which are available either in clinical trials or approval stages.

*Table 11 Examples of plant-produced biopharmaceuticals, which are available in clinical studies or approved for therapeutic use*

<b>Product</b>	<b>Target</b>	<b>Host</b>	<b>Status</b>	<b>Reference</b>
Chimeric mAb (CaroRX)	Dental application	Tobacco	Phase II	(309)
Idiotypic IgG Based vaccine	Cancer immunotherapy	Tobacco	Phase I	(311)
Anti-HIV IgG	HIV treatment	Tobacco	Phase I	(308)
Anti-Ebola IgG cocktail (ZMApp)	Infectious disease treatment	Tobacco	Phase II/III	(127)
IgG (ICAM1)	Infectious disease treatment	Tobacco	Phase I	-
Radiolabeled anti-Ep-CAM IgG	Cancer immunotherapy	Maize	Phase II	(344)
Recombinant human insulin	Treatment of diabetes	Safflower	Phase III	(345, 346)
Lacteron (alpha-interferon)	Treatment of chronic hepatitis C	Duckweed	Phase II	(347)
Glucocerebrosidase enzyme (ELELYSO)	Treatment of Gaucher's disease	Carrot	FDA approval	(312)
Alpha-galactosidase-A (Fabrazyme)	Treatment of Fabry disease	Tobacco	Phase II	(314)
Alpha-galactosidase-A (moss-aGel)	Treatment of Fabry disease	Moss culture	Phase I	(348)
Human deoxyribonuclease I (Alidornase alfa)	Treatment of cystic fibrosis	Tobacco	Phase II	-
Recombinant human Lactoferrin (VEN100)	Treatment of gastrointestinal disorders	Rice	Phase II	(345)
MAPP66	Infectious disease treatment	Tobacco	Phase I	(345)

*Table 12 Examples of plant-produced vaccines, which are available in clinical studies or approved for therapeutic use*

<b>Product</b>	<b>Target</b>	<b>Host</b>	<b>Status</b>	<b>Reference</b>
----------------	---------------	-------------	---------------	------------------

LTB	Enterotoxigenic <i>E. coli</i>	Potato	Phase I	(349)
LTB	Enterotoxigenic <i>E. coli</i>	Maize	Phase I	(350)
Capsid protein	Norovirus	Potato	Phase I	(351)
Capsid protein	Norwalk virus	Potato	Phase I	-
Surface protein	Hepatitis B virus	Lettuce	Phase I	(352)
Surface protein	Hepatitis B virus	Potato	Phase I	(353)
Glycoprotein and nucleoprotein fusion	Rabies virus	Spinach	Phase I	(354)
HA	Influenza virus (H5N1)	Tobacco	Phase I	(355)
HA	Influenza virus (H1N1)	Tobacco	Phase I	(356)
CTB	Cholera	Rice	Phase I	(357, 358)
HA (H5: VLP) pandemic flu	Influenza virus (H7N9)	Tobacco	Phase I	(359, 360)
HA (H5: VLP) pandemic flu	Influenza virus (H5N1)	Tobacco	Phase II	(310)
HA (VLP) seasonal flu	Influenza virus	Tobacco	Phase III	(361)

### **Fc-based therapeutic candidates**

Biological therapeutic products have been successfully produced in various available expression systems and they are used in clinical applications. However, many biological active proteins have short serum half-life due to rapid renal clearance rate from circulation affecting exposure limitation of therapeutic proteins in the target tissues and their pharmacodynamic properties (362, 363). The protein engineering by Fc fusion is an effective strategy to overcome these problems. Fc-fusion proteins consists of a constant region of immunoglobulin (Fc fragment) directly linked to protein of interests such as receptors, ligands, enzymes, soluble cytokines, or proteins. Fc-fusion protein contributes various additional benefits in biological and pharmacological properties. Fc domain increases the serum half-life and prolongs therapeutic protein activities due to pH-dependent binding to the neonatal Fc receptor (FcRn) leading to preventing protein degradation in endosomes and it also reduces renal clearance rate due to larger size molecules (13, 23-25, 362, 364-366). Fc region improves the biophysical properties terms of solubility and stability of its partner

protein *in vitro* and *in vivo* (24, 362, 366). Moreover, Fc portion also improves biological activities by interaction with Fc-receptors (FcRs) presented on immune cells affecting several effector functions including antigen-dependent cellular phagocytosis (ADCP or opsonization), antigen-dependent cellular cytotoxicity (ADCC), and complement-mediated cytotoxicity (CDC), which are important for using in oncological treatments and vaccines (24, 362, 366). As an additional benefit, Fc portion increases higher protein expression and secretion and simplifies downstream manufacturing processes by allowing cost-effective purification by protein A/G affinity chromatography (13, 21, 23, 24, 362, 367). Currently, Fc-fusion proteins has been used as therapeutics in clinical treatment of various diseases, particularly infectious diseases, cancers, immune diseases. There are several approval and commercial Fc-fusion proteins, which are indicated in Table 13.

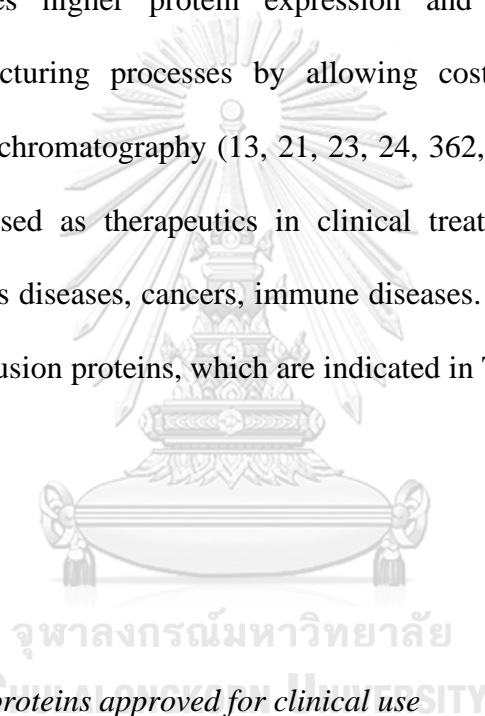


Table 13 Fc-fusion proteins approved for clinical use

Product	Protein partner	Fc portion	Status	Developer
Nulojix (belatacept)	CTLA-4	Fc of human IgG1	FDA approved (2011)	Bristol-Meyers Squibb
Eylea (afibercept)	VEGF1/VEGF2	Fc of human IgG1	FDA approved (2011)	Regeneron pharmaceuticals
Arcalyst (rilonacept)	IL-1R	Fc of human IgG1	FDA approved (2008)	Regeneron pharmaceuticals
NPlate (romiplostim)	Thrombopoietin	Fc of human IgG1	FDA approved (2008)	Amgen/Pfizer
Orencia (abatacept)	Mutated CTLA-4	Fc of human IgG1	FDA approved (2005)	Bristol-Meyers Squibb

Amevive (alefacept)	LFA-3	Fc of human IgG1	FDA approved (2003)	Astellas Pharma
Enbrel (etanercept)	TNFR	Fc of human IgG1	FDA approved (1998)	Amgen/Pfizer



**CHAPTER 2**  
จุฬาลงกรณ์มหาวิทยาลัย  
**MATERIALS AND METHODS**  
CHULALONGKORN UNIVERSITY

## Materials and Equipment

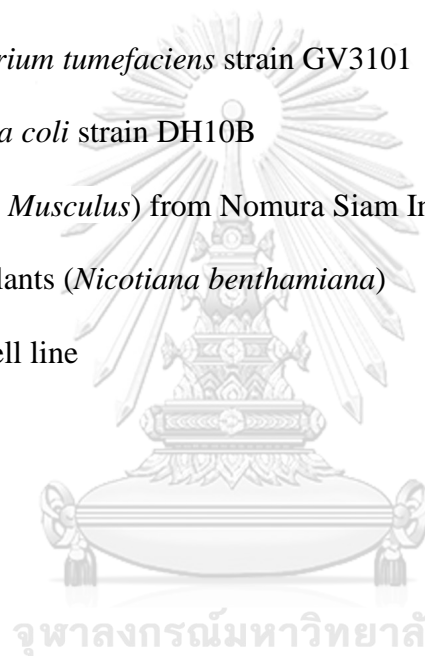
### Genetic materials

- A geminiviral-based plant expression vector (pBYR2eK2Md; pBYR2e)  
(Chen et al., 2011; Dianos and Mason, 2018)

- The synthesize gene of receptor-binding domain (RBD) of SARS-CoV-2 (Genbank accession number: YP\_009724390.1; F318-C617) from Genewiz, Suzhou, China
- The synthesize gene of human angiotensin-converting enzyme 2 (ACE2) (Genbank accession number: 4CDH\_A) from Genewiz, Suzhou, China

### Biological materials

- *Agrobacterium tumefaciens* strain GV3101
- *Escherichia coli* strain DH10B
- Mice (*Mus Musculus*) from Nomura Siam International Co., Ltd. (Thailand)
- Tobacco plants (*Nicotiana benthamiana*)
- Vero E6 cell line



### Equipment

- Biosafety Cabinet (BSC) (ESCO Lifesciences, Thailand)
- ELISpot reader (ImmunoSpot® Analyzer, USA)
- GENESYS™ UV-Vis Spectrophotometer (Thermo Fisher Scientific, USA)
- Hettich® Universal 320/320R centrifuge (Andreas Hettich GmbH & Co. KG, Germany)
- High-content imaging system (PerkinElmer, UK)
- Micropipette 2-1000 µg (Pipetman®, USA)



- Microplate incubator (Hercuvan Lab systems, UK)
- MicroPulser Electroporator (Bio-Rad<sup>®</sup>, USA)
- Mini Centrifuge (Bio-Rad<sup>®</sup>, USA)
- Mini-PROTEAN<sup>®</sup> Tetra handcast systems (Bio-Rad<sup>®</sup>, USA)
- Mini Trans-Blot<sup>®</sup> cell (Bio-Rad<sup>®</sup>, USA)
- MJ Mini Thermo Cycler Machine (Bio-Rad<sup>®</sup>, USA)
- Multichannel pipette (Clever scientific, UK)
- Mupid-EXu Electrophoresis (Mupid Co., Ltd, Japan)
- Nikon Eclipse TS100-T1-SM Microscope (Nikon, Japan)
- NUAIRE<sup>™</sup> DHD Autoflow CO<sub>2</sub> Air-Jacketed Incubator (NUAIRE, UK)
- OTTO<sup>®</sup> Blender (OTTO, Thailand)
- SpectraMax<sup>®</sup> M5 Microplate Reader (Molecular Devices LLC, USA)
- Sunrise<sup>™</sup> microplate reader (Tecan, Switzerland)
- TOMY Autoclave sx series (Amuza Inc., Japan)
- Waterbath WNB 7 (Mettler GmbH + Co. KG, Germany)
- WIS-20 Precise Shaking Incubator (WiseCube<sup>®</sup>, Korea)

### **Materials**

- 0.22 µm Syringe filter (MilliporeSigma, USA)
- 0.22 µm Syringe filter (Pall Corporation, USA)
- 0.45 µm Nitrocellulose Membrane (Bio-Rad<sup>®</sup>, USA)
- 96-well microtiter plates (U-shape bottom) (Corning, USA)

- Centrifuge tube 0.2-50 mL (Axygen<sup>®</sup>, USA)
- Cuvette
- DNA-spin<sup>™</sup> Plasmid DNA Purification Kit (iNtRON Biotechnology, Inc., Korea)
- High binding microplate-96 well (Greiner bio-one, Austria)
- Hycon Petri dishes
- IFN- $\gamma$  ELISpot assay kit (Mabtech, Stockholm, Sweden)
- MEGA quick-spin<sup>™</sup> Plus Total Fragment DNA Purification Kit (iNtRON Biotechnology, Inc., Korea)
- Membrane filter 0.45  $\mu$ m (MilliporeSigma, USA)
- NIPRO<sup>™</sup> Disposable Syringe 1, 10, 20, and 50 mL and needle (Nipro, Thailand)
- Nitrocellulose Membrane plate (96 wells) (Merck, USA)
- PCR tubes/strips (Axygen<sup>®</sup>, USA)
- Pipet Tip sizes: 10, 200, 1000  $\mu$ L and 5 mL (Axygen<sup>®</sup>, USA)
- Protein-A beads (Expedeon, UK)
- Purification column
- T-75 tissue culture flasks, canted neck (Corning, USA)

### **Proteins and antibodies**

- Alexa Fluor 488 conjugated goat anti-rabbit IgG (H+L) highly cross-adsorbed antibody (ThermoFisher Scientific, USA)
- Anti-human IgG-FITC antibody (Santa Cruz Biotechnology, USA)
- Anti-human Kappa chain-HRP fusion antibody (SouthernBiotech, USA)

- Anti-mouse IFN- $\gamma$  (AN18) monoclonal antibody (mAb) (Mabtech, Sweden)
- Anti-mouse IFN- $\gamma$ -biotinylated mAb (R4-6A2 biotin; Mabtech, Sweden)
- Anti-rabbit SARS-CoV nucleoprotein (NP) monoclonal antibody (SinoBiological, USA)
- CHO-produced recombinant ACE2 protein (InvivoGen, USA)
- Goat anti-mouse IgG-HRP conjugated antibody (Jackson ImmunoResearch, USA)
- Goat anti-mouse IgG1-HRP conjugated antibody (Abcam, UK)
- Goat anti-mouse IgG2a-HRP conjugated antibody (Abcam, UK)
- HEK-produced recombinant ACE2 protein (Abcam, UK)
- HRP-conjugated goat anti-rabbit polyclonal antibody (Aligent Dako, USA)
- Plant-produced anti-SARS-CoV-2 (H4) monoclonal antibody (Shanmugaraj et al., 2020)
- Plant-produced S1 protein of porcine epidemic diarrhea virus (PEDV) (Siriwattananon et al., 2021)
- SARS-CoV/SARS-CoV-2 nucleocapsid (N) monoclonal antibody (SinoBiological, China)
- SARS-CoV-2 peptide pools (BioNet-Asia, Thailand, and Mimotopes, Australia)
- SARS-CoV-2 RBD-His tag from Sf9 cells (Genscript, USA)

### **Immunoadjuvants**

- AddaVax<sup>TM</sup> (MF59) (InvivoGen, USA)
- Alhydrogel<sup>®</sup> 2% (alum) (InvivoGen, USA)

- High molecular weight polyinosinic-polycytidylic acid (poly (I:C)) (InvivoGen, USA)
- Monophosphoryl lipid A from *Salmonella Minnesota* R595 (mPLA-SM) (InvivoGen, USA)

### Chemical reagents

- 1x Dulbecco's Phosphate Buffered Saline (1x D-PBS) (GIBCO, USA)
- 1x Phosphate Buffer Saline (PBS) (Sigma-Aldrich, USA)
- 1x Phosphate Buffer Saline (PBS; pH 7.0-7.2) (GE Healthcare, USA)
- 2-(N-morpholino) ethanesulfonic acid monohydrate (MES) (Bio Basic Inc., Canada)
- 2-mercaptoethanol (Sigma-Aldrich, USA)
- 5-bromo-4-chloro-3-indolyl-phosphate/nitro blue tetrazolium; BCIP/NBT substrate (Mabtech, Sweden)
- 50X Tris-Acetate-EDTA (TAE) Buffer, pH8.0, Ultra-Pure Grade (Vivantis, Malaysia)
- $\beta$ -merceptoethanol (Applichem, Germany)
- Acetic acid ( $\text{CH}_3\text{COOH}$ ) (Merck, Germany)
- Acetone ( $\text{C}_3\text{H}_6\text{O}$ ) (Merck, Germany)
- Acrylamide/Bisacrylamide 40% (HiGenoMB<sup>®</sup>, India)
- Agar powder (Titan Biotech Ltd., India)
- Agarose powder (Vivantis, Malaysia)
- Amersham ECL prime western blotting detection reagent (GE Healthcare, UK)

- Ammonium Chloride ( $\text{NH}_4\text{Cl}$ ) (HIMEDIA<sup>®</sup>, India)
- Ammonium Persulfate (APS) (HIMEDIA<sup>®</sup>, India)
- Antibiotics
  - Ampicilin (Panreac AppliChem<sup>®</sup>, USA)
  - Antimycotic (GIBCO, USA)
  - Gentamycin (Panreac AppliChem<sup>®</sup>, USA)
  - Kanamycin sulfate (Panreac AppliChem<sup>®</sup>, USA)
  - Penicillin-Streptomycin (Thermo Fisher Scientific, USA)
  - Rifampicin (Bio Basic Inc., Canada)
- Bovine serum albumin (BSA) powder (Capricorn Scientific, Germany)
- Bromophenol blue (Honeywell Fluka<sup>TM</sup>, Finland)
- Concanavalin A (ConA) Sigma, USA
- Coomassie Blue blue R-250 (AppliChem<sup>®</sup>, USA)
- Deoxynucleoside triphosphate (dNTP): dATP, dCTP, dGTP, dTTP
- Di-Sodium hydrogen phosphate ( $\text{Na}_2\text{HPO}_4$ ) (EMSURE<sup>®</sup>, Germany)
- Dimethyl Sulfoxide (DMSO;  $\text{C}_2\text{H}_6\text{OS}$ ) (Sigma-Aldrich, USA)
- Dulbecco's Modified Eagle Medium (DMEM) powder-High glucose (GIBCO, USA)
- Ethanol (EMSURE<sup>®</sup>, Germany)
- Ethylenediaminetetraacetic acid (EDTA) (HIMEDIA<sup>®</sup>, India)
- Fetal Bovine Serum (FBS) (GIBCO, USA)
- Gel Loading Dye-purple 6x (New England Biolabs, USA)

- Glycerol (HIMEDIA<sup>®</sup>, India)
- Glycine (HIMEDIA<sup>®</sup>, India)
- Hoechst dye (Thermo Fisher Scientific, USA)
- Hydrochloric acid (HCl) (Merck, USA)
- KPL Sureblue<sup>TM</sup> TMB substrate (SeraCare, USA)
- Magnesium sulfate (MgSO<sub>4</sub>) (KEMAUS<sup>®</sup>, Australia)
- Methanol (Merck, Germany)
- Peptone (HIMEDIA<sup>®</sup>, India)
- Potassium bicarbonate (KHCO<sub>3</sub>) (Sigma-Aldrich, USA)
- Potassium chloride (KCL) (Carloerbareagets, Italy)
- Potassium dihydrogen phosphate (KH<sub>2</sub>PO<sub>4</sub>) (Carloerbareagets, Italy)
- Protein ladder (Bio-red<sup>®</sup>, USA)
- RedSafe<sup>TM</sup> nucleic acid staining solution (iNtRON Biotechnology, Inc., Korea)
- Restriction enzymes: *Xba*I, *Bam*HI, *Sac*I (New England Biolabs, UK)
- RPMI 1640 media with phenol red (GIBCO, USA)
- Skim milk (BD Difco<sup>TM</sup>, USA)
- Sodium chloride (NaCl) (Ajax Finechem Pty., Ltd, New Zealand)
- Sodium dodecyl sulfate (SDS) (Carloerbareagets, Italy)
- Sodium hydrogen carbonate (NaHCO<sub>3</sub>) (Sigma-Aldrich, USA)
- Streptavidin-alkaline phosphatase (ALP) (Mabtech, Sweden)
- Sulfuric acid (H<sub>2</sub>SO<sub>4</sub>) (RCI labscan, Thailand)
- T4 DNA ligase (New England BioLabs, UK)

- Taq DNA polymerase (Vivantis, Malaysia)
- Tetramethylethylenediamine (TEMED) (Affymetri<sup>®</sup>, USA)
- TMB stabilized substrate (Promega, USA)
- Tris-base (Vivantis<sup>®</sup>, Malaysia)
- Tween -20 (Vivantis<sup>®</sup>, Malaysia)
- VC 1 kb DNA Ladder (Vivantis<sup>®</sup>, Malaysia)
- Yeast Extract (Himedia Laboratories Pvt. Ltd., India)

#### **Software and database**

- ClustalOmega Multiple Sequence Alignment  
(<https://www.ebi.ac.uk/Tools/msa/clustalo/>)
- ExPASy Bioinformatics Resource Portal  
(<https://web.expasy.org/translate/>)
- GenBank NCBI: NIH genetic sequence database  
(<https://www.ncbi.nlm.nih.gov/genbank/>)
- GeneArt Gene Synthesis Portal  
(<https://www.thermofisher.com/order/geneartgenes/projectmgmt>)
- GraphPad Prism software version 6.0.
- GraphPad Prism software version 8.0.
- Harmony High-Content Imaging and Analysis Software (PerkinElmer, UK)
- National Center for Biotechnology Information (NCBI)  
(<https://www.ncbi.nlm.nih.gov/>)
- NEBcutter V2.0 (New England Biolabs, UK)

(<http://nc2.neb.com/NEBcutter2/>)

### Facilities

- **Certified biosafety level III facility**, Department of Microbiology, Faculty of Science, Mahidol University, Bangkok, Thailand
- **Greenhouse for *N. benthamiana***, Department of Pharmacognosy and Pharmaceutical Botany, Faculty of Pharmaceutical Sciences, Chulalongkorn University, Bangkok, Thailand
- **Hygienic conventional mouse housing system**, Faculty of Medicine, Chulalongkorn University, Bangkok, Thailand

### Experimental Procedures

#### Gene Design and Synthesis

The receptor-binding domain of SARS-CoV-2 (SARS-CoV-2 RBD) and human angiotensin converting enzyme 2 (hACE2) sequences were obtained from NCBI gene database (Genbank accession number: YP\_009724390.1; F318-C617 and NP\_001358344.1, respectively). The nucleotide sequences were codon optimized for expressing in *N. benthamiana* by using GeneArt Gene Synthesis Portal (Thermo Fisher Scientific, USA). The nucleotide sequences of SARS-CoV-2 RBD and ACE2 were designed to anneal with nucleotide-encoding signaling peptides



(MGWSCILFLVATATGVHS) for protein localization in endoplasmic reticulum (ER) at N-terminus. In addition, the nucleotide sequences were added *Xba*I and *Bam*HI restriction sites for cloning with Fc region fragment which contain a peptide linker (GGGGS) (N-terminus), human IgG1, and consensus tetrapeptides Lys-Asp-Glu-Leu (KDEL) for protein retention in ER (C-terminus) with the *Bam*HI and *Sac*I restriction sites at the 5' and 3' ends, respectively to construct SARS-CoV-2 RBD-Fc (Figure 7A) and ACE2-Fc (Figure 7B) sequences. The SARS-CoV-2 RBD and ACE2 sequences were commercially synthesized by Genewiz, Suzhou, China and shipped in the commercial pUC57 vector.

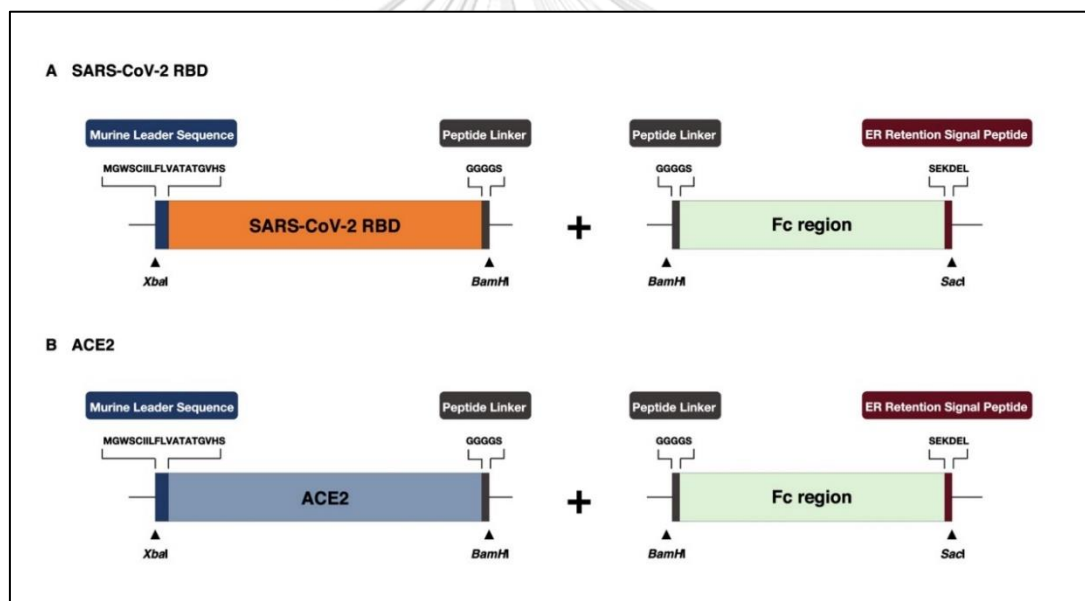


Figure 7 Schematic representation of gene design for cloning with Fc region to construct A. SARS-CoV-2 RBD-Fc and B. ACE2-Fc sequences

### Cloning and Construction of Expression Vectors

The commercial pUC57-SARS-CoV-2 RBD and pUC57-ACE2 plasmids were digested by *Xba*I and *Bam*HI restriction enzymes (New England Biolabs, UK) (Table

14). The SARS-CoV-2 RBD and ACE2 fragments were separated by 0.6% agarose gel with RedSafe™ DNA staining solution (iNtRON Biotechnology, Inc., Korea) for visualization. The target of bands SARS-CoV-2 RBD and ACE2 were sliced from agarose gel and extracted the DNA fragments by using MEGA quick-spin™ Fragment DNA Purification Kit (iNtRON Biotechnology, Inc., Korea) according to the manufacturer's instructions. The extracted DNA fragments were separately ligated with Fc fragment into a geminiviral vector (pBYR2e) using *Xba*I and *Sac*I restriction sites, at the N-terminus and C-terminus (Table 15) to construct the expression vectors pBYR2e-SARS-CoV-2 RBD-Fc and pBYR2e-ACE2-Fc, respectively (Figure 8).

*Table 14 Components for restriction enzyme digestion*

Component	Final concentration
Plasmid DNA	TBD
10xCutsmart buffer	1x
<i>Xba</i> I restriction enzyme	10 units /50 µl reaction
<i>Bam</i> HI restriction enzyme	10 units /50 µl reaction
Nuclease-free water	Adjust into 50 µl

**\*\*TBD: to be determined**

*Table 15 Components for in vitro ligation*

Component	Final concentration/amount
10xT4 DNA ligase buffer	1x
pBY2e vector ( <i>Xba</i> I/ <i>Sac</i> I)	TBD
ACE2 or SARS-CoV-2 RBD ( <i>Xba</i> I/ <i>Bam</i> HI)	TBD
Fc fragment ( <i>Bam</i> HI/ <i>Sac</i> I)	TBD
T4 DNA ligase	1 µl/ 20 µl reaction
Nuclease-free water	Adjust into 20 µl

**\*\*TBD: to be determined**

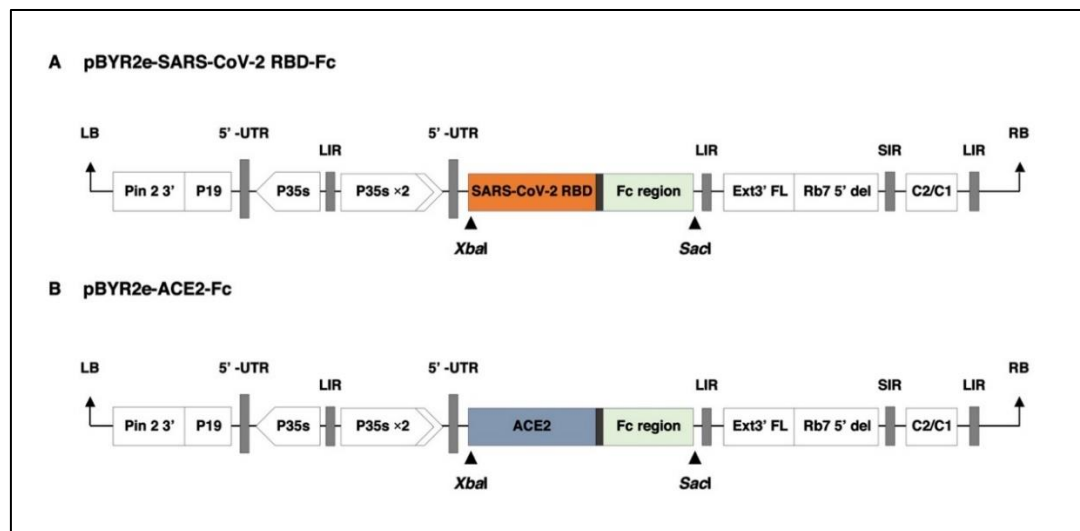


Figure 8 Schematic representation of constructed protein expression vectors for expression in *N. benthamiana* including A. *pBYR2e-SARS-CoV-2 RBD-Fc* and B. *pBYR2e-ACE2-Fc*

### Preparation of Escherichia coli Competent Cells

*E. coli* strain DH10B was cultured in 5 ml Luria Bertani (LB) broth and incubated at 37°C overnight at 200 rpm as a bacterial starter culture. 1 ml starter culture was added into 100 ml fresh LB broth and incubated at 37 °C 200 rpm into OD<sub>600</sub> of 0.3-0.4 (approximately 2h). The *E. coli* was chilled on ice for 10 min and collected the bacterial pellets by centrifugation at 4°C for 10 min at 4000g. The pellets were resuspended by 20 ml 0.1M MgCl<sub>2</sub> and chilled on ice for 10 min. The bacterial suspension was centrifuged at 4°C for 10 min at 4000g to collect the pellets (repeating the 0.1M MgCl<sub>2</sub> resuspension and centrifugation). The bacterial pellets

were resuspended by 0.1M CaCl<sub>2</sub> with 10% glycerol. The competent cell suspension was aliquoted into 1.5 ml microcentrifuge tubes and stored in -80°C

### **Plasmid Propagation in *E. coli***

The expression pBYR2e-SARS-CoV-2 RBD-Fc and pBYR2e-ACE2-Fc vectors were propagated in *E. coli* strain DH10B competent cells by heat shock transformation. 50-100 µl of *E. coli* competent cells were mixed with 1-5 µl of ligated products and incubated on ice for 30 min. After incubation, the competent cell was heated at 42 °C for 30 sec and immediately incubated on ice for 2 min. 500 µl of LB broth (without antibiotic) was added and incubated at 37 °C for 45 min at 200 rpm for recovery the bacterial transformants. Then, the transformants were plated on LB agar with 50 µg/ml selective antibiotic kanamycin and incubated overnight at 37°C. The transformants were confirmed by polymerase chain reaction (PCR) (Table 16 and 17) using vector-specific primers (Table 18). The positive transformants were inoculated into 5 ml LB broth containing 50 µg/ml kanamycin and incubated at 37°C for 16h at 250 rpm. The plasmids were extracted from bacteria by following protocol from DNA-spin™ Plasmid DNA Purification Kit (iNtRON Biotechnology, Inc., Korea) and stored the plasmids in -20 °C.

*Table 16 Components for polymerase chain reaction*

<b>Component</b>	<b>Final concentration</b>
dNTP (dATP/dTTP/dCTP/dGTP)	0.2 mM
Forward primer	0.2 mM
Reverse primer	0.2 mM
DNA template	TBD (0.1-250 ng)
10xViBuffer A	1X
MgCl <sub>2</sub>	2.0 mM

Taq DNA polymerase	2 units/ 50 µl PCR
Nuclease-free water	Adjust into 50 µl
<b>**TBD: to be determined</b>	

Table 17 Conditions for polymerase chain reaction

Reaction step	Temperature	Time
Initial denaturation	95°C	5 min
Denaturation	95°C	30 sec
Annealing	TBD	30 sec
Extension	72°C	30 sec/kb
Final extension	72°C	30 sec
Storage	4°C	10 min
<b>**TBD: to be determined</b>		

Table 18 Primers for polymerase chain reaction

Name	Nucleotide sequence	T <sub>M</sub>
Primers for SARS-CoV-2 RBD-Fc amplification		
BsaI-W-F	5' CTGGTGGAGACCAATTCAGGGTTCAGCCTACCG 3'	68.1°C
2e-Rev	5' GCTTTGCATTCTTGACATC 3'	46.8°C
Primers for ACE2-Fc amplification		
ACE2-F	5' GGGTCTAGAACAATGGGCTGGTCCTGCATCATCCTGTTCC 3'	70.6°C
2e-Rev	5' GCTTTGCATTCTTGACATC 3'	46.8°C

### Preparation of *Agrobacterium tumefaciens* Electrocompetent Cells

*A. tumefaciens* strain GV3101 was cultured in 5 ml Luria Bertani (LB) broth with 50 µg/ml Rifampicin and 50 µg/ml Gentamicin and incubated at 28°C overnight at 200 rpm as a bacterial starter culture. 1 ml starter culture was added into 100 ml fresh LB broth containing 50 µg/ml Rifampicin and 50 µg/ml Gentamicin and incubated at 37 °C 200 rpm into OD<sub>600</sub> of 0.5-1.0. The *A. tumefaciens* was chilled on

ice for 10 min and collected the bacterial pellets by centrifugation at 4°C for 10 min at 4000g. The pellets were resuspended by 20 ml sterile deionized water. The bacterial suspension was centrifuged at 4°C for 10 min at 4000g to collect the pellets (repeating the deionized water resuspension and centrifugation). The bacterial pellets were resuspended by 10% glycerol. The competent cell suspension was aliquoted into 1.5 ml microcentrifuge tubes and stored in -80°C

### **Gene Transformation into *A. tumefaciens* by Electroporation**

The expression vectors containing pBYR2e-SARS-CoV-2 RBD-Fc and pBYR2e-ACE2-Fc were transformed into *Agrobacterium* electrocompetent cells using MicroPulser (Bio-Rad, USA). The recombinant *Agrobacterium* clones were plated on LB agar with selective antibiotics consisting of 50 µg/ml Kanamycin, 50 µg/ml Rifampicin, and 50 µg/ml Gentamicin and incubated at 28°C for 48h. The transformants were confirmed by PCR using vector-specific primers (Table 18). Single positive colony of each vector were inoculated into LB broth with the selective antibiotics and incubated at 28°C overnight at 200 rpm. The growth culture was inoculated into fresh cultures with the ratio of 1:100 and incubated at 28°C overnight at 200 rpm in order to prepare bacterial solutions for agroinfiltration.

### **Transient Expression and Optimization of SARS-CoV-2 RBD-Fc and ACE2-Fc**

*Agrobacterium* containing pBYR2e-SARS-CoV-2 RBD-Fc and pBYR2e-ACE2-Fc pellets were collected by centrifugation at 4000g for 10 min. Cell pellets were resuspended and diluted with 1xInfiltration buffer into OD<sub>600</sub> of 0.2. The SARS-CoV-2 RBD-Fc and ACE2-Fc proteins were transiently expressed in *N. benthamiana*

plants by injecting *Agrobacterium* suspensions into the adaxial side of 6-week-old tobacco leaves using a 1 mL syringe without a needle. The infiltrated plants were maintained in the optimal 16-h light/8-h dark condition at 28°C. The infiltrated leaves were collected from 3 individual plants on days 2, 4, 6, 8, and 10 after agroinfiltration to identify the expression levels of fusion proteins in different time courses.

### **Large-Scale Productions of SARS-CoV-2 RBD-Fc and ACE2-Fc**

After determining the optimal time-course conditions for SARS-CoV-2 RBD-Fc and ACE2-Fc expression, the large-scale productions were performed. *Agrobacterium* stocks containing pBYR2e-SARS-CoV-2 RBD-Fc and pBYR2e-ACE2-Fc were cultured in LB medium with 50 µg/ml Kanamycin, 50 µg/ml Rifampicin, and 50 µg/ml Gentamicin and incubated at 28°C for 48h for bacterial starter culture. The starter cultures were inoculated into 1L LB medium with selective antibiotics and incubated at 28°C for 48h. The *Agrobacterium* pellets were collected by centrifugation and diluted with 1xInfiltration buffer into OD<sub>600</sub> of 0.2. The *Agrobacterium* suspensions were infiltrated into tobacco plants by using vacuum infiltration. The infiltrated plants were harvested on day 4, and 6 after agroinfiltration for SARS-CoV-2 RBD-Fc and ACE2-Fc, respectively.

### **Protein Extraction and Purification**

Infiltrated leaves were extracted with 1xPBS pH 7.4 and clarified by centrifugation at 4°C for 45 min at 26,000g. The supernatants were filtered by using 0.45 µm filter membrane (MilliporeSigma, USA) for removal of the contaminated macromolecules. The plant-produced SARS-CoV-2 RBD-Fc and ACE2-Fc were

purified by affinity chromatography using protein A resin (Expedeon, UK). The affinity columns containing protein-A beads were equilibrated by 1xPBS pH 7.4 and followed by addition of clarified supernatants. The purified columns were washed by 1xPBS pH 7.4 for 2 times. The plant-produced proteins were eluted by 0.1M glycine buffer pH 3. The eluted solutions were instantly neutralized by addition of Tris-HCl pH 8.8 buffer. The purified plant-produced SARS-CoV-2 RBD-Fc and ACE2-Fc were concentrated using Amicon® ultracentrifugal filter (Merck, Massachusetts, USA) and filtered with 0.22 µm syringe filter (Merck, Massachusetts, USA) for protein sterilization.

#### **Protein Characterization by Sodium Dodecyl Sulfate Polyacrylamide Gel Electrophoresis (SDS-PAGE) and Western Blotting**

The purified plant-produced SARS-CoV-2 RBD-Fc and ACE2-Fc were analyzed by sodium dodecyl sulfate-polyacrylamide gel electrophoresis (SDS-PAGE). The purified samples were prepared by addition of reducing and non-reducing dyes and denatured at 95°C for 5 min. The SARS-CoV-2 RBD-Fc and ACE2-Fc samples were subjected into 10% and 8% sodium dodecyl sulfate polyacrylamide gel electrophoresis, respectively for protein separation and stained by Coomassie staining solution for protein visualization.

For western blot analysis, separated proteins were transferred to nitrocellulose membranes (Biorad, USA) at 100 V for 2h. The membranes were blocked by 5% skim milk (BD Difco, USA) diluted in 1xPBS for 45 min. The membranes were probed with a rabbit anti-SARS-CoV-2 RBD antibody (Thermo Fisher Scientific, USA) and a rabbit anti-human ACE2 antibody (SinoBiological, USA) diluted in



1xPBS with a dilution of 1:2,500 as primary antibodies for detection of plant-produced SARS-CoV-2 RBD and ACE2 proteins, respectively at 4°C overnight. The detection antibody, a 1:5,000 dilution of goat anti-rabbit-IgG HRP conjugate antibody (BosterBio, USA), were added to membranes and incubated for 1h. Fc portions in SARS-CoV-2 RBD and ACE2 proteins were detected by Fc-domain-specific antibody using a sheep anti-human Gamma chain-HRP fusion (The Binding Sites, UK) diluted with ratio of 1:5,000 in 1xPBS for 2h. The membranes were washed three times by 1xPBS-T and developed using an enhanced chemiluminescent (ECL) detection reagent (Abcam, UK).

#### **Protein Quantification by Enzyme-linked Immunoassay (ELISA) Assay**

The yields of plant-produced SARS-CoV-2 RBD were measured by sandwich ELISA assay starting by addition of a rabbit anti-SARS-CoV-2 RBD antibody diluted in 1xPBS with ratio of 1:1000 in 96-well plates (Greiner Bio-One GmbH, Austria) and incubated at 4°C overnight. The plates were blocked by 5% skim milk in 1xPBS at 37°C for 2h. Subsequently, the plant-produced SARS-CoV-2 RBD-Fc samples and HEK-produced SARS-CoV-2 Spike RBD-Fc chimera (R&D Systems, USA) as a protein standard diluted in 1xPBS were loaded on the wells and incubated at 37°C for 2h. The SARS-CoV-2 RBD-Fc proteins were detected by a 1:1,000 anti-human Gamma chain-HRP fusion in 1xPBS, at 37 °C for 1h.

Plant-produced ACE2-Fc was quantified by indirect ELISA assay. The ELISA well plates were coated with plant-produced ACE2-Fc and commercial HEK-produced ACE2-Fc proteins (Abcam, UK) as a protein standard in 1xPBS at 4°C overnight. Then, the plates were blocked by 5% skim milk in 1xPBS at 37 °C for 2h

and incubated with a 1:2,000 rabbit anti-human ACE2 at 37 °C for 2h and a 1:1,000 goat-anti-rabbit-IgG HRP fusion antibody as detection antibody at 37 °C for 1h, respectively. A 3,3',5,5'-Tetramethylbenzidine (TMB) solution (Promega, USA) was added to the plates as colorimetric developer followed by 1M H<sub>2</sub>SO<sub>4</sub> for termination of enzymatic reactions. The absorbance was read at 450 nm in a 96-well plate reader (BMG Labtech, Germany). Between each step, the plates were washed three times by 1xPBS-T.

### **In vitro Binding Activity of Plant-Produced SARS-CoV-2 RBD-Fc**

The binding activity of plant-produced RBD-Fc fusion protein to ACE2 receptor was performed by ELISA assay. A 96-well ELISA plate was coated by 100 ng of two commercial proteins including HEK-produced ACE2 (Abcam, UK) and CHO-produced ACE2 (InvivoGen, USA) proteins incubated at 4°C overnight. For blocking, 5% skim milk in 1xPBS was added into the wells and incubated at 37°C for 2h. The plate was washed three times with 1xPBS-T and incubated with various concentrations of plant-produced SARS-CoV-2 RBD-Fc diluted in 1xPBS starting with the protein concentration of 1,000 µg/ml at 37°C for 2h. A 1:100 plant-produced anti-SARS-CoV-2 (H4) mAb (368) was incubated into the wells at 37°C for 2h. Subsequently, the 96-well plate was incubated with a 1:1,000 dilution of anti-human Kappa chain-HRP fusion (SouthernBiotech, USA) in 1xPBS for 1h at 37°C. For colorimetric development, a TMB solution (Promega, USA) will be added into the wells and followed by 1M H<sub>2</sub>SO<sub>4</sub> for terminating the enzymatic reactions. The absorbance at 450 nm will be measured using a microplate reader.

### ***In vitro* Binding Activity of Plant-Produced ACE2-Fc**

A 96-well plate was coated with 100 ng of plant-produced ACE2-Fc and incubated at 4°C overnight. The plate was blocked by 5% skim milk in 1xPBS at 37°C for 2h. The wells were washed three times by 1xPBS-T and incubated with various dilutions of proteins including the commercial Sf9-produced SARS-CoV-2 RBD (Genscript Biotech, USA), an unrelated S1 protein of porcine epidemic diarrhea virus (PEDV) (13) starting with the protein concentration of 100 µg/ml and 1xPBS as negative controls at 37°C for 2h. After washing, a 1:1,000 anti-6X His tag-HRP fusion (Abcam, UK) in 1xPBS was incubated into the wells for 2h at 37°C. For detection, a TMB solution was added into the plate. The reactions were stopped by adding 1M H<sub>2</sub>SO<sub>4</sub>. The absorbance at 450 nm was read using a 96-well microplate reader.

### **Vaccine Preparation and Formulation for Mice Immunization**

Purified plant-produced SARS-CoV-2 RBD-Fc was dialyzed for supplanting the buffer into 1xPBS at pH 7.0-7.2 (GE Healthcare, USA) and concentrated by using Amicon® ultracentrifugal filter. The protein was sterilized by using 0.22 µm syringe filter and conducted in biosafety cabinet class II. Sterile plant-produced SARS-CoV-2 RBD-Fc was formulated with various commercial immunoadjuvants consisting of aluminium hydroxide gel (alum), AddaVax™ (MF59 adjuvant), mPLA from *Salmonella Minnesota* R595 (mPLA-SM), and high molecular weight poly (I:C) (poly (I:C) HMW) (InvivoGen, USA). All the adjuvants were prepared by following manufacturer's protocols in the sterile condition for preparing the vaccine formulations for immunogenicity studies in mice (Table 19).

*Table 19 Experiment groups for immunogenicity study in mice*

<b>Group</b>	<b>Antigen content</b>	<b>Adjuvant content</b>	<b>Immunized volume (μl)</b>	<b>Number</b>
1	PBS control	-	50	5
2	10 μg SARS-CoV-2 RBD-Fc	-	50	5
3	10 μg SARS-CoV-2 RBD-Fc	0.1 mg alum	50	5
4	10 μg SARS-CoV-2 RBD-Fc	10 μg MF59	50	5
5	10 μg SARS-CoV-2 RBD-Fc	10 μg mPLA-SM	50	5
6	10 μg SARS-CoV-2 RBD-Fc	20 μg poly (I:C)	50	5

### **Ethics Statement**

Seven-week-old female ICR mice were ordered from Nomura Siam International Co., Ltd. (Thailand) and were maintained in animal facilities with strictly hygienic conventional system in Faculty of Medicine, Chulalongkorn University, Bangkok, Thailand. The use of animal protocol was approved by the Institutional Animal Care and Use Committee, Faculty of Medicine, Chulalongkorn University (permit number: 012/2563).

### **Mice Immunogenicity Studies**

The thirty female ICR mice (n = 5 per group) were intramuscularly (IM) immunized *via.*, anterior tibialis by 50 μl of several SARS-CoV-2 RBD-Fc vaccine formulations (Table 19) on days 0 and 21. Mice sera was collected prior to the first immunization (pre-bleed, day 0) and 14 days post-vaccination (days 14 and 35) to

investigate SARS-CoV-2 RBD-specific antibody responses. The mice were sacrificed on day 35 (14 days after second booster) to collect the spleen for quantitative measurement of SARS-CoV-2 RBD-specific T-cells (Figure 9). Health status was monitored by clinical signs and body weight changes among vaccinated mice.

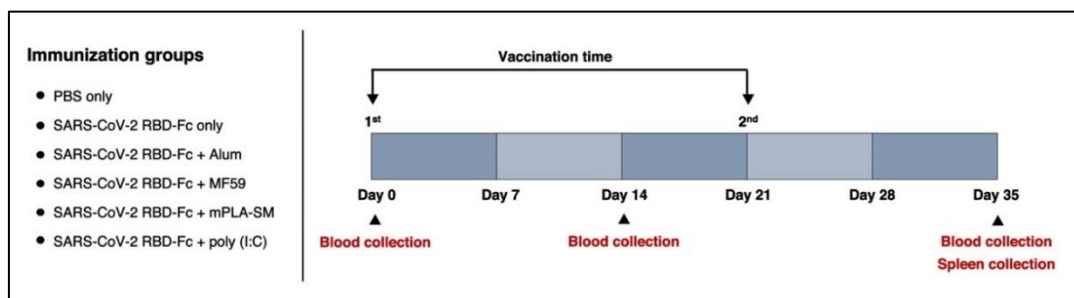


*Figure 9 Experimental design of plant-produced SARS-CoV-2 RBD-Fc immunization and sample collection in mice immunogenicity studies*

## Evaluation of SARS-CoV-2 RBD-Specific Antibody Responses by ELISA

### Assay

96-well plates were captured by SARS-CoV-2 spike protein RBD from Sf9 insect cells (GenScript, USA) diluted in 1xPBS at the final concentration of 2  $\mu\text{g/ml}$  and incubated at 4°C overnight. Then, the wells were blocked by 5% skim milk in 1xPBS and incubated at 37°C for 2h. Subsequently, the animal sera were 10-fold serially diluted with 1xPBS starting at 1:100 and loaded on the wells at 37°C for 2h. A goat anti-mouse IgG HRP conjugate antibody (Jackson ImmunoResearch, Pennsylvania, USA) diluted 1:2000 in 1xPBS was added into the wells and incubated at 37°C for 1h for detection of SARS-CoV-2 RBD-specific antibodies. TMB substrate was added into the plates for colorimetric development. The enzymatic reactions were terminated by adding 1M H<sub>2</sub>SO<sub>4</sub>. The absorbance was measured at 450 nm ( $A_{450}$ )

using a microplate reader. Between each step, the plates will be washed by 1xPBS-T for three times.

For mouse IgG1 and IgG2a analyses, the mice sera were 10-fold serially diluted with 1xPBS starting 1:100 in the same fashion and detected by 1:2000 goat anti-mouse IgG1 (HRP) and goat anti-mouse IgG2a (HRP) (Abcam, UK), respectively in 1xPBS at 37°C for 2h. The endpoint titers of IgG1 and IgG2a were also computed for monitoring Th2 and Th1 lymphocyte responses, respectively.

The endpoint titers were determined as the highest dilution of immunized sera, which had  $A_{450}$  more than cut off, which is calculated from  $A_{450}$  of pre-immunized sera in the dilution of 1:100 in 1xPBS as following equation (369).

$$cut\ off = X + SD \sqrt{1 + \left(\frac{1}{n}\right)}$$

Where X is the mean of  $A_{450}$  reading from independent controls of pre-immune sera, SD is standard deviation,  $n$  is the number of independent controls,  $t$  is  $1 - \alpha$ , and  $\alpha$  is significance level.

### Cell culture

The Vero E6 cells, African green monkey (*Cercopithecus aethiops*) kidney epithelial cells (ATCC, USA) were used for microneutralization assay for quantification of neutralizing antibody in animal sera anti-SARS-CoV-2 activities of plant-produced ACE2-Fc. The Vero E6 cells were cultured in Dulbecco's Modified Eagle Medium High glucose (DMEM) (Gibco, USA) with 10% fetal bovine serum (FBS) (Gibco, USA) and Penicillin-Streptomycin antibiotics.

### **Virus preparation**

Live SARS-CoV-2 virus (SARS-CoV-2/01/human/Jan2020/Thailand), which was used in a microneutralization and antiviral assay, was obtained from nasopharyngeal swabs isolation of a confirmed COVID-19 case in Thailand. The virus was prepared by Vero E6 cells propagation to establish a high-titer stock and stored at  $-80^{\circ}\text{C}$ . Virus titration was performed using the Reed Muench method and expressed terms of 50% tissue culture infectious dose ( $\text{TCID}_{50}$ ) per ml of culture media (370).

### **In Vitro Microneutralization Assay**

A microneutralization assay was conducted in a certified biosafety level III facility in Department of Microbiology, Faculty of Science, Mahidol University, Bangkok, Thailand. The Vero E6 cells were seeded with the concentration of  $1 \times 10^4$  cells/well in complete DMEM medium in 96-well plates and incubated at  $37^{\circ}\text{C}$  with  $5\% \text{CO}_2$  for overnight. The immunized sera and positive convalescent serum from COVID-19 patient were prepared by heat-inactivation at  $56^{\circ}\text{C}$  for 30 min. The heat-inactivated sera were 2-fold serially diluted for loading in independent duplicate wells and incubated with 100 of 50% tissue culture infective dose ( $100\text{TCID}_{50}$ ) of the live SARS-CoV-2 virus in DMEM medium at  $37^{\circ}\text{C}$  for 1h. Virus control at  $100 \text{TCID}_{50}$  and uninfected cell control wells were included in all plates. Subsequently, the mixtures of diluted serum and virus were transferred to the monolayer of Vero E6 cells and incubated at  $37^{\circ}\text{C}$  with  $5\% \text{CO}_2$  for 2 days. After incubation, the cells were washed with 1xPBS and followed by fixing and permeabilizing the cells by ice-cold 1:1 methanol/acetone fixative solution at  $4^{\circ}\text{C}$  for 20 min. The cells were washed 3 times

with 1xPBS-T and blocked with blocking solution at room temperature (RT) for 1h. After washing, the viral nucleocapsids were detected using a 1: 5,000 of SARS-CoV/SARS-CoV-2 nucleocapsid (N) monoclonal antibody (SinoBiological, USA) and incubated at 37°C for 1h followed by a 1:2,000 HRP-conjugated goat anti-rabbit polyclonal antibody (Dako, Denmark) in 1xPBS at 37 °C for 1h. The KPL Sureblue™ TMB substrate (SeraCare, USA) was added for colorimetric development. Afterwards, the reactions were stopped by the addition of 1N HCl. The absorbance was read at 450 nm and 620 nm using a Sunrise™ microplate reader (Tecan, Switzerland). The absorbance differences between 450 and 620 nm ( $A_{450}-A_{620}$ ) of diluted samples were computed and compared with the 50% specific signal of the cut point, which was calculated by the following equation to determine the potent neutralization titers of the immunized sera.

$$A_{cut\ point} = \frac{A_{virus\ control} - A_{cell\ control}}{2} + A_{cell\ control}$$

Where  $A_{virus\ control}$  and  $A_{cell\ control}$  are the average of  $A_{450}-A_{620}$  of virus control wells and cell control wells, respectively. The neutralizing titers will be defined as the reciprocal highest dilution providing the average of  $A_{450}-A_{620}$  of the diluted serum well more than the cut point. The neutralizing antibody titers of each experimental group will be compared by using GraphPad Prism. The significant differences will be considered when  $p < 0.05$ .



### **Quantification of Mouse IFN- $\gamma$ by ELISpot Assay**

Mouse spleen tissues were prepared by removal of surrounding fatty tissue and soaking into RPMI1640 medium. Mouse spleens were transferred by using 70  $\mu\text{m}$  nylon cell strainer and loaded into the petri-dish. Then, the spleen cells were dissociated into single-cell suspension using needle #21 for 2-3 times. After cell dissociation, R5 medium was added into the cells. The splenocytes were clarified by centrifugation at 4°C for 5 min at 1,200 rpm. Then, the cells were washed and lysed by 1xACK lysis buffer. The cells were centrifuged for 5 min at 1,200 rpm and resuspended by R5 medium into a final concentration of  $5 \times 10^6$  cells/ml. The nitrocellulose membrane plates (Millipore, Bedford, MA, USA) were coated by anti-mouse IFN- $\gamma$  (AN18) monoclonal antibody (mAb) (Mabtech, Sweden) at the concentration of 10  $\mu\text{g}/\text{mL}$  in 1xPBS at 37°C with 5%CO<sub>2</sub> for 3h. Then, the plates were washed six times by 1xPBS and blocked with R10 medium at RT for 1h. The mouse splenocytes were activated by incubating with SARS-CoV-2 peptide pools (BioNet-Asia, Thailand, and Mimotopes, Australia) and incubated at 37°C with 5% CO<sub>2</sub> for 4h. Then, the activated splenocytes were added in to the wells. Culture medium and concanavalin A (ConA) were served as a negative and positive control, respectively. The unbound splenocytes were removed by washing with 1xPBS-T for six times followed by 1xPBS for three times. The plates were incubated with the detection antibody, which is anti-mouse IFN- $\gamma$ -biotinylated mAb (R4-6A2 biotin; Mabtech, Sweden) in 1xPBS, at RT for 3h. The streptavidin-alkaline phosphatase (ALP; Mabtech, Stockholm, Sweden) was then added and incubated at RT for 1h. For the enzymatic development, the substrate solution (5-bromo-4-chloro-3-indolyl-

phosphate/nitro blue tetrazolium; BCIP/NBT) was added into the wells after washing the plates. The enzymatic reactions were terminated by washing with tap water and removed the underdrain by rinsing the tap water underside of the membrane. The spots were counted by using ELISpot reader (ImmunoSpot<sup>®</sup> Analyzer, USA). Results were expressed term of spot-forming cells (SFCs)/10<sup>6</sup> splenocytes). The number of spots were compared to the controls for determining the positive responses. A positive response was defined at more than 50 SFCs/10<sup>6</sup> splenocytes over the background signal.

#### **In Vitro Antiviral Activity of Plant-Produced ACE2-Fc**

Anti-viral activity of plant-produced ACE2-Fc was also conducted in a certified biosafety level III facility in Department of Microbiology, Faculty of Science, Mahidol University, Bangkok, Thailand. Vero E6 cells were seeded in a 96-black well plate (Corning, USA) at 37°C with 5% CO<sub>2</sub> overnight. For the post-treatment condition, 25TCID<sub>50</sub> (50% tissue culture infective dose) of live SARS-CoV-2 was incubated with the cells at 37°C for 2h and then washed the plate by 1xPBS. After washing, the fresh culture medium (DMEM with 2% FBS) was added. Various 10-fold serial dilutions of plant-produced ACE2-Fc were directly added to the wells and maintained at 37°C with 5%CO<sub>2</sub> for 48h (Figure 10A) (371).

For pre-treatment condition, a 25TCID<sub>50</sub> of live SARS-CoV-2 was incubated with the various dilutions of plant-produced ACE2-Fc at 37°C for 1h prior to viral adsorption for 2h. The cells were washed two times with 1xPBS followed by the addition of fresh culture medium (DMEM with 2% FBS). Vero E6 cells were

incubated with the prepared mixtures of live SARS-CoV-2 and plant-produced ACE2-Fc under standard conditions for 48h (Figure 10B) (371).

The heat-inactivated Positive convalescent serum from a COVID-19 patient and an anti-human IgG-FITC antibody (Santa Cruz Biotechnology, USA) were served as positive and negative controls, respectively. The cells in the 96-well plate were fixed and permeabilized with 50% (v/v) acetone in methanol on ice for 20 min and washed by 1xPBS-T. The plates were blocked by blocking solution. After blocking, the plates were incubated with a 1:500 of a rabbit monoclonal primary antibody (SinoBiological, USA) at 37°C for 1h for the detection of the SARS-CoV-2 nucleocapsid. The unbound antibodies were removed by washing with 1xPBS-T for three times. Then, the cells were incubated with a 1:500 dilution of an Alexa Fluor 488 conjugated goat anti-rabbit IgG (H+L) highly cross-adsorbed secondary antibody (ThermoFisher Scientific, USA). Nuclei of the cells were stained with Hoechst dye (Thermo Fisher Scientific, USA). The fluorescent signals were detected and analyzed using a high-content imaging system (PerkinElmer, UK) at 40x magnitude. The percentage of infected cells in each well was automatically obtained randomly from 13 images per well using Harmony software (PerkinElmer, UK).

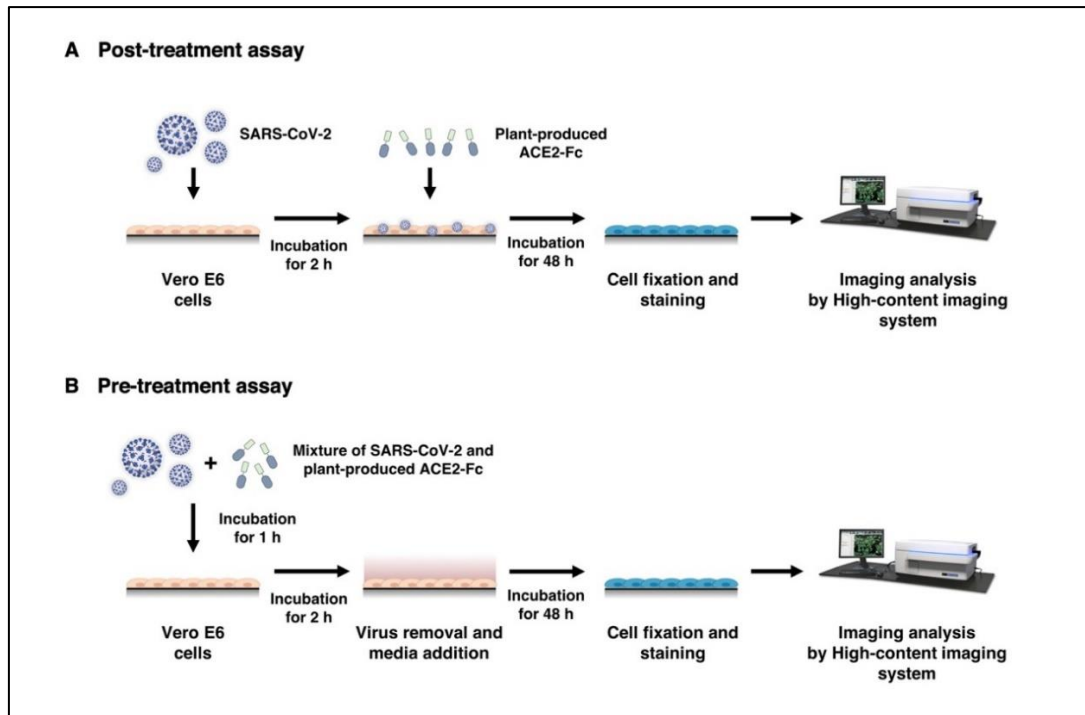


Figure 10 Experimental design of *in vitro* anti-SARS-CoV-2 assay including A. post-infection phase; plant-produced ACE2-Fc added to SARS-CoV-2-infected Vero E6 cells (at 25TCID<sub>50</sub>) and B. pre-infection phase; plant-produced ACE2-Fc and SARS-CoV-2 (at 25TCID<sub>50</sub>) mixture added to Vero E6 cells

### Statistical analysis

The immunological results were analyzed using Prism 8.0 (GraphPad software, USA) Data are expressed as mean  $\pm$  standard deviation (SD). Dunnett's Tests of Multiple Comparison were also carried out. The values of  $p < 0.05$  were considered as statistically significant.

### CHAPTER 3

## RESULTS AND DISCUSSION

A newly emerging disease, caused by the novel *betacoronavirus* SARS-CoV-2 is responsible for an ongoing COVID-19 pandemic. The SARS-CoV-2 has continually spread to more than 200 countries worldwide with millions of cumulative infected cases and deaths (372). Moreover, the COVID-19 allows unprecedented impacts on humans, especially public health, the global economy and society. The effective therapeutic interventions such as specific anti-viral drug, neutralizing antibodies, or preventive vaccines are urgently demanded for COVID-19 therapy and prophylaxis of lethal SARS-CoV-2 virus (10, 13, 50, 170, 373).

SARS-CoV-2 utilizes its S glycoprotein, particularly the RBD domain, which specifically interacts with the cellular ACE2 receptor for viral entry. Importantly, SARS-CoV-2 RBD was found to be dominant conformational epitopes, which showed great immunogenicity and effectively elicited potent neutralizing antibodies and protective effects against SARS-CoV-2 infection in pre-clinical models suggesting a vaccine consisting of RBD is considered to be a promising immunogen for possible COVID-19 vaccine development (9, 11, 190, 374). As well, previous reports have shown the therapeutic potential of recombinant ACE2 in protection of SARS-CoV infection *in vitro* with high protective efficacy compared with the use of virus-specific monoclonal antibodies (161, 162). Hence, SARS-CoV-2 RBD and ACE2 have the potential to be targets for development of therapeutic interventions against the disease-associated with SARS-CoV-2.

For three decades ago, plants have been utilized to produce recombinant biopharmaceuticals and vaccine candidates for several human and veterinary diseases (12, 288, 331, 339-343, 375). Many reports have shown the potential of plant expression system for production of biopharmaceutical products as effective as the mammalian cell-produced counterparts in producing neutralizing antibodies against a particular pathogen or infection as judged by generated products, which are recruiting in either clinical evaluations or approval stage by FDA (296, 303, 307, 343, 376). Additionally, plants are advantageous and can overcome the challenges in biopharmaceutical production during the pandemic situation by providing an efficient system for bulk production with the rapid-scalable processes to fulfil the demands of biopharmaceuticals against infectious diseases (377). Hence, plants expression system is fascinating platform and it can be served as an alternative platform for producing biologics or therapeutic proteins with economical process during the pandemic circumstances.

Fusion protein based on the immunoglobulin Fc domain offers enable easy purification method of recombinant protein by protein A chromatography. Additionally, the Fc provide several favorable characteristics consisting of facilitating expression and secretion of the recombinant proteins and increasing the protein solubility and stability (24, 362, 366). Moreover, Fc portion prolongs the serum half-life and therapeutic activities by pH-dependent binding to the neonatal Fc receptor (FcRn) allowing prevention of protein degradation in endosomes and reduction of renal clearance rate due to larger molecular weight (21, 25, 366, 378, 379). Fc region have been used as a fusion protein partner for several recombinant proteins such as

receptors, ligands, enzymes, and soluble cytokines for therapeutic applications (9, 23, 24, 380, 381).

Hence, we engineered the SARS-CoV-2 RBD and ACE2 by fusing N-terminus of the Fc region of human immunoglobulin IgG1 as preventive subunit vaccine and therapeutic against SARS-CoV-2 and transiently expressed the construct in *N. benthamiana* using geminiviral vector. The geminiviral-based expression system was developed from the genome structure of the Bean yellow dwarf virus (BeYDV), a *Mastrevirus* in the *Geminiviridae* family, to improve the protein expression in plants with higher yields of recombinant proteins by a rolling cycle of its genome replication, resulting in high yield of copies (382). Earlier reports applied geminiviral-based vector in several protein production in plants such as Ebola GP-based immune complex was expressed in *N. benthamiana* using geminiviral-based transient expression vector. The maximum expression level of the antigen was on day 4 after agroinfiltration with the yield of approximately 50 µg antigen per g leaf mass (12). In addition, a geminiviral expression vector was used for producing anti-Enterovirus 71 (EV71) mAb (305) and anti-human PD1 antibody (306) by co-infiltration of heavy chain (HC) and light chain (LC) of antibody protein in *N. benthamiana* yielded to 50 and 140 µg/ g FW, respectively and showed complete biological activities *in vitro* studies.

### **Construction of SARS-CoV-2 RBD-Fc and ACE2-Fc for Plant Expression**

The RBD of SARS-CoV-2 (Genbank accession number: YP\_009724390.1; F318-C617) and human ACE2 (GenBank accession number: NP\_001358344.1) was designed to join with murine leader sequence as a signal peptide for protein

localization and protein linker (GGGGs) at the N-terminus and C-terminus, respectively. The nucleotide sequences were codon optimized for expression in plants and annealed with *Xba*I and *Bam*HI restriction site at 5' and 3' ends, respectively for ligating with Fc portion, which includes SEKDEL retention peptide sequence, at the C-terminus. The nucleotide sequences were synthesized into commercial pUC57 vector with ampicillin resistance. The commercial recombinant pUC57 plasmids consisting of pUC57-SARS-CoV-2 RBD and pUC57-ACE2 were cut by *Xba*I and *Bam*HI restriction enzymes to provide SARS-CoV-2 RBD and ACE2 fragments. The digested products were subjected onto 0.6% agarose gel to visualize the expected sizes of DNA with approximately 1,000 bp (Figure 11A) and 1,900 bp (Figure 11B), respectively.

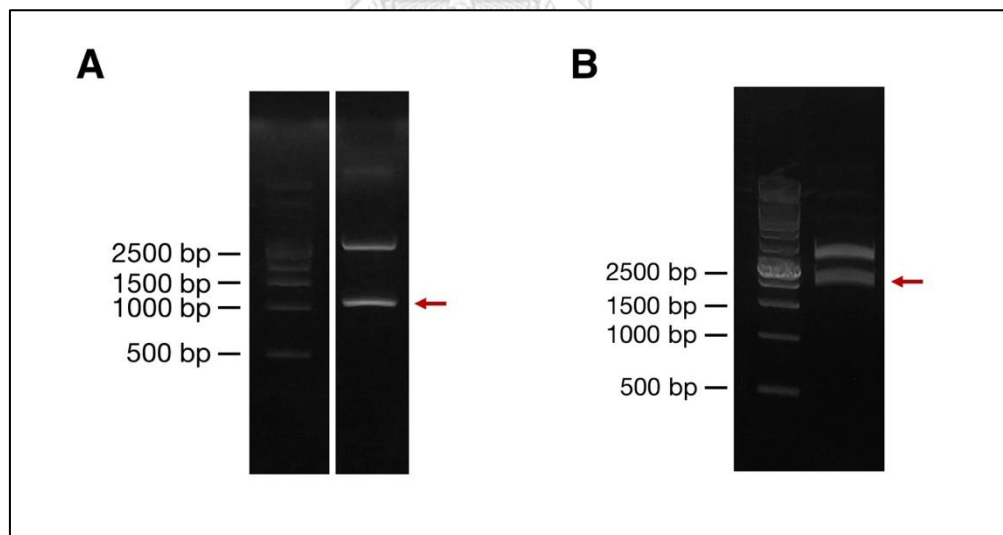
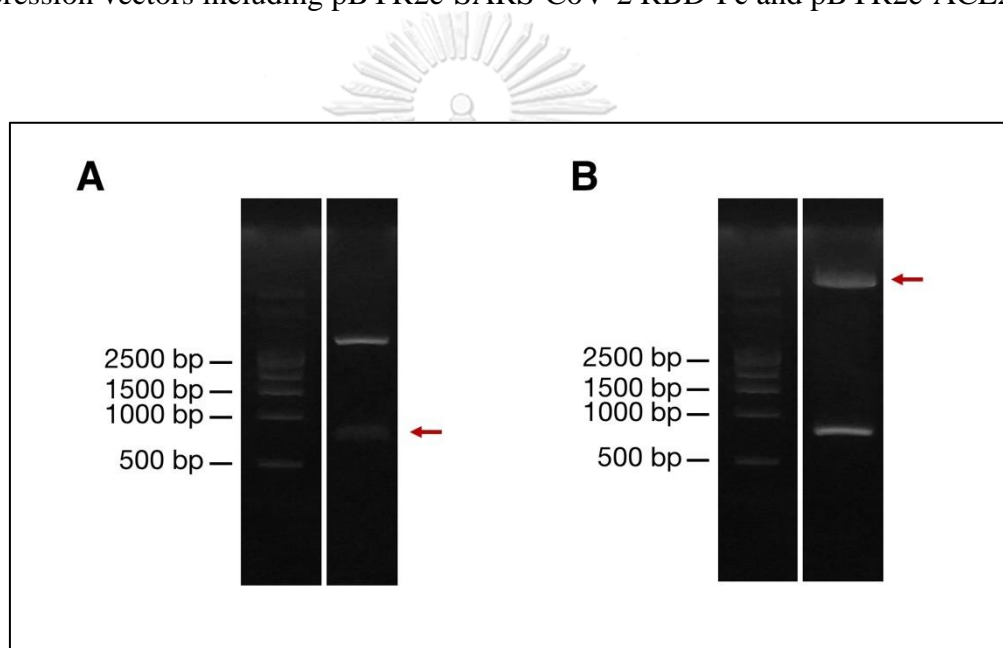


*Figure 11 Digestion of commercially synthesized genes including A. pUC57-SARS-CoV-2 and B. pUC57-ACE2 by XbaI and BamHI restriction enzymes*



The Fc fragment and pBYR2e vector were also prepared by digestion using its specific restriction enzymes including *Bam*HI and *Sac*I (Figure 12A) and *Xba*I and *Sac*I (Figure 12B) restriction enzymes, respectively for *in vitro* ligation. The DNA fragments including SARS-CoV-2 RBD, and ACE2 fragment were extracted and separately ligated with Fc fragment into geminiviral expression vector (pBYR2e) provided from Professor Hugh Mason (Arizona State University, USA) to construct expression vectors including pBYR2e-SARS-CoV-2 RBD-Fc and pBYR2e-ACE2-Fc.



CHULALONGKORN UNIVERSITY

Figure 12 Digestion of A. Fc fragment and B. pBYR2e vector by using its specific restriction enzymes including *Bam*HI and *Sac*I and *Xba*I and *Sac*I restriction enzymes, respectively for preparation of expression constructs in plants

The expression vectors were propagated in *E. coli* strain DH10B by heat shock transformation and plated on LB agar with kanamycin. The *E. coli* transformants were picked for 4 colonies to confirm by colony PCR using specific primers. The PCR products were loaded on 0.8% agarose gel to visualize the positive bands with the expected size of approximately 1,700 bp for SARS-CoV-2 RBD-Fc (Figure 13A) and 2,700 bp for ACE2-Fc (Figure 13B).

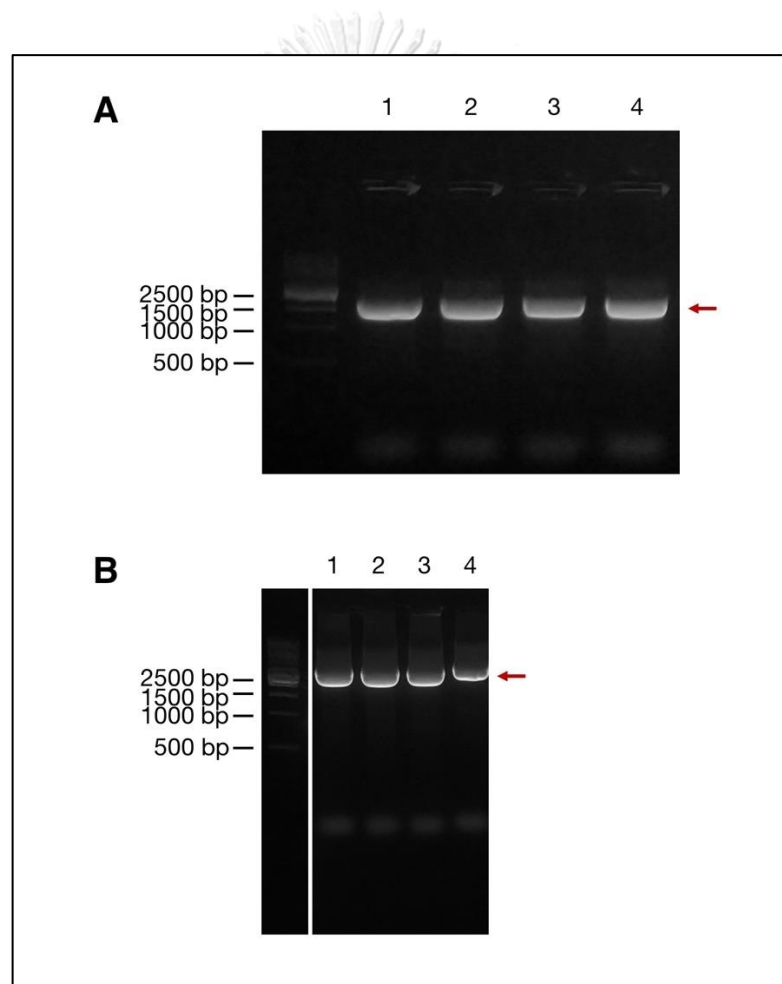


Figure 13 0.8% agarose gel of transformant *E. coli* colony PCR containing A. *pBYR2e-SARS-CoV-2 RBD-Fc* and B. *pBYR2e-ACE2-Fc*

The expression vectors were extracted from the positive *E. coli* clones used for gene transformation into *A. tumefaciens* strain GV3101 by electroporation transformation. *A. tumefaciens*-harboring pBYR2e-SARS-CoV-2 RBD-Fc and pBYR2e-ACE2-Fc clones were also confirmed by colony PCR prior to agroinfiltration in plants, which were shown in Figure 14A and B, respectively.

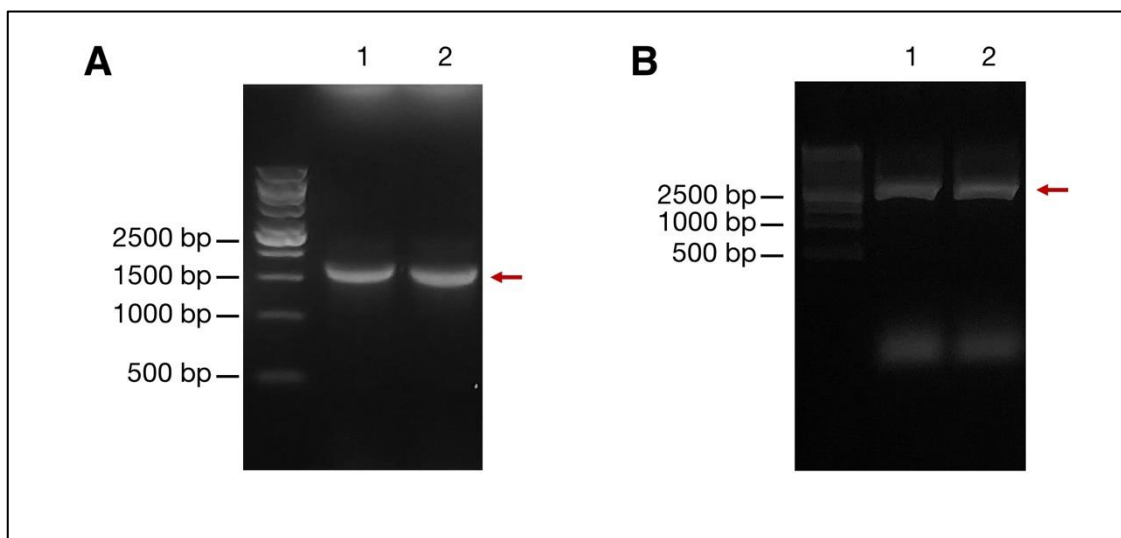
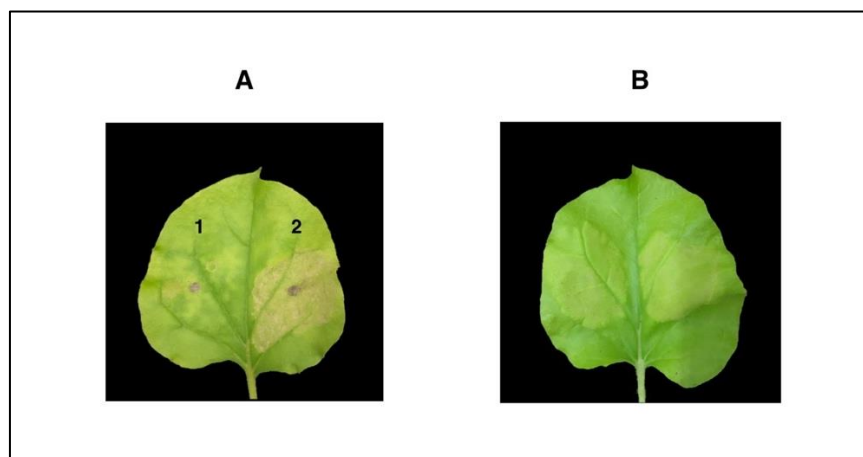


Figure 14 0.8% agarose gel of transformant *A. tumefaciens* colony PCR containing A. pBYR2e-SARS-CoV-2 RBD-Fc and B. pBYR2e-ACE2-Fc

### Transient Expression of SARS-CoV-2 RBD-Fc and ACE2-Fc in *N. benthamiana* via., Agroinfiltration

*N. benthamiana* plants were infiltrated with *Agrobacterium*-containing pBYR2e-SARS-CoV-2 RBD-Fc and pBYR2e-ACE2-Fc through syringe infiltration. The expression of the SARS-CoV-2 RBD-Fc (Figure 15A) and ACE2-Fc (Figure 15B) fusion proteins induced mild necrosis in infiltrated leaves. The infiltrated leaves were incubated and harvested from 3 individual the plants on days 2, 4, 6, 8, and 10

after agroinfiltration. The yields of recombinant proteins were measured from the crude protein by ELISA assay compare with its specific protein standard. The protein SARS-CoV-2 RBD-Fc was expressed with the level of 25 µg/g leaf fresh weight on 4 days post infiltration whereas ACE2-Fc were expressed highest on day 6 post-infiltration, with the yields up to 100 µg/g leaf fresh weight. (Figure 16).



*Figure 15 Phenotypic expression of infiltrated N. benthamiana leaves. A. leaf infiltrated with 1; Agrobacterium control and 2; Agrobacterium containing pBYR2e-SARS-CoV-2 RBD-Fc after 4 dpi. B. leaf infiltrated with Agrobacterium containing pBYR2e-ACE2-Fc after 6 dpi*

For rapid production of recombinant SARS-CoV-2 RBD-Fc protein, time-course optimization of recombinant protein did not include in the study. However, our earlier study with viral antigen expression showed that the high protein accumulation was observed between 3-5 days (295). Hence, 4 dpi was an optimal time-course, which we chose for the present study. Time course study needs to be performed for industrial scale manufacturing.

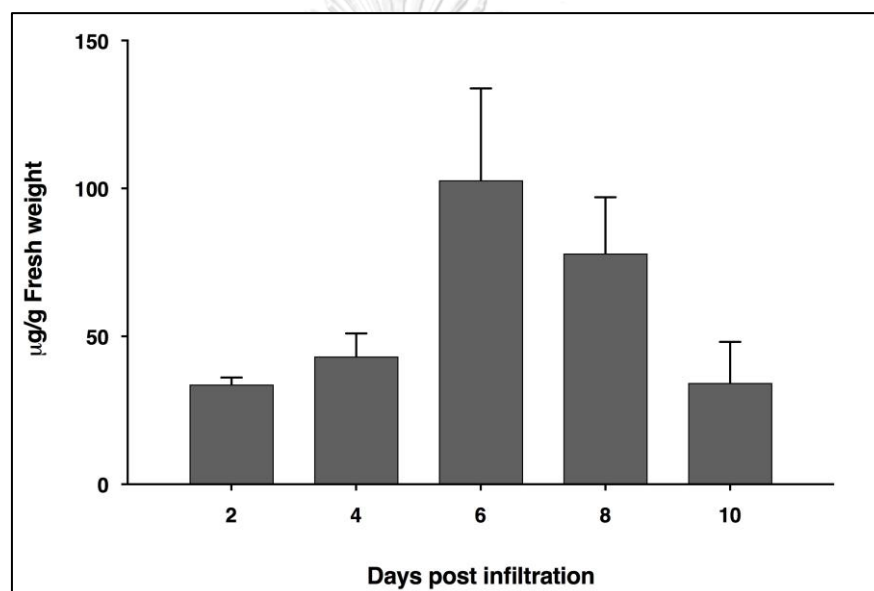


*Figure 16 Expression levels of plant-produced ACE2-Fc in each time course. The infiltrated leaves were collected from 3 individual plants in each day post infiltration. Data were analyzed by indirect ELISA assay using ACE2-specific antibody and presented as mean  $\pm$  SD of triplicates*

## **Purification and Characterization of SARS-CoV-2 RBD-Fc and ACE2-Fc Fusion Protein from *N. benthamiana* Leaves**

After time-course optimization of Fc fusion proteins, the SARS-CoV-2 RBD-Fc and ACE2-Fc were performed in large-scale protein production by vacuum infiltration, which is used as rapid-scalable production of several therapeutic proteins and vaccines in plants such as human Dental Matrix Protein 1 (hDMP1) (383) and anti-receptor activator of nuclear factor-kappa B ligand antibody (anti-RANKL) (384) for bone and dental application, human epidermal growth factor (hEGF) (385), human vascular endothelial growth factor (VEGF) (386), Ebola immune complex vaccine (12), and recombinant gp51 (rgp51) (387) and E2 glycoprotein (388) as preventive vaccines for Bovine leukemia virus (BLV), and Classical Swine Fever Virus (CSFV), respectively. The vacuum infiltration method was also applied in production of therapeutic monoclonal antibodies against viral infections including anti-Enterovirus 71 (D5) mAb (305), anti-SARS-CoV (CR3022) mAb (295), and anti-SARS-CoV-2 H4 and B38 antibodies (368).

The plant-produced SARS-CoV-2 RBD-Fc and ACE2-Fc were extracted with 1x PBS (pH 7.4) and purified from crude extract by single-step protein A affinity chromatography. Protein A is an useful and cost-effective purification method for immunoglobulins and Fc fusion proteins due to specific binding to Fc portion of IgG with high affinity providing the separation of desired IgG-related products from crude supernatants (389, 390). The protein A affinity chromatography was successfully used for purification of several IgG or IgG-related proteins (23, 295, 305, 306, 368, 384). However, additional purification is required in order to meet the quality standards for commercial use.

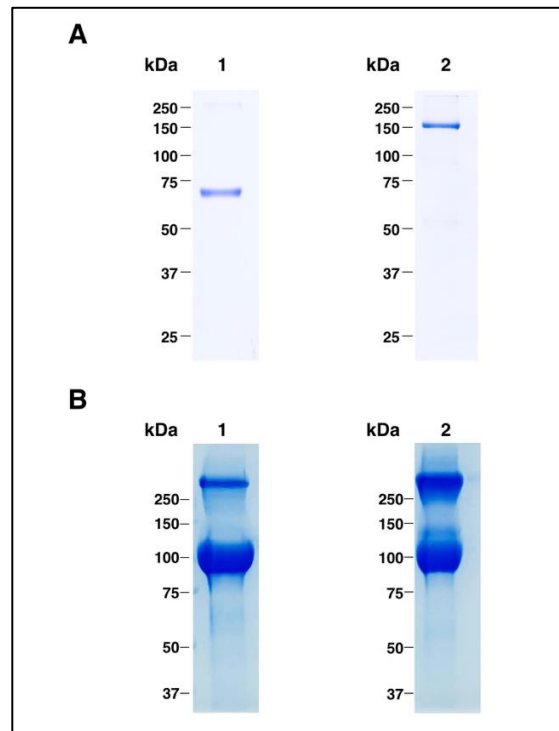


*Figure 17 SDS-PAGE analysis of plant-produced A. SARS-CoV-2 RBD-Fc and B. ACE2-Fc fusion proteins stained with Coomassie staining. 1; SDS gel under reducing condition, 2; SDS gel under non-reducing condition*

The purity of the purified plant-produced SARS-CoV-2 RBD-Fc was analyzed by SDS-PAGE gel stained with Coomassie blue staining under reducing and non-reducing condition. The results indicated that plant-produced SARS-CoV-2 RBD-Fc and ACE2-Fc fusion proteins were approximately 90% purity based on visual inspection of a Coomassie blue stained gel.

The protein bands of plant-produced SARS-CoV-2 RBD-Fc corresponding to the molecular weights of 65 and 150 kDa were observed in reducing and non-reducing condition gels (Figure 17A) whereas purified plant-produced ACE2-Fc showed two major bands at approximately 100 and 250 kDa under reducing and non-reducing condition, respectively (Figure 17B). which implies that the SARS-CoV-2 RBD-Fc and ACE2-Fc fusion proteins could be linked by disulfide bond into dimeric form. The folding of plant-produced SARS-CoV-2 RBD-Fc and ACE2-Fc fusion proteins was further confirmed by western blot analysis using the specific antibodies including a rabbit anti-SARS-CoV-2 RBD antibody and rabbit anti-human ACE2 antibody, respectively. Both plant-produced SARS-CoV-2 RBD-Fc (Figure 18A) and ACE2-Fc (Figure 18B) could be detected by its specific detection antibodies and displayed the pattern bands same as the profiles on its Coomassie blue stained gels.

To confirm the folding of Fc portion in each recombinant protein, the membranes were probed by an anti-human Gamma chain HRP conjugate antibody. The results indicated that plant-produced SARS-CoV-2 RBD-Fc and ACE2-Fc could be detected by Fc-specific antibody as shown in Figure 19. The full-length of plant-produced SARS-CoV-2 RBD-Fc and ACE2 fusion proteins could be by western blotting by using its specific antibody and goat anti-human Gamma chain-HRP conjugated antibody, which are specific to protein partner and Fc domain, respectively. The results showed that the molecular weight of both plant-produced SARS-CoV-2 RBD-Fc and ACE2-Fc fusion proteins in nitrocellulose membranes probed by different antibodies were the same molecular weight sizes (Figure 18 and 19). The plant-produced SARS-CoV-2 RBD-Fc and ACE2-Fc also showed the



several degraded bands of protein, which could be detected by its specific antibody (Figure 18 and 19).

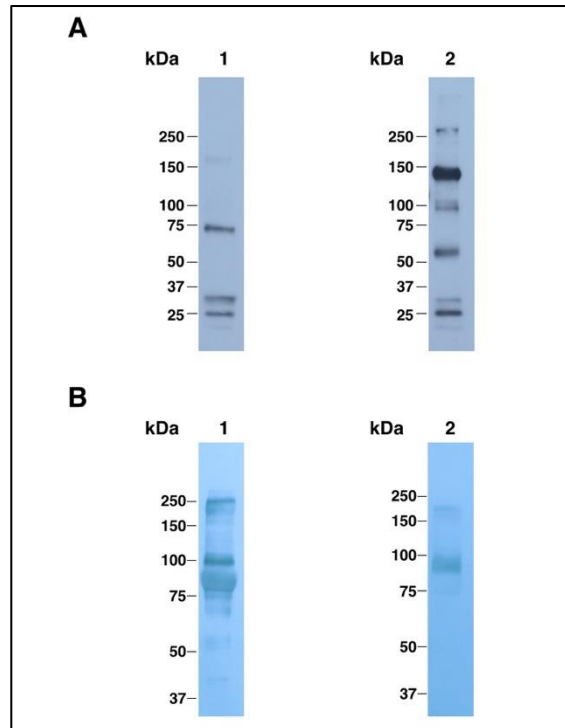
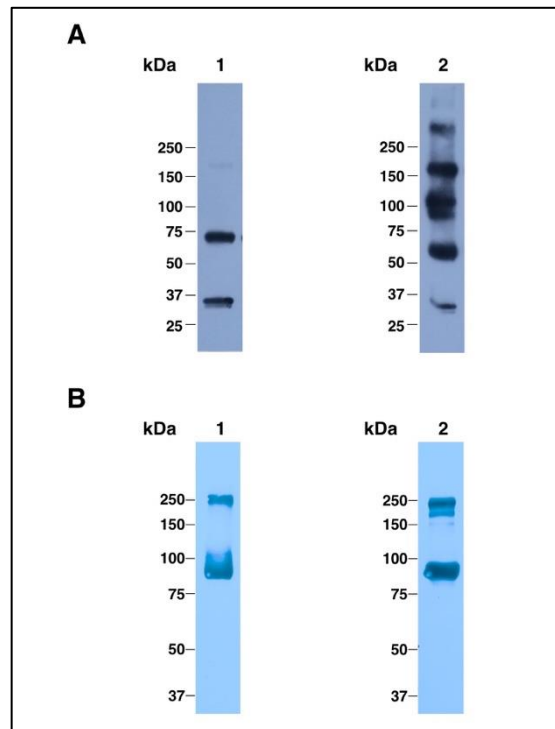


Figure 18 Western blotting analysis of A. plant-produced SARS-CoV-2 RBD-Fc and B. plant-produced ACE2-Fc fusion proteins probed with its specific antibody including a rabbit anti-SARS-CoV-2 RBD antibody and rabbit anti-human ACE2 antibody. 1; SDS gel under reducing condition, 2; SDS gel under non-reducing condition



*Figure 19 Western blotting analysis of A. plant-produced SARS-CoV-2 RBD-Fc and B. plant-produced ACE2-Fc fusion proteins probed with Fc-specific antibody 1; SDS gel under reducing condition, 2; SDS gel under non-reducing condition*

### ***In vitro* Binding Activity of Plant-Produced RBD-Fc and ACE2-Fc Fusion Proteins**

Commonly, SARS-CoV-2 RBD is able to interact with ACE2 receptor (5, 10, 391). Hence, the plant-produced SARS-CoV-2 RBD-Fc could be initially confirmed the authenticity of proteins by binding assay using the commercial ACE2-Fc protein. The binding of plant-produced SARS-CoV-2 RBD-Fc fusion protein was confirmed by ELISA by using commercial HEK293 and CHO-produced ACE2 proteins as the capture reagents. The various dilutions of purified plant-produced SARS-CoV-2 RBD-Fc were incubated with commercial ACE2 proteins with triplicate wells. Anti-

SARS-CoV-2 (H4) mAb (368) was added into the wells for SARS-CoV-2 RBD detection, followed by anti-human kappa chain-HRP conjugate antibody. Plant-produced SARS-CoV-2 RBD-Fc fusion protein produced saturable binding to both commercial ACE2 proteins with substantially high affinity in comparison to PBS control used as a negative control which confirms the authenticity of plant-produced SARS-CoV-2 RBD-Fc (Figure 20).

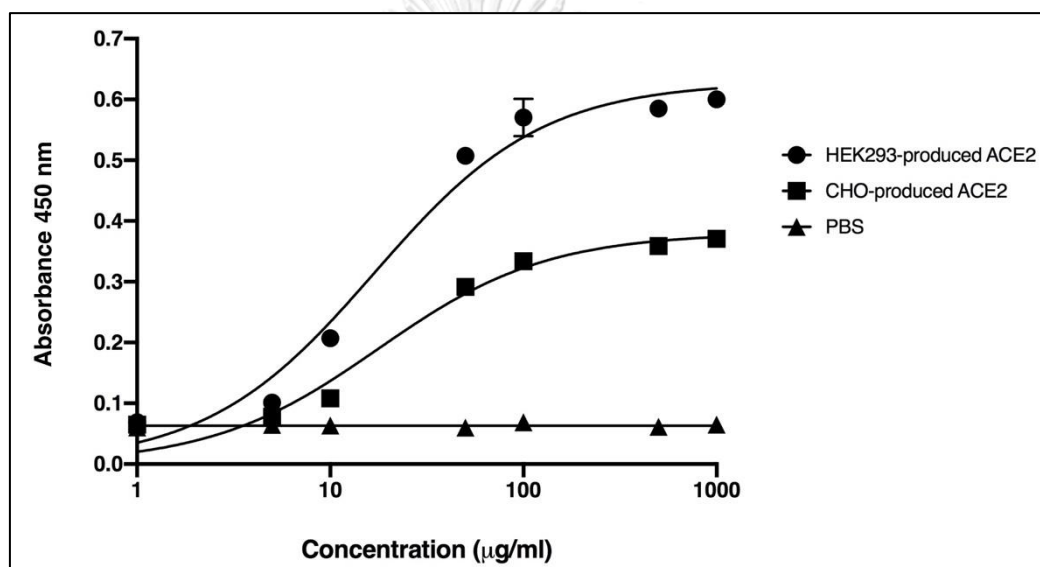


Figure 20 Binding activity of the plant-produced SARS-CoV-2 RBD-Fc using the commercial angiotensin-converting enzyme 2 (ACE2 proteins) derived from HEK293 and CHO cells and analyzed by ELISA. 1xPBS was used as negative control. Data are presented as mean  $\pm$  standard deviation (SD) of triplicates in each sample dilution

As well, the authenticity of plant-produced ACE2-Fc could be confirmed by *in vitro* binding assay using the commercial SARS-CoV-2 RBD protein. The purified ACE2-Fc fusion protein was immobilized in the wells of a microtiter plate. Eight different dilutions of the commercial Sf9-produced RBD protein of SARS-CoV-2 were incubated with plant-produced ACE2-Fc with triplicate wells. The S1 protein of the porcine epidemic diarrhea virus (PEDV) (Figure 21), and 1xPBS were used as negative controls. PEDV belongs to a monophyletic member in the order *Nidovirales* with *alphacoronavirus* subfamily, which utilizes a zinc peptidase, aminopeptidase N (APN) receptor for viral entry. Hence, S1 protein of PEDV could be used as a possible negative control in *in vitro* binding assay of plant-produced ACE2-Fc (392). The results showed that the plant-produced ACE2-Fc fusion protein produced substantially high OD signals with the RBD of SARS-CoV-2, compared to the negative PBS control and the PEDV S1 protein (Figure 22). Our data are consistent with the binding of the RBD of SARS-CoV-2 to the plant-produced ACE2-Fc fusion protein.

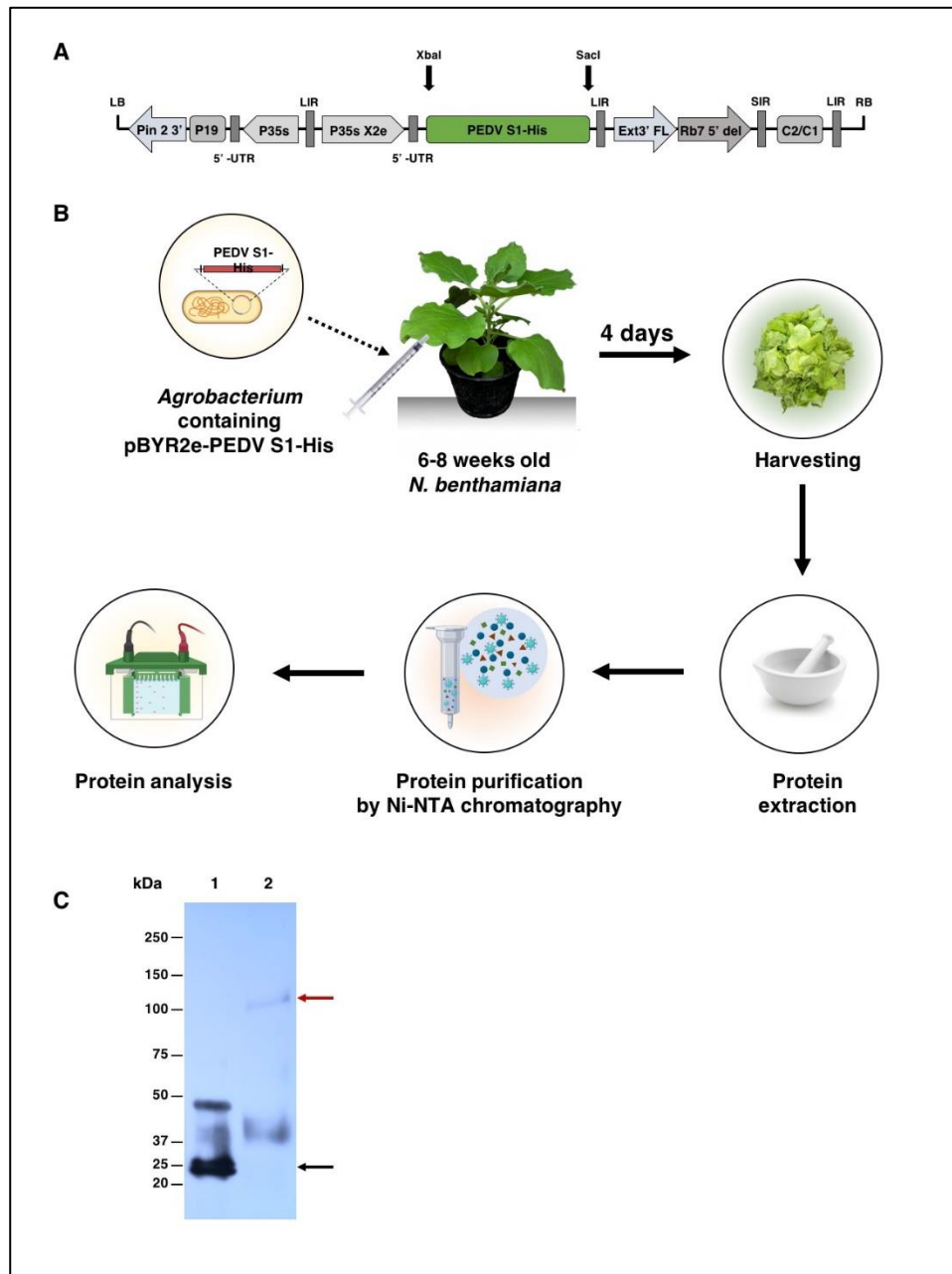


Figure 21 Expression of S1 protein of porcine epidemic diarrhea virus (PEDV) in *N. benthamiana*. A. Schematic representation showing the plant expression construct pBYR2e PEDV S1-His used. B. Diagrammatic representation showing the overview of transient expression of PEDV S1 protein in *N. benthamiana*. C. Western blotting of plant-produced PEDV S1 under reducing conditions. SARS-CoV-2 RBD-His from Sf9 cells (Genscript Biotech, USA) (lane 1; positive control) and lane 2; purified plant-

produced PEDV S1-His probed with anti-His-HRP conjugate antibody. The red and black arrows indicate the presence of S1-His of PEDV and SARS-CoV-2 RBD-His, respectively

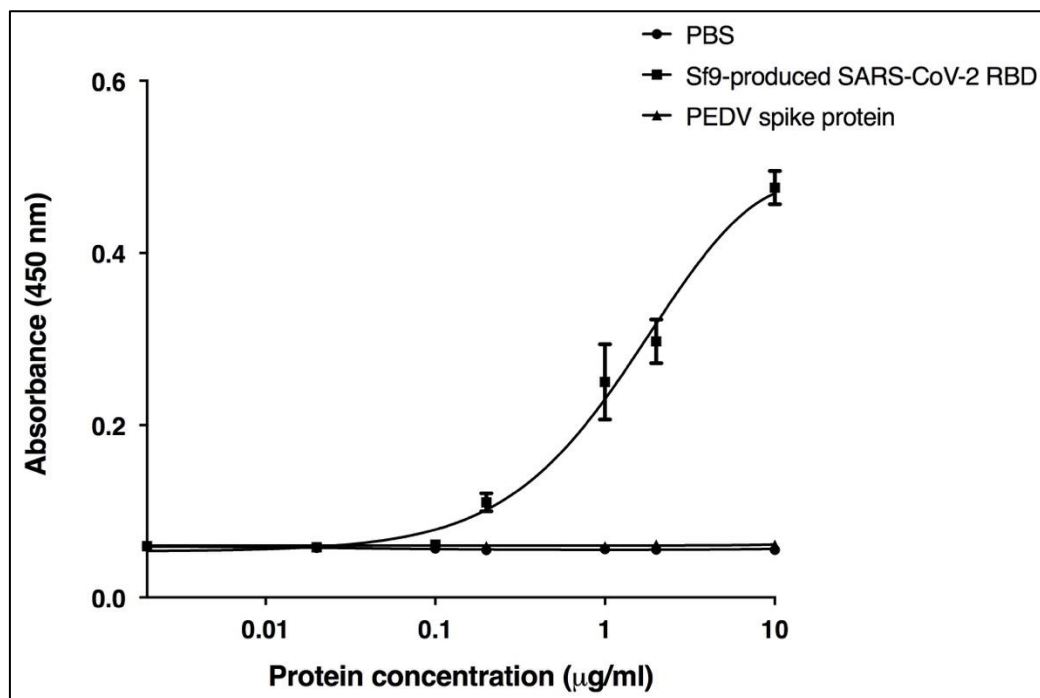


Figure 22 Binding activity of the plant-produced ACE2-Fc using the commercial Sf9-produced SARS-CoV-2 RBD protein and analyzed by ELISA. PBS buffer and S1 protein of PEDV were used as negative controls. Data are presented as mean  $\pm$  standard deviation (SD) of triplicates in each sample dilution

### **Identification of Immunoadjuvants and Mice Immunogenicity**

Compared with the other commercially available platforms of preventive vaccines, recombinant protein-based subunit vaccines provide several advantageous features, particularly high safety profiles with no risk of the vaccine-triggering disease due to the lack of live pathogen components. Hence, the protein-based subunit vaccines are considered as attractive vaccine platform and suitable for the recipients, especially immunocompromised patients. Additionally, protein subunit vaccines are easy to produce by utilizing recombinant protein techniques and relatively stable in comparison to whole virus and viral-vectored vaccines (170-173, 182). However, the absence of the immunomodulatory components associated with viral particles provide the poor immunogenicity induced by protein subunit immunogens (225, 393-397). Formulation of vaccine antigen with the potent immunologicadjuvants or immunostimulatory molecules is an attractive strategy for enhancing the immunogenicity and improving the quality of specific immune responses induced by the vaccine antigens (227, 234, 393, 394, 397, 398). Additionally, immunologic adjuvants facilitate the subunit vaccine development by several beneficial mechanisms of action such as preventing the rapid degradation of the proteins *in vivo*, enhancing the dose effectiveness of vaccines, and inducing the production of cytokines with favor development of T-helper I and II responses to vaccine antigens (242, 393, 394, 396, 399-401). Identification and selection of immunologic adjuvants are thus important for successful protein-based subunit vaccine development.

In fact, few adjuvants were approved for use in the licensed human vaccines, particularly alum was used in various human vaccines (242, 397), MF59 was used in influenza vaccines (242, 397, 402), and combination adjuvant systems such as AS01

and AS04 containing mPLA was used in malaria, hepatitis B (HBV) virus, and human papilloma virus (HPV) vaccines (242, 397, 403). In addition, there are also several experimental adjuvants, which are recruiting in clinical trials, especially poly(I:C), which are used for formulation with H5N1 influenza and cancer vaccines currently in phase III and I/II clinical stages, respectively (397, 404, 405). Immunologic adjuvants induce diverse mechanisms of action, which are critical for adjuvant selection and vaccine design to elicit appropriate immune responses against specific viral pathogens. Aluminum salts increase the stability and immunogenicity of the vaccine antigens by antigen adsorption onto alum particles and facilitate gradual release of antigens, resulting in extension of local pro-inflammatory induction at the administration site (242, 397, 406). Alum-based vaccines induce innate immunity by promoting antigen presentation by human macrophage, leading to upregulation of MHC class II and co-stimulatory molecules, especially CD40, CD 80, and CD86. Additionally, alum salts act on interleukin-4 (IL-4) secretion involving in stimulation of Th2 responses and production of IgG1 and IgE immunoglobulins, and eosinophils suggesting alum is strong inducer of Th2 responses in mice and humans (234, 397, 402, 406-408). However, alum salts suppress the protective Th1 associated immunity, which is significant for combating the intracellular pathogens (234, 242, 397). MF59, oil-in-water emulsion-based adjuvant, also induces a local immunostimulatory molecules at the injection site up-regulating several cytokines and chemokines and providing the recruitment of immune cells in the muscle (234, 242, 251, 397, 402). MF59 preferentially stimulates Th2-based immunity or a mixed Th1/Th17 and Th1/Th2 responses, which are required for intracellular pathogen protection (242, 251, 398). Interestingly, MF59 showed more effective adjuvanticity in induction of



cell-mediated immunity with safety profile against influenza virus in human populations compared to the alum salts (225, 234). mPLA allows the preferential recruitment of TIR-domain-containing adapter-inducing interferon- $\beta$  (TRIF) responding to activation of TLR4, which leads to decreasing the induction of inflammatory cytokines (260-263). MPL promotes monocytes to produce IL-10 and induces IFN- $\gamma$  expression from NK cells and CD8<sup>+</sup> T cells in mice (225, 397, 409). mPLA is found to be Th1 inducer, which increases Th1 immune responses in combination with alum adjuvant in AS04 and results to IgG2a subtype eliciting in mice (266, 397). In addition, mPLA also improves cell-mediated immunity against hepatitis B antigens in comparison to vaccine-formulated with alum alone (234, 399). Poly (I:C) activates immune responses through endosomal TLR3 and cytosolic sensors including melanocyte differentiation-associated 5 (MDA-5) and retinoic acid-inducible protein I (RIG-I), resulting in MHC class I expression and type I IFN production. Poly (I:C) promotes cross-presentation of antigens to CD8<sup>+</sup> T lymphocytes and induces the production of several chemokines and cytokines in murine respiratory tissues, which generate the activation of dendritic cells, macrophages, and neutrophils (397, 410-413). Poly (I:C) also stimulates a strong type I interferon, type III interferon, and Th1 cytokine responses, resulting in IgG2a subtype eliciting in mice that is required for the clearance of virus and other pathogens (279, 281, 397, 410, 414, 415).

### **SARS-CoV-2 RBD-specific IgG responses elicited in mice immunized by several plant-produced SARS-CoV-2 subunit vaccine formulations**

Mice immunogenicity was assessed in female ICR mice by immunizing intramuscularly with 2 doses on days 0 and 21 with 10 µg of plant-produced SARS-CoV-2 RBD-Fc fusion protein with or without several commercial adjuvants including alum, MF59, mPLA-SM, and poly (I:C). The mice immunized with PBS were served as a negative control group. Mice sera were collected for 3 timepoints on days 0, 14, and 35 to investigate the immunological profiles in terms of SARS-CoV-2-specific IgG and neutralizing antibodies. SARS-CoV-2 RBD-specific antibodies were evaluated by ELISA using commercial Sf9-produced SARS-CoV-2 RBD-His protein as a capture antigen. The plant-produced SARS-CoV-2 RBD-Fc was found to be an immunogenic, which could induce SARS-CoV-2 RBD-specific IgG antibodies in mice within second immunization (Figure 23). After second boost, the detection of anti-RBD specific IgG were significantly increased in mice immunized with plant-produced SARS-CoV-2 RBD-Fc along with aforementioned adjuvants over control group (Figure 23). Notably, mPLA-SM adjuvanted with plant-produced SARS-CoV-2 RBD-Fc showed the slight increase in SARS-CoV-2 RBD-specific IgG responses after first immunization whereas no statistical differences in total IgG antibody response were observed between the different adjuvants tested after the second immunization. In addition, mice-immunized with PBS failed to induce specific antibody responses (Figure 23).

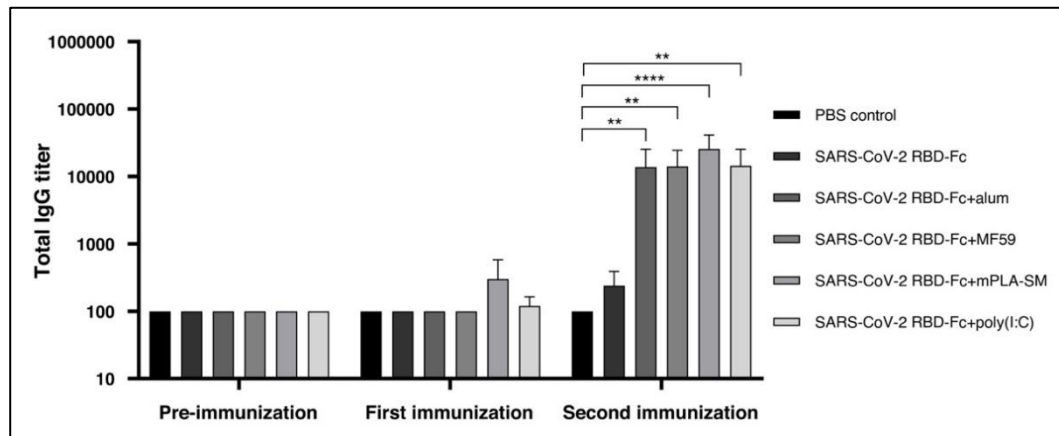


Figure 23 The SARS-CoV-2 RBD-specific total IgG antibody response elicited by mice immunized with different plant-produced SARS-CoV-2 RBD-Fc vaccine formulations. The titers were expressed as endpoint titers, which were analyzed by indirect ELISA using commercial SARS-CoV-2 RBD produced from Sf9 cells as a capture antigen and detected with goat-anti mouse IgG-HRP conjugated antibody. The immunological data were presented as mean  $\pm$  SD of the endpoint titers from five mice in each vaccination group ( $n = 5$ ). \* $p < 0.05$ ; \*\* $p < 0.01$ ; \*\*\* $p < 0.001$ ; \*\*\*\* $p < 0.0001$

**SARS-CoV-2 RBD-specific IgG1 and IgG2a subtype responses elicited in mice immunized by several plant-produced SARS-CoV-2 subunit vaccine formulations**

The levels of SARS-CoV-2 RBD-specific IgG1 and IgG2a subtypes were also comparatively evaluated, which can refer to Th2 and Th1 cellular responses in mice, respectively. The plant-produced SARS-CoV-2 RBD-Fc alone could induce detectable IgG1 and IgG2a responses in mice after the second immunization. Specifically, all of tested adjuvants enhance significant level of IgG1 responses in mice (Figure 24), whereas both mPLA-SM and poly (I:C) showed significant increase in IgG2a subtype responses in mice immunized with two doses of plant-produced SARS-CoV-2 RBD-Fc protein compared to control. (Figure 25).

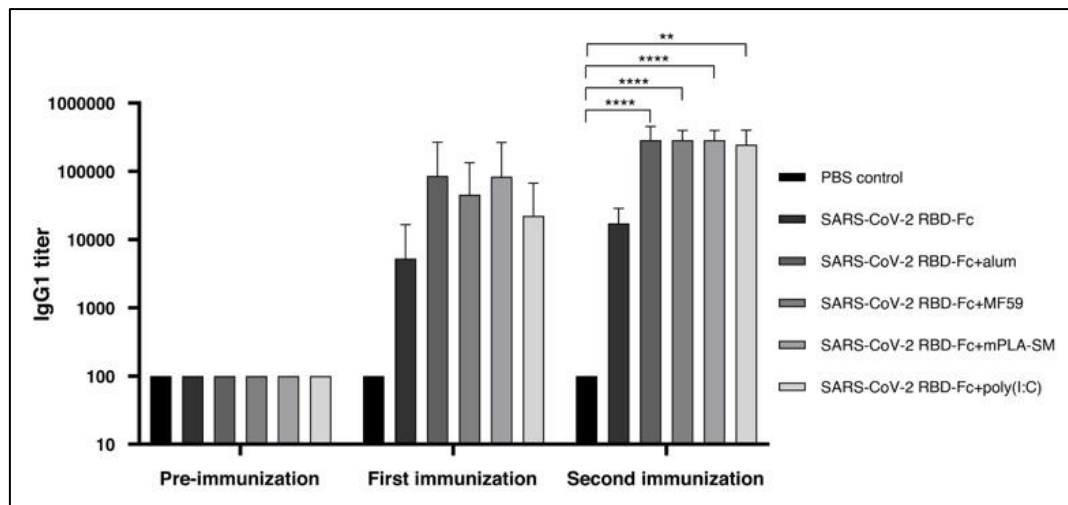


Figure 24 The endpoint titers of SARS-CoV-2 RBD-specific IgG1 detected in the immunized sera, which were collected on day 0, 14, and 35 and analyzed by indirect ELISA using commercial SARS-CoV-2 RBD produced from Sf9 cells as a capture antigen and the mouse-specific detection antibodies including goat-anti mouse IgG1-HRP and goat anti-mouse IgG2a-HRP antibody, respectively. The immunological data were presented as mean  $\pm$  SD of the endpoint titers from five mice in each vaccination group ( $n = 5$ ). \* $p < 0.05$ ; \*\* $p < 0.01$ ; \*\*\* $p < 0.001$ ; \*\*\*\* $p < 0.0001$

Interestingly, mPLA-SM and poly (I:C) induce significant levels of IgG2a subtype, which can refer to Th1-biased responses in plant-produced SARS-CoV-2 RBD-Fc vaccination as confirmed by IgG2a titers with more than 51,200-fold dilution of immunized sera after second immunization whereas alum and MF59 provided the Th2-biased immune responses (Figure 22). IgG2a subtype antibody plays a dominant role in viral clearance with high-affinity interaction of activatory Fc receptors providing effective Fc receptor-mediated immune responses (225, 416, 417). The activation of IgG2a subtype could also increase survival rate from viral infections and enhance the efficacy of vaccination and viral protection *in vivo* (416, 418-420).

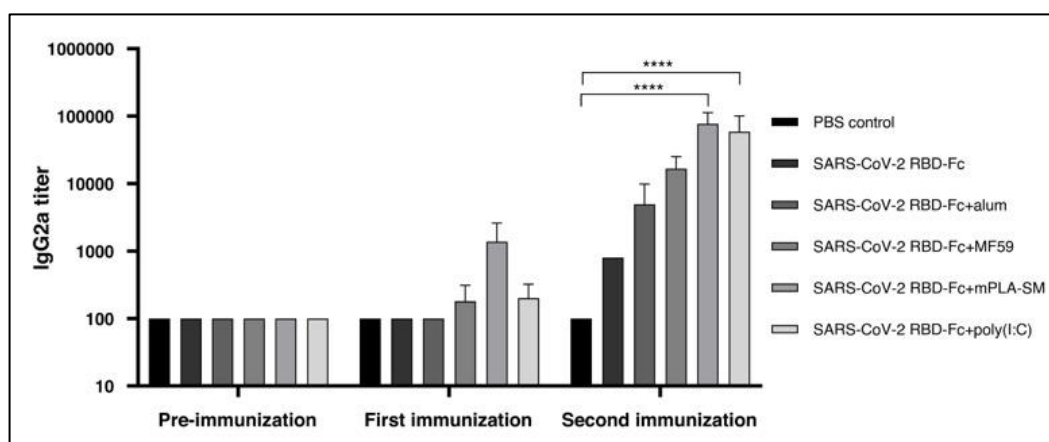


Figure 25 The endpoint titers of SARS-CoV-2 RBD-specific IgG2a detected in the immunized sera, which were collected on day 0, 14, and 35 and analyzed by indirect ELISA using commercial SARS-CoV-2 RBD produced from Sf9 cells as a capture antigen and the mouse-specific detection antibodies including goat-anti mouse IgG1-HRP and goat anti-mouse IgG2a-HRP antibody, respectively. The immunological data were presented as mean  $\pm$  SD of the endpoint titers from five mice in each vaccination group ( $n = 5$ ). \* $p < 0.05$ ; \*\* $p < 0.01$ ; \*\*\* $p < 0.001$ ; \*\*\*\* $p < 0.0001$

### Protective efficacy against live SARS-CoV-2 *in vitro*

We further assessed the neutralizing activity of immunized sera by *in vitro* microneutralization assay using Vero E6 cells. The results showed that no detectable neutralizing antibody responses were observed in mice immunized with plant-produced SARS-CoV-2 RBD-Fc alone after first immunization, whilst the neutralization titer was slightly increased with a dilution of 1:40 after the second boost (Figure 26). The plant-produced SARS-CoV-2 RBD-Fc alone was capable of eliciting neutralizing antibodies to an extent after two doses of the antigen (Figure

26). In contrast, the addition of all tested adjuvants improves its immunogenicity profiles and elicit higher neutralizing titers, which were observed after the second vaccination compared to the mice immunized with PBS and plant-produced SARS-CoV-2 RBD-Fc alone with a dilution of approximately 1:5,000 (Figure 26). However, there was no significant differences in the neutralizing titer between different tested adjuvants.

Upon SARS-CoV-2 RBD-Fc immunization, we observed that alum and mPLA-SM could significantly induce neutralizing antibody response which inhibits SARS-CoV-2 infection *in vitro* in comparison to PBS control group after the second boost (Figure 26). However, alum induced Th1 (IgG2a) responses inefficiently, hence the co-administration of alum combining with other Th1 adjuvants is needed (225, 234, 242).

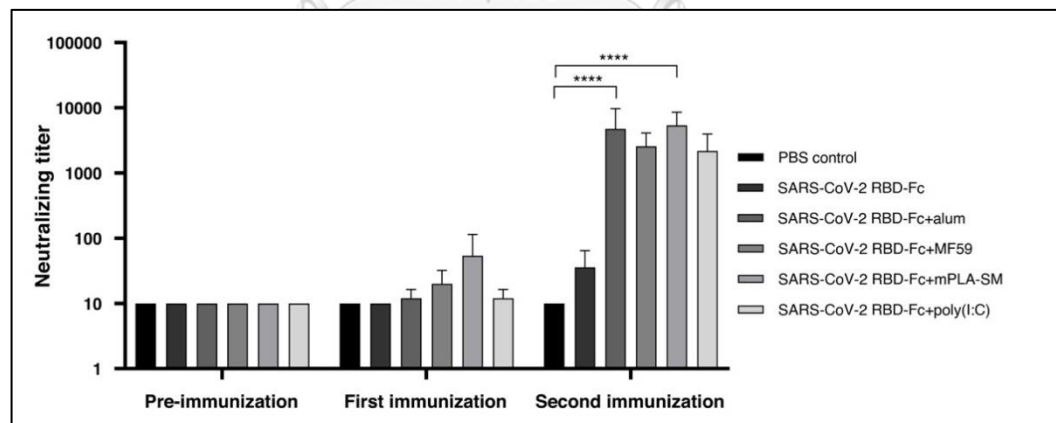


Figure 26 The neutralizing titers detected in mouse sera, which were elicited by mice immunized with several plant-produced SARS-CoV-2 RBD-Fc vaccine formulations against SARS-CoV-2. The *in vitro* neutralizing responses were assessed by microneutralization assay using Vero E6 cells. The infected cells were detected by

*anti-SARS-CoV-2 nucleocapsid mAb and goat anti-rabbit IgG-HRP antibody. The immunological data were presented as mean  $\pm$  SD of the endpoint titers from five mice in each vaccination group (n = 5). \*p < 0.05; \*\*p < 0.01; \*\*\*p < 0.001; \*\*\*\*p < 0.0001*

In ELISA, there was no or less detectable RBD-specific IgG response was observed in the mice immunized either SARS-CoV-2 RBD-Fc with or without adjuvants after first immunization (Figure 23), whereas titers were observed in IgG1 (Figure 24) after first immunization. This might be due to the high background values caused by the pre-bleed sera with the different antibodies used for analysis of IgG and IgG subtypes. However, the IgG titer values are consistent with the neutralizing antibody titer analyzed by *in vitro* neutralization assay.

#### **IFN- $\gamma$ -expressing T cells induced by several plant-produced SARS-CoV-2 subunit vaccine formulations**

The SARS-CoV-2 RBD-specific T cell immunity, which was induced by different formulations of plant-produced SARS-CoV-2 RBD-Fc was evaluated. Additionally, we appraised the comparison of the ability of immunoadjuvants including alum, MF59, mPLA-SM, and poly (I:C) in enhancing the IFN- $\gamma$  expression. To accomplish the comparative T cell-mediated immune responses, the mouse spleens were collected on day 35 (14 days after second immunization) and the levels of SARS-CoV-2 RBD-specific IFN- $\gamma$  expression were assessed from mouse splenocytes by IFN- $\gamma$  ELISpot assay. Plant-produced SARS-CoV-2 RBD-Fc itself can capable of inducing cellular immunity which can be exhibited by the expression level of IFN- $\gamma$  compared with control (Figure 27). However, formulation of antigen with the tested



adjuvants such as alum, MF59, mPLA-SM, and poly (I:C) increase the frequency of IFN- $\gamma$  secreting cells when compared with mice-immunized with plant-produced SARS-CoV-2 RBD-Fc alone or control group. The poly (I:C) elicited significantly higher level of IFN- $\gamma$  expression in comparison to the PBS control whereas no significant difference was observed between the adjuvanted groups (Figure 27). Poly (I:C) enhanced vaccine-specific cellular immunity in mice and showed the highest level of specific IFN- $\gamma$  expression at the level of 75 spots forming cell (SFCs)/ $10^6$  splenocytes. (Figure 27).



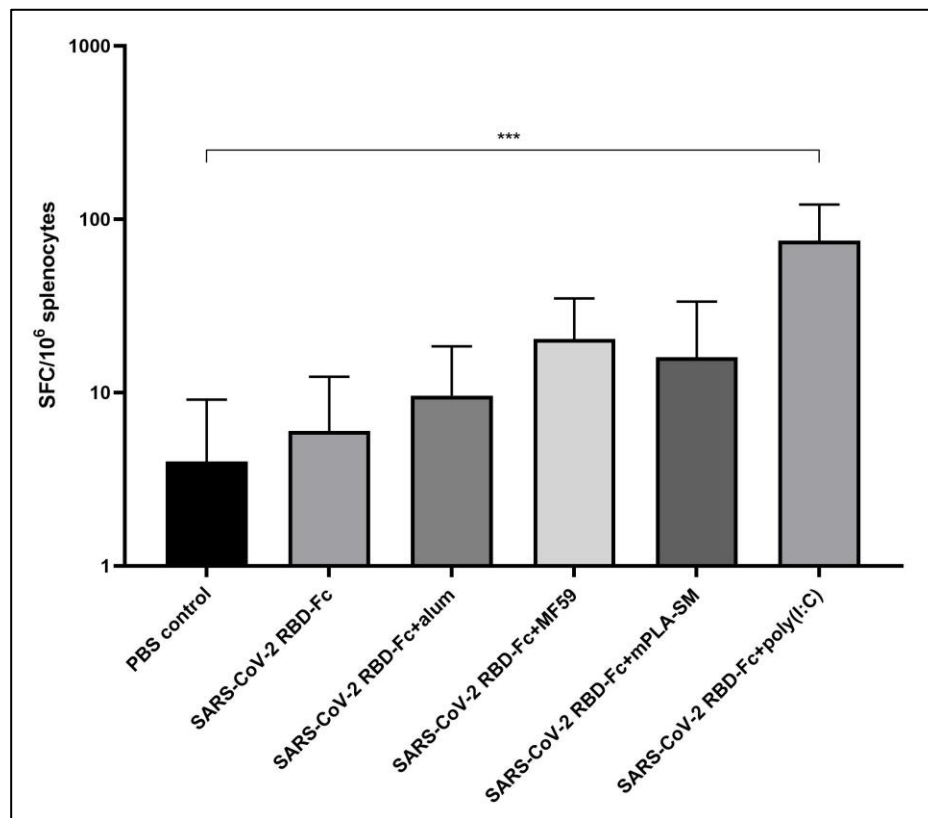


Figure 27 The levels of SARS-CoV-2 RBD-specific IFN- $\gamma$ -producing T cells expressing from mouse splenocytes immunized with different plant-produced SARS-CoV-2 RBD-Fc vaccine formulations. The IFN- $\gamma$  expression levels were quantified by mouse ELISpot assay. Data are expressed as mean  $\pm$  SD of the spot-forming cells (SFCs)/10<sup>6</sup> splenocytes from five mice in each vaccination group ( $n = 5$ ). \*  $p < 0.05$ ; \*\*  $p < 0.01$ ; \*\*\*  $p < 0.001$ ; \*\*\*\*  $p < 0.0001$

IFN- $\gamma$  is secreted from T-lymphocytes, especially CD4<sup>+</sup> T cells, which promotes the activation of macrophage and innate immunity and enhances antigen presentation mediating antiviral activity (421-423). IFN- $\gamma$  also induces the differentiation of CD4<sup>+</sup> to Th1 responses, which are required for pathogen clearance, indicating that IFN- $\gamma$  plays a critical role in vaccine-induced immunity (424-426). Based on these results, all of the adjuvants effectively elicited both humoral and cell-

mediated immune responses against the viral infection in mice compared to control. However, further studies are needed to investigate the desired effects and efficacy of the tested adjuvants in different vaccine formulations

### **Anti-SARS-CoV-2 Activity of the Plant-Produced ACE2-Fc Fusion Protein**

The plant-produced ACE2-Fc fusion protein was assessed anti-SARS-CoV-2 activities *in vitro* at the pre- and post-entry phases using live SARS-CoV-2. The serum from COVID-19 patient and an anti-human IgG were used as the positive and negative controls, respectively, for both pre- and post-treatment experiments. For the pre-entry treatment, the plant-produced ACE2-Fc protein was pre-incubated with SARS-CoV-2 at 37°C for 1 h before inoculation onto Vero E6 cells. Viral adsorption was undertaken for 2 h in the presence of the protein before removing any unbound virus. The cells were cultured for 48 h before harvesting for analysis. The ACE2-Fc fusion protein in pre-entry treatment showed lower efficiency of SARS-CoV-2 inhibition in Vero E6 cells (Figure 28A and B) The IC<sub>50</sub> of the plant-produced ACE2-Fc fusion protein for the pre-entry treatment was measured by the percentage of SARS-CoV-2 inhibition curve with 94.66 µg/ml (Figure 28C). For the post-entry treatment, the Vero E6 cells were inoculated with SARS-CoV-2 for 2h. After washing, the plant-produced ACE2-Fc protein was added and the cells were incubated for 48 h before harvesting for analysis. The results showed that the post-treatment inhibited SARS-CoV-2 infection at the concentration starting with 1 µg/ml (Figure 29A and B). The IC<sub>50</sub> for post-entry treatment was 0.84 µg/ml (Figure 29C).



infection the cells through ACE2-RBD interaction, whereas the post-infectious assay required lower concentration due to plant-produced ACE2-Fc circulation onto the infected cells providing the inhibition of SARS-CoV-2 virion release in order to infect other cells. The results suggested that the post-treatment strategy is optimal way for recombinant ACE2 therapy in COVID-19 patients.

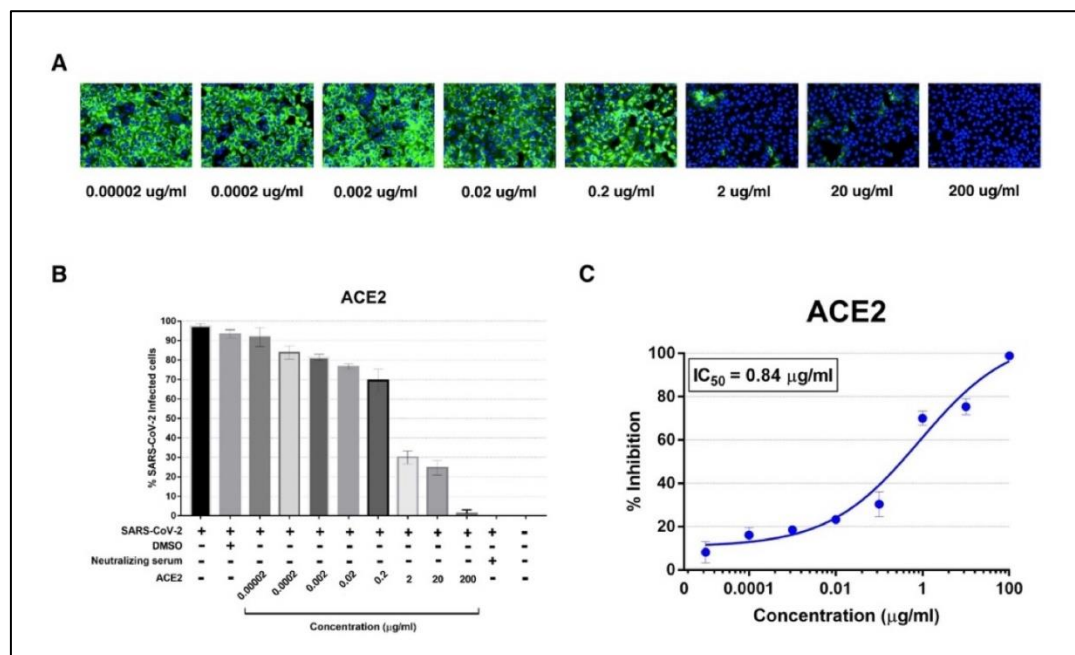


Figure 29 Dose-dependent effect of plant-produced ACE2-Fc on live SARS-CoV-2 inhibition in vitro at the post-infection phase. A. SARS-CoV-2 infection profiles in Vero E6 cells which were treated with eight concentrations of plant-produced ACE2-Fc. B. Percentage of SARS-CoV-2 inhibition in Vero E6 cells, which were treated with eight concentrations of plant-produced ACE2-Fc starting with 200  $\mu\text{g/ml}$ . C. Efficacy of SARS-CoV-2 inhibition in Vero E6 cells, which were treated by eight concentrations of plant-produced ACE2-Fc. The data were showed as mean  $\pm$  SD of triplicates in individual concentrations

## CHAPTER 4

### CONCLUSION

The emergence of SARS-CoV-2 in December 2019 has caused the global challenges in serious public health demanding the rapid development of therapeutic interventions, especially efficient vaccines, and anti-virals to counteract against the coronavirus diseases. Plant-based recombinant therapeutic proteins play a greater role in preventing and treating viral infectious diseases due to their rapid-scalable processes resulting to the establishment of numerous clinical products as shown in the use of plant-produced antibody cocktail for Ebola treatment. The strengths of plant-based technologies allow them to be served as high potential natural bioreactors and effective production system for production of valuable biopharmaceuticals and medicinal molecules, especially the ability of manufacture recombinant proteins with glycan modification providing the more complexity and complete biological activities as well as mammalian cell platform (288, 294, 330). Specifically, the use of plant-based transient expression system provides time-saving upstream processes in the recombinant proteins production with a few days, which can accelerate the therapeutic proteins against pathogen infections for testing the practical efficacy in preclinical and clinical stages before FDA approval and commercialization and allow competitive therapeutic products in the biopharmaceutical market (295, 427, 428). Plants are also used for producing vaccine candidates and therapeutic interventions for both veterinary and human applications, which show highly immunogenic and protective activities against infectious diseases and cancers (12, 288, 331, 339-343, 375). Nowadays, more plant-derived biologics have been found to be accepted by

government regulatory, particularly U.S. FDA published the GMP guidelines for production of plant-derived recombinant proteins used in human clinical trials (429).

In summary, our data demonstrated that that it was feasible to produce SARS-CoV-2 RBD protein in *N. benthamiana* plants by transient expression system. Further plant-produced recombinant protein was shown to be immunogenic in mice. The plant-based vaccine elicited both humoral and cell mediated immune responses suggesting the potential of plant-produced RBD as the effective vaccine against SARS-CoV-2. The immunogenicity of plant-produced SARS-CoV-2 RBD-Fc subunit vaccine could be enhanced by all tested adjuvants, especially mPLA-SM and poly (I:C). As well, this study showed that a plant expression system can rapidly and effectively produce a functional ACE2-Fc fusion protein on a large scale. Moreover, the plant-produced ACE2-Fc fusion protein exhibited anti-SARS-CoV-2 activities in both pre- and post-entry treatment *in vitro* but the protein showed more effective in post-infection treatment suggesting it could be used as a single therapy in post-exposure therapeutic to treat COVID-19. However, additional research is essential to further investigate the efficacy and safety of plant-produced SARS-CoV-2 RBD-Fc and ACE2-Fc to support this preliminary data. To our knowledge, this is the first report demonstrating the immunogenicity of plant-produced SARS-CoV-2 RBD subunit vaccine in mice and antiviral activities of plant-produced ACE2-Fc. Collectively, this proof-of-concept study demonstrated that the plant-produced SARS-CoV-2 RBD and ACE2 proteins could possibly be further developed as candidate vaccines and therapeutics for early-stage clinical development.

## REFERENCES

1. World Health Organization. Novel Coronavirus-China 2020 [Available from: <http://www.who.int/csr/don/12-january-2020-novel-coronavirus-china/en/>].
2. Wang M-Y, Zhao R, Gao L-J, Gao X-F, Wang D-P, Cao J-M. SARS-CoV-2: Structure, biology, and structure-based therapeutics development. *Front Cell Infect Microbiol.* 2020;10(587269).
3. Sun P, Lu X, Xu C, Sun W, Pan B. Understanding of COVID-19 based on current evidence. *J Med Virol.* 2020;92(6):548-51.
4. World Health Organization. Weekly epidemiological update on COVID-19 - 16 November 2021 2021 [Available from: <https://www.who.int/publications/m/item/weekly-epidemiological-update-on-covid-19--16-november-2021>].
5. V'kovski P, Kratzel A, Steiner S, Stalder H, Thiel V. Coronavirus biology and replication: implications for SARS-CoV-2. *Nat Rev Microbiol.* 2021;19(3):155-70.
6. Bahrami A, Ferns GA. Genetic and pathogenic characterization of SARS-CoV-2: a review. *Future Virol.* 2020.
7. Hoffmann M, Kleine-Weber H, Schroeder S, Ger NK, Herrler T, Erichsen S, et al. SARS-CoV-2 cell entry depends on ACE2 and TMPRSS2 and is blocked by a clinically proven protease inhibitor. *Cell.* 2020;181(2):271-80.
8. Walls AC, Park Y-J, Tortorici MA, Wall A, McGuire AT, Veesler D. Structure, function, and antigenicity of the SARS-CoV-2 spike glycoprotein. *Cell.* 2020;181(2):281-92.
9. Liu Z, Xu W, Xia S, Gu C, Wang X, Wang Q, et al. RBD-Fc-based COVID-19 vaccine candidate induces highly potent SARS-CoV-2 neutralizing antibody response. *Signal Transduct Target Ther.* 2020;5(282).
10. Shanmugaraj B, Siri wattananon K, Wangkanont K, Phoolcharoen W. Perspectives on monoclonal antibody therapy as potential therapeutic intervention for Coronavirus disease-19 (COVID-19). *Asian Pac J Allergy Immunol.* 2020;38(1):10-8.
11. Yang J, Wang W, Chen Z, Lu S, Yang F, Bi Z, et al. A vaccine targeting the RBD of the S protein of SARS-CoV-2 induces protective immunity. *Nature.* 2020;586:572-7.
12. Phoolcharoen W, Bhoo SH, Lai H, Ma J, Arntzen CJ, Chen Q, et al. Expression of an immunogenic Ebola immune complex in *Nicotiana benthamiana*. *Plant Biotechnol J.* 2011;9(7):807-16.
13. Siri wattananon K, Manopwisedjaroen S, Kanjanasirirat P, Purwono PB, Rattanapisit K, Shanmugaraj B, et al. Development of plant-produced recombinant ACE2-Fc fusion protein as a potential therapeutic agent against SARS-CoV-2. *Front Plant Sci.* 2021;11(604663).
14. Bellucci M, Marchis FD, Pompa A. The endoplasmic reticulum is a hub to sort proteins toward unconventional traffic pathways and endosymbiotic organelles. *J Exp Bot.* 2017;69(1):7-20.
15. Komarova TV, Baschieri S, Donini M, Marusic C, Benvenuto E, Dorokhov YL. Transient expression systems for plant-derived biopharmaceuticals. *Expert Rev Vaccines.* 2010;9(8):859-76.
16. Teh AYH, Maresch D, Klein K, Ma JKC. Characterization of VRC01, a potent and broadly neutralizing anti-HIV mAb, produced in transiently and stably transformed



tobacco. *Plant Biotechnol J*. 2014;12(3):300-11.

17. Dianos AG, Mason HS. High-level expression and enrichment of norovirus virus-like particles in T plants using modified geminiviral vectors. *Protein Expr Purif*. 2018;151:86-92.
18. Ko K, Koprowski H. Plant biopharming of monoclonal antibodies. *Virus Res*. 2005;111(1):93-100.
19. Miao Y, Ding Y, Sun Q-Y, Xu Z-F, Jiang L. Plant bioreactors for pharmaceuticals. *Biotechnol Genet Eng Rev*. 2008;25:363-80.
20. Basaran P, Rodríguez-Cerezo E. Plant molecular farming: opportunities and challenges. *Crit Rev Biotechnol*. 2008;28(3):153-72.
21. Carter PJ. Introduction to current and future protein therapeutics: a protein engineering perspective. *Exp Cell Res*. 2011;317(9):1261-9.
22. Park Y, Lee S, Kang H, Park M, Min K, Kim NH, et al. A classical swine fever virus E2 fusion protein produced in plants elicits a neutralizing humoral immune response in mice and pigs. *Biotechnol Lett*. 2020;42(7):1247-61.
23. Rattanasit K, Srifa S, Kaewpungsup P, Pavasant P, Phoolcharoen W. Plant-produced recombinant Osteopontin-Fc fusion protein enhanced osteogenesis. *Biotechnol Rep (Amst)*. 2019;21.
24. Czajkowsky DM, Hu J, Shao Z, Pleass RJ. Fc-fusion proteins: new developments and future perspectives. *EMBO Mol Med*. 2012;4:1015-28.
25. Suzuki T, Ishii-Watabe A, Tada M, Kobayashi T, Kanayasu-Toyoda T, Kawanishi T, et al. Importance of neonatal FcR in regulating the serum half-life of therapeutic proteins containing the Fc domain of human IgG1: a comparative study of the affinity of monoclonal antibodies and Fc-fusion proteins to human neonatal FcR. *J Immunol*. 2010;184(4):1968-76.
26. Kruse RL. Therapeutic strategies in an outbreak scenario to treat the novel coronavirus originating in Wuhan, China. *F1000Res*. 2020;9(72).
27. World Health Organization. WHO coronavirus disease (COVID-19) dashboard 2020 [Available from: <https://covid19.who.int>].
28. Gautret P, Million M, Jarrot P-A, Camoin-Jau L, Colson P, Fenollar F, et al. Natural history of COVID-19 and therapeutic options. *Expert Rev Clin Immunol*. 2020;16(12):1159-84.
29. Wang W, Xu Y, Gao R, Lu R, Han K, Wu G, et al. Detection of SARS-CoV-2 in different types of clinical specimens. *JAMA*. 2020;323(18):1843-4.
30. Zhai P, Ding Y, Wu X, Long J, Zhong Y, Li Y. The epidemiology, diagnosis and treatment of COVID-19. *Int J Antimicrob Agents*. 2020;55(5).
31. Carlos WG, Cruz CSD, Cao B, Pasnick S, Jamil S. Novel Wuhan (2019-nCoV) coronavirus. *Am J Respir Crit Care Med*. 2020;201(4):7-8.
32. Lauxman MA, Santucci NE, Aufrán-Gómez AM. The SARS-CoV-2 Coronavirus and the COVID-19 Outbreak. *Int Braz J Urol*. 2020;46 (Suppl 1):6-18.
33. Lu C-W, Liu X-F, Jia Z-F. 2019-nCoV transmission through the ocular surface must not be ignored. *Lancet*. 2020;395(10224).
34. Wiersinga WJ, Rhodes A, Cheng AC, Peacock SJ, Prescott HC. Pathophysiology, transmission, diagnosis, and treatment of Coronavirus Disease 2019 (COVID-19). *JAMA*. 2020;324(8):782-93.
35. Mao R, Qiu Y, He J-S, Tan J-Y, Li X-H, Liang J, et al. Manifestations and prognosis of gastrointestinal and liver involvement in patients with COVID-19: a

systematic review and meta-analysis. 2020;5(7):667-78.

36. Long B, Brady WJ, Koyfman A, Gottlieb M. Cardiovascular complications in COVID-19. *Am J Emerg Med.* 2020;38(7):1504-7.

37. Mao L, Jin H, Wang M, Hu Y, Chen S, He Q, et al. Neurologic manifestations of hospitalized patients with coronavirus disease 2019 in Wuhan, China. *JAMA Neurol.* 2020;77(6):683-90.

38. Middeldorp S, Coppens M, Haaps TFv, Foppen M, Vlaar AP, Müller MCA, et al. Incidence of venous thromboembolism in hospitalized patients with COVID-19. *J Thromb Haemost.* 2020;18(8):1995-2002.

39. Chen Y-T, Shao S-C, Hsu C-K, Wu I-W, Hung M-J, Chen Y-C. Incidence of acute kidney injury in COVID-19 infection: a systematic review and meta-analysis. *Crit Care.* 2020;24(1).

40. Rodríguez-Morales AJ, Cardona-Ospina JA, Gutiérrez-Ocampo E, Villamizar-Peña R, Holguin-Rivera Y, Escalera-Antezana JP, et al. Clinical, laboratory and imaging features of COVID-19: A systematic review and meta-analysis. *Travel Med Infect Dis.* 2020;34(101623).

41. Rothe C, Schunk M, Sothmann P, Bretzel G, Froeschl G, Wallrauch C, et al. Transmission of 2019-nCoV infection from an asymptomatic contact in Germany. *N Engl J Med.* 2020;382(10):970-1.

42. Department of Disease Control MoPH. Corona Virus Disease (COVID-19) 2021 [Available from: <https://ddc.moph.go.th/viralpneumonia/eng/index.php>.

43. Poon LLM, Peiris M. Emergence of a novel human coronavirus threatening human health. *Nat Med.* 2020;26(3):317-9.

44. Neerukonda SN, Katneni U. A review on SARS-CoV-2 virology, pathophysiology, animal Models, and anti-Viral interventions. *Pathogens.* 2020;9(6).

45. Cui J, Li F, Shi Z-L. Origin and evolution of pathogenic coronaviruses. *Nat Rev Microbiol.* 2019;17(3):181-92.

46. Masters PS. The Molecular Biology of Coronaviruses. *Adv Virus Res.* 2006;66:193-292.

47. Cheng VCC, Lau SKP, Woo PCY, Yuen KY. Severe acute respiratory syndrome coronavirus as an agent of emerging and reemerging infection. *Clin Microbiol Rev.* 2007;20(4):660-94.

48. Zhou P, Yang X-L, Wang X-G, Hu B, Zhang L, Zhang W, et al. A pneumonia outbreak associated with a new coronavirus of probable bat origin. *Nature.* 2020;579(7798):270-3.

49. Wit Ed, Doremalen Nv, Falzarano D, Munster VJ. SARS and MERS: recent insights into emerging coronaviruses. *Nat Rev Microbiol.* 2016;14(8):523-34.

50. Li Y-D, Chi W-Y, Su J-H, Ferrall L, Hung C-F, Wu T-C. Coronavirus vaccine development: from SARS and MERS to COVID-19. *J Biomed Sci.* 2020;27(1).

51. Zhu N, Zhang D, Wang W, Li X, Yang B, Song J, et al. A novel coronavirus from patients with pneumonia in China, 2019. *N Engl J Med.* 2020;382(8):727-33.

52. World Health Organization. Summary of probable SARS cases with onset of illness from 1 November 2002 to 31 July 2003 2015 [Available from: <https://www.who.int/publications/m/item/summary-of-probable-sars-cases-with-onset-of-illness-from-1-november-2002-to-31-july-2003>.

53. Organization WH. MERS situation update September 2019 2016 [Available from: <https://applications.emro.who.int/docs/EMROPub-MERS-SEP-2019->

[EN.pdf?ua=1&ua=1.](#)

54. Zhang T, Wu Q, Zhang Z. Probable pangolin origin of SARS-CoV-2 associated with the COVID-19 outbreak. *Curr Biol.* 2020;30(8).
55. Lam TT-Y, Jia N, Zhang Y-W, Shum MH-H, Jiang J-F, Zhu H-C, et al. Identifying SARS-CoV-2-related coronaviruses in Malayan pangolins. *Nature.* 2020;5837815:282-5.
56. Liu Y-C, Kuo R-L, Shih S-R. COVID-19: The first documented coronavirus pandemic in history. *Biomed J.* 2020;43(4):328-33.
57. Gorbalenya AE, Enjuanes L, Ziebuhr J, Snijder EJ. *Nidovirales*: evolving the largest RNA virus genome. *Virus Res.* 2006;117(1):17-37.
58. Khan M, Adil SF, Alkhatlan HZ, Tahir MN, Saif S, Khan M, et al. COVID-19: A global challenge with old history, epidemiology and progress so far. *Molecules.* 2021;26(1).
59. Kim D, Lee J-Y, Yang J-S, Kim JW, Kim VN, Chang H. The architecture of SARS-CoV-2 transcriptome. *Cell.* 2020;181(4):914-21.
60. Bojkova D, Klann K, Koch B, Widera M, Krause D, Ciesek S, et al. Proteomics of SARS-CoV-2-infected host cells reveals therapy targets. *Nature.* 2020;583(7816):469-72.
61. Viruses CSGotICoTo. The species Severe acute respiratory syndrome-related coronavirus: classifying 2019-nCoV and naming it SARS-CoV-2. *Nat Microbiol.* 2020;5(4):536-44.
62. Akram A, Mannan N. Molecular structure, pathogenesis and virology of SARS-CoV-2: A review. *Bangladesh J Infect Dis.* 2020;7:36-40.
63. Hu B, Guo H, Zhou P, Shi Z-L. Characteristics of SARS-CoV-2 and COVID-19. *Nat Rev Microbiol.* 2020;19(3):141-54.
64. Ou X, Liu Y, Lei X, Li P, Mi D, Ren L, et al. Characterization of spike glycoprotein of SARS-CoV-2 on virus entry and its immune cross-reactivity with SARS-CoV. *Nat Commun.* 2020;11(1).
65. Shang J, Wan Y, Luo C, Ye G, Geng Q, Auerbach A, et al. Cell entry mechanisms of SARS-CoV-2. *Proc Natl Acad Sci U S A.* 2020;117(21):11727-34.
66. Wrapp D, Wang N, Corbett KS, Goldsmith JA, Hsieh C-L, Abiona O, et al. Cryo-EM structure of the 2019-nCoV spike in the prefusion conformation. *Science.* 2020;367(6483):1260-3.
67. Stertz S, Reichelt M, Spiegel M, Kuri T, Martínez-Sobrido L, García-Sastre A, et al. The intracellular sites of early replication and budding of SARS-coronavirus. *Virology.* 2007;361(2):304-15.
68. Haan CAMd, Rottier PJM. Molecular interactions in the assembly of coronaviruses. *Adv Virus Res.* 2005;64:165-230.
69. Klein S, Cortese M, Winter SL, Wachsmuth-Melm M, Neufeldt CJ, Cerikan B, et al. SARS-CoV-2 structure and replication characterized by in situ cryo-electron tomography. *Nat Commun.* 2020;11(1).
70. Li W, Zhang C, Sui J, Kuhn JH, Moore MJ, Luo S, et al. Receptor and viral determinants of SARS-coronavirus adaptation to human ACE2. *EMBO J.* 2005;24(8):1634-43.
71. Bestle D, Heindl MR, Limburg H, van TVL, Pilgram O, Moulton H, et al. TMPRSS2 and furin are both essential for proteolytic activation of SARS-CoV-2 in human airway cells. *Life Sci Alliance.* 2020;3(9).

72. Matsuyama S, Nao N, Shirato K, Kawase M, Saito S, Takayama I, et al. Enhanced isolation of SARS-CoV-2 by TMPRSS2-expressing cells. *Proc Natl Acad Sci U S A*. 2020;117(13):7001-3.
73. Ulrich H, Pillat MM. CD147 as a target for COVID-19 treatment: Suggested effects of azithromycin and stem cell engagement. *Stem Cell Rev Rep*. 2020;16(3):434-40.
74. Iacono KT, Brown AL, Greene MI, Saouaf SJ. CD147 immunoglobulin superfamily receptor function and role in pathology. *Exp Mol Pathol*. 2007;83(3):283-95.
75. Wang K, Chen W, Zhang Z, Deng Y, Lian J-Q, Du P, et al. CD147-spike protein is a novel route for SARS-CoV-2 infection to host cells. *Signal Transduct Target Ther*. 2020;5(1).
76. Nguyen HL, Lan PD, Thai NQ, Nissley DA, O'Brien EP, Li MS. Does SARS-CoV-2 bind to human ACE2 more strongly than does SARS-CoV? *Phys Chem B*. 2020;124(34):7336-47.
77. Bakhiet M, Taurin S. SARS-CoV-2: Targeted managements and vaccine development. *Cytokine Growth Factor Rev*. 2021;58:16-29.
78. Ehlers MRW, Riordan JF. Angiotensin-converting enzyme. Zinc- and inhibitor-binding stoichiometries of the somatic and testis isozymes. *Biochemistry*. 1991;30(29):7118-26.
79. Donoghue M, F Hsieh EB, Godbout K, Gosselin M, Stagliano N, Donovan M, et al. A novel angiotensin-converting enzyme-related carboxypeptidase (ACE2) converts angiotensin I to angiotensin 1-9. *Circ Res*. 2000;87(5).
80. Skeggs LT, Dorer FE, Kahn JR, Lentz KE, Levine M. The biochemistry of the renin-angiotensin system. *Am J Med*. 1976;60(6):737-48.
81. Corvol P, Williams TA, Soubrier F. Peptidyl dipeptidase A: angiotensin I-converting enzyme. *Methods Enzymol*. 1995;248:283-305.
82. Boehm M, Nabel EG. Angiotensin-converting enzyme 2--a new cardiac regulator. *N Engl J Med*. 2002;347(22):1795-7.
83. Ni W, Yang X, Yang D, Bao J, Li R, Xiao Y, et al. Role of angiotensin-converting enzyme 2 (ACE2) in COVID-19. *Crit Care*. 2020;24(1).
84. Keidar S, Kaplan M, Gamliel-Lazarovich A. ACE2 of the heart: From angiotensin I to angiotensin (1-7). *Cardiovasc Res*. 2007;73(3):463-9.
85. Beyerstedt S, Casaro EB, Rangel ÉB. COVID-19: angiotensin-converting enzyme 2 (ACE2) expression and tissue susceptibility to SARS-CoV-2 infection. *Eur J Clin Microbiol Infect Dis*. 2021;40(5):905-19.
86. Tipnis SR, Hooper NM, Hyde R, Karran E, Christie G, Turner AJ. A human homolog of angiotensin-converting enzyme. Cloning and functional expression as a captopril-insensitive carboxypeptidase. *J Biol Chem*. 2000;275(43):33238-43.
87. Zou X, Chen K, Zou J, Han P, Hao J, Han Z. Single-cell RNA-seq data analysis on the receptor ACE2 expression reveals the potential risk of different human organs vulnerable to 2019-nCoV infection. *Front Med*. 2020;14(2):185-92.
88. Monteil V, Kwon H, Prado P, Hagelkrüys A, Wimmer RA, Stahl M, et al. Inhibition of SARS-CoV-2 infections in engineered human tissues using clinical-grade soluble human ACE2. *Cell*. 2020;181(4):905-13.
89. Yap JKY, Moriyama M, Iwasaki A. Inflammasomes and pyroptosis as therapeutic targets for COVID-19. *J Immunol*. 2020;205(2):307-12.

90. Li S, Jiang L, Li X, Lin F, Wang Y, Li B, et al. Clinical and pathological investigation of patients with severe COVID-19. *JCI Insight*. 2020;5(12).
91. Huang C, Wang Y, Li X, Ren L, Zhao J, Hu Y, et al. Clinical features of patients infected with 2019 novel coronavirus in Wuhan, China. *Lancet*. 2020;395(10223):497-506.
92. Zhou Y, Fu B, Zheng X, Wang D, Zhao C, Qi Y, et al. Pathogenic T cells and inflammatory monocytes incite inflammatory storm in severe COVID-19 patients. *Natl Sci Rev*. 2020.
93. Qin C, Zhou L, Hu Z, Zhang S, Yang S, Tao Y, et al. Dysregulation of Immune Response in Patients With Coronavirus 2019 (COVID-19) in Wuhan, China. *Clin Infect Dis*. 2020;71(15):762-8.
94. Tufan A, Güler AA, Matucci-Cerinic M. COVID-19, immune system response, hyperinflammation and repurposing antirheumatic drugs. *Turk J Med Sci*. 2020;50(SI-1):620-32.
95. Bautista-Vargas M, Bonilla-Abadía F, Cañas CA. Potential role for tissue factor in the pathogenesis of hypercoagulability associated with in COVID-19. *J Thromb Thrombolysis*. 2020.
96. Leisman DE, Ronner L, Pinotti R, Taylor MD, Sinha P, Calfee CS, et al. Cytokine elevation in severe and critical COVID-19: a rapid systematic review, meta-analysis, and comparison with other inflammatory syndromes. *Lancet Respir Med*. 2020;8(12):1233-44.
97. Xu Z, Shi L, Wang Y, Zhang J, Huang L, Zhang C, et al. Pathological findings of COVID-19 associated with acute respiratory distress syndrome. *Lancet Respir Med*. 2020;8(4):420-2.
98. ClinicalTrials.gov. CORIMUNO-19 - Tocilizumab Trial - TOCI (CORIMUNO-TOCI) (CORIMUNO-TOC) 2020 [Available from: <https://clinicaltrials.gov/ct2/show/NCT04331808>].
99. Cennimo DJ. Coronavirus Disease 2019 (COVID-19) clinical presentation 2021 [Available from: <https://emedicine.medscape.com/article/2500114-clinical>].
100. Young K. COVID-19: Steroid Lowered Mortality / Rural America / Potential Drug-Drug Interaction 2020 [Available from: <https://www.jwatch.org/fw116743/2020/06/16/covid-19-steroid-lowered-mortality-rural-america>].
101. Tang N, Bai H, Chen X, Gong J, Li D, Sun Z. Anticoagulant treatment is associated with decreased mortality in severe coronavirus disease 2019 patients with coagulopathy. *J Thromb Haemost*. 2020;18(5):1094-9.
102. Debnath SK, Srivastava R, Omri A. Emerging therapeutics for the management of COVID 19. *Expert Opin Emerg Drugs*. 2020;25(3):337-51.
103. Rattanawong P, Shen W, Masry HE, Sorajja D, Srivathsan K, Valverde A, et al. Guidance on acute management of atrial fibrillation in COVID-19. *J Am Heart Assoc*. 2020;9(14).
104. Duddu P. Coronavirus outbreak: top coronavirus drugs and vaccines in development. *Clin Trials Arena*. 2020.
105. Jeevaratnam K. Chloroquine and hydroxychloroquine for COVID-19: implications for cardiac safety. *Eur Heart J Cardiovasc Pharmacother*. 2020;6(4):256-7.
106. Mehra MR, Ruschitzka F, Patel AN. Retraction-Hydroxychloroquine or chloroquine with or without a macrolide for treatment of COVID-19: a multinational

- registry analysis. *Lancet*. 2020;395(10240).
107. Meng J, Xiao G, Zhang J, He X, Ou M, Bi J, et al. Renin-angiotensin system inhibitors improve the clinical outcomes of COVID-19 patients with hypertension. *Emerg Microbes Infect*. 2020;9(1):757-60.
108. Vaduganathan M, Vardeny O, Michel T, McMurray JJV, Pfeffer MA, Scott D. Solomon. Renin-angiotensin-aldosterone system inhibitors in patients with COVID-19. *N Engl J Med*. 2020;382:1653-9.
109. Hoffmann M, Schroeder S, Kleine-Weber H, Müller MA, Drosten C, Pöhlmann S. Nafamostat mesylate blocks activation of SARS-CoV-2: new treatment option for COVID-19. *Antimicrob Agents Chemother*. 2020;64(6).
110. Xu T, Gao X, Wu Z, Selinger DW, Zhou Z. Indomethacin has a potent antiviral activity against SARS CoV-2 in vitro and canine coronavirus in vivo. *bioRxiv*. 2020.
111. Sanders JM, Monogue ML, Jodlowski TZ, Cutrell JB. Pharmacologic treatments for coronavirus disease 2019 (COVID-19): A review. *JAMA*. 2020;323(18).
112. Scavone C, Brusco S, Bertini M, Sportiello L, Rafaniello C, Zoccoli A, et al. Current pharmacological treatments for COVID-19: What's next? *Br J Pharmacol*. 2020;177(21):4813-24.
113. Cao B, Wang Y, Wen D, Liu W, Wang J, Fan G, et al. A trial of lopinavir-ritonavir in adults hospitalized with severe Covid-19. *N Engl J Med*. 2020;382(19):1787-99.
114. Xu Z, Yao H, Shen J, Wu N, Xu Y, Lu X, et al. Nelfinavir is active against SARS-CoV-2 in Vero E6 cells. *ChemRxiv*. 2020.
115. Xu Z, Peng C, Shi Y, Zhu Z, Mu K, Wang X, et al. Nelfinavir was predicted to be a potential inhibitor of 2019-nCov main protease by an integrative approach combining homology modelling, molecular docking and binding free energy calculation. *bioRxiv*. 2020.
116. Amirian ES, Levy JK. Current knowledge about the antivirals remdesivir (GS-5734) and GS-441524 as therapeutic options for coronaviruses. *One Health*. 2020;9(100128).
117. Gordon CJ, Tchesnokov EP, Feng JY, Porter DP, Götte M. The antiviral compound remdesivir potently inhibits RNA-dependent RNA polymerase from Middle East respiratory syndrome coronavirus. *J Biol Chem*. 2020;295(15):4773-9.
118. Grein J, Ohmagari N, Shin D, Diaz G, Asperges E, Castagna A, et al. Compassionate use of remdesivir for patients with severe Covid-19. *N Engl J Med*. 2020;382(24):2327-36.
119. Joshi S, Parkar J, Ansari A, Vora A, Talwar D, Tiwaskar M, et al. Role of favipiravir in the treatment of COVID-19. *Int J Infect Dis*. 2021;102.
120. Both L, Banyard AC, Dolleweerd Cv, Wright E, Ma JK-C, Fooks AR. Monoclonal antibodies for prophylactic and therapeutic use against viral infections. *Vaccine*. 2013;31(12):1553-9.
121. Zeitlin L, Cone RA, Moench TR, Whaley KJ. Preventing infectious disease with passive immunization. *Microbes Infect*. 2000;2(6):701-8.
122. Chen L, Xiong J, Bao L, Shi Y. Convalescent plasma as a potential therapy for COVID-19. *Lancet Infect Dis*. 2020;20(4):398-400.
123. Roback JD, Guarner J. Convalescent plasma to treat COVID-19: possibilities and challenges. *JAMA*. 2020;323(16):1561-2.
124. Tanne JH. Covid-19: FDA approves use of convalescent plasma to treat

critically ill patients. *BMJ*. 2020;368(m1256).

125. Nagoba B, Gavkare A, Jamadar N, Mumbre S, Selkar S. Positive aspects, negative aspects and limitations of plasma therapy with special reference to COVID-19. *J Infect Public Health*. 2020;13(12):1818-22.

126. Lu R-M, Hwang Y-C, Liu I-J, Lee C-C, Tsai H-Z, Li H-J, et al. Development of therapeutic antibodies for the treatment of diseases. *J Biomed Sci*. 2020;27(1).

127. Group PIW, Team M-NPIS, Jr RTD, Dodd L, Proschan MA, Neaton J, et al. A randomized, controlled trial of ZMapp for ebola virus infection. *N Engl J Med*. 2016;375(15):1448-56.

128. Bayry J, Lacroix-Desmazes Sb, Kazatchkine MD, Kaveri SV. Monoclonal antibody and intravenous immunoglobulin therapy for rheumatic diseases: rationale and mechanisms of action. *Nat Clin Pract Rheumatol*. 2007;3(5):262-72.

129. Tuccori M, Ferraro S, Convertino I, Cappello E, Valdiserra G, Blandizzi C, et al. Anti-SARS-CoV-2 neutralizing monoclonal antibodies: clinical pipeline. *mAbs*. 2020;12(1).

130. Jaworski JP. Neutralizing monoclonal antibodies for COVID-19 treatment and prevention. *Biomed J*. 2020.

131. Marovich M, Mascola JR, Cohen MS. Monoclonal antibodies for prevention and treatment of COVID-19. *JAMA*. 2020;324(2):131-2.

132. Ju B, Zhang Q, Ge X, Wang R, Yu J, Shan S, et al. Potent human neutralizing antibodies elicited by SARS-CoV-2 infection. *Nature*. 2020;584:115-9.

133. Pinto D, Park Y-J, Beltramello M, Walls AC, Tortorici MA, Bianchi S, et al. Cross-neutralization of SARS-CoV-2 by a human monoclonal SARS-CoV antibody. *Nature*. 2020;583(7815):290-5.

134. Hansen J, Baum A, Pascal KE, Russo V, Giordano S, Wloga E, et al. Studies in humanized mice and convalescent humans yield a SARS-CoV-2 antibody cocktail. *Science*. 2020;369(6506):1010-4.

135. Baum A, Fulton BO, Wloga E, Copin R, Pascal KE, Russo V, et al. Antibody cocktail to SARS-CoV-2 spike protein prevents rapid mutational escape seen with individual antibodies. *Science*. 2020;369(6506):1014-8.

136. Baum A, Ajithdoss D, Copin R, Zhou A, Lanza K, Negron N, et al. REGN-COV2 antibodies prevent and treat SARS-CoV-2 infection in rhesus macaques and hamsters. *Science*. 2020;370(6520):1110-5.

137. Ju B, Zhang Q, Ge J, Wang R, Sun J, Ge X, et al. Human neutralizing antibodies elicited by SARS-CoV-2 infection. *Nature*. 2020;584(7819):115-9.

138. Shi R, Shan C, Duan X, Chen Z, Liu P, Song J, et al. A human neutralizing antibody targets the receptor-binding site of SARS-CoV-2. *Nature*. 2020;584(7819):129-4.

139. Barnes CO, Jr APW, Huey-Tubman KE, Hoffmann MAG, Sharaf NG, Hoffman PR, et al. Structures of human antibodies bound to SARS-CoV-2 spike reveal common epitopes and recurrent features of antibodies. *Cell*. 2020;182(4):828-42.

140. Robbiani DF, Gaebler C, Muecksch F, Lorenzi JCC, Wang Z, Cho A, et al. Convergent antibody responses to SARS-CoV-2 in convalescent individuals. *Nature*. 2020;584(7821):437-42.

141. Rogers TF, Zhao F, Huang D, Beutler N, Burns A, He W-T, et al. Isolation of potent SARS-CoV-2 neutralizing antibodies and protection from disease in a small animal model. *Science*. 2020;369(6506):956-63.

142. Wu Y, Wang F, Shen C, Peng W, Li D, Zhao C, et al. A noncompeting pair of human neutralizing antibodies block COVID-19 virus binding to its receptor ACE2. *Science*. 2020;368(6496):1274-8.
143. Chen X, Li R, Pan Z, Qian C, Yang Y, You R, et al. Human monoclonal antibodies block the binding of SARS-CoV-2 spike protein to angiotensin converting enzyme 2 receptor. *Cell Mol Immunol*. 2020;17:647-9.
144. Brouwer PJM, Caniels TG, Straten Kvd, Snitselaar JL, Aldon Y, Bangaru S, et al. Potent neutralizing antibodies from COVID-19 patients define multiple targets of vulnerability. *Science*. 2020;369(6504):643-50.
145. Seydoux E, Homad LJ, MacCamy AJ, Parks KR, Hurlburt NK, Jennewein MF, et al. Analysis of a SARS-CoV-2-infected individual reveals development of potent neutralizing antibodies with limited somatic mutation. *Immunity*. 2020;53(1):98-105.
146. Zost SJ, Gilchuk P, Chen RE, Case JB, Reidy JX, Trivette A, et al. Rapid isolation and profiling of a diverse panel of human monoclonal antibodies targeting the SARS-CoV-2 spike protein. *Nat Med*. 2020;26(9):1422-7.
147. Cao Y, Su B, Guo X, Sun W, Deng Y, Bao L, et al. Potent neutralizing antibodies against SARS-CoV-2 identified by high-throughput single-cell sequencing of convalescent patients' B cells. *Cell*. 2020;182(1):73-84.
148. Chi X, Yan R, Zhang J, Zhang G, Zhang Y, Hao M, et al. A neutralizing human antibody binds to the N-terminal domain of the Spike protein of SARS-CoV-2. *Science*. 2020;369(6504):650-5.
149. Meulen Jt, Brink ENvd, Poon LLM, Marissen WE, Leung CSW, Cox F, et al. Human monoclonal antibody combination against SARS coronavirus: synergy and coverage of escape mutants. *PLoS Med*. 2006;3(7):1071-9.
150. Huo J, Zhao Y, Ren J, Zhou D, Duyvesteyn HME, Ginn HM, et al. Neutralization of SARS-CoV-2 by destruction of the prefusion spike. *Cell Host Microbe*. 2020;28(3):445-54.
151. Yuan M, Wu NC, Zhu X, Lee C-CD, So RTY, Lv H, et al. A highly conserved cryptic epitope in the receptor-binding domains of SARS-CoV-2 and SARS-CoV. *Science*. 2020;368(6491):630-3.
152. Wang C, Li W, Drabek D, Okba NMA, Haperen Rv, Osterhaus ADME, et al. A human monoclonal antibody blocking SARS-CoV-2 infection. *Nat Commun*. 2020;11(1).
153. Lv Z, Deng Y-Q, Ye Q, Cao L, Sun C-Y, Fan C, et al. Structural basis for neutralization of SARS-CoV-2 and SARS-CoV by a potent therapeutic antibody. *Science*. 2020;369(6510):1505-9.
154. Wec AZ, Wrapp D, Herbert AS, Maurer DP, Haslwanter D, Sakharkar M, et al. Broad neutralization of SARS-related viruses by human monoclonal antibodies. *Science*. 2020;369(6504):731-6.
155. Wrapp D, Vliieger DD, Corbett KS, Torres GM, Wang N, Breedam WV, et al. Structural basis for potent neutralization of betacoronaviruses by single-domain camelid antibodies. *Cell*. 2020;181(5):1004-15.
156. Glasgow A, Glasgow J, Limonta D, Solomon P, Lui I, Zhang Y, et al. Engineered ACE2 receptor traps potentially neutralize SARS-CoV-2. *Proc Natl Acad Sci U S A*. 2020;117(45):28046-55.
157. Wang Q, Zhang Y, Wu L, Niu S, Song C, Zhang Z, et al. Structural and functional basis of SARS-CoV-2 entry by using human ACE2. *Cell*. 2020;181(4):894-



904.

158. Lei C, Qian K, Li T, Zhang S, Fu W, Ding M, et al. Neutralization of SARS-CoV-2 spike pseudotyped virus by recombinant ACE2-Ig. *Nat Commun.* 2020;11(2070).

159. Li F, Li W, Farzan M, Harrison SC. Structure of SARS coronavirus spike receptor-binding domain complexed with receptor. *Science.* 2005;309(5472):1864-688.

160. Wu K, Li W, Peng G, Li F. Crystal structure of NL63 respiratory coronavirus receptor-binding domain complexed with its human receptor. *Proc Natl Acad Sci U S A.* 2009;106(47):19970-4.

161. Li W, Moore MJ, Vasilieva N, Sui J, Wong SK, Berne MA, et al. Angiotensin-converting enzyme 2 is a functional receptor for the SARS coronavirus. *Nature.* 2003;426(6965):450-4.

162. Sui J, Li W, Murakami A, Tamin A, Matthews LJ, Wong SK, et al. Potent neutralization of severe acute respiratory syndrome (SARS) coronavirus by a human mAb to S1 protein that blocks receptor association. *Proc Natl Acad Sci U S A.* 2004;101(8):2536-41.

163. Moore MJ, Dorfman T, Li W, Wong SK, Li Y, Kuhn JH, et al. Retroviruses pseudotyped with the severe acute respiratory syndrome coronavirus spike protein efficiently infect cells expressing angiotensin-converting enzyme 2. *J Virol.* 2004;78(19):10628-35.

164. Karakus U, Pohl MO, Stertz S. Breaking the convention: sialoglycan variants, co-receptors and alternative receptors for influenza A virus entry. *J Virol.* 2020;94(4).

165. Apeiron Biologics. APN01 – Our work on a potential drug candidate for COVID-19 treatment 2021 [Available from: <https://www.apeiron-biologics.com/our-work-on-a-potential-drug-candidate-for-covid-19/>].

166. Zou Z, Yan Y, Shu Y, Gao R, Sun Y, Li X, et al. Angiotensin-converting enzyme 2 protects from lethal avian influenza A H5N1 infections. *Nat Commun.* 2014;5(3594).

167. Haschke M, Schuster M, Poglitsch M, Loibner H, Salzberg M, Bruggisser M, et al. Pharmacokinetics and pharmacodynamics of recombinant human angiotensin-converting enzyme 2 in healthy human subjects. *Clin Pharmacokinet.* 2013;52(9):783-92.

168. Khan A, Benthin C, Zeno B, Albertson TE, Boyd J, Christie JD, et al. A pilot clinical trial of recombinant human angiotensin-converting enzyme 2 in acute respiratory distress syndrome. *Crit Care.* 2017;21(1).

169. Nichol KL, Mendelman PM, Mallon KP, Jackson LA, Gorse GJ, Belshe RB, et al. Effectiveness of live, attenuated intranasal influenza virus vaccine in healthy, working adults: a randomized controlled trial. *JAMA.* 1999;282(2):137-44.

170. Amanat F, Krammer F. SARS-CoV-2 vaccines: status report. *Immunity.* 2020;52(4):583-9.

171. Kaur SP, Gupta V. COVID-19 vaccine: A comprehensive status report. *Virus Res.* 2020;288(198114).

172. Ng WH, Liu X, Mahalingam S. Development of vaccines for SARS-CoV-2. *F1000Res.* 2020;9.

173. Riel Dv, Wit Ed. Next-generation vaccine platforms for COVID-19. *Nat Mater.* 2020;19(8):810-2.

174. Hussein IH, Chams N, Chams S, Sayegh SE, Badran R, Raad M, et al. Vaccines

through centuries: Major cornerstones of global health. *Front Public Health*. 2015;3(269).

175. Poland GA, Ovsyannikova IG, Crooke SN, Kennedy RB. SARS-CoV-2 vaccine development: current status. *Mayo Clin Proc*. 2020;95(10):2172-88.

176. Gao Q, Bao L, Mao H, Wang L, Xu K, Yang M, et al. Development of an inactivated vaccine candidate for SARS-CoV-2. *Science*. 2020;369(6499):77-81.

177. Xia S, Zhang Y, Wang Y, Wang H, Yang Y, Gao GF, et al. Safety and immunogenicity of an inactivated SARS-CoV-2 vaccine, BBIBP-CorV: a randomised, double-blind, placebo-controlled, phase 1/2 trial. *Lancet Infect Dis*. 2021;21(1):39-51.

178. Mathew S, Faheem M, Hassain NA, Benslimane FM, Thani AAA, Zaraket H, et al. Platforms exploited for SARS-CoV-2 vaccine development. *Vaccines*. 2021;9(11).

179. Wang H, Zhang Y, Huang B, Deng W, Quan Y, Wang W, et al. Development of an Inactivated Vaccine Candidate, BBIBP-CorV, with Potent Protection against SARS-CoV-2. *Cell*. 2020;182(3):713-21.

180. Xia S, Zhang Y, Wang Y, Wang H, Yang Y, Gao GF, et al. Safety and immunogenicity of an inactivated SARS-CoV-2 vaccine, BBIBP-CorV: a randomised, double-blind, placebo-controlled, phase 1/2 trial. *Lancet Infect Dis*. 2021;21(1):39-51.

181. Xia S, Duan K, Zhang Y, Zhao D, Zhang H, Xie Z, et al. Effect of an inactivated vaccine against SARS-CoV-2 on safety and immunogenicity outcomes: interim analysis of 2 randomized clinical trials. *JAMA*. 2020;324(10):951-60.

182. Fuenmayor J, Gòdia F, Cervera L. Production of virus-like particles for vaccines. *N Biotechnol*. 2017;39:174-80.

183. Jackson LA, Anderson EJ, Roupheal NG, Roberts PC, Makhene M, Coler RN, et al. An mRNA vaccine against SARS-CoV-2 — Preliminary report. *N Engl J Med*. 2020.

184. Anderson EJ, Roupheal NG, Widge AT, Jackson LA, Roberts PC, Makhene M, et al. Safety and immunogenicity of SARS-CoV-2 mRNA-1273 vaccine in older adults. *N Engl J Med*. 2020;383(25):2427-38.

185. Vogel AB, Kanevsky I, Che Y, Swanson KA, Muik A, Vormehr M, et al. BNT162b vaccines protect rhesus macaques from SARS-CoV-2. *Nature*. 2021;592(7853):283-9.

186. Mulligan MJ, Lyke KE, Kitchin N, Absalon J, Gurtman A, Lockhart S, et al. Phase 1/2 study of COVID-19 RNA vaccine BNT162b1 in adults. *Nature*. 2020;586(7830):589-93.

187. Walsh EE, Frenck R, Falsey AR, Kitchin N, Absalon J, Gurtman A, et al. RNA-based COVID-19 vaccine BNT162b2 selected for a pivotal efficacy study. *medRxiv*. 2020.

188. Walsh EE, Jr RWF, Falsey AR, Kitchin N, Absalon J, Gurtman A, et al. Safety and immunogenicity of two RNA-based covid-19 vaccine candidates. *N Engl J Med*. 2020;383(25):2439-50.

189. Sahin U, Muik A, Derhovanessian E, Vogler I, Kranz LM, Vormehr M, et al. COVID-19 vaccine BNT162b1 elicits human antibody and TH1 T-cell responses. *Nature*. 2020;586(7830):594-9.

190. Smith TRF, Patel A, Ramos S, Elwood D, Zhu X, Yan J, et al. Immunogenicity of a DNA vaccine candidate for COVID-19. *Nat Commun*. 2020;11(2601).

191. Tebas P, Yang S, Boyer JD, Reuschel EL, Patel A, Christensen-Quick A, et al. Safety and immunogenicity of INO-4800 DNA vaccine against SARS-CoV-2: A

- preliminary report of an open-label, Phase 1 clinical trial. *EClinicalMedicine*. 2021;31(100689).
192. Trials G-C. Safety and immunogenicity study of GX-19, a COVID-19 preventive DNA vaccine in healthy adults 2020 [Available from: <https://clinicaltrials.gov/ct2/show/NCT04445389?term=vaccine&cond=covid-19&draw=3>].
193. Wu S, Zhong G, Zhang J, Shuai L, Zhang Z, Wen Z, et al. A single dose of an adenovirus-vectored vaccine provides protection against SARS-CoV-2 challenge. *Nat Commun*. 2020;11(1).
194. Zhu F-C, Li Y-H, Guan X-H, Hou L-H, Wang W-J, Li J-X, et al. Safety, tolerability, and immunogenicity of a recombinant adenovirus type-5 vectored COVID-19 vaccine: a dose-escalation, open-label, non-randomised, first-in-human trial. *Lancet*. 2020;395(10240):1845-54.
195. Zhu F-C, Guan X-H, Li Y-H, Huang J-Y, Jiang T, Hou L-H, et al. Immunogenicity and safety of a recombinant adenovirus type-5-vectored COVID-19 vaccine in healthy adults aged 18 years or older: a randomised, double-blind, placebo-controlled, phase 2 trial. *Lancet*. 2020;396(10249):479-88.
196. Doremalen Nv, Lambe T, Spencer A, Belij-Rammerstorfer S, Purushotham JN, Port JR, et al. ChAdOx1 nCoV-19 vaccine prevents SARS-CoV-2 pneumonia in rhesus macaques. *Nature*. 2020;586(7830):578-82.
197. Folegatti PM, Ewer KJ, Aley PK, Angus B, Becker S, Belij-Rammerstorfer S, et al. Safety and immunogenicity of the ChAdOx1 nCoV-19 vaccine against SARS-CoV-2: a preliminary report of a phase 1/2, single-blind, randomised controlled trial. *Lancet*. 2020;396(10249):467-78.
198. AstraZeneca. AZD1222 vaccine met primary efficacy endpoint in preventing COVID-19 2020 [Available from: <https://www.astrazeneca.com/media-centre/press-releases/2020/azd1222h1r.html>].
199. Phillips N, Cyranoski D, Mallapaty S. A leading coronavirus vaccine trial is on hold: scientists react. *Nature*. 2020.
200. Logunov DY, Dolzhikova IV, Zubkova OV, Tukhvatulin AI, Shcheblyakov DV, Dzharrullaeva AS, et al. Safety and immunogenicity of an rAd26 and rAd5 vector-based heterologous prime-boost COVID-19 vaccine in two formulations: two open, non-randomised phase 1/2 studies from Russia. *Lancet*. 2020;396(10255):887-97.
201. Johnson J. Johnson & Johnson prepares to resume Phase 3 ENSEMBLE trial of its Janssen COVID-19 vaccine candidate in the U.S. 2020 [Available from: <https://www.jnj.com/our-company/johnson-johnson-prepares-to-resume-phase-3-ensemble-trial-of-its-janssen-covid-19-vaccine-candidate-in-the-us>].
202. Tian J-H, Patel N, Haupt R, Zhou H, Weston S, Hammond H, et al. SARS-CoV-2 spike glycoprotein vaccine candidate NVX-CoV2373 immunogenicity in baboons and protection in mice. *Nat Commun*. 2021;12(372).
203. Guebre-Xabier M, Patel N, Tian J-H, Zhou B, Maciejewski S, Lam K, et al. NVX-CoV2373 vaccine protects cynomolgus macaque upper and lower airways against SARS-CoV-2 challenge. *Vaccine*. 2020;38(50):7892-6.
204. Keech C, Albert G, Cho I, Robertson A, Reed P, Neal S, et al. Phase 1-2 trial of a SARS-CoV-2 recombinant spike protein nanoparticle vaccine. *N Engl J Med*. 2020;383(24):2320-32.
205. Ward BJ, Gobeil P, Séguin A, Atkins J, Boulay I, Charbonneau P-Y, et al. Phase

- 1 randomized trial of a plant-derived virus-like particle vaccine for COVID-19. *Nat Med.* 2021;27(6):1071-8.
206. To KK-W, Tsang OT-Y, Leung W-S, Tam AR, Wu T-C, Lung DC, et al. Temporal profiles of viral load in posterior oropharyngeal saliva samples and serum antibody responses during infection by SARS-CoV-2: an observational cohort study. *Lancet Infect Dis.* 2020;20(5):565-74.
207. Awadasseid A, Wu Y, Tanaka Y, Zhang W. Current advances in the development of SARS-CoV-2 vaccines. *Int J Biol Sci.* 2021;17(1):8-19.
208. Du L, He Y, Zhou Y, Liu S, Zheng B-J, Jiang S. The spike protein of SARS-CoV--a target for vaccine and therapeutic development. *Nat Rev Microbiol.* 2009;7(3):226-36.
209. Zakhartchouk AN, Sharon C, Satkunarajah M, Auperin T, Viswanathan S, Mutwiri G, et al. Immunogenicity of a receptor-binding domain of SARS coronavirus spike protein in mice: implications for a subunit vaccine. *Vaccine.* 2007;25(1):136-43.
210. Li F. Structure, function, and evolution of coronavirus spike proteins. *Annu Rev Virol.* 2016;3(1):237-61.
211. Quinlan BD, Mou H, Zhang L, Guo Y, He W, Ojha A, et al. The SARS-CoV-2 receptor-binding domain elicits a potent neutralizing response without antibody-dependent enhancement. *bioRxiv.* 2020.
212. Suthar MS, Zimmerman MG, Kauffman RC, Mantus G, Linderman SL, Hudson WH, et al. Rapid generation of neutralizing antibody responses in COVID-19 patients. *Cell Rep Med.* 2020;1(3).
213. Ni L, Fang, Cheng M-L, Feng Y, Deng Y-Q, Zhao H, et al. Detection of SARS-CoV-2-specific humoral and cellular immunity in COVID-19 convalescent individuals. *Immunity.* 2020;52(6):971-7.
214. Liu J, Sun Y, Qi J, Chu F, Wu H, Gao F, et al. The membrane protein of severe acute respiratory syndrome coronavirus acts as a dominant immunogen revealed by a clustering region of novel functionally and structurally defined cytotoxic T-lymphocyte epitopes. *J Infect Dis.* 2010;202(8):1171-80.
215. Nieto-Torres JL, DeDiego ML, Verdía-Báguena C, Jimenez-Guardeño JM, Regla-Nava JA, Fernandez-Delgado R, et al. Severe acute respiratory syndrome coronavirus envelope protein ion channel activity promotes virus fitness and pathogenesis. *PLoS Pathog.* 2014;10(5).
216. Kim TW, Lee JH, Hung C-F, Peng S, Roden R, Wang M-C, et al. Generation and characterization of DNA vaccines targeting the nucleocapsid protein of severe acute respiratory syndrome coronavirus. *J Virol.* 2004;78(9):4638-45.
217. Collisson EW, Pei J, Dzielawa J, Seo SH. Cytotoxic T lymphocytes are critical in the control of infectious bronchitis virus in poultry. *Dev Comp Immunol.* 2000;24(2-3):187-200.
218. Buchholz UJ, Bukreyev A, Yang L, Lamirande EW, Murphy BR, Subbarao K, et al. Contributions of the structural proteins of severe acute respiratory syndrome coronavirus to protective immunity. *Proc Natl Acad Sci U S A.* 2004;101(26):9804-9.
219. Zhang Y, Zhang J, Chen Y, Luo B, Yuan Y, Huang F, et al. The ORF8 Protein of SARS-CoV-2 Mediates Immune Evasion through Potently Downregulating MHC-I. *bioRxiv.* 2020.
220. Gordon DE, Jang GM, Bouhaddou M, Xu J, Obernier K, White KM, et al. A SARS-CoV-2 protein interaction map reveals targets for drug repurposing. *Nature.*

2020;583(7816):459-68.

221. Wang M, Jiang S, Wang Y. Recent advances in the production of recombinant subunit vaccines in *Pichia pastoris*. *Bioengineered*. 2016;7(3):155-65.
222. Bill RM. Recombinant protein subunit vaccine synthesis in microbes: a role for yeast? *J Pharm Pharmacol*. 2015;67(3):319-28.
223. Bill RM. Playing catch-up with *Escherichia coli*: using yeast to increase success rates in recombinant protein production experiments. *Front Microbiol*. 2014;5(85).
224. Vartak A, Sucheck SJ. Recent advances in subunit vaccine carriers. *Vaccines (Basel)*. 2016;4(2).
225. Zhang N, Channappanavar R, Ma C, Wang L, Tang J, Garron T, et al. Identification of an ideal adjuvant for receptor-binding domain-based subunit vaccines against Middle East respiratory syndrome coronavirus. *Cell Mol Immunol*. 2016;13(2):180-90.
226. Kurella S, Manocha M, Sabhnani L, Thomas B, Rao DN. New age adjuvants and delivery systems for subunit vaccines. *Indian J Clin Biochem*. 2000;15:83-100.
227. Zhang N, Jiang S, Du L. Current advancements and potential strategies in the development of MERS-CoV vaccines. *Expert Rev Vaccines*. 2014;13(6):761-74.
228. Chen DJ, Osterrieder N, Metzger SM, Buckles E, Doody AM, DeLisa MP, et al. Delivery of foreign antigens by engineered outer membrane vesicle vaccines. *Proc Natl Acad Sci U S A*. 2010;107:7.
229. Foged C. Subunit vaccines of the future: the need for safe, customized and optimized particulate delivery systems. *Ther Deliv*. 2011;2(8):1057-77.
230. Petrovsky N, Aguilar JC. Vaccine adjuvants: current state and future trends. *Immunol Cell Biol*. 2004;82(5):488-96.
231. McElrath MJ. Selection of potent immunological adjuvants for vaccine construction. *Semin Cancer Biol*. 1995;6(6):375-85.
232. Marx PA, Compans RW, Gettie A, Staas JK, Gilley RM, Mulligan MJ, et al. Protection against vaginal SIV transmission with microencapsulated vaccine. *J Virol*. 1993;260(5112):1323-7.
233. Douce G, Turcotte C, Cropley I, Roberts M, Pizza M, Domenghini M, et al. Mutants of *Escherichia coli* heat-labile toxin lacking ADP-ribosyltransferase activity act as nontoxic, mucosal adjuvants. *Proc Natl Acad Sci U S A*. 1995;92(5):1644-8.
234. Burakova Y, Madera R, McVey S, Schlup JR, Shi J. Adjuvants for animal vaccines. *Viral Immunol*. 2018;31(1):11-22.
235. Gupta T, Gupta SK. Potential adjuvants for the development of a SARS-CoV-2 vaccine based on T experimental results from similar coronaviruses. *Int Immunopharmacol*. 2020;86(106717).
236. plc. G. Developing COVID-19 vaccines 2020 [Available from: <https://www.gsk.com/en-gb/media/resource-centre/our-contribution-to-the-fight-against-2019-ncov/>].
237. Coler RN, Bertholet S, Moutaftsi M, Guderian JA, Windish HP, Baldwin SL, et al. Development and characterization of synthetic glucopyranosyl lipid adjuvant system as a vaccine adjuvant. *PLoS One*. 2011;6(1).
238. iBio I. IBIO-201 demonstrates ability to elicit anti-SARS-CoV-2 immune response in preclinical studies 2020 [Available from: <https://www.ibioinc.com/ibio-provides-update-on-ibio-201-covid-19-vaccine-program/>].
239. Soligenix I. Soligenix licenses BTG's CoVaccine HT for SARS-CoV-2 2020

[Available from: <https://www.contractpharma.com/content-microsite/covid-19/2020-04-16/soligenix-licenses-btgs-covaccine-ht-for-sars-cov-2>.

240. Lakhan N, Stevens NE, Diener KR, Hayball JD. CoVaccine HT™ adjuvant is superior to Freund's adjuvants in eliciting antibodies against the endogenous alarmin HMGB1. *J Immunol Methods*. 2016;439:37-43.
241. Bodewes R, Kreijtz JHCM, Amerongen Gv, Geelhoed-Mieras MM, Verburgh RJ, Heldens JGM, et al. A single immunization with CoVaccine HT-adjuvanted H5N1 influenza virus vaccine induces protective cellular and humoral immune responses in ferrets. *J Virol*. 2010;84(16):7943-52.
242. Mbow ML, Gregorio ED, Valiante NM, Rappuoli R. New adjuvants for human vaccines. *Curr Opin Immunol*. 2010;22(3):411-6.
243. Gupta R. Aluminum compounds as vaccine adjuvants. *Adv Drug Deliv Rev*. 1998;32(3):155-72.
244. HogenEsch H. Mechanisms of stimulation of the immune response by aluminum adjuvants. *Front Immunol*. 2012;3.
245. Ulanova M, Tarkowski A, Hahn-Zoric M, Hanson LA. The common vaccine adjuvant aluminum hydroxide up-regulates accessory properties of human monocytes via an interleukin-4-dependent mechanism. *Infect Immun*. 2001;69(2):1151-9.
246. Brewer JM, Conacher M, Satoskar A, Bluethmann H, Alexander J. In interleukin-4-deficient mice, alum not only generates T helper 1 responses equivalent to Freund's complete adjuvant, but continues to induce T helper 2 cytokine production. *Eur J Immunol*. 1996;26(9):2062-6.
247. HogenEsch H, O'Hagan DT, Fox CB. Optimizing the utilization of aluminum adjuvants in vaccines: you might just get what you want. *NPJ Vaccines*. 2018;3(51).
248. Pini A, Danskin D, Coackley W. Comparative evaluation of the potency of beta-propiolactone inactivated Newcastle disease vaccines prepared from a lentogenic strain and a velogenic strain. *Vet Rec*. 1965;30:127-9.
249. Sellers RF, Herniman KA. Early protection of pigs against foot and mouth disease. *Br Vet J*. 1974;130(5):440-5.
250. O'Hagan DT, Ott GS, Nest GV, Rappuoli R, Giudice GD. The history of MF59® adjuvant: a phoenix that arose from the ashes. *Expert Rev Vaccines*. 2013;12(1):13-30.
251. Ko E-J, Kang S-M. Immunology and efficacy of MF59-adjuvanted vaccines. *Hum Vaccin Immunother*. 2018;14(12):3041-5.
252. Podda A. The adjuvanted influenza vaccines with novel adjuvants: experience with the MF59-adjuvanted vaccine. *Vaccine*. 2001;19(17-19):2673-80.
253. Clark TW, Pareek M, Hoschler K, Dillon H, Nicholson KG, Groth N, et al. Trial of 2009 influenza A (H1N1) monovalent MF59-adjuvanted vaccine. *N Engl J Med*. 2009;361(25):2424-35.
254. Fang J-H, Hora M. The adjuvant MF59: A 10-year perspective. *Methods Mol Med*. 2000;42:211-28.
255. Mosca F, Tritto E, Muzzi A, Monaci E, Bagnoli F, Iavarone C, et al. Molecular and cellular signatures of human vaccine adjuvants. *Proc Natl Acad Sci U S A*. 2008;105(30):10501-6.
256. Seubert A, Monaci E, Pizza M, O'Hagan DT, Wack A. The adjuvants aluminum hydroxide and MF59 induce monocyte and granulocyte chemoattractants and enhance monocyte differentiation toward dendritic cells. *J Immunol*. 2008;180(8):5402-12.

257. O'Hagan DT, Ott GS, Gregorio ED, Seubert A. The mechanism of action of MF59 – An innately attractive adjuvant formulation. *Vaccine*. 2012;30(29):4341-8.
258. Dupuis M, Murphy TJ, Higgins D, Ugozzoli M, Nest Gv, Ott G, et al. Dendritic cells internalize vaccine adjuvant after intramuscular injection. *Cell Immunol*. 1998;186(1):18-27.
259. Baudner BC, Ronconi V, Casini D, Tortoli M, Kazzaz J, Singh M, et al. MF59 emulsion is an effective delivery system for a synthetic TLR4 agonist (E6020). *Pharm Res*. 2009;26(6):1477-85.
260. Casella CR, Mitchell TC. Putting endotoxin to work for us: monophosphoryl lipid A as a safe and effective vaccine adjuvant. *Cell Mol Life Sci*. 2008;65(20):3231-40.
261. Sivakumar SM, Safhi MM, Kannadasan M, Sukumaran N. Vaccine adjuvants – Current status and prospects on controlled release adjuvancity. *Saudi Pharm J*. 2011;19(4):197-206.
262. Mata-Haro V, Cekic C, Martin M, Chilton PM, Casella CR, Mitchell TC. The vaccine adjuvant monophosphoryl lipid A as a TRIF-biased agonist of TLR4. *Science*. 2007;316(5831):1628-32.
263. Patil HP, Murugappan S, Veer Wt, Meijerhof T, Haan Ad, Frijlink HW, et al. Evaluation of monophosphoryl lipid A as adjuvant for pulmonary delivered influenza vaccine. *J Control Release*. 2014;174:51-62.
264. Fransen F, Boog CJ, Putten Jpv, Ley Pvd. Agonists of Toll-like receptors 3, 4, 7, and 9 are candidates for use as adjuvants in an outer membrane vaccine against *Neisseria meningitidis* serogroup. *Infect Immun*. 2007;75(12):5939-46.
265. Rhee EG, Kelley RP, Agarwal I, Lynch DM, Porte AL, Simmons NL, et al. TLR4 Ligands Augment Antigen-Specific CD8+ T Lymphocyte Responses Elicited by a Viral Vaccine Vector. *J Virol*. 2010;84(19):10413-9.
266. Didierlaurent AM, Morel S, Lockman L, Giannini SL, Bisteau M, Carlsen H, et al. AS04, an aluminum salt- and TLR4 agonist-based adjuvant system, induces a transient localized innate immune response leading to enhanced adaptive immunity. *J Immunol*. 2009;183(10):6186-97.
267. Du X, Poltorak A, Wei Y, Beutler B. Three novel mammalian toll-like receptors: gene structure, expression, and evolution. *Eur Cytokine Netw*. 2000;11(3):362-71.
268. Martínez-Campos C, Burguete-García AI, Madrid-Marina V. Role of TLR9 in oncogenic virus-produced cancer. *Viral Immunol*. 2017;30(2):98-105.
269. Notley CA, Jordan CK, McGovern JL, Brown MA, Ehrenstein MR. DNA methylation governs the dynamic regulation of inflammation by apoptotic cells during efferocytosis. *Sci Rep*. 2017;7(42204).
270. Barry M, Cooper C. Review of hepatitis B surface antigen-1018 ISS adjuvant-containing vaccine safety and efficacy. *Expert Opin Biol Ther*. 2007;7(11):1731-7.
271. Schellack C, Prinz K, Egyed A, Fritz JH, Wittmann B, Ginzler M, et al. IC31, a novel adjuvant signaling via TLR9, induces potent cellular and humoral immune responses. *Vaccine*. 2006;24(26):5461-72.
272. Schijns VEJC. Mechanisms of vaccine adjuvant activity: initiation and regulation of immune responses by vaccine adjuvants. *Vaccine*. 2003;21(9-10):829-31.
273. Agger EM, Rosenkrands I, Olsen AW, Hatch G, Williams A, Kritsch C, et al. Protective immunity to tuberculosis with Ag85B-ESAT-6 in a synthetic cationic adjuvant system IC31. *Vaccine*. 2006;24(26):5452-60.

274. Aagaard C, Hoang TTKT, Izzo A, Billeskov R, Troudt J, Arnett K, et al. Protection and polyfunctional T cells induced by Ag85B-TB10.4/IC31 against *Mycobacterium tuberculosis* is highly dependent on the antigen dose. *PLoS Med*. 2009;4(6).
275. Kane M, Case LK, Wang C, Yurkovetskiy L, Dikiy S, Golovkina TV. Innate immune sensing of retroviral infection via Toll-like receptor 7 occurs upon viral entry. *Immunity*. 2011;35(1):135-45.
276. Patel MC, Shirey KA, Pletneva LM, Boukhvalova MS, Garzino-Demo A, Vogel SN, et al. Novel drugs targeting Toll-like receptors for antiviral therapy. *Future Virol*. 2014;9(9):811-29.
277. Vender RB, Goldberg O. Innovative uses of imiquimod. *J Drugs Dermatol*. 2005;4(1):58-63.
278. Kumar A, Zhang J, Yu F-SX. Toll-like receptor 3 agonist poly(I:C)-induced antiviral response in human corneal epithelial cells. *Immunology*. 2006;117(1):11-21.
279. Frank-Bertoncelj M, Pisetsky DS, Kolling C, Michel BA, Gay RE, Jüngel A, et al. TLR3 ligand Poly(I:C) exerts distinct actions in synovial fibroblasts when delivered by extracellular vesicles. *Front Immunol*. 2018;9(28).
280. Harris P, Sridhar S, Peng R, Phillips JE, Cohn RG, Burns L, et al. Double-stranded RNA induces molecular and inflammatory signatures that are directly relevant to COPD. *Mucosal Immunol*. 2012;6(3):474-84.
281. Li Y-G, Siripanyaphinyo U, Tumkosit U, Noranate N, A-Nuegoonpipat A, Pan Y, et al. Poly (I:C), an agonist of toll-like receptor-3, inhibits replication of the Chikungunya virus in BEAS-2B cells. *Virology*. 2012;9(114).
282. Guillot L, Goffic RL, Bloch S, Escriou N, Akira S, Chignard M, et al. Involvement of Toll-like receptor 3 in the immune response of lung epithelial cells to double-stranded RNA and influenza A virus. *J Biol Chem*. 2005;280(7):5571-80.
283. Isogawa M, Robek MD, Furuichi Y, Chisari FV. Toll-like receptor signaling inhibits hepatitis B virus replication in vivo. *J Virol*. 2005;79(11):7269-72.
284. Zhou Y, Wang X, Liu M, Hu Q, Song L, Ye L, et al. A critical function of Toll-like receptor-3 in the induction of anti-human immunodeficiency virus activities in macrophages. *Immunology*. 2010;131(1):40-9.
285. Mazaleuskaya L, Veltrop R, Ikpeze N, Martin-Garcia J, Navas-Martin S. Protective role of Toll-like receptor 3-induced type I interferon in murine coronavirus infection of macrophages. *Viruses*. 2012;4(5):901-23.
286. Naumann K, Wehner R, Schwarze A, Petzold C, Schmitz M, Rohayem J. Activation of dendritic cells by the novel Toll-like receptor 3 agonist RGC100. *Clin Dev Immunol*. 2013;2013(283649).
287. Yao J, Weng Y, Dickey A, Wang KY. Plants as factories for human pharmaceuticals: applications and challenges. *Int J Mol Sci*. 2015;16(12):28549-65.
288. Shanmugaraj B, Bulaon CJI, Phoolcharoen W. Plant molecular farming: A viable platform for recombinant biopharmaceutical production. *Plants*. 2020;9(842).
289. Demain AL, Vaishnav P. Production of recombinant proteins by microbes and higher organisms. *Biotechnol Adv*. 2009;27(3):297-306.
290. Vitale A, Denecke Jr. The endoplasmic reticulum-gateway of the secretory pathway. *Plant Cell*. 1999;11(4):615-28.
291. Strasser R, Stadlmann J, Schähs M, Stiegler G, Quendler H, Mach L, et al. Generation of glyco-engineered *Nicotiana benthamiana* for the production of



- monoclonal antibodies with a homogeneous human-like N-glycan structure. *Plant Biotechnol J*. 2008;6(4):392-402.
292. Gomes AR, Munivenkatappa S, Belamaranahally B, Veeregowda M, Balamurugan V. An overview of heterologous expression host systems for the production of recombinant proteins. *Adv Anim Vet Sci*. 2016;4(7):346-56.
293. Ma JK-C, Drake PMW, Christou P. The production of recombinant pharmaceutical proteins in plants. *Nat Rev Genet*. 2003;4(10):794-805.
294. Burnett MJB, Burnett AC. Therapeutic recombinant protein production in plants: Challenges and opportunities. *Plants, People, Planet*. 2019;2(2):121-32.
295. Rattanapisit K, Shanmugaraj B, Manopwisedjaroen S, Purwono PB, Siriwattananon K, Khorattanakulchai N, et al. Rapid production of SARS-CoV-2 receptor binding domain (RBD) and spike specific monoclonal antibody CR3022 in *Nicotiana benthamiana*. *Sci Rep*. 2020;10(17698).
296. Donini M, Marusic C. Current state-of-the-art in plant-based antibody production systems. *Biotechnol Lett*. 2019;41(3):335-46.
297. Kopertekh L, Schiemann J. Transient production of recombinant pharmaceutical proteins in plants: evolution and perspectives. *Curr Med Chem*. 2019;26(3):365-80.
298. Komori T, Imayama T, Kato N, Ishida Y, Ueki J, Komari T. Current status of binary vectors and superbinary vectors. *PIAnt Physio*. 2007;145(4):1155-60.
299. Lee L-Y, Gelvin SB. T-DNA binary vectors and systems. *PIAnt Physio*. 2008;146(2):325-32.
300. Goodin MM, Zaitlin D, Naidu RA, Lommel SA. *Nicotiana benthamiana*: its history and future as a model for plant-pathogen interactions. *Mol Plant Microbe Interact*. 2008;21(8):1015-26.
301. Krenek P, Samajova O, Luptovciak I, Doskocilova A, Komis G, Samaj J. Transient plant transformation mediated by *Agrobacterium tumefaciens*: principles, methods and applications. *Biotechnol Adv*. 2015;33(6 Pt 2):1024-42.
302. Wigdorovitz A, Filgueira DMP, Robertson N, Carrillo C, Sadir AM, Morris TJ, et al. Protection of mice against challenge with foot and mouth disease virus (FMDV) by immunization with foliar extracts from plants infected with recombinant tobacco mosaic virus expressing the FMDV structural protein VP1. *Virology*. 1999;264(1):85-91.
303. Huang Z, Santi L, LePore K, Kilbourne J, Arntzen CJ, Mason HS. Rapid, high-level production of hepatitis B core antigen in plant leaf and its immunogenicity in mice. *Vaccine*. 2006;24(14):2506-13.
304. Santi L, Batchelor L, Huang Z, Hjelm B, Kilbourne J, Arntzen CJ, et al. An efficient plant viral expression system generating orally immunogenic Norwalk virus-like particles. *Vaccine*. 2008;26(15):1846-54.
305. Rattanapisit K, Chao Z, Siriwattananon K, Huang Z, Phoolcharoen W. Plant-produced anti-enterovirus 71 (EV71) monoclonal antibody efficiently protects mice against EV71 infection. *Plants (Basel)*. 2019;8(12).
306. Rattanapisit K, phakham T, Buranapraditkun S, Siriwattananon K, Boonkrai C, pisitkun T, et al. Structural and *in vitro* functional analyses of novel plant-produced anti-Human PD1 antibody. *Sci Rep*. 2019;9(15205).
307. Park KY, Wi SJ. Potential of plants to produce recombinant protein products. *J Plant Biol*. 2016;59(6):559-68.
308. Ma JK-C, Drossard J, Lewis D, Altmann F, Boyle J, Christou P, et al.

- Regulatory approval and a first-in-human phase I clinical trial of a monoclonal antibody produced in transgenic tobacco plants. *Plant Biotechnol J*. 2015;13(8):1106-20.
309. Weintraub JA, Hilton JF, White JM, Hoover CI, Wycoff KL, Yu L, et al. Clinical trial of a plant-derived antibody on recolonization of mutans streptococci. *Caries Res*. 2005;39(3):241-50.
310. Hendin HE, Pillet S, Lara AN, Wu C-Y, Charland N, Landry N, et al. Plant-made virus-like particle vaccines bearing the hemagglutinin of either seasonal (H1) or avian (H5) influenza have distinct patterns of interaction with human immune cells *in vitro*. *Vaccine*. 2017;35(19):2592-9.
311. Tusé D, Ku N, Bendandi M, Becerra C, Jr RC, Langford N, et al. Clinical safety and immunogenicity of tumor-targeted, plant-made Id-KLH conjugate vaccines for follicular lymphoma. *Biomed Res Int*. 2015;2015(648143).
312. Mor TS. Molecular pharming's foot in the FDA's door: protalix's trailblazing story. *Biotechnol Lett*. 2015;37(11):2147-50.
313. Mercx S, Smargiasso N, Chaumont F, Pauw ED, Boutry M, Navarre C. Inactivation of the  $\beta(1,2)$ -xylosyltransferase and the  $\alpha(1,3)$ -fucosyltransferase genes in *Nicotiana tabacum* BY-2 Cells by a Multiplex CRISPR/cas9 strategy results in glycoproteins without plant-specific glycans. *Front Plant Sci*. 2017;8(403).
314. Kizhner T, Azulay Y, Hainrichson M, Tekoah Y, Arvatz G, Shulman A, et al. Characterization of a chemically modified plant cell culture expressed human  $\alpha$ -Galactosidase-A enzyme for treatment of Fabry disease. *Mol Genet Metab*. 2015;114(2):259-67.
315. Karg SR, Kallio PT. The production of biopharmaceuticals in plant systems. *Biotechnol Adv*. 2009;27(6):879-94.
316. Warzecha H. Biopharmaceuticals from plants: A multitude of options for posttranslational modifications. *Biotechnol Genet Eng Rev*. 2008;25:315-30.
317. Cymer F, Beck H, Rohde A, Reusch D. Therapeutic monoclonal antibody N-glycosylation-Structure, function and therapeutic potential. *Biologicals*. 2018;52.
318. Moremen KW, Tiemeyer M, Nairn AV. Vertebrate protein glycosylation: diversity, synthesis and function. *Nat Rev Mol Cell Biol*. 2021;13(7):448-62.
319. Hebert DN, Lamriben L, Powers ET, Kelly JW. The intrinsic and extrinsic effects of N-linked glycans on glycoproteostasis. *Nat Chem Biol*. 2014;10(11):902-10.
320. Helenius A, Aebi M. Intracellular functions of N-linked glycans. *Science*. 2001;291(5512):2364-9.
321. Vincenz-Donnelly L, Holthusen H, Körner R, Hansen EC, Presto J, Johansson J, et al. High capacity of the endoplasmic reticulum to prevent secretion and aggregation of amyloidogenic proteins. *EMBO J*. 2018;37(3):337-50.
322. Gomord V, Wee E, Faye L. Protein retention and localization in the endoplasmic reticulum and the Golgi apparatus. *Biochimie*. 1999;81(6):607-18.
323. Denecke J, Rycke RD, Botterman J. Plant and mammalian sorting signals for protein retention in the endoplasmic reticulum contain a conserved epitope. *EMBO J*. 1992;11(6):2345-55.
324. Gomord V, Denmat LA, Fitchette-Lainé AC, Satiat-Jeunemaitre B, Hawes LF. The C-terminal HDEL sequence is sufficient for retention of secretory proteins in the endoplasmic reticulum (ER) but promotes vacuolar targeting of proteins that escape the ER. *Plant J*. 1997;11(2):313-25.
325. Fiedler U, Phillips J, Artsaenko O, Conrad U. Optimization of scFv antibody

- production in transgenic plants. *Immunotechnology*. 1997;3(3):205-16.
326. Petruccelli S, Otegui MS, Lareu F, Dinh OT, Fitchette A-C, Circosta A, et al. A KDEL-tagged monoclonal antibody is efficiently retained in the endoplasmic reticulum in leaves, but is both partially secreted and sorted to protein storage vacuoles in seeds. *Plant Biotechnol J*. 2006;4(5):511-27.
327. Meyer TD, Depicker A. Trafficking of endoplasmic reticulum-retained recombinant proteins is unpredictable in *Arabidopsis thaliana*. *Front Plant Sci*. 2014;5(473).
328. Torres E, Vaquero C, Nicholson L, Sack M, Stöger E, Drossard J, et al. Rice cell culture as an alternative production system for functional diagnostic and therapeutic antibodies. *Transgenic res*. 1999;8(6):441-9.
329. Moon K-B, Park J-S, Park Y-I, Song I-J, Lee H-J, Cho HS, et al. Development of systems for the production of plant-derived biopharmaceuticals. *Plant (Basel)*. 2020;9(1).
330. Moustafa K, Makhzoum A, mouillaux-Guiller JT. Molecular farming on rescue of pharma industry for next generations. *Crit Rev Biotechnol*. 2016;36(5):840-50.
331. Ko K. Expression of recombinant vaccines and antibodies in plants. *Monoclon Antib Immunodiagn Immunother*. 2014;33(3):192-8.
332. Ko K, Tekoah Y, Rudd PM, Harvey DJ, Dwek RA, Spitsin S, et al. Function and glycosylation of plant-derived antiviral monoclonal antibody. *Proc Natl Acad Sci U S A*. 2003;100(13):8013-8.
333. Wycoff KL. Secretory Ig antibodies from plants. *Curr Pharm Des*. 2005;11(19):2429-37.
334. Loos A, Gruber C, Altmann F, Mehofer U, Hensel F, Grandits M, et al. Expression and glycoengineering of functionally active heteromultimeric IgM in plants. *Proc Natl Acad Sci U S A*. 2014;111(17):6263-8.
335. Ismaili A, Jalali-Javaran M, Rasae MJ, Rahbarizadeh F, Forouzandeh-Moghadam M, Memari HR. Production and characterization of anti-(mucin MUC1) single-domain antibody in tobacco (*Nicotiana tabacum* cultivar Xanthi). *Biotechnol Appl Biochem*. 2007;47(Pt 1):11-9.
336. Galeffi P, Lombardi A, Pietraforte I, Novelli F, Donato MD, Sperandei M, et al. Functional expression of a single-chain antibody to ErbB-2 in plants and cell-free systems. *J Transl Med*. 2006;4(39).
337. Xu B, Copolla M, Herr JC, Timko MP. Expression of a recombinant human sperm-agglutinating mini-antibody in tobacco (*Nicotiana tabacum* L.). *Soc Reprod Fertil Suppl*. 2007;63:465-77.
338. Makvandi-Nejad S, McLean MD, Hiramata T, Almquist KC, Mackenzie CR, Hall JC. Transgenic tobacco plants expressing a dimeric single-chain variable fragment (scfv) antibody against *Salmonella enterica* serotype Paratyphi B. *Transgen Res*. 2005;14(5):785-92.
339. Sohrab SS, Suhail M, Kamal MA, Husen A, Azhar EI. Recent Development and Future Prospects of Plant-Based Vaccines. *Curr Drug Metab*. 2017;18(9):831-41.
340. Phoolcharoen W, Dye JM, Kilbourne J, Piensook K, Pratt WD, Arntzen CJ, et al. A nonreplicating subunit vaccine protects mice against lethal Ebola virus challenge. *Proc Natl Acad Sci U S A*. 2011;108(51):20695-700.
341. Shchelkunov SN, Salyaev RK, Pozdnyakov SG, Rekoslavskaya NI, Nesterov AE, Ryzhova TS, et al. Immunogenicity of a novel, bivalent, plant-based oral vaccine

- against hepatitis B and human immunodeficiency viruses. *Biotechnol Lett*. 2006;28(13):959-67.
342. Fitchen J, Beachy RN, Hein MB. Plant virus expressing hybrid coat protein with added murine epitope elicits autoantibody response. *Vaccine*. 1995;13(12):1051-7.
343. Takeyama N, Kiyono H, Yuki Y. Plant-based vaccines for animals and humans: recent advances in technology and clinical trials. *Ther Adv Vaccines*. 2015;3(5-6):139-54.
344. Gavilondo JV, Larrick JW. Antibody engineering at the millennium. *Biotechniques*. 2000;29(1):128-32.
345. Fischer R, Schillberg S, Hellwig S, Twyman RM, Drossard J. GMP issues for recombinant plant-derived pharmaceutical proteins. *Biotechnol Adv*. 2012;30(2):434-9.
346. Frey AD, Karg SR, Kallio PT. Expression of rat beta(1,4)-N-acetylglucosaminyltransferase III in *Nicotiana tabacum* remodels the plant-specific N-glycosylation. *Plant Biotechnol J*. 2009;7(1):33-48.
347. Paul M, Ma JK-C. Plant-made pharmaceuticals: leading products and production platforms. *Biotechnol Appl Biochem*. 2011;58(1):58-67.
348. Shen J-S, Busch A, Day TS, Meng X-L, Yu CI, Dabrowska-Schlepp P, et al. Mannose receptor-mediated delivery of moss-made  $\alpha$ -galactosidase A efficiently corrects enzyme deficiency in Fabry mice. *J Inher Metab Dis*. 2016;39:293-303.
349. Tacket CO, Mason HS, Lososky G, Clements JD, Levine MM, Arntzen CJ. Immunogenicity in humans of a recombinant bacterial antigen delivered in a transgenic potato. *Nat Med*. 1998;4(5):607-9.
350. Tacket CO, Pasetti MF, Edelman R, Howard JA, Streatfield S. Immunogenicity of recombinant LT-B delivered orally to humans in transgenic corn. *Vaccine*. 2004;22(31-32):4385-9.
351. Tacket CO, Mason HS, Lososky G, Estes MK, Levine MM, Arntzen CJ. Human immune responses to a novel norwalk virus vaccine delivered in transgenic potatoes. *J Infect Dis*. 2000;182(1):302-5.
352. Kapusta J, Modelska A, Figlerowicz M, Pniewski T, Letellier M, Lisowa O, et al. A plant-derived edible vaccine against hepatitis B virus. *FASEB J*. 1999;13(13):1796-9.
353. Thanavala Y, Mahoney M, Sribani Pal AS, Richter L, Natarajan N, Goodwin P, et al. Immunogenicity in humans of an edible vaccine for hepatitis B. *Proc Natl Acad Sci U S A*. 2005;102(9):3378-82.
354. Yusibov V, Hooper DC, Spitsin SV, Fleysh N, Kean RB, Mikheeva T, et al. Expression in plants and immunogenicity of plant virus-based experimental rabies vaccine. *Vaccine*. 2002;20(25-26):3155-64.
355. Chichester JA, Jones RM, Green BJ, Stow M, Miao F, Moonsammy G, et al. Safety and immunogenicity of a plant-produced recombinant hemagglutinin-based influenza vaccine (HAI-05) derived from A/Indonesia/05/2005 (H5N1) influenza virus: a phase 1 randomized, double-blind, placebo-controlled, dose-escalation study in healthy adults. *Viruses*. 2012;4(11):3227-44.
356. Cummings JF, Guerrero ML, Moon JE, Waterman P, Nielsen RK, Jefferson S, et al. Safety and immunogenicity of a plant-produced recombinant monomer hemagglutinin-based influenza vaccine derived from influenza A (H1N1)pdm09 virus: a phase 1 dose-escalation study in healthy adults. *Vaccine*. 2014;32(19):2251-9.
357. Nochi T, Yuki Y, Katakai Y, Shibata H, Tokuhara D, Mejima M, et al. A rice-

- based oral cholera vaccine induces macaque-specific systemic neutralizing antibodies but does not influence pre-existing intestinal immunity. *J Immunol.* 2009;183(10):6538-44.
358. Yuki Y, Mejima M, Kurokawa S, Hiroiwa T, Takahashi Y, Tokuhara D, et al. Induction of toxin-specific neutralizing immunity by molecularly uniform rice-based oral cholera toxin B subunit vaccine without plant-associated sugar modification. *Plant Biotechnol J.* 2013;11(7):799-808.
359. D'Aoust M-A, Lavoie P-O, Couture MM-J, Trépanier S, Guay J-M, Dargis M, et al. Influenza virus-like particles produced by transient expression in *Nicotiana benthamiana* induce a protective immune response against a lethal viral challenge in mice. *Plant Biotechnol J.* 2008;6(9):930-40.
360. Landry N, Ward BJ, Trépanier S, Montomoli E, Dargis M, Lapini G, et al. Preclinical and clinical development of plant-made virus-like particle vaccine against avian H5N1 influenza. *PLoS One.* 2010;5(12).
361. Pillet S, Aubin É, Trépanier S, Bussière D, Dargis M, Poulin J-F, et al. A plant-derived quadrivalent virus like particle influenza vaccine induces cross-reactive antibody and T cell response in healthy adults. *Clin Immunol.* 2016;168:72-87.
362. Huang C. Receptor-Fc fusion therapeutics, traps, and MIMETIBODY technology. *Curr Opin Biotechnol.* 2009;20(6):692-9.
363. Beck A, Reichert JM. Therapeutic Fc-fusion proteins and peptides as successful alternatives to antibodies. *mAbs.* 2011;3(5):415-6.
364. Roopenian DC, Akilesh S. FcRn: the neonatal Fc receptor comes of age. *Nat Rev Immunol.* 2007;7(9):715-25.
365. Kontermann RE. Strategies for extended serum half-life of protein therapeutics. *Curr Opin Biotechnol.* 2011;22(6):868-76.
366. Yang C, Gao X, Gong R. Engineering of Fc fragments with optimized physicochemical properties implying improvement of clinical potentials for Fc-based therapeutics. *Front Immunol.* 2018;8(1860).
367. Goldenberg MM. Etanercept, a novel drug for the treatment of patients with severe, active rheumatoid arthritis. *Clin Ther.* 1999;21(1):75-87.
368. Shanmugaraj B, Rattanapisit K, Manopwisedjaroen S, Thitithanyanont A, Phoolcharoen W. Monoclonal antibodies B38 and H4 produced in *Nicotiana benthamiana* neutralize SARS-CoV-2 *in vitro*. *Front Plant Sci.* 2020;11(589995).
369. Frey A, Canzio JD, Zurakowski D. A statistically defined endpoint titer determination method for immunoassays. *J Immunol Methods.* 1998;221(1-2):35-41.
370. Reed LJ, Muench H. A simple method of estimating fifty percent endpoints. *Am J Hyg.* 1938;27(3):493-7.
371. Kanjanasirirat P, Suksatu A, Manopwisedjaroen S, Munyoo B, Tuchinda P, Jearawuttanakul K, et al. High-content screening of Thai medicinal plants reveals *Boesenbergia rotunda* extract and its component Panduratin A as anti-SARS-CoV-2 agents. *Sci Rep.* 2020;10(19963).
372. World Health Organization. Weekly operational update on COVID-19 - 31 August 2021 2021 [Available from: <https://www.who.int/publications/m/item/weekly-epidemiological-update-on-covid-19---31-august-2021>].
373. Jeyanathan M, Afkhami S, Smaill F, Miller MS, Lichty BD, Xing Z. Immunological considerations for COVID-19 vaccine strategies. *Nat Rev Immunol.* 2020;20(10):615-32.

374. Li H, Liu S-M, Yu X-H, Tang S-L, Tang C-K. Coronavirus disease 2019 (COVID-19): current status and future perspectives. *Int J Antimicrob Agents*. 2020;55(5)(105951).
375. Siri wattananon K, Manopwisedjaroen S, Shanmugaraj B, Rattanapisit K, Phumiamorn S, Sapsutthipas S, et al. Plant-produced receptor-binding domain of SARS-CoV-2 elicits potent neutralizing responses in mice and non-human primates. *Front Plant Sci*. 2021;12(847).
376. D'Aoust M-A, Couture MM-J, Charland N, Trépanier S, Landry N, Ors F, et al. The production of hemagglutinin-based virus-like particles in plants: a rapid, efficient and safe response to pandemic influenza. *Plant Biotechnol J*. 2010;8(5):607-19.
377. Kumar AU, Kadiresen K, Gan WC, Ling APK. Current updates and research on plant-based vaccines for coronavirus disease 2019. *Clin Exp Vaccine Res*. 2021;10(1):13-23.
378. Jazayeri JA, Carroll GJ. Fc-based cytokines: prospects for engineering superior therapeutics. *Biodrugs*. 2008;22(1):11-26.
379. Rath T, Baker K, Dumont JA, Peters RT, Jiang H, Qiao S-W, et al. Fc-fusion proteins and FcRn: structural insights for longer-lasting and more effective therapeutics. *Crit Rev Biotechnol*. 2015;35(2):235-54.
380. Strohl WR, Knight DM. Discovery and development of biopharmaceuticals: current issues. *Curr Opin Biotechnol*. 2009;20(6):668-72.
381. Li F, Ravetch JV. Inhibitory Fc $\gamma$  receptor engagement drives adjuvant and anti-tumor activities of agonistic CD40 antibodies. *Science*. 2011;333(6045):1030-4.
382. Yamamoto T, Hoshikawa K, Ezura K, Okazawa R, Fujita S, Takaoka M, et al. Improvement of the transient expression system for production of recombinant proteins in plants. *Sci Rep*. 2018;8(4755).
383. Ahmad AR, Kaewpungsup P, Khorattanakulchai N, Rattanapisit K, Pavasant P, Phoolcharoen W. Recombinant human dentin matrix protein 1 (hDMP1) expressed in *Nicotiana benthamiana* potentially induces osteogenic differentiation. *Plants (Basel)*. 2019;8(12).
384. Boonyayothin W, Sinnung S, Shanmugaraj B, Abe Y, Strasser R, Pavasant P, et al. Expression and functional evaluation of recombinant anti-receptor activator of nuclear factor kappa-B ligand monoclonal antibody produced in *Nicotiana benthamiana*. *Front Plant Sci*. 2021;12(683417).
385. Hanittinan O, Oo Y, Chaotham C, Rattanapisit K, Shanmugaraj B, Phoolcharoen W. Expression optimization, purification and in vitro characterization of human epidermal growth factor produced in *Nicotiana benthamiana*. *Biotechnol Rep (Amst)*. 2020;28.
386. Bulaon CJI, Shanmugaraj B, Oo Y, Rattanapisit K, Chuanasa T, Chaotham C, et al. Rapid transient expression of functional human vascular endothelial growth factor in *Nicotiana benthamiana* and characterization of its biological activity. *Biotechnol Rep (Amst)*. 2020;27.
387. Zhumabek AT, Abeuova LS, Mukhametzhanov NS, Scholthof HB, Ramankulov YM, Manabayeva SA. Transient expression of a bovine leukemia virus envelope glycoprotein in plants by a recombinant TBSV vector. *J Virol Methods*. 2018;255.
388. Laughlin RC, Madera R, Peres Y, Berquist BR, Wang L, Buist S, et al. Plant-made E2 glycoprotein single-dose vaccine protects pigs against classical swine fever. *Plant Biotechnol J*. 2019;17(2):410-20.

389. Bauer K, Bayer PM, Deutsch E, Gabl F. Binding of enzyme-IgG complexes in human serum to Protein-A Sepharose CL-4B. *Clin Chem*. 1980;26(2):297-300.
390. Hober S, Nord K, Linhult M. Protein A chromatography for antibody purification. *J Chromatogr B Analyt Technol Biomed Life Sci*. 2007;848(1):40-7.
391. Rabi FA, Zoubi MSA, Kasasbeh GA, Salameh DM, Al-Nasser AD. SARS-CoV-2 and coronavirus disease 2019: what we know so far. *Pathogens*. 2020;9(231).
392. Liu C, Tang J, Ma Y, Liang X, Yang Y, Peng G, et al. Receptor usage and cell entry of porcine epidemic diarrhea coronavirus. *J Virol*. 2015;89(11):6121-5.
393. Reed SG, Orr MT, Fox CB. Key roles of adjuvants in modern vaccines. *Nat Med*. 2013;19(12):1597-608.
394. Vogel FR. Improving vaccine performance with adjuvants *Clin Infect Dis*. 2000;30:266-70.
395. Aoshi T. Modes of action for mucosal vaccine adjuvants. *Viral Immunol*. 2017;30(6):463-70.
396. Pasquale AD, Preiss S, Silva FTD, Garçon N. Vaccine adjuvants: from 1920 to 2015 and beyond. *Vaccines (Basel)*. 2015;3(2):320-43.
397. Sarkar I, Garg R, Hurk SvDL-vd. Selection of adjuvants for vaccines targeting specific pathogens. *Expert Rev Vaccines*. 2019;18(5):505-21.
398. Mastelic B, Ahmed S, Egan WM, Giudice GD, Golding H, Gust I, et al. Mode of action of adjuvants: implications for vaccine safety and design. *Biologicals*. 2010;38(5):594-601.
399. Tong NKC, Beran J, Kee SA, Miguel JL, Sánchez C, Bayas JM, et al. Immunogenicity and safety of an adjuvanted hepatitis B vaccine in pre-hemodialysis and hemodialysis patients. *Kidney Int*. 2005;68(5):2298-303.
400. Levie K, Gjorup I, Skinhøj P, Stoffel M. A 2-dose regimen of a recombinant hepatitis B vaccine with the immune stimulant AS04 compared with the standard 3-dose regimen of Engerix-B in healthy young adults. *Scand J Infect Dis*. 2002;34(8):610-4.
401. McCluskie MJ, Pryde DC, Gervais DP, Stead DR, Zhang N, Benoit M, et al. Enhancing immunogenicity of a 3'aminomethylnicotine-DT-conjugate anti-nicotine vaccine with CpG adjuvant in mice and non-human primates. *Int Immunopharmacol*. 2013;16(1):50-6.
402. Giudice GD, Rappuoli R, Didierlaurent AM. Correlates of adjuvanticity: A review on adjuvants in licensed vaccines. *Semin Immunol*. 2018;39:14-21.
403. Garçon N, Pasquale AD. From discovery to licensure, the adjuvant system story. *Hum Vaccin Immunother*. 2017;13(1):19-33.
404. Ichinohe T, Kawaguchi A, Tamura S-i, Takahashi H, Sawa H, Ninomiya A, et al. Intranasal immunization with H5N1 vaccine plus Poly I:Poly C12U, a Toll-like receptor agonist, protects mice against homologous and heterologous virus challenge. *Microbes Infect*. 2007;9(11):1333-40.
405. Sharma S, Zhu L, Davoodi M, Harris-White M, Lee JM, John MS, et al. TLR3 agonists and proinflammatory antitumor activities. *Expert Opin Ther Targets*. 2013;17(5):481-3.
406. Marrack P, McKee AS, Munks1 MW. Towards an understanding of the adjuvant action of aluminium. *Nat Rev Immunol*. 2009;9(4):287-93.
407. Toussi DN, Massari P. Immune adjuvant effect of molecularly-defined Toll-like receptor ligands. *Vaccines (Basel)*. 2014;2(2):323-53.
408. Exley C, Siesjö P, Eriksson H. The immunobiology of aluminium adjuvants:

- how do they really work? Trends Immunol. 2010;31(3):103-9.
409. Cekic C, Casella CR, Eaves CA, Matsuzawa A, Ichijo H, Mitchell TC. Selective activation of the p38 MAPK pathway by synthetic monophosphoryl lipid A. J Biol Chem. 2009;284(46):31982-91.
410. Martins KAO, Bavari S, Salazar AM. Vaccine adjuvant uses of poly-IC and derivatives. Expert Rev Vaccines. 2015;14(3):447-59.
411. Ho NI, Veld LGMHIt, Raaijmakers TK, Adema GJ. Adjuvants enhancing cross-presentation by dendritic cells: the key to more effective vaccines? Front Immunol. 2018;9(2874).
412. Sarkar I, Garg R, Hurk SvDL-vd. Formulation of the respiratory syncytial virus fusion protein with a polymer-based combination adjuvant promotes transient and local innate immune responses and leads to improved adaptive immunity. Vaccine. 2016;34(42):5114-24.
413. Longhi MP, Trumpfheller C, Idoyaga J, Caskey M, Matos I, Kluger C, et al. Dendritic cells require a systemic type I interferon response to mature and induce CD4+ Th1 immunity with poly IC as adjuvant. J Exp Med. 2009;206(7):1589-602.
414. Bon AL, Thompson C, Kamphuis E, Durand V, Rossmann C, Kalinke U, et al. Cutting edge: enhancement of antibody responses through direct stimulation of B and T cells by type I IFN. J Immunol. 2006;176(4):2078-4.
415. Bon AL, Schiavoni G, D'Agostino G, Gresser I, Belardelli F, Tough DF. Type I interferons potently enhance humoral immunity and can promote isotype switching by stimulating dendritic cells *in vivo*. Immunity. 2001;14(4):461-70.
416. Huber VC, McKeon RM, Brackin MN, Miller LA, Keating R, Brown SA, et al. Distinct contributions of vaccine-induced immunoglobulin G1 (IgG1) and IgG2a antibodies to protective Immunity against Influenza. Clin Vaccine Immunol. 2006;13(9):981-90.
417. Hofmeister Y, Planitzer CB, Farcet MR, Teschner W, Butterweck HA, Weber A, et al. Human IgG subclasses: *in vitro* neutralization of and *in vivo* protection against West Nile virus. J Virol. 2011;85(4):1896-9.
418. Hovden A-O, Cox RJ, Haaheim LR. Whole influenza virus vaccine is more immunogenic than split influenza virus vaccine and induces primarily an IgG2a response in BALB/c mice. Scand J Immunol. 2005;62(1):36-44.
419. Coutelier JP, Logt JTvd, Heessen FW, Vink A, Snick Jv. Virally induced modulation of murine IgG antibody subclasses. J Exp Med. 1988;168(6):2373-8.
420. Moran TM, Park H, Fernandez-Sesma A, Schulman JL. Th2 responses to inactivated influenza virus can be converted to Th1 responses and facilitate recovery from heterosubtypic virus infection. J Infect Dis. 1999;180(3):579-85.
421. Tau G, Rothman P. Biologic functions of the IFN- $\gamma$  receptors. Allergy. 1999;54(12):1233-51.
422. Billiau A. Interferon-gamma: biology and role in pathogenesis. Adv Immunol. 1996;62:61-130.
423. Boehm U, Klamp T, Groot M, Howard JC. Cellular responses to interferon-gamma. Annu Rev Immunol. 1997;15:749-95.
424. Chin KL, Anis FZ, Sarmiento ME, Norazmi MN, Acosta A. Role of interferons in the development of diagnostics, vaccines, and therapy for tuberculosis. J Immunol Res. 2017;2017(5212910).
425. Xu Y, Zhu B, Wang Q, Chen J, Qie Y, Wang J, et al. Recombinant BCG



coexpressing Ag85B, ESAT-6 and mouse-IFN-gamma confers effective protection against Mycobacterium tuberculosis in C57BL/6 mice. *FEMS Immunol Med Microbiol.* 2007;51(3):480-7.

426. Bradley LM, Dalton DK, Croft M. A direct role for IFN-gamma in regulation of Th1 cell development. *J Immunol.* 1996;157(4):1350-8.

427. Dhama K, Natesan S, Yatoo MI, Patel SK, Tiwari R, Saxena SK, et al. Plant-based vaccines and antibodies to combat COVID-19: current status and prospects. *Hum Vaccin Immunother.* 2020;16(12):2913-20.

428. Sainsbury F. Innovation in plant-based transient protein expression for infectious disease prevention and preparedness. *Curr Opin Biotechnol.* 2020;61:110-5.

429. Gomes C, Oliveira F, Vieira SI, Duque AS. Prospects for the production of recombinant therapeutic proteins and peptides in plants: special focus on angiotensin I-converting enzyme inhibitory (ACEI) peptides. London: IntechOpen; 2019.





**APPENDICES**

จุฬาลงกรณ์มหาวิทยาลัย  
**CHULALONGKORN UNIVERSITY**

## APPENDIX 1

## NUCLEOTIDE SEQUENCES IN SARS-CoV-2 RBD CONSTRUCT

## Synthesized Sequence of Signal Peptide-SARS-CoV-2 RBD-Peptide

## Linker

**TCT AGA** ACA ATG GGC TGG TCC TGC ATC ATC CTG TTC CTT GTT GCT ACT GCT ACC GGC GTT  
 S R T M G W S C I I L F L V A T A T G V  
CAC TCT GAT GTT CAA CTT CTC GAG TTC AGG GTT CAG CCT ACC GAG TCT ATT GTG CGG TTC  
 H S D V Q L L E F R V Q P T E S I V R F  
 CCT AAC ATC ACC AAC TTG TGC CCT TTC GGC GAG GTG TTC AAT GCT ACT AGG TTC GCT TCT  
 P N I T N L C P F G E V F N A T R F A S  
 GTG TAC GCC TGG AAC CGG AAG AGG ATT TCT AAC TGC GTG GCC GAT TAC AGC GTG CTG TAC  
 V Y A W N R K R I S N C V A D Y S V L Y  
 AAC TCT GCT TCC TTC AGC ACC TTC AAG TGC TAC GGT GTG TCT CCT ACC AAG CTG AAC GAT  
 N S A S F S T F K C Y G V S P T K L N D  
 CTG TGC TTC ACC AAC GTG TAC GCT GAC TCT TTC GTG ATC AGG GGT GAT GAG GTT AGG CAG  
 L C F T N V Y A D S F V I R G D E V R Q  
 ATT GCT CCT GGT CAG ACC GGA AAG ATC GCT GAC TAC AAC TAC AAG CTG CCG GAT GAT TTC  
 I A P G Q T G K I A D Y N Y K L P D D F  
 ACC GGA TGC GTT ATC GCT TGG AAC AGC AAC AAC CTG GAC TCT AAG GTT GGC GGC AAT TAC  
 T G C V I A W N S N N L D S K V G G N Y  
 AAC TAC CTC TAC CGG CTG TTC CGG AAG TCT AAC TTG AAG CCT TTC GAG CGG GAC ATC AGC  
 N Y L Y R L F R K S N L K P F E R D I S  
 ACC GAA ATC TAT CAG GCT GGT TCT ACC CCT TGC AAC GGT GTT GAG GGT TTC AAC TGC TAC  
 T E I Y Q A G S T P C N G V E G F N C Y  
 TTC CCG CTT CAG TCT TAC GGT TTC CAG CCT ACT AAT GGT GTG GGC TAC CAG CCT TAC AGA  
 F P L Q S Y G F Q P T N G V G Y Q P Y R  
 GTG GTG GTT TTG TCT TTC GAG CTT CTG CAT GCT CCT GCT ACT GTT TGC GGT CCT AAG AAG  
 V V V L S F E L L H A P A T V C G P K K  
 TCT ACC AAC CTG GTC AAG AAC AAG TGC GTG AAC TTC AAC TTC AAC GGC CTT ACC GGA ACT  
 S T N L V K N K C V N F N F N G L T G T  
 GGT GTG CTG ACT GAG TCT AAC AAG AAG TTC CTG CCG TTC CAG CAG TTC GGC AGA GAT ATT  
 G V L T E S N K K F L P F Q Q F G R D I

GCT GAT ACC ACC GAT GCT GTG AGG GAC CCT CAG ACT CTT GAG ATC CTT GAT ATT ACC CCG  
 A D T T D A V R D P Q T L E I L D I T P  
 TGC AGC TTC GGT GGT GTG TCT GTT ATT ACT CCT GGC ACC AAC ACC TCT AAC CAG GTG GCA  
 C S F G G V S V I T P G T N T S N Q V A  
 GTT CTT TAC CAG GAT GTG AAC TGC GAT ATC TCT GGT GGT GGT GGA TCC  
 V L Y Q D V N C D I S G G G G S

## Synthesized Sequence of Human Fc of Immunoglobulin G1-SEKDEL

### Retention Signal

GGT GGT GGT GGA TCC GGA GGT GGA GGT TCT GGA GGT GGA GGT TCA CCA CCA TGT CCA GCT  
 G G G G S G G G G S G G G S P P C P A  
 CCA GAA CTT CTT GGT GGT CCT TCT GTT TTT TTG TTC CCA CCA AAG CCA AAG GAT ACT CTC  
 P E L L G G P S V F L F P P K P K D T L  
 ATG ATC TCT AGG ACT CCA GAG GTT ACA TGC GTT GTG GTT GAT GTG TCT CAT GAA GAT CCA  
 M I S R T P E V T C V V V D V S H E D P  
 GAG GTG AAG TTC AAC TGG TAT GTG GAT GGT GTT GAG GTG CAC AAC GCT AAG ACT AAG CCA  
 E V K F N W Y V D G V E V H N A K T K P  
 AGA GAG GAA CAG TAC AAC TCC ACT TAC AGG GTT GTG TCT GTG CTT ACT GTT CTT CAC CAG  
 R E E Q Y N S T Y R V V S V L T V L H Q  
 GAT TGG CTT AAC GGC AAA GAG TAC AAG TGC AAG GTG TCC AAC AAG GCT TTG CCA GCT CCA  
 D W L N G K E Y K C K V S N K A L P A P  
 ATC GAA AAG ACT ATC TCT AAG GCT AAG GGA CAG CCA AGG GAA CCT CAA GTT TAC ACT CTT  
 I E K T I S K A K G Q P R E P Q V Y T L  
 CCA CCA TCT AGG GAT GAG CTT ACT AAG AAC CAG GTG TCC CTT ACT TGC CTT GTG AAG GGA  
 P P S R D E L T K N Q V S L T C L V K G  
 TTT TAC CCA TCC GAT ATT GCT GTT GAG TGG GAG TCT AAT GGA CAG CCT GAG AAC AAC TAC  
 F Y P S D I A V E W E S N G Q P E N N Y  
 AAG ACT ACT CCA CCA GTG CTC GAT TCC GAT GGA TCA TTC TTC TTG TAC TCC AAG CTC ACT  
 K T T P P V L D S D G S F F L Y S K L T  
 GTG GAT AAG TCT AGG TGG CAA CAG GGA AAC GTT TTC TCT TGC TCT GTT ATG CAT GAG GCT  
 V D K S R W Q Q G N V F S C S V M H E A  
 CTC CAC AAT CAC TAC ACT CAG AAG TCC CTT TCT TTG TCC CCT GGC AAG TCT GAG AAG GAT  
 L H N H Y T Q K S L S L S P G K S E K D

GAG CTT TAA **GAG CTC**

E L - E L

### Sequence of SARS-CoV-2 RBD-Fc construct

**TCT AGA** ACA ATG GGC TGG TCC TGC ATC ATC CTG TTC CTT GTT GCT ACT GCT ACC GGC GTT  
 S R T M G W S C I I L F L V A T A T G V  
CAC TCT GAT GTT CAA CTT CTC GAG TTC AGG GTT CAG CCT ACC GAG TCT ATT GTG CGG TTC  
 H S D V Q L L E F R V Q P T E S I V R F  
 CCT AAC ATC ACC AAC TTG TGC CCT TTC GGC GAG GTG TTC AAT GCT ACT AGG TTC GCT TCT  
 P N I T N L C P F G E V F N A T R F A S  
 GTG TAC GCC TGG AAC CGG AAG AGG ATT TCT AAC TGC GTG GCC GAT TAC AGC GTG CTG TAC  
 V Y A W N R K R I S N C V A D Y S V L Y  
 AAC TCT GCT TCC TTC AGC ACC AAG TGC TAC GGT GTG TCT CCT ACC AAG CTG AAC GAT  
 N S A S F S T F K C Y G V S P T K L N D  
 CTG TGC TTC ACC AAC GTG TAC GCT GAC TCT TTC GTG ATC AGG GGT GAT GAG GTT AGG CAG  
 L C F T N V Y A D S F V I R G D E V R Q  
 ATT GCT CCT GGT CAG ACC GGA AAG ATC GCT GAC TAC AAC TAC AAG CTG CCG GAT GAT TTC  
 I A P G Q T G K I A D Y N Y K L P D D F  
 ACC GGA TGC GTT ATC GCT TGG AAC AGC AAC AAC CTG GAC TCT AAG GTT GGC GGC AAT TAC  
 T G C V I A W N S N N L D S K V G G N Y  
 AAC TAC CTC TAC CGG CTG TTC CGG AAG TCT AAC TTG AAG CCT TTC GAG CGG GAC ATC AGC  
 N Y L Y R L F R K S N L K P F E R D I S  
 ACC GAA ATC TAT CAG GCT GGT TCT ACC CCT TGC AAC GGT GTT GAG GGT TTC AAC TGC TAC  
 T E I Y Q A G S T P C N G V E G F N C Y  
 TTC CCG CTT CAG TCT TAC GGT TTC CAG CCT ACT AAT GGT GTG GGC TAC CAG CCT TAC AGA  
 F P L Q S Y G F Q P T N G V G Y Q P Y R  
 GTG GTG GTT TTG TCT TTC GAG CTT CTG CAT GCT CCT GCT ACT GTT TGC GGT CCT AAG AAG  
 V V V L S F E L L H A P A T V C G P K K  
 TCT ACC AAC CTG GTC AAG AAC AAG TGC GTG AAC TTC AAC TTC AAC GGC CTT ACC GGA ACT  
 S T N L V K N K C V N F N F N G L T G T  
 GGT GTG CTG ACT GAG TCT AAC AAG AAG TTC CTG CCG TTC CAG CAG TTC GGC AGA GAT ATT  
 G V L T E S N K K F L P F Q Q F G R D I  
 GCT GAT ACC ACC GAT GCT GTG AGG GAC CCT CAG ACT CTT GAG ATC CTT GAT ATT ACC CCG  
 A D T T D A V R D P Q T L E I L D I T P  
 TGC AGC TTC GGT GGT GTG TCT GTT ATT ACT CCT GGC ACC AAC ACC TCT AAC CAG GTG GCA  
 C S F G G V S V I T P G T N T S N Q V A

GTT CTT TAC CAG GAT GTG AAC TGC GAT ATC TCT GGT GGT GGT GGA TCC GGA GGT GGA GGT  
 V L Y Q D V N C D I S G G G G S G G G G

TCT GGA GGT GGA GGT TCA CCA CCA TGT CCA GCT CCA GAA CTT CTT GGT GGT CCT TCT GTT  
 S G G G G S P P C P A P E L L G G P S V  
 TTT TTG TTC CCA CCA AAG CCA AAG GAT ACT CTC ATG ATC TCT AGG ACT CCA GAG GTT ACA  
 F L F P P K P K D T L M I S R T P E V T  
 TGC GTT GTG GTT GAT GTG TCT CAT GAA GAT CCA GAG GTG AAG TTC AAC TGG TAT GTG GAT  
 C V V V D V S H E D P E V K F N W Y V D  
 GGT GTT GAG GTG CAC AAC GCT AAG ACT AAG CCA AGA GAG GAA CAG TAC AAC TCC ACT TAC  
 G V E V H N A K T K P R E E Q Y N S T Y  
 AGG GTT GTG TCT GTG CTT ACT GTT CTT CAC CAG GAT TGG CTT AAC GGC AAA GAG TAC AAG  
 R V V S V L T V L H Q D W L N G K E Y K  
 TGC AAG GTG TCC AAC AAG GCT TTG CCA GCT CCA ATC GAA AAG ACT ATC TCT AAG GCT AAG  
 C K V S N K A L P A P I E K T I S K A K  
 GGA CAG CCA AGG GAA CCT CAA GTT TAC ACT CTT CCA CCA TCT AGG GAT GAG CTT ACT AAG  
 G Q P R E P Q V Y T L P P S R D E L T K  
 AAC CAG GTG TCC CTT ACT TGC CTT GTG AAG GGA TTT TAC CCA TCC GAT ATT GCT GTT GAG  
 N Q V S L T C L V K G F Y P S D I A V E  
 TGG GAG TCT AAT GGA CAG CCT GAG AAC AAC TAC AAG ACT ACT CCA CCA GTG CTC GAT TCC  
 W E S N G Q P E N N Y K T T P P V L D S  
 GAT GGA TCA TTC TTC TTG TAC TCC AAG CTC ACT GTG GAT AAG TCT AGG TGG CAA CAG GGA  
 D G S F F L Y S K L T V D K S R W Q Q G  
 AAC GTT TTC TCT TGC TCT GTT ATG CAT GAG GCT CTC CAC AAT CAC TAC ACT CAG AAG TCC  
 N V F S C S V M H E A L H N H Y T Q K S  
 CTT TCT TTG TCC CCT GGC AAG TCT GAG AAG GAT GAG CTT TAA GAG CTC  
 L S L S P G K S E K D E L - E L

## APPENDIX 2

### NUCLEOTIDE SEQUENCES IN ACE2-Fc CONSTRUCT

#### Synthesized Sequence of Signal Peptide-ACE2-Peptide Linker

GGG **TCT AGA** ACA ATG GGC TGG TCC TGC ATC ATC CTG TTC CTT GTT GCT ACT GCT ACC GGC  
 G S R T M G W S C I I L F L V A T A T G  
GTT CAC TCT GAT GTT CAA CTT CTC GAG CAG TCT ACC ATT GAG GAA CAG GCT AAG ACC TTC  
 V H S D V Q L L E Q S T I E E Q A K T F  
 CTG GAC AAG TTC AAT CAC GAG GCT GAG GAC CTG TTC TAC CAG TCC TCT CTT GCT TCC TGG  
 L D K F N H E A E D L F Y Q S S L A S W  
 AAC TAC AAC ACC AAC ATC ACC GAA GAG AAC GTG CAG AAC ATG AAC AAC GCT GGC GAT AAG  
 N Y N T N I T E E N V Q N M N N A G D K  
 TGG TCC GCC TTC CTT AAA GAG CAG TCT ACC CTT GCT CAG ATG TAC CCG CTT CAA GAG ATT  
 W S A F L K E Q S T L A Q M Y P L Q E I  
 CAG AAC CTG ACC GTG AAG CTC CAG CTT CAA GCA CTT CAG CAG AAC GGT TCT TCT GTG CTG  
 Q N L T V K L Q L Q A L Q Q N G S S V L  
 AGC GAG GAT AAG AGC AAG AGG CTT AAC ACC ATC CTG AAC ACC ATG AGC ACC ATC TAC AGC  
 S E D K S K R L N T I L N T M S T I Y S  
 ACT GGT AAG GTG TGC AAC CCT GAC AAT CCT CAA GAG TGC CTT TTG CTT GAG CCT GGC CTT  
 T G K V C N P D N P Q E C L L L E P G L  
 AAC GAG ATC ATG GCT AAC AGC CTG GAT TAC AAC GAG AGG CTT TGG GCT TGG GAG TCT TGG  
 N E I M A N S L D Y N E R L W A W E S W  
 AGA TCT GAG GTG GGA AAG CAG CTT AGG CCT CTG TAC GAA GAG TAC GTG GTG CTG AAG AAT  
 R S E V G K Q L R P L Y E E Y V V L K N  
 GAG ATG GCT AGG GCT AAC CAC TAC GAG GAC TAC GGT GAT TAT TGG AGG GGC GAT TAC GAG  
 E M A R A N H Y E D Y G D Y W R G D Y E  
 GTG AAC GGT GTG GAT GGT TAC GAT TAC TCT AGG GGT CAG CTG ATC GAG GAT GTT GAG CAT  
 V N G V D G Y D Y S R G Q L I E D V E H  
 ACC TTC GAA GAG ATC AAG CCG CTG TAC GAG CAT CTT CAT GCT TAC GTG AGG GCC AAG CTG  
 T F E E I K P L Y E H L H A Y V R A K L  
 ATG AAC GCT TAC CCG TCT TAC ATC AGC CCT ATT GGT TGC CTT CCT GCT CAC CTT CTT GGT  
 M N A Y P S Y I S P I G C L P A H L L G

GAT ATG TGG GGA AGA TTC TGG ACC AAC CTG TAC TCT CTT ACC GTG CCT TTC GGC CAA AAG  
 D M W G R F W T N L Y S L T V P F G Q K  
 CCG AAC ATT GAT GTG ACC GAT GCT ATG GTG GAT CAG GCT TGG GAT GCT CAG AGG ATC TTC  
 P N I D V T D A M V D Q A W D A Q R I F  
 AAA GAG GCC GAG AAG TTC TTC GTG TCT GTG GGT TTG CCT AAC ATG ACC CAA GGA TTC TGG  
 K E A E K F F V S V G L P N M T Q G F W  
 GAG AAC TCC ATG CTT ACC GAT CCT GGC AAT GTG CAG AAG GCT GTT TGT CAT CCT ACC GCT  
 E N S M L T D P G N V Q K A V C H P T A  
 TGG GAC CTT GGT AAG GGC GAT TTC AGG ATT CTG ATG TGC ACC AAG GTG ACA ATG GAC GAC  
 W D L G K G D F R I L M C T K V T M D D  
 TTC CTT ACT GCA CAC CAC GAG ATG GGT CAC ATC CAG TAC GAT ATG GCT TAT GCT GCT CAG  
 F L T A H H E M G H I Q Y D M A Y A A Q  
 CCT TTC CTG CTT AGG AAT GGT GCT AAT GAG GGT TTC CAT GAG GCT GTG GGT GAG ATC ATG  
 P F L L R N G A N E G F H E A V G E I M  
 TCT CTT TCT GCT GCT ACC CCT AAG CAC CTG AAG TCT ATT GGT CTG CTG AGC CCT GAT TTC  
 S L S A A T P K H L K S I G L L S P D F  
 CAA GAG GAC AAT GAG ACT GAG ATC AAC TTC CTG CTG AAG CAG GCT CTG ACT ATT GTG GGA  
 Q E D N E T E I N F L L K Q A L T I V G  
 ACT CTG CCC TTC ACC TAC ATG CTT GAA AAG TGG CGG TGG ATG GTC TTT AAG GGC GAG ATT  
 T L P F T Y M L E K W R W M V F K G E I  
 CCT AAG GAC CAG TGG ATG AAG AAA TGG TGG GAG ATG AAG CGT GAG ATC GTC GGT GTT GTT  
 P K D Q W M K K W W E M K R E I V G V V  
 GAG CCA GTT CCT CAC GAT GAG ACT TAC TGC GAT CCT GCC TCT CTG TTC CAC GTG AGC AAC  
 E P V P H D E T Y C D P A S L F H V S N  
 GAC TAC TCT TTC ATC CGG TAC TAC ACC CGG ACC TTG TAC CAG TTT CAG TTT CAA GAG GCT  
 D Y S F I R Y Y T R T L Y Q F Q F Q E A  
 CTG TGC CAG GCT GCT AAA CAT GAA GGT CCT CTT CAC AAG TGC GAC ATC AGC AAT TCT ACT  
 L C Q A A K H E G P L H K C D I S N S T  
 GAG GCT GGG CAA AAG CTG TTC AAC ATG CTG AGG CTT GGT AAG TCC GAG CCT TGG ACT CTT  
 E A G Q K L F N M L R L G K S E P W T L  
 GCT TTG GAG AAT GTT GTG GGC GCC AAG AAT ATG AAC GTG AGG CCT CTT CTG AAC TAC TTC  
 A L E N V V G A K N M N V R P L L N Y F  
 GAG CCT TTG TTC ACC TGG CTG AAG GAC CAG AAC AAG AAC AGC TTC GTT GGC TGG TCT ACC  
 E P L F T W L K D Q N K N S F V G W S T  
 GAC TGG TCA CCT TAT GCT GAT GGT GGT GGA TCC  
 D W S P Y A D G G G S



### Sequence of ACE2-Fc construct

GGG **TCT AGA** ACA ATG GGC TGG TCC TGC ATC ATC CTG TTC CTT GTT GCT ACT GCT ACC GGC  
 G S R T M G W S C I I L F L V A T A T G  
 GTT CAC TCT GAT GTT CAA CTT CTC GAG CAG TCT ACC ATT GAG GAA CAG GCT AAG ACC TTC  
 V H S D V Q L L E Q S T I E E Q A K T F  
 CTG GAC AAG TTC AAT CAC GAG GCT GAG GAC CTG TTC TAC CAG TCC TCT CTT GCT TCC TGG  
 L D K F N H E A E D L F Y Q S S L A S W  
 AAC TAC AAC ACC AAC ATC ACC GAA GAG AAC GTG CAG AAC ATG AAC AAC GCT GGC GAT AAG  
 N Y N T N I T E E N V Q N M N N A G D K  
 TGG TCC GCC TTC CTT AAA GAG CAG TCT ACC CTT GCT CAG ATG TAC CCG CTT CAA GAG ATT  
 W S A F L K E Q S T L A Q M Y P L Q E I  
 CAG AAC CTG ACC GTG AAG CTC CAG CTT CAA GCA CTT CAG CAG AAC GGT TCT TCT GTG CTG  
 Q N L T V K L Q L Q A L Q Q N G S S V L  
 AGC GAG GAT AAG AGC AAG AGG CTT AAC ACC ATC CTG AAC ACC ATG AGC ACC ATC TAC AGC  
 S E D K S K R L N T I L N T M S T I Y S  
 ACT GGT AAG GTG TGC AAC CCT GAC AAT CCT CAA GAG TGC CTT TTG CTT GAG CCT GGC CTT  
 T G K V C N P D N P Q E C L L L E P G L  
 AAC GAG ATC ATG GCT AAC AGC CTG GAT TAC AAC GAG AGG CTT TGG GCT TGG GAG TCT TGG  
 N E I M A N S L D Y N E R L W A W E S W  
 AGA TCT GAG GTG GGA AAG CAG CTT AGG CCT CTG TAC GAA GAG TAC GTG GTG CTG AAG AAT  
 R S E V G K Q L R P L Y E E Y V V L K N  
 GAG ATG GCT AGG GCT AAC CAC TAC GAG GAC TAC GGT GAT TAT TGG AGG GGC GAT TAC GAG  
 E M A R A N H Y E D Y G D Y W R G D Y E  
 GTG AAC GGT GTG GAT GGT TAC GAT TAC TCT AGG GGT CAG CTG ATC GAG GAT GTT GAG CAT  
 V N G V D G Y D Y S R G Q L I E D V E H  
 ACC TTC GAA GAG ATC AAG CCG CTG TAC GAG CAT CTT CAT GCT TAC GTG AGG GCC AAG CTG  
 T F E E I K P L Y E H L H A Y V R A K L  
 ATG AAC GCT TAC CCG TCT TAC ATC AGC CCT ATT GGT TGC CTT CCT GCT CAC CTT CTT GGT  
 M N A Y P S Y I S P I G C L P A H L L G  
 GAT ATG TGG GGA AGA TTC TGG ACC AAC CTG TAC TCT CTT ACC GTG CCT TTC GGC CAA AAG  
 D M W G R F W T N L Y S L T V P F G Q K  
 CCG AAC ATT GAT GTG ACC GAT GCT ATG GTG GAT CAG GCT TGG GAT GCT CAG AGG ATC TTC  
 P N I D V T D A M V D Q A W D A Q R I F  
 AAA GAG GCC GAG AAG TTC TTC GTG TCT GTG GGT TTG CCT AAC ATG ACC CAA GGA TTC TGG  
 K E A E K F F V S V G L P N M T Q G F W

GAG AAC TCC ATG CTT ACC GAT CCT GGC AAT GTG CAG AAG GCT GTT TGT CAT CCT ACC GCT  
 E N S M L T D P G N V Q K A V C H P T A  
 TGG GAC CTT GGT AAG GGC GAT TTC AGG ATT CTG ATG TGC ACC AAG GTG ACA ATG GAC GAC  
 W D L G K G D F R I L M C T K V T M D D  
 TTC CTT ACT GCA CAC CAC GAG ATG GGT CAC ATC CAG TAC GAT ATG GCT TAT GCT GCT CAG  
 F L T A H H E M G H I Q Y D M A Y A A Q  
 CCT TTC CTG CTT AGG AAT GGT GCT AAT GAG GGT TTC CAT GAG GCT GTG GGT GAG ATC ATG  
 P F L L R N G A N E G F H E A V G E I M  
 TCT CTT TCT GCT GCT ACC CCT AAG CAC CTG AAG TCT ATT GGT CTG CTG AGC CCT GAT TTC  
 S L S A A T P K H L K S I G L L S P D F  
 CAA GAG GAC AAT GAG ACT GAG ATC AAC TTC CTG CTG AAG CAG GCT CTG ACT ATT GTG GGA  
 Q E D N E T E I N F L L K Q A L T I V G  
 ACT CTG CCC TTC ACC TAC ATG CTT GAA AAG TGG CGG TGG ATG GTC TTT AAG GGC GAG ATT  
 T L P F T Y M L E K W R W M V F K G E I  
 CCT AAG GAC CAG TGG ATG AAG AAA TGG TGG GAG ATG AAG CGT GAG ATC GTC GGT GTT GTT  
 P K D Q W M K K W W E M K R E I V G V V  
 GAG CCA GTT CCT CAC GAT GAG ACT TAC TGC GAT CCT GCC TCT CTG TTC CAC GTG AGC AAC  
 E P V P H D E T Y C D P A S L F H V S N  
 GAC TAC TCT TTC ATC CGG TAC TAC ACC CGG ACC TTG TAC CAG TTT CAG TTT CAA GAG GCT  
 D Y S F I R Y Y T R T L Y Q F Q F Q E A  
 CTG TGC CAG GCT GCT AAA CAT GAA GGT CCT CTT CAC AAG TGC GAC ATC AGC AAT TCT ACT  
 L C Q A A K H E G P L H K C D I S N S T  
 GAG GCT GGG CAA AAG CTG TTC AAC ATG CTG AGG CTT GGT AAG TCC GAG CCT TGG ACT CTT  
 E A G Q K L F N M L R L G K S E P W T L  
 GCT TTG GAG AAT GTT GTG GGC GCC AAG AAT ATG AAC GTG AGG CCT CTT CTG AAC TAC TTC  
 A L E N V V G A K N M N V R P L L N Y F  
 GAG CCT TTG TTC ACC TGG CTG AAG GAC CAG AAC AAG AAC AGC TTC GTT GGC TGG TCT ACC  
 E P L F T W L K D Q N K N S F V G W S T  
 GAC TGG TCA CCT TAT GCT GAT GGT GGT GGA TCC GGA GGT GGA GGT TCT GGA GGT GGA GGT  
 D W S P Y A D G G G S G G G G S G G G G  
  
TCA CCA CCA TGT CCA GCT CCA GAA CTT CTT GGT GGT CCT TCT GTT TTT TTG TTC CCA CCA  
 S P P C P A P E L L G G P S V F L F P P  
 AAG CCA AAG GAT ACT CTC ATG ATC TCT AGG ACT CCA GAG GTT ACA TGC GTT GTG GTT GAT  
 K P K D T L M I S R T P E V T C V V V D  
 GTG TCT CAT GAA GAT CCA GAG GTG AAG TTC AAC TGG TAT GTG GAT GGT GTT GAG GTG CAC  
 V S H E D P E V K F N W Y V D G V E V H

AAC GCT AAG ACT AAG CCA AGA GAG GAA CAG TAC AAC TCC ACT TAC AGG GTT GTG TCT GTG  
 N A K T K P R E E Q Y N S T Y R V V S V  
 CTT ACT GTT CTT CAC CAG GAT TGG CTT AAC GGC AAA GAG TAC AAG TGC AAG GTG TCC AAC  
 L T V L H Q D W L N G K E Y K C K V S N  
 AAG GCT TTG CCA GCT CCA ATC GAA AAG ACT ATC TCT AAG GCT AAG GGA CAG CCA AGG GAA  
 K A L P A P I E K T I S K A K G Q P R E  
 CCT CAA GTT TAC ACT CTT CCA CCA TCT AGG GAT GAG CTT ACT AAG AAC CAG GTG TCC CTT  
 P Q V Y T L P P S R D E L T K N Q V S L  
 ACT TGC CTT GTG AAG GGA TTT TAC CCA TCC GAT ATT GCT GTT GAG TGG GAG TCT AAT GGA  
 T C L V K G F Y P S D I A V E W E S N G  
 CAG CCT GAG AAC AAC TAC AAG ACT ACT CCA CCA GTG CTC GAT TCC GAT GGA TCA TTC TTC  
 Q P E N N Y K T T P P V L D S D G S F F  
 TTG TAC TCC AAG CTC ACT GTG GAT AAG TCT AGG TGG CAA CAG GGA AAC GTT TTC TCT TGC  
 L Y S K L T V D K S R W Q Q G N V F S C  
 TCT GTT ATG CAT GAG GCT CTC CAC AAT CAC TAC ACT CAG AAG TCC CTT TCT TTG TCC CCT  
 S V M H E A L H N H Y T Q K S L S L S P  
 GGC AAG TCT GAG AAG GAT GAG CTT TAA **GAG CTC**  
 G K S E K D E L - E L

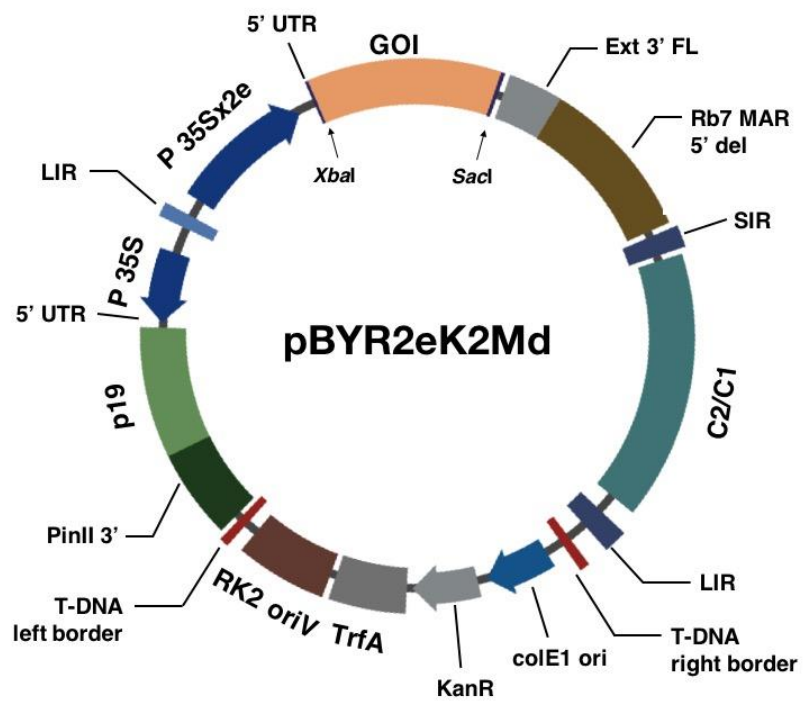
## APPENDIX 3

## RESTRICTION ENZYMES

*Xba*I Restriction Enzyme*Bam*HI Restriction Enzyme*Sac*I Restriction Enzyme

## APPENDIX 4

## GEMINIVIRAL-BASED PLANT EXPRESSION VECTOR (pBYR2eK2Md)



## APPENDIX 5

### REAGENT PREPARATION

#### LB Broth (Miller)

Yeast extract	5.0	g/l
NaCl	10.0	g/l
Tryptone	10.0	g/l

#### LB Agar (Miller)

Yeast extract	5.0	g/l
NaCl	10.0	g/l
Tryptone	10.0	g/l
Agar	1.5	%

#### 1xPBS Buffer (pH7.4)

KCl	2.68	g
KH <sub>2</sub> PO <sub>4</sub>	1.76	mM
Na <sub>2</sub> HPO <sub>4</sub>	10.10	mM
NaCl	137.00	mM

Adjust the pH into 7.4

**1xInfiltration Buffer (pH 5.5)**

2-(N-morpholino) ethanesulfonic acid (MES)	2.68	g
KH <sub>2</sub> PO <sub>4</sub>	1.76	mM
Na <sub>2</sub> HPO <sub>4</sub>	10.10	mM
NaCl	137.00	mM
Adjust the pH into 5.5		

**1xRunning Buffer for SDS-PAGE**

SDS	3	mM
Tris base	25	mM
Glycine	0.2	M

**1xTransfer Buffer for Western Blotting**

Tris base	20	mM
Glycine	0.1	M
Methanol	15	%

**Coomassie Staining Solution**

Glacial acetic acid	10.0	%
Methanol	50.0	%
Coomassie R250		

**De-staining Solution**

Glacial acetic acid	10.0	%
Methanol	20.0	%

**Z-buffer for Reducing Protein Loading Dye**

Glycerol	10.0	%
SDS	12.0	%
$\beta$ -mercaptoethanol	22.0	%
1M Tris-HCl pH 6.8	125	mM
Bromophenol blue		

**Z-buffer for Non-Reducing Protein Loading Dye**

Glycerol	10.0	%
SDS	12.0	%
1M Tris-HCl pH 6.8	125	mM
Bromophenol blue		

จุฬาลงกรณ์มหาวิทยาลัย  
CHULALONGKORN UNIVERSITY

**Complete DMEM Medium**

Heat-inactivated FBS	10	%
Penicillin solution	100	U/ml
Streptomycin solution	100	$\mu$ g/ml
1xDMEM medium		



**Blocking Solution for Microneutralization Assay**

Tween-20	0.1	%
BSA	2.0	%
1xPBS buffer		

**Diluent Solution for Antibody**

Tween-20	0.1	%
BSA	0.5	%
1xPBS buffer		

**R5 Medium**

2-mercaptoethanol	35	$\mu\text{M}$
Heat-inactivated FBS	5.0	%
Antimycotic	1.0	%
1xRPMI1640 medium		

**R10 Medium**

Heat-inactivated FBS	10.0	%
Antimycotic	1.0	%
1xRPMI1640 medium		

**1xACK Lysis Buffer**

NH <sub>4</sub> Cl	0.15	M
KHCO <sub>3</sub>	0.01	M
Na <sub>2</sub> EDTA	0.10	mM

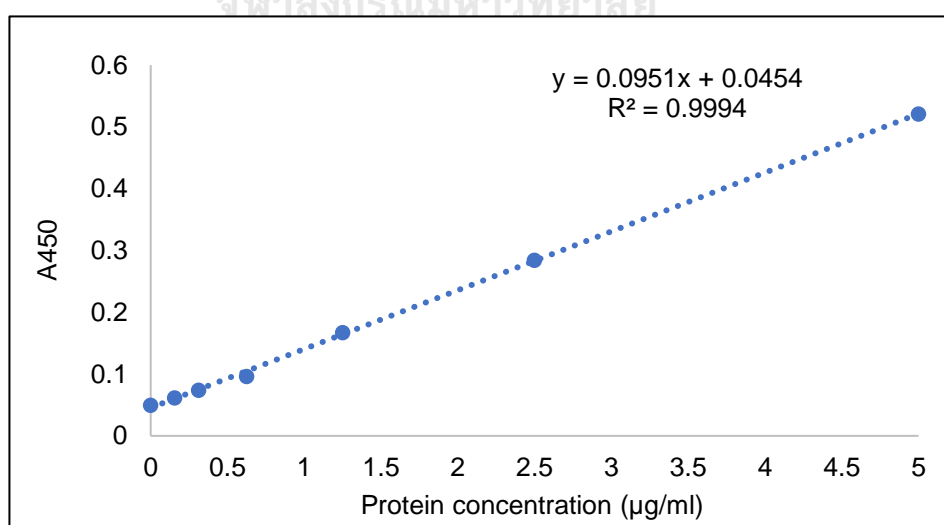


## APPENDIX 6

### TIME-COURSE OPTIMIZATION OF PLANT-PRODUCED ACE2-Fc

#### Commercial HEK-Produced ACE2-Fc Protein Standard

Concentration ( $\mu\text{g/ml}$ )	Absorbance at 450 nm			
	Rep 1	Rep 2	Rep 3	Average
0.000	0.0495	0.0505	0.0497	0.0499
0.156	0.0629	0.0622	0.0602	0.0618
0.313	0.0737	0.0733	0.0748	0.0739
0.625	0.1226	0.0830	0.0830	0.0962
1.250	0.1699	0.1695	0.1627	0.1674
2.500	0.2829	0.2851	0.2855	0.2845
5.000	0.5104	0.5167	0.5356	0.5209



### Expression Levels of Plant-Produced ACE2-Fc Proteins

Days	Concentration ( $\mu\text{g/g FW}$ )				
	Rep 1	Rep 2	Rep 3	Average	SD
2	32.130	26.250	36.474	31.618	5.131
4	34.419	57.903	45.487	45.936	11.749
6	137.967	121.693	79.272	107.498	27.060
8	67.062	99.961	55.573	74.199	23.038
10	27.549	25.058	50.210	34.272	13.858

## APPENDIX 7

### *IN VITRO* BINDING ACTIVITIES OF PLANT-PRODUCED

#### SARS-CoV-2 RBD-Fc

**Absorbance at 450 nm of Sample in the Various Concentrations Tested  
by Using HEK293-Produced ACE2 Protein.**

Concentration (µg/ml)	Absorbance at 450 nm				
	Rep 1	Rep 2	Rep 3	Average	SD
0.0010	0.0609	0.0623	0.0655	0.0629	0.0024
0.0050	0.0593	0.0606	0.0611	0.0603	0.0009
0.0100	0.0608	0.0585	0.0621	0.0605	0.0018
0.0500	0.0611	0.0608	0.0598	0.0606	0.0007
0.1000	0.0600	0.0617	0.0665	0.0627	0.0034
0.5000	0.0646	0.0654	0.0645	0.0648	0.0005
1.0000	0.0693	0.0708	0.0668	0.0690	0.0020
5.0000	0.1017	0.1049	0.0973	0.1013	0.0038
10.0000	0.2063	0.2153	0.2000	0.2072	0.0077
50.0000	0.5081	0.5075	0.5059	0.5072	0.0011
100.0000	0.5347	0.5878	0.5881	0.5702	0.0307
500.0000	0.5840	0.5858	0.5859	0.5852	0.0011
1000.0000	0.6000	0.6026	0.5985	0.6004	0.0021

**Absorbance at 450 nm of Sample in the Various Concentrations Tested  
by Using CHO-Produced ACE2 Protein.**

Concentration ( $\mu\text{g/ml}$ )	Absorbance at 450 nm				
	Rep 1	Rep 2	Rep 3	Average	SD
0.0010	0.0590	0.0623	0.0613	0.0609	0.0017
0.0050	0.0588	0.0626	0.0604	0.0606	0.0019
0.0100	0.0593	0.0601	0.0601	0.0598	0.0005
0.0500	0.0595	0.0604	0.0610	0.0603	0.0008
0.1000	0.0643	0.0603	0.0619	0.0622	0.0020
0.5000	0.0639	0.0626	0.0626	0.0630	0.0008
1.0000	0.0646	0.0657	0.0644	0.0649	0.0007
5.0000	0.0791	0.0783	0.0765	0.0780	0.0013
10.0000	0.1142	0.1092	0.1012	0.1082	0.0066
50.0000	0.2806	0.3028	0.2918	0.2917	0.0111
100.0000	0.3368	0.3402	0.3248	0.3339	0.0081
500.0000	0.3613	0.3570	0.3579	0.3587	0.0023
1000.0000	0.3723	0.3698	0.3702	0.3708	0.0013

**Absorbance at 450 nm of Sample in the Various Concentrations Tested  
by Using 1xPBS Buffer (Negative Control)**

Concentration ( $\mu\text{g/ml}$ )	Absorbance at 450 nm				
	Rep 1	Rep 2	Rep 3	Average	SD
0.0010	0.0619	0.0610	0.0776	0.0668	0.0093
0.0050	0.0630	0.0633	0.0645	0.0636	0.0008
0.0100	0.0664	0.0649	0.0635	0.0649	0.0015
0.0500	0.0603	0.0645	0.0623	0.0624	0.0021
0.1000	0.0664	0.0652	0.0643	0.0653	0.0011
0.5000	0.0595	0.0602	0.0618	0.0605	0.0012
1.0000	0.0580	0.0603	0.0625	0.0603	0.0023
5.0000	0.0691	0.0613	0.0637	0.0647	0.0040
10.0000	0.0612	0.0628	0.0669	0.0636	0.0029
50.0000	0.0587	0.0608	0.0610	0.0602	0.0013
100.0000	0.0670	0.0702	0.0687	0.0686	0.0016
500.0000	0.0632	0.0589	0.0621	0.0614	0.0022
1000.0000	0.0632	0.0675	0.0645	0.0651	0.0022

## APPENDIX 8

### *IN VITRO* BINDING ACTIVITIES OF PLANT-PRODUCED ACE2-Fc

**Absorbance at 450 nm of Sample in the Various Concentrations Tested  
by Using Sf9-Produced SARS-CoV-2 RBD-His Protein.**

Concentration (µg/ml)	Absorbance at 450 nm				
	Rep 1	Rep 2	Rep 3	Average	SD
0.0010	0.0490	0.0493	0.0491	0.2505	0.0002
0.0100	0.0497	0.0471	0.0495	0.1982	0.0001
0.1000	0.0654	0.0523	0.0529	0.1126	0.0074
0.5000	0.1034	0.0889	0.0961	0.0961	0.0072
1.0000	0.1279	0.1111	0.0988	0.0569	0.0146
5.0000	0.2018	0.1862	0.2067	0.0488	0.0107
10.0000	0.1921	0.2838	0.2756	0.0491	0.0507



**Absorbance at 450 nm of Sample in the Various Concentrations Tested  
by Using Plant-Produced S1 of PEDV-His Protein (Negative Control).**

Concentration ( $\mu\text{g/ml}$ )	Absorbance at 450 nm				
	Rep 1	Rep 2	Rep 3	Average	SD
0.0010	0.0514	0.0514	0.0518	0.0515	0.0002
0.0100	0.0512	0.0518	0.0519	0.0516	0.0004
0.1000	0.0492	0.0581	0.0502	0.0525	0.0049
0.5000	0.0505	0.0499	0.0506	0.0503	0.0004
1.0000	0.0513	0.0509	0.0507	0.0510	0.0003
5.0000	0.0547	0.0537	0.0561	0.0548	0.0012
10.0000	0.0555	0.0567	0.0541	0.0554	0.0013



**Absorbance at 450 nm of Sample in the Various Concentrations Tested  
by Using 1xPBS Buffer (Negative Control).**

Concentration ( $\mu\text{g/ml}$ )	Absorbance at 450 nm				
	Rep 1	Rep 2	Rep 3	Average	SD
0.0010	0.0499	0.0501	0.0507	0.0502	0.0004
0.0100	0.0509	0.0510	0.0497	0.0505	0.0007
0.1000	0.0498	0.0498	0.0504	0.0500	0.0003
0.5000	0.0510	0.0498	0.0505	0.0504	0.0006
1.0000	0.0504	0.0499	0.0503	0.0502	0.0003
5.0000	0.0506	0.0494	0.0497	0.0499	0.0006
10.0000	0.0503	0.0503	0.0507	0.0504	0.0002

## APPENDIX 9

## SARS-CoV-2 RBD-Specific IgG Titers

## Total IgG Titers

Group	Vaccination Group	No.	Total mouse-IgG titer		
			Day 0	Day 14	Day 35
1	PBS + 0.1 mg alum (Control)	1	100	100	100
		2	100	100	100
		3	100	100	100
		4	100	100	100
		5	100	100	100
2	10 µg SARS-CoV-2 RBD-Fc	1	100	100	200
		2	100	100	100
		3	100	100	100
		4	100	100	400
		5	100	100	400
3	10 µg SARS-CoV-2 RBD-Fc + alum	1	100	100	12,800
		2	100	100	1,600
		3	100	100	3,200
		4	100	100	25,600
		5	100	100	25,600

Group	Vaccination Group	No.	Total mouse-IgG titer		
			Day 0	Day 14	Day 35
4	10 µg SARS-CoV-2 RBD-Fc + MF59	1	100	100	25,600
		2	100	100	6,400
		3	100	100	25,600
		4	100	100	6,400
		5	100	100	6,400
5	10 µg SARS-CoV-2 RBD-Fc + mPLA-SM	1	100	800	51,200
		2	100	200	25,600
		3	100	100	12,800
		4	100	200	12,800
		5	100	200	25,600
6	10 µg SARS-CoV-2 RBD-Fc + Poly (I:C)	1	100	100	6,400
		2	100	100	12,800
		3	100	200	25,600
		4	100	100	25,600
		5	100	100	1,600

### IgG1 subtype Titers

Group	Vaccination Group	No.	Total mouse-IgG1 titer		
			Day 0	Day 14	Day 35
1	PBS + 0.1 mg alum (Control)	1	100	100	100
		2	100	100	100
		3	100	100	100
		4	100	100	100
		5	100	100	100
2	10 µg SARS-CoV-2 RBD-Fc	1	100	400	25,600
		2	100	100	6,400
		3	100	100	3,200
		4	100	400	25,600
		5	100	100	25,600
3	10 µg SARS-CoV-2 RBD-Fc + alum	1	100	3,200	409,600
		2	100	3,200	102,400
		3	100	6,400	102,400
		4	100	3,200	409,600
		5	100	6,400	409,600
4	10 µg SARS-CoV-2 RBD-Fc + MF59	1	100	3,200	204,800
		2	100	3,200	204,800

Group	Vaccination Group	No.	Total mouse-IgG1 titer		
			Day 0	Day 14	Day 35
		3	100	6,400	409,600
		4	100	6,400	409,600
		5	100	6,400	204,800
5	10 µg SARS-CoV-2 RBD-Fc + mPLA-SM	1	100	12,800	409,600
		2	100	3,200	409,600
		3	100	100	204,800
		4	100	1,600	204,800
		5	100	800	204,800
6	10 µg SARS-CoV-2 RBD-Fc + Poly (I:C)	1	100	400	102,400
		2	100	3,200	409,600
		3	100	1,600	204,800
		4	100	3,200	409,600
		5	100	800	102,400

## IgG2a subtype Titers

Group	Vaccination Group	No.	Total mouse-IgG2a titer		
			Day 0	Day 14	Day 35
1	PBS + 0.1 mg alum  (Control)	1	100	100	100
		2	100	100	100
		3	100	100	100
		4	100	100	100
		5	100	100	100
2	10 µg  SARS-CoV-2 RBD-Fc	1	100	100	800
		2	100	100	800
		3	100	100	800
		4	100	100	800
		5	100	100	800
3	10 µg  SARS-CoV-2 RBD-Fc + alum	1	100	100	3,200
		2	100	100	800
		3	100	100	1,600
		4	100	100	6,400
		5	100	100	12,800
4	10 µg  SARS-CoV-2 RBD-Fc + MF59	1	100	100	12,800
		2	100	100	6,400

Group	Vaccination Group	No.	Total mouse-IgG2a titer		
			Day 0	Day 14	Day 35
		3	100	200	25,600
		4	100	400	12,800
		5	100	100	25,600
5	10 µg SARS-CoV-2 RBD-Fc + mPLA-SM	1	100	3,200	102,400
		2	100	400	102,400
		3	100	100	25,600
		4	100	1,600	51,200
		5	100	1,600	102,400
6	10 µg SARS-CoV-2 RBD-Fc + Poly (I:C)	1	100	100	25,600
		2	100	200	51,200
		3	100	400	102,400
		4	100	200	102,400
		5	100	100	12,800



## APPENDIX 10

## SARS-CoV-2-Specific Neutralizing Antibody Titers

Group	Vaccination Group	No.	Neutralizing titer		
			Day 0	Day 14	Day 35
1	PBS + 0.1 mg alum (Control)	1	10	10	10
		2	10	10	10
		3	10	10	10
		4	10	10	10
		5	10	10	10
2	10 µg SARS-CoV-2 RBD-Fc	1	10	10	40
		2	10	10	10
		3	10	10	10
		4	10	10	40
		5	10	10	80
3	10 µg SARS-CoV-2 RBD-Fc + alum	1	10	10	10,240
		2	10	10	640
		3	10	20	1,280
		4	10	10	1,280
		5	10	10	10,240
4	10 µg	1	10	10	1,280

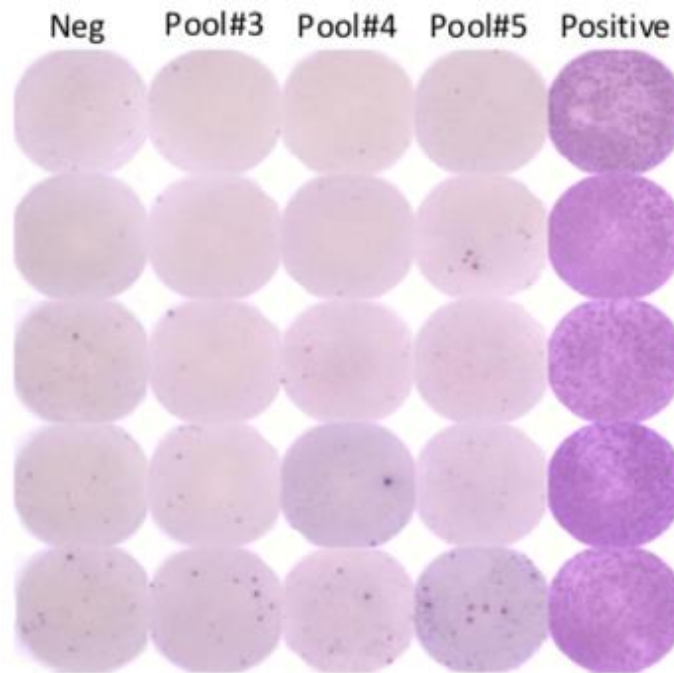
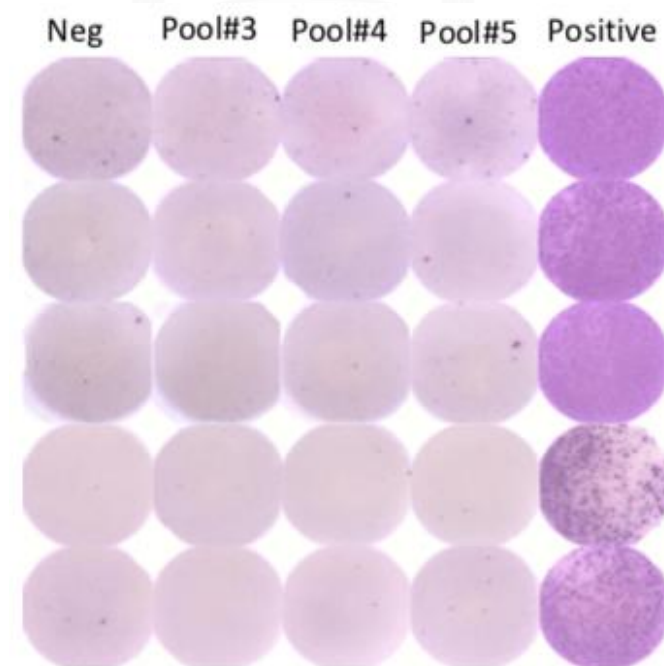
Group	Vaccination Group	No.	Neutralizing titer		
			Day 0	Day 14	Day 35
	SARS-CoV-2 RBD-Fc + MF59	2	10	10	2,560
		3	10	20	2,560
		4	10	20	1,280
		5	10	40	5,120
5	10 µg SARS-CoV-2 RBD-Fc + mPLA-SM	1	10	160	10,240
		2	10	40	5,120
		3	10	10	1,280
		4	10	20	5,120
		5	10	40	5,120
6	10 µg SARS-CoV-2 RBD-Fc + Poly (I:C)	1	10	10	1,280
		2	10	10	2,560
		3	10	20	1,280
		4	10	10	5,120
		5	10	10	640

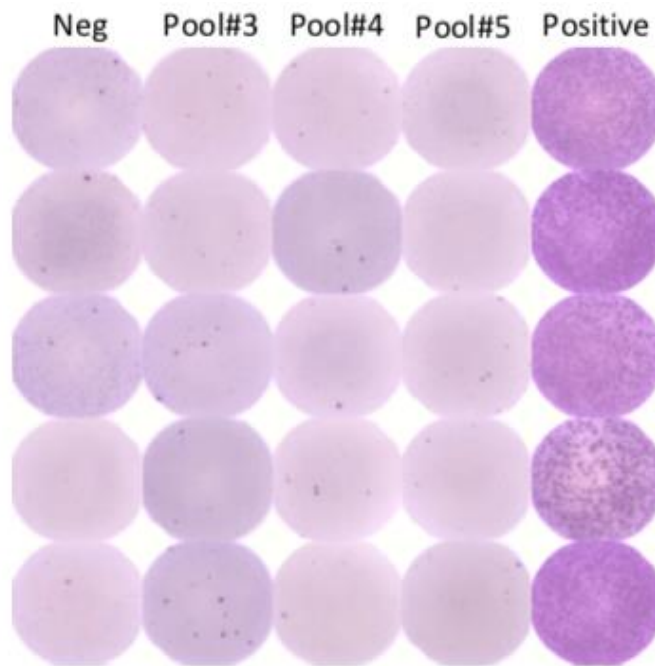
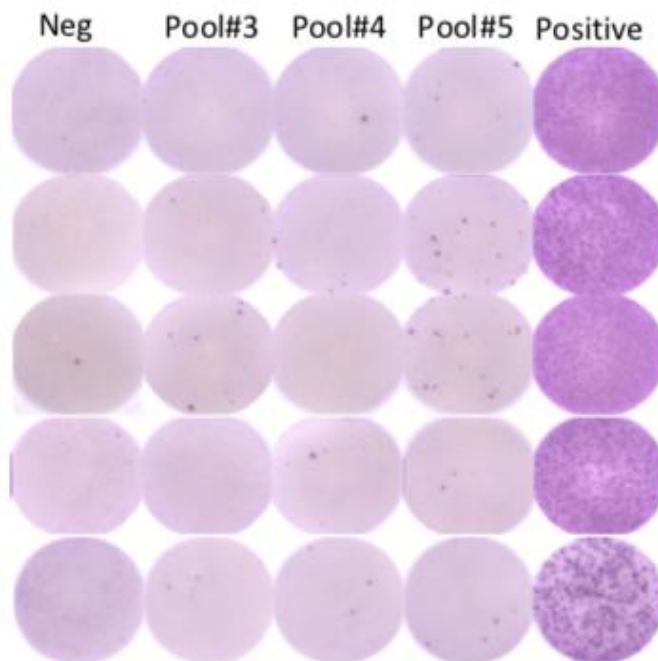
## APPENDIX 11

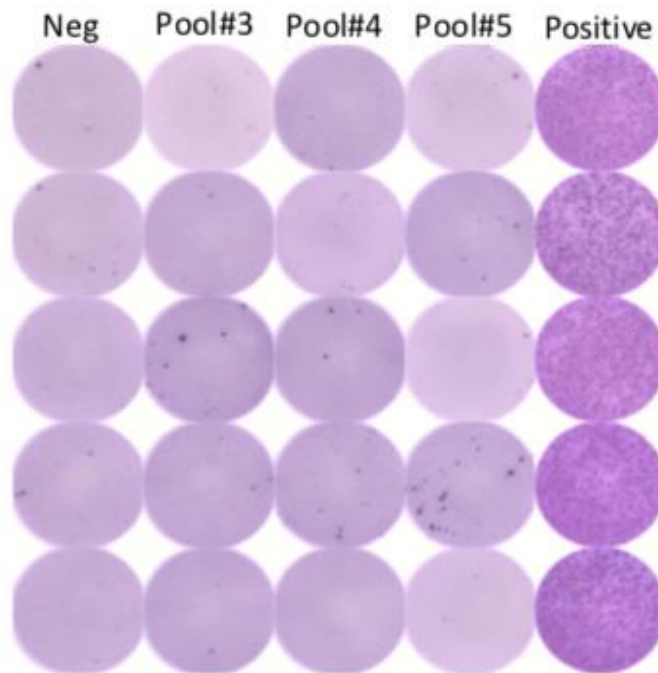
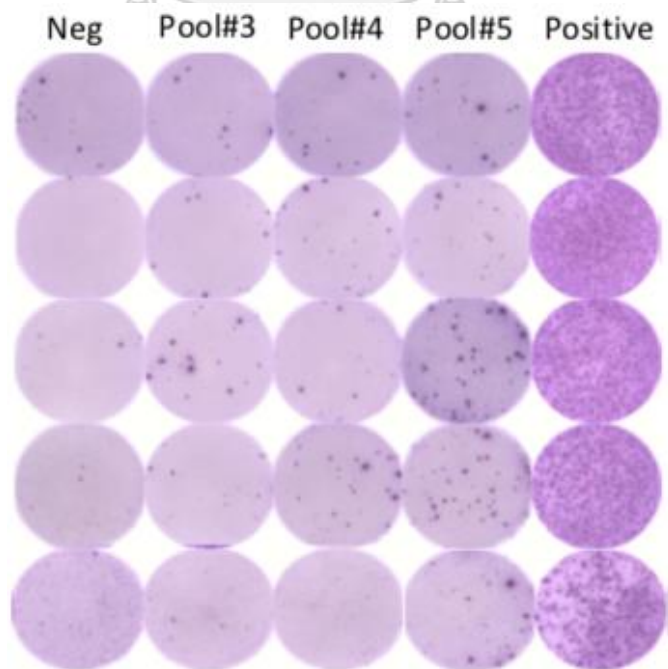
QUANTIFICATION OF SARS-CoV-2-SPECIFIC IFN- $\gamma$ 

Group	Vaccination Group	No.	IFN- $\gamma$ ELISpot (SFU/10 <sup>6</sup> Splenocyte)				
			Negative	Positive	SARS-CoV-2 Pool# 3	SARS-CoV-2 Pool# 4	SARS-CoV-2 Pool# 5
1	PBS + 0.1 mg alum (Control)	1	0	2,206	0	0	0
		2	0	2,204	0	2	10
		3	0	1,962	0	0	0
		4	0	1,938	2	0	0
		5	0	1,992	0	0	6
2	10 $\mu$ g SARS-CoV-2 RBD-Fc	1	0	2,128	4	2	10
		2	0	2,110	0	2	0
		3	0	2,500	0	0	8
		4	0	1,340	0	0	0
		5	0	1,932	0	0	4
3	10 $\mu$ g SARS-CoV-2 RBD-Fc + alum	1	0	2,620	2	4	0
		2	0	2,020	0	4	0
		3	0	1,858	0	0	0

		4	0	1,802	6	8	4
		5	0	1,894	20	0	0
4	10 µg SARS-CoV-2 RBD-Fc + MF59	1	0	1,954	0	2	4
		2	0	1,960	4	6	20
		3	0	2,288	10	0	30
		4	0	1,906	0	6	2
		5	0	1,562	4	6	8
5	10 µg SARS-CoV-2 RBD-Fc + mPLA- SM	1	0	2,084	0	4	4
		2	0	1,926	0	0	2
		3	0	1,954	14	6	2
		4	0	1,644	0	6	38
		5	0	1,544	2	0	2
6	10 µg SARS-CoV-2 RBD-Fc + poly (I:C)	1	0	1,868	2	2	18
		2	0	1,698	10	30	26
		3	0	1,886	32	12	90
		4	0	1,974	4	36	70
		5	0	1,696	4	0	40

**Group 1: PBS + 0.1 mg alum (Control)****Group 2: 10  $\mu$ g SARS-CoV-2 RBD-Fc**

**Group 3: 10 µg SARS-CoV-2 RBD-Fc + alum****Group 4: 10 µg SARS-CoV-2 RBD-Fc + MF59**

**Group 5: 10 µg SARS-CoV-2 RBD-Fc + mPLA-SM****Group 6: 10 µg SARS-CoV-2 RBD-Fc + poly (I:C)**

## APPENDIX 12

## WEIGHT OF MICE

Group	Vaccination Group	No.	Weight (g)		
			Day 0	Day 14	Day 35
1	PBS + 0.1 mg alum (Control)	1	25.92	27.89	31.00
		2	28.03	30.08	34.5
		3	24.52	27.20	30.95
		4	28.49	31.87	38.30
		5	31.24	37.59	39.19
2	10 µg SARS-CoV-2 RBD-Fc	1	27.49	30.78	34.22
		2	25.39	30.82	37.02
		3	24.68	23.75	26.59
		4	28.85	31.50	33.95
		5	28.61	30.29	34.13
3	10 µg SARS-CoV-2 RBD-Fc + alum	1	27.54	31.47	33.83
		2	24.98	29.07	31.34
		3	27.76	30.98	33.64
		4	29.00	33.39	37.38
		5	23.80	32.74	39.16



Group	Vaccination Group	No.	Weight (g)		
			Day 0	Day 14	Day 35
4	10 µg SARS-CoV-2 RBD-Fc + MF59	1	26.23	30.26	34.47
		2	24.47	26.16	28.18
		3	26.29	30.27	34.70
		4	27.01	30.96	33.94
		5	27.38	29.26	33.60
5	10 µg SARS-CoV-2 RBD-Fc + mPLA-SM	1	26.24	27.59	36.53
		2	24.46	29.15	33.54
		3	27.01	30.99	35.63
		4	28.41	31.91	38.06
		5	27.02	30.04	32.00
6	10 µg SARS-CoV-2 RBD-Fc + Poly (I:C)	1	27.76	32.85	35.15
		2	21.91	26.07	31.64
		3	24.91	28.75	33.10
		4	30.10	36.45	41.30
		5	28.88	32.05	34.89

## APPENDIX 13

## SPLEEN SIZE AND HEALTH STATUS

Group	Vaccination Group	No.	Spleen size (mm)	Health status
1	PBS + 0.1 mg alum (Control)	1	23.2	Normal
		2	20.6	Normal
		3	22.8	Normal
		4	20.7	Normal
		5	22.4	Normal
2	10 µg SARS-CoV-2 RBD-Fc	1	22.8	Normal
		2	21.0	Normal
		3	19.6	Normal
		4	19.9	Normal
		5	20.9	Normal
3	10 µg SARS-CoV-2 RBD-Fc + alum	1	22.4	Normal
		2	20.6	Normal
		3	23.6	Normal
		4	21.0	Normal
		5	22.5	Normal
4	10 µg	1	20.8	Normal

Group	Vaccination Group	No.	Spleen size (mm)	Health status
	SARS-CoV-2 RBD-Fc + MF59	2	23.5	Normal
		3	21.2	Normal
		4	23.0	Normal
		5	24.5	Normal
5	10 µg SARS-CoV-2 RBD-Fc + mPLA-SM	1	23.8	Normal
		2	19.7	Normal
		3	20.9	Normal
		4	20.6	Normal
		5	17.9	Normal
6	10 µg SARS-CoV-2 RBD-Fc + Poly (I:C)	1	23.9	Normal
		2	22.4	Normal
		3	21.3	Normal
		4	20.8	Normal
		5	25.6	Normal

## APPENDIX 14

## COMMERCIAL IMMUNOADJUVANT DATASHEET

## Alum Adjuvant

## Alhydrogel® adjuvant 2%

Aluminium hydroxide gel

Catalog code: vac-alu-250

<https://www.invivogen.com/alhydrogel>

Distributed by InvivoGen for research use only

Version 20J08-MM

## PRODUCT INFORMATION

## Contents

• 250 ml of Alhydrogel® adjuvant 2% is provided as a ready-to-use, aluminium hydroxide wet gel (colloidal) suspension. Alhydrogel® adjuvant is sterilized by autoclavation and aseptically filled.

## Storage and stability

• Alhydrogel® adjuvant 2% is shipped at room temperature and should be stored at room temperature. The expiry date is specified on the product label. **DO NOT FREEZE.**

*Note:* Do not expose to frost as product will be destroyed if ice crystals form in the gel.

## Quality control

• Alhydrogel® adjuvant 2% is tested for pyrogenicity and sterility.

## CHEMICAL PROPERTIES

CAS Number: 21645-51-2

Formulation: Al(OH)<sub>3</sub>, Aluminium hydroxide gel

Appearance: White gelatinous precipitate

Aluminium content: 9.0 - 11.0 mg/ml

pH: ~6.5

## DESCRIPTION

Alhydrogel® adjuvant is an aluminium hydroxide (referred to as alum) wet gel suspension. Alum improves attraction and uptake of antigen by antigen presenting cells (APCs)<sup>1</sup>. Recently, it has been suggested that the antigens adsorbed on the aluminum salts are presented in a particulate form, making them more efficiently internalized by APCs. Moreover, alum activates the NLRP3 inflammasome complex implicated in the induction of several pro-inflammatory cytokines including IL-1 $\beta$  and IL-18<sup>2</sup>. Alum increases Th2 antibodies but does not promote significant Th1 cellular response<sup>3</sup>. Alhydrogel® particles have a net positive electrical charge at pH 5-7 and thus are well suited for adsorption of negatively charged antigens (e.g. antigens with isoelectric points below the pH of formulation)<sup>4</sup>. Alhydrogel® adjuvant 2% is made by Croda (following its acquisition of Brenntag Biosector A/S), a leader in the global vaccine adjuvants market with a long history of producing high quality products. Alhydrogel® adjuvant 2% was elected as the International Standard Preparation for aluminium hydroxide gels<sup>5</sup>. Alhydrogel® adjuvant 2% is present in multiple commercial vaccine formulations<sup>6</sup>. Typical results obtained with Alhydrogel® adjuvant 2% are shown in figure 1.

1. **Coffman R, et al. 2010.** Vaccine adjuvants: Putting innate immunity to work. *Immunity* 33(4):492-503. 2. **Merrick P, et al. 2009.** Towards an understanding of adjuvant action of aluminium. *Nat Rev Immunol*, 9(4): 287-93. 3. **Huang M & Wang W, 2014.** Factors affecting alum-protein interactions. *Int J Pharm*, 466(1-2):139-46. 4. **Stewart-Tull D., 1989.** Recommendations for the assessment of adjuvants (immunopotentiators). In: *Immunological adjuvants and vaccines* (Gregoriadis, G., Allison, A. & Poste, G., eds.), Plenum, New York, pp.213-226. 5. **Stewart-Tull D., 1991.** The assessment and use of adjuvants. In: *Vaccines* (Gregoriadis, G., Allison, A. & Poste, G., eds.), Plenum, New York, pp85-92. 6. **Lindblad E. & Schenberg N, 2010.** Aluminium adjuvants: preparation, application, dosage, and formulation with antigen. *Methods Mol Biol*, 626:41-58.

## METHODS

## Preparation of antigen-Alhydrogel® adjuvant 2% mixture

Antigens are preferentially diluted in saline or phosphate buffers. The amount of protein or conjugated peptide used for the primary immunization can be adjusted depending upon availability and immunogenicity of the antigen. For example, mice can be injected subcutaneously (s.c.) with 1 to 10  $\mu$ g of endotoxin-free ovalbumin (cat. code: vac-pova). The adsorption capacity for a model protein such as diphtheroid toxoid, human growth hormone or ovalbumin in Alhydrogel® adjuvant varies from 1 to 3 mg (mg/mg Al)<sup>1</sup>.

1. **Shake well before use** the capped bottle of Alhydrogel® adjuvant 2%.  
2. Add Alhydrogel® adjuvant 2% to the antigen solution; the final volume ratio of Alhydrogel® adjuvant 2% to antigen should be 1:1 (100  $\mu$ l Alhydrogel® adjuvant 2% for 100  $\mu$ l of antigen) to 1:9 (100  $\mu$ l Alhydrogel® adjuvant 2% for 900  $\mu$ l of antigen).  
3. Mix well by pipetting up and down for at least 5 minutes to allow Alhydrogel® adjuvant 2% to effectively adsorb the antigen.

The volume of injection depends on the site of administration. For example, 100  $\mu$ l can be injected s.c. in mice.

*Note:* To avoid anaphylaxis, do not use adjuvants for intravenous injection.

Recommended maximum volumes for injection of antigen/adjuvant mixtures per site of injection for laboratory animals.

Species	Max. volume	Injection Site
Mice, hamsters	100 $\mu$ l	subcutaneous (s.c.)
Mice, hamsters	50 $\mu$ l	intramuscular (im.)
Guinea pigs	200 $\mu$ l	s.c. or im.
Rats	200 $\mu$ l	s.c. or im.
Rabbits	250 $\mu$ l	s.c. or im.

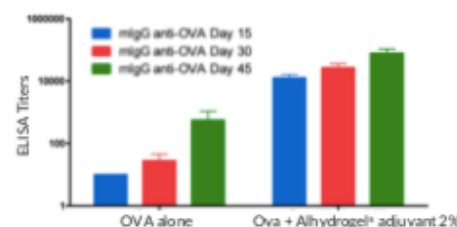


**Figure 1.** Anti-Ova mlgG levels at 15, 30 and 45 days after the initial immunization in different groups. Mice were immunized s.c. at 0, 2 and 3 weeks with 1  $\mu$ g of EndoFIT™ Ovalbumin alone or 1  $\mu$ g of EndoFIT™ Ovalbumin/Alhydrogel® adjuvant 2% (1:1, w/v) in a final volume of 100  $\mu$ l. Serum anti-OVA mlgG was monitored by ELISA (coated with ovalbumin at 10  $\mu$ g/ml in PBS).

Alhydrogel® is a trademark of Croda

## TECHNICAL SUPPORT

InvivoGen USA (Toll-Free): 888-457-5873

InvivoGen USA (International): +1 (858) 457-5873

InvivoGen Europe: +33 (0) 5-62-71-69-39

InvivoGen Hong Kong: +852 3622-34-80

E-mail: [info@invivogen.com](mailto:info@invivogen.com)

 **InvivoGen**  
www.invivogen.com

## AddaVax™ (MF59) Adjuvant

# AddaVax™

Squalene-based oil-in-water adjuvant

Catalog code: vac-adx-10

<https://www.invivogen.com/addavax>

For research use only. Not for use in humans.

Version 20J08-MM

### PRODUCT INFORMATION

#### Contents

- 10 ml of AddaVax™ provided as a ready-to-use sterile emulsion

#### Storage and stability

- AddaVax™ is shipped at room temperature.
- Store at 4°C. AddaVax™ is stable for 2 years. **DO NOT FREEZE.**

#### Formulation

AddaVax™ is based on nano-emulsification of 2 components:

- Sorbitan trioleate (0.5% w/v) in squalene oil (5% w/v)
  - Tween 80 (0.5% w/v) in sodium citrate buffer (10 mM, pH 6.5)
- The nano-emulsion is produced using a microfluidizer and filtered through a 0.22-µm filter to remove large droplets and sterilize the final product. The particle size is ~ 160 nm.

#### Quality control

- AddaVax™ is VacciGrade™ (preclinical grade). It is prepared under strict aseptic conditions and is tested for the presence of endotoxins. AddaVax™ is guaranteed sterile and its endotoxin level is < 1 EU/ml (measurement by kinetic chromogenic LAL assay).
- Adjuvanticity of AddaVax™ was evaluated by assessing the levels of total mouse IgG (mIgG) and the mIgG1 and mIgG2 isotypes after two subcutaneous injections of EndoFit™ Ovalbumin/AddaVax™ (1:1, v/v) in mice. Results were compared to mice receiving antigen alone.

### DESCRIPTION

AddaVax™ is a squalene-based oil-in-water nano-emulsion based on the formulation of MF59® that has been licensed in Europe for adjuvanted flu vaccines<sup>1</sup>. Squalene is an oil that is more readily metabolized than the paraffin oil used in Freund's adjuvants<sup>2</sup>. Squalene oil-in-water emulsions, such as MF59®, elicit both cellular (Th1) and humoral (Th2) immune responses<sup>3,4</sup>. This class of adjuvants is believed to act through a depot effect, enhancement of antigen persistence at the injection site, recruitment and activation of antigen presenting cells, and direct stimulation of cytokine and chemokine production by macrophages and granulocytes<sup>5</sup>.

Typical results obtained with AddaVax™ are shown in Figure 1.

MF59® is a registered trademark used for adjuvants for vaccine owned by Novartis AG.

1. Mbow ML, et al., 2010. New adjuvants for human vaccines. *Curr Opin Immunol* 22(3):411-6. 2. Calabro S, et al., 2013. The adjuvant effect of MF59 is due to the oil-in-water emulsion formulation, none of the individual components induce a comparable adjuvant effect. *Vaccine* 31:3363-9. 3. Ott G, et al., 1995. MF59: Design and evaluation of a safe and potent adjuvant for human vaccines. *Pharm Biotechnol* 6:277-96.

#### TECHNICAL SUPPORT

InvivoGen USA (Toll-Free): 888-457-5873  
 InvivoGen USA (International): +1 (858) 457-5873  
 InvivoGen Europe: +33 (0) 5-62-71-69-39  
 InvivoGen Hong Kong: +852 3622-34-80  
 E-mail: [info@invivogen.com](mailto:info@invivogen.com)

### METHODS

#### Preparation of antigen-AddaVax™ mixture

Antigens are preferentially diluted in saline or phosphate buffers. The amount of protein or conjugated peptide used for the primary immunization can be adjusted depending upon availability and immunogenicity of the antigen. Mice can be injected subcutaneously (s.c.) with 1 to 10 µg of endotoxin-free ovalbumin (cat. code vac-pova).

1. Bring AddaVax™ to room temperature.
2. Shake the capped bottle of AddaVax™ before opening.
3. Mix equal volumes of antigen and AddaVax™ by pipetting.

The volume of injection depends of the site of administration. For example, 100 µl can be injected s.c. in mice.

**Note:** To avoid anaphylaxis, do not use adjuvants for intravenous injection.

Recommended maximum volumes for injection of antigen/adjuvant mixtures per site of injection for laboratory animals. (Jindblad EB, 2000. Freund's Adjuvants. In: Vaccine adjuvants: Preparation Methods and Research Protocols. Humana Press, Totowa, NJ).

Species	Max. volume	Injection Site
Mice, hamsters	100 µl	subcutaneous (s.c.)
Mice, hamsters	50 µl	intramuscular (im.)
Guinea pigs	200 µl	s.c. or i.m.
Rats	200 µl	s.c. or i.m.
Rabbits	250 µl	s.c. or i.m.

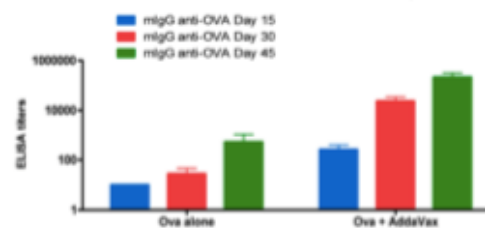


Figure 1. Anti-Ova mIgG levels at 15, 30 and 45 days after the initial immunization in different groups. Mice were immunized s.c. at 0, 2 and 3 weeks with 1 µg of EndoFit™ Ovalbumin alone or 1 µg of EndoFit™ Ovalbumin/AddaVax™ (1:1, v/v) in a final volume of 100 µl. Serum anti-OVA mIgG was monitored by ELISA (coated with ovalbumin at 10 µg/ml in PBS).

## mPLA-SM Adjuvant

# MPLA-SM VacciGrade™

Monophosphoryl Lipid A from *S. minnesota* R595; TLR4-based adjuvant

Catalog code: vac-mpla

<https://www.invivogen.com/mpla-vaccigrade>

For research use only. Not for use in humans.

Version 19A23-MM

### PRODUCT INFORMATION

#### Contents:

- 1 mg MPLA-SM VacciGrade™
- 10 ml sterile endotoxin-free physiological water (NaCl 0.9%)

#### Storage and stability

- MPLA-SM VacciGrade™ is provided as a clear, lipidic film and shipped at room temperature. Store at -20°C. Product is stable for 1 year when properly stored.
- Upon resuspension, prepare aliquots of MPLA-SM VacciGrade™ and store at -20°C. Resuspended product is stable for 6 months when properly stored. Avoid repeated freeze-thaw cycles.

#### Quality control

MPLA-SM VacciGrade™ is a preclinical grade preparation of monophosphoryl lipid A (MPLA) derived from *Salmonella enterica* serovar Minnesota R595 LPS. It is prepared under strict aseptic conditions. MPLA-SM VacciGrade™ is guaranteed sterile.

### DESCRIPTION

Monophosphoryl Lipid A (MPLA) is extracted from lipopolysaccharide (LPS or endotoxin) produced by the Re mutant of a rough strain *Salmonella minnesota* R595. Lipid A, a disaccharide with fatty acid side chains, is the component responsible for the endotoxic activity of LPS<sup>1,2</sup>. Removal of one phosphate group from lipid A produces MPLA which has reduced toxicity while retaining the ability to stimulate the immune system<sup>3,4</sup>.

Both LPS and MPLA are TLR4 agonists, but they signal through different adaptors, MyD88 and TRIF, respectively. The reduced toxicity of MPLA is attributed to the preferential recruitment of TRIF upon TLR4 activation, resulting in decreased induction of inflammatory cytokines<sup>5</sup>. MPLA has been tested as an adjuvant in mice and reported to induce a strong Th1 response<sup>6,7</sup>. Although the mechanism of action of MPLA has not been fully elucidated, it has been suggested that MPLA improves vaccine immunogenicity by enhancing antigen presenting cell maturation<sup>8</sup>.

MPLA-SM is a potent activator of TLR4 with negligible TLR2 activity. MPLA-SM was extracted from LPS using treatment with acid and heat followed by chromatography. Preparations of natural MPLA, such as MPLA-SM, contain a mixture of 5, 6, and 7 acyl lipid A<sup>9</sup>.

**Note:** Due to the intrinsic structural complexity of lipid A, some batch-to-batch variation may occur.

1. Martin M, et al., 2003. Role of innate immune factors in the adjuvant activity of monophosphoryl lipid A. *Infect Immun* 71(5):2498-507.
2. Ogawa T, et al., 2002. Cell activation by *Porphyromonas gingivalis* lipid A molecule through Toll-like receptor 4- and myeloid differentiation factor 88-dependent signaling pathway. *Int. Immunol.* 14(11):1325-32.
3. Qureshi N, et al., 1982. Purification and structural determination of nontoxic lipid A obtained from the lipopolysaccharide of *Salmonella typhimurium*. *J. Biol. Chem.* 257(19):11808-15.
4. Romero CD, et al., 2011. The Toll-Like Receptor 4 agonist monophosphoryl Lipid A augments innate host resistance to systemic bacterial infection. *Infect Immun* 79(9): 3576-3587.
5. Mata-Haro V, et al., 2007. The vaccine adjuvant monophosphoryl lipid A as a TRIF-based agonist of TLR4. *Science* 316(5831):1628-32.
6. Fransen F, et al., 2007. Agonists of Toll-like receptors 3, 4, 7, and 9 are candidates for use as adjuvants in an outer membrane vaccine against *Neisseria meningitidis* serogroup. *Infect Immun* 75(12): 5939-46.
7. Rhee EG, et al., 2010. TLR4 Ligands Augment Antigen-Specific CD8+ T Lymphocyte Responses Elicited by a Viral Vaccine Vector. *J. Virol.* 84: 10413 - 10419.
8. Didierlaurent A, et al., 2009. AS04, an aluminum salt- and TLR4 agonist-based adjuvant system, induces a transient localized innate immune response leading to enhanced adaptive immunity. *J Immunol* 183(10): 6186-97.

### METHODS

#### Preparation of sterile stock solution (1 mg/ml)

- Add 1 ml of DMSO to 1 mg of MPLA-SM VacciGrade™ and vortex until complete solubilization, then sonicate.
- Prepare aliquots of stock solution and store at -20°C. Further dilutions can be prepared with endotoxin-free physiological water (provided).

#### Notes:

- The suspension may appear to contain floating fine particles. Difficulties may be encountered for solubilization at higher concentrations.
- Alternatively, MPLA-SM VacciGrade™ can be resuspended in DMSO containing 0.2 % triethylamine.

**Working Concentration:** 2 - 20 µg/mouse

### TECHNICAL SUPPORT

InvivoGen USA (Toll-Free): 888-457-5873  
 InvivoGen USA (International): +1 (858) 457-5873  
 InvivoGen Europe: +33 (0) 5-62-71-69-09  
 InvivoGen Hong Kong: +852 3622-3480  
 E-mail: [info@invivogen.com](mailto:info@invivogen.com)



## Poly (I:C)-High Molecular Weight Adjuvant

# Poly(I:C) HMW

## High Molecular Weight

Synthetic analog of dsRNA; TLR3 ligand  
Catalog code: tlr1-pic, tlr1-pic-5  
<https://www.invivogen.com/polyic-hmw>

For research use only  
Version 19D27-MM

### PRODUCT INFORMATION

#### Contents

- Poly(I:C) HMW is provided lyophilized and is available in two sizes:
  - tlr1-pic: 10 mg
  - tlr1-pic-5: 50 mg
- Sterile endotoxin-free physiological water (NaClO<sub>9</sub>)
  - 10 ml with catalog code tlr1-pic
  - 2 x 25 ml with catalog code tlr1-pic-5

#### Storage and stability

- Product is shipped at room temperature. Upon receipt, store at 4°C.
- Lyophilized product is stable for 1 year at 4°C when properly stored.
- Upon resuspension, prepare aliquots of Poly(I:C) HMW and store at 4°C or at -20°C. Resuspended product is stable for 1 month at 4°C and 1 year at -20°C. Avoid repeated freeze-thaw cycles.

#### Quality control:

- Absorbance spectrum
- TLR3 activity has been verified using HEK-Blue™ TLR3 cells
- The absence of bacterial contamination (e.g. lipoproteins and endotoxins) has been confirmed using cellular assays.

### BACKGROUND

Polyinosinic-polycytidylic acid (poly(I:C)) is a synthetic analog of double stranded RNA (dsRNA), a molecular pattern associated with viral infection. Both natural and synthetic dsRNAs are known to induce type I interferons (IFN) and other cytokines production. Poly(I:C) is recognized by Toll-like receptor 3 (TLR3)<sup>1,2</sup>. Upon poly(I:C) recognition, TLR3 activates the transcription factor interferon regulatory factor 3 (IRF3), through the adapter protein Toll-IL-1 receptor (TIR) domain-containing adapter inducing IFN- $\beta$  (TRIF, also known as TICAM-1)<sup>3</sup>. Activation of IRF3 leads to the production of type I IFNs, especially IFN- $\beta$ . A second pathway involves the recruitment of TNF receptor-associated factor 6 (TRAF6) or receptor interacting protein 1 (RIP1), with the subsequent activation of the transcription factors NF- $\kappa$ B and AP-1<sup>4</sup>. Activation of this pathway triggers the production of inflammatory cytokines and chemokines such as TNF- $\alpha$ , IL-6 and CXCL10. Poly(I:C) is also recognized by the cytosolic RNA helicases retinoic acid-inducible protein 1 (RIG-I) and melanoma differentiation-associated gene 5 (MDA-5)<sup>5</sup>.

1. **Alexopoulos L et al., 2001.** Recognition of double-stranded RNA and activation of NF- $\kappa$ B by Toll-like receptor 3. *Nature*, 413(6857):732-6. 2. **Matsumoto M et al., 2002.** Establishment of a monoclonal antibody against human Toll-like receptor 3 that binds double-stranded RNA-mediated signaling. *BBRC*, 275(5):1364-9. 3. **Yamanoto M et al., 2003.** Role of Adapter TRIF in the MyD88-Independent Toll-Like Receptor Signaling Pathway. *Science* 301: 640. 4. **Kawai T & Akira S., 2005.** Toll-like receptor and RIG-I-like receptor signaling. *Ann NY Acad Sci*, 1143:1-20. Review. 5. **Kato H et al., 2006.** Differential roles of MDA5 and RIG-I helicases in the recognition of RNA viruses. *Nature*, 441(7089): 101-5.

### PRODUCT DESCRIPTION

Polyinosinic-polycytidylic acid (usually abbreviated as poly(I:C) or poly(I);poly(C)) is a synthetic analog of double-stranded RNA (dsRNA), a molecular pattern associated with viral infection. Poly(I:C) activates the antiviral pattern recognition receptors TLR3, RIG-1/MDA5 and PKR, thereby inducing signaling via multiple inflammatory pathways, including NF- $\kappa$ B and IRF. High Molecular Weight Poly(I:C) comprises long strands of inosine poly(I) homopolymer annealed to strands of cytidine poly(C) homopolymer. The average size of Poly(I:C) HMW is 1.5 to 8 kb.

### METHODS

#### Preparation of stock solution (1 mg/ml)

- Stimulation of TLR3 can be achieved with 30ng - 10 $\mu$ g/ml Poly(I:C).
- Add 10 ml of the endotoxin-free physiological water provided to the 10 mg Poly(I:C) vial or 50 ml to the 50 mg Poly(I:C) vial to obtain a solution at 1 mg/ml.
  - Mix the solution by pipetting up and down.
  - Heat the mixture for 10 minutes at 65-70°C. Allow the solution to cool for 1 hour at room temperature to ensure proper annealing.

#### TLR3 activation of TLR3 with Poly(I:C) HMW

Poly(I:C) HMW can be used to stimulate hTLR3 in HEK-Blue™ hTLR3 cells. These cells are designed for studying the stimulation of hTLR3 by monitoring the activation of NF- $\kappa$ B. Stimulation with a TLR3 ligand activates NF- $\kappa$ B and AP-1 which induces the production of SEAP. Levels of SEAP can be easily determined with QUANTI-Blue™ (a detection medium that turns purple/blue in the presence of alkaline phosphatase).

1. Prepare a HEK-Blue™ hTLR3 cell suspension (250,000 cells/ml).
2. Add 180  $\mu$ l of the cell suspension per well of a 96-well plate.
3. Stimulate cells with 30 ng-10  $\mu$ g/ml Poly(I:C) HMW for 6 to 24 hours.
4. Determine poly(I:C) stimulation on TLR3 by assessing reporter gene expression using QUANTI-Blue™ Solution or HEK-Blue™ detection.

**Note:** InvivoGen provides also a low molecular weight poly(I:C), named poly(I:C)-LMW (see "Related Products"), with an average size of 0.2-2 kb that may activate the immune system differently.

### RELATED PRODUCTS

Product	Catalog Code
HEK-Blue™ hTLR3	hkb-htlr3
QUANTI-Blue™	rep-qb1
Poly(I:C)-LMW	tlr1-picw

### TECHNICAL SUPPORT

InvivoGen USA (Toll-Free): 888-457-5873  
InvivoGen USA (International): +1 (858) 457-5873  
InvivoGen Europe: +33 (0) 5-62-71-69-39  
InvivoGen Hong Kong: +852 3622-3480  
E-mail: [info@invivogen.com](mailto:info@invivogen.com)





จุฬาลงกรณ์มหาวิทยาลัย  
**CHULALONGKORN UNIVERSITY**



## VITA

**NAME** Konlavat Siriwattananon

**DATE OF BIRTH** 17 Dec 1995

**PLACE OF BIRTH** Saraburi, Thailand

**INSTITUTIONS ATTENDED** Chulalongkorn University

**HOME ADDRESS** 475 Pichai road, Pak Phriao, Muang, Saraburi 18000

**PUBLICATION**

1. Development of plant-produced recombinant ACE2-Fc fusion protein as a potential therapeutic agent against SARS-CoV-2
2. Plant-produced receptor-binding domain of SARS-CoV-2 elicits potent neutralizing responses in mice and non-human primates
3. Immunogenicity studies of plant-produced SARS-CoV-2 receptor binding domain-based subunit vaccine candidate with different adjuvant formulations